MATHEMATICAL MODELING OF ARBORESCENT POLYISOBUTYLENE PRODUCTION IN BATCH REACTOR USING NOVEL MATERIAL BALANCE AND MONTE CARLO METHODS

by

Yutian (Ryan) Zhao

A thesis submitted to the Department of Chemical Engineering

In conformity with the requirements for the

Degree of Doctor of Philosophy

Queen's University

Kingston, Ontario, Canada

(October, 2014)

Abstract

Four mathematical models have been developed to describe copolymerization of inimer and isobutylene via living carbocationic polymerization in batch reactors. In this system, there are six different propagation rate constants that result from two kinds of vinyl groups and three different propagating end groups. The models are developed with the following goals: 1) to account for all six propagation rate constants without making equal-reactivity assumptions; 2) to predict concentration changes of inimer, isobutylene and polymer over time; 3) to predict values of average branching level, number and weight average molecular weight; 4) to predict molecular weight distribution; 5) to estimate model parameters.

First, a simplified but lengthy PREDICI model is developed. Due to simplifying assumptions, this model can only be used for systems with low branching levels (*i.e.*, less than 5 branches per molecule, on average), and only four of the six propagation rate constants are included. This model achieves goals 2 to 5 above, with parameters being estimated using low-branching-level data. Next, a traditional Monte Carlo (MC) model is developed. This MC model achieves all of the goals, except parameter estimation, due to the excessive computational effort that would be required. Third, a more advanced MC model is developed using a combination of dynamic material balances and stochastic calculations. With much shorter computational times (by a factor of ~200), this MC model provides information similar to that provided by the traditional MC model, and also provides information about dangling and internal segments in the polymer molecules. However, this model is still not suitable for parameter estimation. Finally, a "parallel" model is developed in PREDICI, which contains three simulation systems that are solved simultaneously. This model achieves goals 1 to 3 and 5, but cannot predict the weight average molecular weight. For the first time, all six propagation rate constants are included in the parameter estimation, resulting in improved fit to the experimental data. Three of the parameter estimates are not significantly different from zero at the 95% confidence level. Additional data, with higher branching levels should be used, in future, to improve the precision of parameter estimates.

Co-Authorship

The research that is presented in this thesis is mainly conducted by me under the supervision of Dr. Kim B. McAuley of the Department of Chemical Engineering, Queen's University and Dr. Judit E. Puskas of the Department of Chemical & Biomolecular Engineering, University of Akron.

Materials in Chapters 2 to 4 have been published in Macromolecular Theory and Simulations and materials in Chapter 5 have been submitted to the AIChE journal. These journal papers were drafted by me and carefully edited and revised by Dr. McAuley and Dr. Puskas. Dr. McAuley and Dr. Puskas are co-authors and helped to develop the objectives of the research for the journal papers in Chapters 2 to 5. Dr. Lucas Dos Santos (Goodyear Tire & Rubber Company) and Dr. Alejandra Alvarez (Univ. of Akron) are also co-authors for the journal paper in Chapter 2. Dr. Dos Santos and Dr. Alvarez provided the experimental data and helped me to understand them. Dr. Piet Iedema (Univ. of Amsterdam) is a co-author for the journal paper in Chapter 4. Dr. Iedema contributed to the development of the advanced Monte Carlo algorithm.

Acknowledgements

First of all, I would like to give my thanks to GOD, who has shown great mercy on me, led me through my Ph.D. program and enabled me to finish ahead of schedule. He has given me comfort and provided research ideas at times when I struggled.

I would like to thank my supervisors Dr. Kim McAuley and Dr. Judit Puskas, for their kind guidance and advice through my whole Ph.D. program. Whenever I had questions or requests, they were always patient and willing to help. Especially, I would like to extend my sincerest and deepest appreciation to Kim who shows genuine care for students. In addition to research advice, Kim generously offered her time to help me improve my English, editing my written work word by word, regardless of whether it was an academic journal article or a simple course report.

I would like to thank Dr. Lucas Dos Santos and Dr. Alejandra Alvarez from University of Akron, for their kind support in providing the experimental data.

I would like to thank all the professors, staffs and students in the Department of Chemical Engineering at Queen's University, especially my office mates, Abdullah, Emily, Hui, Liang, Wei, Zahra, Yasmine, and John for making the office a pleasant place to work.

A special thanks to my family. Words cannot express how grateful I am for the consistent love and support from my father, Yingxiao Zhao, and mother, Yange Li. Thank-you to my dear fiancée Stacey Hildebrand for your love, encouragement and prayers. You are a great blessing to me. I would also like to thank my friends in Kingston for making my life in Canada wonderful.

Table of Contents

Abstract ii
Co-Authorship iii
Acknowledgements iv
List of Figures viii
List of Tables xii
Nomenclature for Chapter 2 xiv
Nomenclature for Chapter 3 xvi
Nomenclature for Chapter 4 xviii
Nomenclature for Chapter 5 xx
Chapter 1 Introduction 1
1.1 Arborescent Polymers 3
1.2 Mathematical Models And Parameter Estimation 4
1.3 Reference 7
Chapter 2 Mathematical Modeling of Arborescent Polyisobutylene Production in Batch Reactor 8
2.1 Abstract 8
2.2 Introduction 9
2.2.1 Mathematical Modeling of Branched Polymer Production 12
2.2.2 Models for Branched Polymer Systems Involving IM 13
2.2.3 Mathematical Models for Linear Isobutylene Polymerization 15
2.3 Model Development 19
2.3.1 Mechanism and Notation 19
2.3.2 Model Implementation in PREDICI 25
2.3.2.1 Experimental Data and Parameter Estimation 27
2.3.2.2 Initial Guesses and Uncertainties for Rate Constants 27
2.4 Simulation Results 32
2.5 Conclusion 41
2.6 Reference 44
Appendix 2.1 Examples of Reaction Steps Implemented in PREDICI 48
Appendix 2.2 Calculation of Mw from Different Polymer Species 49
Appendix 2.3 Scaling Factor Used in PREDICI 52
Appendix 2.4 Simulation results compared with SEC results 54
Chapter 3 Monte Carlo Model for Arborescent Polyisobutylene Production in Batch Reactor 56

3.1 Abstract 56
3.2 Introduction 57
3.3 Model Development 66
3.3.1 Monte Carlo Model Development 69
3.4 Results 72
3.5 Conclusions 79
3.6 Reference 81
Appendix 3.1 MC Simulation with Only 10000 Initial IM Molecules 84
Appendix 3.2 Simple PREDICI Simulation for k_{pIIapp} And k_{pSIapp} 85
Appendix 3.3 Matlab Code for MC Model with Six Parameters 86
Appendix 3.4 Matlab Code for MC Model with Four Parameters 94
Chapter 4 Advanced Monte Carlo for Arborescent Polyisobutylene Production in Batch Reactor 100
4.1 Abstract 100
4.2 Introduction 101
4.3 Model Development 110
4.4 Simulation Results 122
4.5 Conclusion 130
4.6 Reference 131
Appendix 4.1 Implementation Details in PREDICI for Internal Segments 134
Appendix 4.2 Matlab Code for Advanced MC Model with 3 Minutes Interval 137
Chapter 5 Parallel Models for Arborescent Polyisobutylene Synthesized in Batch Reactor 146
5.1 Abstract 146
5.2 Introduction 147
5.3 Model Development 155
5.4 Parameter Estimation and Simulation Results 163
5.4.1 Parameter Estimation 163
5.4.2 Simulation Results 169
5.5 Conclusions 175
5.6 References 176
Appendix 5.1 Additional Information about Parameter Estimation Attempts 183
Chapter 6 Conclusions and Recommendations 185
6.1 Conclusions 185
6.2 Recommendations for Future Work 189
6.2.1 Modifications of Current Models 189

6.2.2 More Experimental Data for Parameter Estimation 189

List of Figures

Figure 1.1 Carbenium ion 1
Figure 1.2 a) Isobutylene molecule and isoprene molecule; b) the inimer molecule 4-(2-chloro-isopropyl)styrene has a vinyl group that can undergo propagation reactions and a chloride that can be removed to initiate cationic polymerization 2
Figure 2.1 Synthetic strategy for production of *arb*PIB.[7] This scheme involves two types of vinyl groups, V_I and V_M and three types of cations arising from C_I, C_S and C_M 9
Figure 2.2 Aromatic link destruction reaction[22] 11
Figure 2.3 Comprehensive mechanism for living IB polymerization using $TiCl_4$ as the Lewis acid[51] 16
Figure 2.4 Two examples of $P_9^{2I,2S}$(18) molecules that have 9 benzene groups from IM units, 18 isobutylene units, 2 chloride ends of type C_I from IM and 2 secondary chlorides of type C_S. . 20
Figure 2.5 Six reactions corresponding to the different true propagation rate coefficients. The new bond that forms is shown in bold. 22
Figure 2.6 Comparison of experimental data from replicate experiments in Table 2.4 and model predictions using parameter values in Table 2.8. a) [IB] ▲data, ─ prediction; b) ■ M_n and▲ M_w data, ─ prediction c) B_{kin} ▲data, ─ prediction 34
Figure 2.7 Comparison of experimental data from 06DNX090 and 06DNX100 in Table 2.4 and model predictions using parameter values in Table 2.8. a) [IB] 06DNX090 Δ data, - - - prediction; 06DNX100 ■ data, ─ prediction; b) 06DNX090 □ M_n, Δ M_w data, - - - prediction; 06DNX100 ■ M_n, ▲ M_w data, ─ prediction. c) B_{kin} 06DNX090 □ data, - - - prediction; 06DNX100 ■ data, ─ prediction 35
Figure 2.8 Predicted [IM] vs. time from the replicate runs, a) simulation results from using estimated value k_{pIMapp} in Table 2.8; b) simulation result from using initial value of k_{pIMapp} in Table 2.8, which we most believed. Note the different time scales for a) and b). 38
Figure 2.9 Detailed simulation results for polymer species with different numbers of IM units using the conditions for 06DNX100. a) Polymer concentrations vs. time; b) M_n vs. time; c) M_w vs. time. ■ 1 IM per molecule, ▲ 3 IM per molecule, ▼ 5 IM per molecule, ○ 10 IM per molecule and × 15 IM per molecule. 39
Figure 2.10 Simulation results for MWD using experimental conditions for run 06DNX100. The left-most peak of the overall MWD corresponds primarily to linear polymer with only one inimer unit. The second peak corresponds mainly to branched polymer with two or three inimer units.

Note that area of the peaks decreases as the number of inimer units increases, except for peak 15. 40
Figure 2.11 Simulation results for MWD using experimental conditions for run 06DNX001, 06DNX010 and 06DNX030. 54
Figure 2.12 SEC traces of selected *arb*PIB samples obtained from Dos Santos[21]. (a) 06DNX001; (b) 06DNX010 55
Figure 3.1 Reaction scheme to produce *arborescent* polyisobutylene. Step a) is the exchange reaction that generates IM from MeOIM.[13] Step b) is the overall reaction scheme to produce an *arb*PIB molecule from several IM and isobutylene molecules.[15] 57
Figure 3.2 Comprehensive mechanism for living IB polymerization using $TiCl_4$ as the Lewis acid[16]..... 61
Figure 3.3 a) Comparison of predicted chainlength distributions obtained using different initial numbers of IM molecules ─ · ─ 50000, - - - 1500000 and ── PREDICI predictions; b) individual MWD curves for polymer molecules with different numbers of IM units from MC simulation with 1500000 initial IM molecules. 73
Figure 3.4 . Comparison between MC and PREDICI model predictions for simulations with $[IM]_0$ = 0.00454 M. The MC simulations used 50000 IM and 19162996 IB molecules initially ─ · ─ MC, ─ ─ PREDICI. The MC results are difficult to see in a) because they overlap with the PREDICI results..... 75
Figure 3.5 Comparison between MC model with only 4 parameters and MC model with all 6 parameters when $[IM]_0$ = 0.00454 M. Note that 50000 IM and 19162996 IB molecules are used initially in the MC simulations. The thinner dash-dot lines correspond to MC simulations with only 4 parameters and the thicker dash-dot lines correspond to MC model with 6 parameters. In a) the results are overlaid so that the thinner line cannot be seen. 77
Figure 3.6 SCVP results with $[IM]_0$ = 1 M and 2000000 initial IM units 78
Figure 3.7 MC predictions for simulations with $[IM]_0$ = 0.00454 M. The MC simulations used 10000 IM and 3832599 IB molecules initially. These figures agree well with the MC simulations in Figure 3.4 for less computing time. 84
Figure 3.8 PREDICI rough simulation results for k_{pIIapp} = 0.00075 $Lmol^{-1}s^{-1}$ and k_{pSIapp} = 0.00001 $Lmol^{-1}s^{-1}$ with experimental data. ── simulation results; ■ is the experimental data..... 85
Figure 4.1 Typical structure of an inimer 101
Figure 4.2 a) Exchange reaction that converts 4-(2-methoxyisopropyl)styrene to IM;[19] b) a simplified reaction scheme for the "one-pot" living copolymerization of IM and IB[21] 103
Figure 4.3 Two different paths for carbocationic polymerization using different amount of Lewis acid coinitiator. Path A is dominant when LA concentration is lower than the concentration of

initiator; Path B is dominant when LA concentration is much higher than the concentration of initiator. Note I is initiator and M is monomer.[26] 104
Figure 4.4 Detailed illustration of dangling segments and internal segments. 112
Figure 4.5 Detailed process for assembling the polymer molecule shown in Figure 4.4. The Cl groups that uncaps to initiate the next segment is shown in bold 115
Figure 4.6 Fraction of the total C_I end groups that are eventually converted to C_M groups (via reaction 2 in Table 4.2) at any time during a batch with $[IB]_0$ = 1.74 M and $[IM]_0$ = 0.00454 M that ends at t_f = 5400 s. The values of r_2 and t_M shown on the plot indicate that 75% of the reactions of this type have occurred by a time of 528 s. 122
Figure 4.7 Model predictions for hypothetical species from Table 4.4, a) $C_{HI \rightarrow S}$; b) C_{HM}; c) C_{HS}; d) $C_{HS \rightarrow M}$ and $C_{HS \rightarrow S}$ obtained by starting with $[IB]_0$ = 1.74 M and $[IM]_0$ = 0.00454 M. Note that only the first 600 seconds of the simulated results are shown in c) and d). 123
Figure 4.8 Predicted concentrations of vinyl groups and end groups obtained by solving ODEs in Table 4.4, a) V_I and V_M vinyl groups; b) ── is C_I groups; - - - is C_M groups; ⋯⋯ is C_S groups, starting with $[IB]_0$ = 1.74 M and $[IM]_0$ = 0.00454 M 123
Figure 4.9 MWDs obtained using different number of random polymer chains and discretization intervals of 180 s in Tables 4.7 and 4.8, for a batch with $[IB]_0$ = 1.74 M and $[IM]_0$ = 0.00454 M and t_f = 5400 s. - - - is a distribution with 1×10^4 polymer chains; ── is a distribution with 1×10^5 polymer chains; ⋯⋯ is a distribution with 2×10^5 polymer chains. 125
Figure 4.10 MWDs with different time intervals in Tables 4.7 and 4.8, using $[IB]_0$ = 1.74 M and $[IM]_0$ = 0.00454 M and t_f = 5400 s and 1×10^5 polymer chains. - - - is a distribution with 60 s discretization intervals; ── is a distribution with 180 s intervals; ⋯⋯ is a distribution with 600 s intervals. 125
Figure 4.11 MWDs for results from traditional MC and advanced MC for a batch with $[IB]_0$ = 1.74 M and $[IM]_0$ = 0.00454 M and t_f = 5400 s. ── is advanced MC and there are 1×10^5 polymer chains, using 180 s intervals in Tables 4.7 and 4.8; - - - is from a traditional MC simulation that results in 0.99313×10^5 polymer chains. 126
Figure 4.12 MWDs results for dangling segments and internal segments from advanced MC with $[IB]_0$ = 1.74 M and $[IM]_0$ = 0.00454 M and t_f = 5400 s and 1×10^5 polymer chains. ── are dangling segments (36236 pieces); - - - are internal segments (308953 pieces). Note internal segment with length 0 is not considered here 128
Figure 4.13 Captured photo from PREDICI. L0 is the concentration of segments that start growing at t = 0; L1 is the concentration of the segments that start growing at t = 1 min.; L2,L3… are linear

segments that are born at different time. M0, M1… are the corresponding initiator that initiates the linear segments. 135
Figure 4.14 PREDICI file for kp1.fun that controls the birth time of L1(1). 136
Figure 5.1 a) Typical structure of an inimer; b) a simplified reaction scheme for the "one-pot" living copolymerization of IM and IB.[13] 148
Figure 5.2 Two different paths for carbocationic polymerization using different amount of Lewis acid coinitiator. Path A is dominant when LA concentration is lower than that of the initiator; Path B is dominant when LA concentration is higher than that of the initiator. Note I is initiator and M is monomer.[33] 150
Figure 5.3 Comparison of the calculated MWD between simulation 3 using PREDICI and our previous advanced MC model[15] using the initial condition $[IM]_0$ = 0.00454 M and $[IB]_0$ = 1.74 M and the parameter values in Table 5.2. - - - is the MWD calculated by PREDICI; ─ is the MWD calculated by advanced MC with 10^5 polymer chains. 161
Figure 5.4 Comparison among experimental results and simulation results using old parameter values in Table 5.2 and new estimates in Table 5.7 for a batch reactor run with $[IM]_0$ = 0.00114 M and $[IB]_0$ = 1.74 M . ── simulation with newly estimated parameters; - - - simulation with old parameters; ■ experimental values; ▲ B_{kin} calculated from data with assumption [IM]=0; Δ B_{kin} calculated from data using simulated [IM]; a) [IB], b) [IM], c) polymer concentration, d) B_{kin}, e) M_n f) M_w. 171
Figure 5.5 Comparison among experimental results and simulation results using old parameter values in Table 5.2 and new estimates in Table 5.7 for a batch reactor run with $[IM]_0$ = 0.00227 M and $[IB]_0$ = 1.74 M . ── simulation with newly estimated parameters; - - - simulation with old parameters; ■ experimental values; ▲ B_{kin} calculated from data with assumption [IM]=0; Δ B_{kin} calculated from data using simulated [IM]; a) [IB], b) [IM], c) polymer concentration, d) B_{kin}, e) M_n f) M_w. 172
Figure 5.6 Comparison among experimental results and simulation results using old parameter values in Table 5.2 and new estimates in Table 5.7 for a batch reactor run with$[IM]_0$ = 0.00454 M and $[IB]_0$ = 1.74 M . ── simulation with newly estimated parameters; - - - simulation with old parameters; ■ experimental values; ▲ B_{kin} calculated from data with assumption [IM]=0; Δ B_{kin} calculated from data using simulated [IM]; a) [IB], b) [IM], c) polymer concentration, d) B_{kin}, e) M_n f) M_w. 173
Figure 5.7 Predicted MWDs for a) internal segments and b) dangling segments at t = 5400 s from experiment with $[IM]_0$ = 0.00454 M and $[IB]_0$ = 1.74 M and parameter values from Table 5.7; ─ PREDICI, -- Advanced Monte Carlo. Note that the two curves in a) overlap. 174

List of Tables

Table 2.1 Summary of typical reactions based on end groups 23
Table 2.2 Summary of reactions and rate expressions in terms of the apparent and true propagation rate constants assuming that all propagation reactions occur via both path A and path B. C_M, C_I and C_S in the second column indicate the type of cation that is participating in the reaction. 24
Table 2.3 Assumptions for model development 26
Table 2.4 Experiments from Dos Santos[21] $[IB]_0$ = 1.74 M, $[TiCl_4]_0$ = 0.0313 M, T = -95 ℃ in Hx/MeCl (60/40). The inimer that initiated the polymerization was formed in situ from a precursor (MeOIM), as shown in Figure 3.1. 28
Table 2.5 Initial values, upper and lower values, and uncertainties of each parameter 29
Table 2.6 Literature values for kinetic parameters from IB and styrene homopolymerization and copolymerization 29
Table 2.7 The actual apparent rate constants for parameter estimation 31
Table 2.8 Parameter estimation results 33
Table 3.1 Assumptions for PREDICI material balance model development[15] 62
Table 3.2 Parameter estimation results for four lumped parameters.[15] 63
Table 3.3 Summary of six possible propagation reactions and corresponding reaction rates between end groups and vinyl groups during copolymerization of IM and IB 67
Table 3.4 Summary of reactions and rate expressions for reactions between different types of molecules during copolymerization of IM and IB. C_M, C_I and C_S in the second column indicate the type of cation that is participating in the reaction.[15] 68
Table 3.5 special matrix for counting IM and polymers 70
Table 4.1 Six apparent propagation rate constants and their estimated values.[21,22] 104
Table 4.2 Summary of six possible propagation reactions between end groups and vinyl groups during copolymerization of IM and IB 105
Table 4.3 Assumptions from our previous PREDICI model[21] 107
Table 4.4 Dynamic material balances and initial conditions (IC) used in advanced MC calculations. 111
Table 4.5 Algorithm for assembling a random polymer molecule using information available at the end of the batch. 113
Table 4.6 Random numbers, Criteria and Outcomes used in the MC algorithm in Table 4.5 114
Table 4.7 Probabilities of lengths of internal segments that are born at t_M = 2520 s and that end at different times t_S. The probability values were obtained using the parameter values in Table 4.1 for a

batch with $[IB]_0$=1.74 M, $[IM]_0$=0.00454 M and t_f = 5400 s. Similar tables are required for different values of t_M. 118
Table 4.8 ODEs for different chain lengths that are solved by an alternative way using Matlab. 118
Table 4.9 Probabilities for dangling segments born at different times with time interval 180 s. 120
Table 5.1 Summary of six possible propagation reactions between end groups and vinyl groups using apparent propagation rate constants during copolymerization of IM and IB. 149
Table 5.2 Six apparent propagation rate constants and their estimated values.[13-15] 149
Table 5.3 Assumptions from our previous PREDICI model.[13] 153
Table 5.4 Four parallel polymerization simulations that focus on different arborescent polymerization characteristics 157
Table 5.5 Pseudo rate constants derived using reactions in corresponding rows in Table 5.4 for Simulations 1, 3 and 4. 158
Table 5.6 Initial values and lower and upper bounds used for estimation of six apparent rate constants 164
Table 5.7 Parameter ranking and estimation results for all six apparent rate constants. 168
Table 5.8 Twenty different initial guesses used for parameter estimation. Note that the estimable parameters determined in each attempt are marked in bold and the best trial (Trial 19) is highlighted. 183
Table 5.9 Estimation results from all 20 trials. Values shown as –- did not change from their initial values because the corresponding parameters were not selected for estimation. 184

Nomenclature for Chapter 2

B_{LD}	branching level determined by link destruction method
B_{kin}	branching level determined by kinetic calculations and measured molecular weight
C_I	chloride-capped groups from the IM
C_M	chloride-capped groups on a chain end formed after propagation with monomer
C_S	chloride-capped groups along the side of a chain, produced after propagation with a V_I type vinyl group, either on IM or polymer
Hx	Hexane
IB	Isobutylene
IM	Inimer, a small molecule that functions of both initiator and monomer
k_{pIM}	true rate constant for reactions involving $C_I + V_M$
k_{pII}	true rate constant for reactions involving $C_I + V_I$
k_{pMM}	true rate constant for reactions involving $C_M + V_M$
k_{pMI}	true rate constant for reactions involving $C_M + V_I$
k_{pSM}	true rate constant for reactions involving $C_S + V_M$
k_{pSI}	true rate constant for reactions involving $C_S + V_I$
k_{app}	apparent rate constant that accounts for ionization equilibrium
k_{pIMapp}	apparent rate constant for reactions involving $C_I + V_M$
k_{pMMapp}	apparent rate constant for reactions involving $C_M + V_M$
k_{pMIapp}	apparent rate constant for reactions involving $C_M + V_I$
k_{pSMapp}	apparent rate constant for reactions involving $C_S + V_M$
k_{p12}	cross-propagation rate constant in IB (1) and styrene (2) copolymerization
k_{p21}	cross-propagation rate constant in IB (1) and styrene (2) copolymerization
k_0	rate constant for intermediate formation, $L \cdot mol^{-1}s^{-1}$
$k\text{-}_0$	rate constant for intermediate dissociation, s^{-1}
K_0	$k_0/k\text{-}_0$, equilibrium constant for intermediate formation, $L \cdot mol^{-1}$
k_1	ionization rate constant to form active species with monomeric gegenion, s^{-1}
$k\text{-}_1$	deactivation rate constant for active species with monomeric gegenion, s^{-1}
K_1	$k_1/k\text{-}_1$, equilibrium constant for active species with monomeric gegenion
k_2	ionization rate constant to form active species with dimeric gegenion, $L \cdot mol^{-1}s^{-1}$
$k\text{-}_2$	deactivation rate constant for active species with dimeric gegenion, s^{-1}
K_2	$k_2/k\text{-}_2$, equilibrium constant for active species with dimeric gegenion, $L \cdot mol^{-1}$
LA	Lewis Acid
MeCl	methyl chloride
$M_{n,theo}$	the molecular weight that would be obtained if all *IM* was consumed as initiator only
M_{IB}	the molar mass of isobutylene
M_{IM}	the molar mass of inimer
M_n	number average molecular weight
M_w	weight average molecular weight
MWD	molecular weight distribution
P_n^*LA	polymer/Lewis acid intermediate with chain of length *n*, *n*>1
$P_n^+LA^-$	active growing chain of length *n*, with monomeric Lewis acid gegenion, *n*>1

$P_n^+LA_2^-$	active growing chain of length *n*, with dimeric Lewis acid gegenion, *n*>1
$P_i^{xI,yS}(m)$	polymer molecules with *i* IM units, *m* IB units, *x* C_I end groups and *y* C_S side groups
r_1	k_{p11}/k_{p12} in IB (1) and styrene (2) copolymerization
r_2	k_{p22}/k_{p21} in IB (1) and styrene (2) copolymerization
R_{pA}	rate expressions for reactions via path A, *i.e.*, with monomeric gegenion
R_{pB}	rate expressions for reactions via path B, *i.e.*, with dimeric gegenion
R_{pTot}	rate expressions for combination of both path A and path B
SCVP	self-condensing vinyl polymerization
SCVCP	self-condensing vinyl copolymerization
TMPCl	2-chloro-2,4,4-trimethylpentane
V_I	vinyl groups on IM and polymer
V_M	vinyl groups on isobutylene
$\mu_{i,0}^{yS}$	zeroth moment for polymer chains with *i* IM units and *y* C_S side groups
$\mu_{i,1}^{yS}$	first moment for polymer chains with *i* IM units and *y* C_S side groups
$\mu_{i,2}^{yS}$	second moment for polymer chains with *i* IM units and *y* C_S side groups

Nomenclature for Chapter 3

B_{kin}	branching level determined by kinetic calculations and measured molecular weight
C_I	chloride-capped groups from the IM
C_{Itot}	total number of C_I groups in MC simulation
C_j	concentration of species j in the system
C_M	chloride-capped groups on a chain end formed after propagation with monomer
C_{Mtot}	total number of C_M groups in MC simulation
C_S	chloride-capped groups along the side of a chain, produced after propagation with an IM vinyl group
C_{Stot}	total number of C_S groups in MC simulation
Δt	small time interval between two successive reactions in MC
DP	Degree of polymerization, here includes both IM and IB
IB	Isobutylene
IM	Inimer, a small molecule that functions of both initiator and monomer
k_i^{MC}	rate constant for initiation used in MC model
k_p^{MC}	rate constant for propagation used in MC model
k_{pII}	true rate constant for reactions involving C_I + V_I
k_{pIIapp}	apparent rate constant for reactions involving C_I + V_I
k_{pIIapp}^{MC}	apparent rate constant for reactions involving C_I + V_I used in MC model
k_{pIM}	true rate constant for reactions involving C_I + V_M
k_{pIMapp}	apparent rate constant for reactions involving C_I + V_M
k_{pIMapp}^{MC}	apparent rate constant for reactions involving C_I + V_M used in MC model
k_{pMI}	true rate constant for reactions involving C_M + V_I
k_{pMIapp}	apparent rate constant for reactions involving C_M + V_I
k_{pMIapp}^{MC}	apparent rate constant for reactions involving C_M + V_I used in MC model
k_{pMM}	true rate constant for reactions involving C_M + V_M
k_{pMMapp}	apparent rate constant for reactions involving C_M + V_M
k_{pMMapp}^{MC}	apparent rate constant for reactions involving C_M + V_M used in MC model
k_{pSI}	true rate constant for reactions involving C_S + V_I
k_{pSIapp}	apparent rate constant for reactions involving C_S + V_I
k_{pSIapp}^{MC}	apparent rate constant for reactions involving C_S + V_I used in MC model
k_{pSM}	true rate constant for reactions involving C_S + V_M
k_{pSMapp}	apparent rate constant for reactions involving C_S + V_M
k_{pSMapp}^{MC}	apparent rate constant for reactions involving C_S + V_M used in MC model
k_t^{MC}	rate constant for termination used in MC model
k_0	rate constant for intermediate formation, $L \cdot mol^{-1}s^{-1}$
k_{-0}	rate constant for intermediate dissociation, s^{-1}
K_0	k_0/k_{-0}, equilibrium constant for intermediate formation, $L \cdot mol^{-1}$
k_1	ionization rate constant to form active species with monomeric gegenion, s^{-1}
k_{-1}	deactivation rate constant for active species with monomeric gegenion, s^{-1}

K_1	k_1/ k_{-1}, equilibrium constant for active species with monomeric gegenion
k_2	ionization rate constant to form active species with dimeric gegenion, $L \cdot mol^{-1}s^{-1}$
k_{-2}	deactivation rate constant for active species with dimeric gegenion, s^{-1}
K_2	k_2/ k_{-2}, equilibrium constant for active species with dimeric gegenion, $L \cdot mol^{-1}$
LA	Lewis Acid
MeOIM	4-(2-methoxyisopropyl)styrene
M_n	number average molecular weight
M_w	weight average molecular weight
MWD	molecular weight distribution
N_A	*Avogadro*'s constant
N_{C_I}	number of C_I end groups in MC model
N_{C_M}	number of C_M end groups in MC model
N_{C_S}	number of C_S end groups in MC model
N_i	number of initiator in MC model
N_m	number of monomer in MC model
N_p	number of polymer in MC model
N_{V_I}	number of V_I vinyl groups in MC model
N_{V_M}	number of V_M vinyl groups in MC model
p_j	probability of the *j*th reaction
P_n^*LA	polymer/Lewis acid intermediate with chain of length *n*, *n*>1
$P_n^+LA^-$	active growing chain of length *n*, with monomeric Lewis acid gegenion, *n*>1
$P_n^+LA_2^-$	active growing chain of length *n*, with dimeric Lewis acid gegenion, *n*>1
$P_i^{xI,yS}(m)$	polymer molecules with *I* IM units, *m* IB units, *x* C_I end groups and *y* C_S side groups
R_i^{MC}	the reaction rate of initiation in MC model
R_j^{MC}	the reaction rate of *j*th reaction in MC model
R_p^{MC}	the reaction rate of propagation reaction in MC model
R_t^{MC}	the reaction rate of termination reaction in MC model
R_{total}^{MC}	total reaction rate of all reactions in MC model
R_{pA}	rate expressions for reactions via path A, *i.e.*, with monomeric gegenion
R_{pB}	rate expressions for reactions via path B, *i.e.*, with dimeric gegenion
R_{pTot}	rate expressions for combination of both path A and path B
r_1 *to* r_4	uniformly distributed random number from 0 to 1
SCVP	self-condensing vinyl polymerization
SCVCP	self-condensing vinyl copolymerization
V	specific volume used in MC model
V_I	vinyl groups on IM and polymer
V_{Itot}	total number of V_I groups in MC simulation
V_M	vinyl groups on isobutylene

Nomenclature for Chapter 4

B_{kin}	branching level determined from kinetic calculations and measured molecular weight
C_I	chloride-capped groups from the inimer
C_M	chloride-capped groups on a chain end formed after propagation with monomer
C_S	chloride-capped groups along the side of a chain, produced after propagation with an inimer vinyl group
$C_{HI\rightarrow M}$	hypothetical counter species that counts the total number of moles (per liter) of C_I groups that have been converted to C_M at a particular time in the batch (see Table 4.4)
$C_{HI\rightarrow S}$	hypothetical counter species that counts the total number of moles (per liter) of C_I groups that have been converted to C_S at a particular time in the batch (see Table 4.4)
C_{HM}	hypothetical counter species that counts the number of C_M groups per unit volume that change to C_S (see Table 4.4)
C_{HS}	hypothetical counter species that counts the number of C_S groups that are consumed by either V_I groups or V_M groups (see Table 4.4)
$C_{HS\rightarrow M}$	hypothetical counter species that counts only the C_S groups that are converted to C_M groups. (see Table 4.4)
$C_{HS\rightarrow S}$	hypothetical counter species that counts only the C_S groups that are converted to other C_S groups. (see Table 4.4)
Δt	small time interval between two successive reactions using traditional Monte Carlo method
IB	Isobutylene
IM	Inimer, a small molecule that functions as both initiator and monomer
k_{pII}	true rate constant for propagation reactions involving C_I and V_I
k_{pIIapp}	apparent rate constant for propagation reactions involving C_I and V_I
k_{pIM}	true rate constant for propagation reactions involving C_I and V_M
k_{pIMapp}	apparent rate constant for propagation reactions involving C_I and V_M
k_{pMI}	true rate constant for propagation reactions involving C_M and V_I
k_{pMIapp}	apparent rate constant for propagation reactions involving C_M and V_I
k_{pMM}	true rate constant for propagation reactions involving C_M and V_M
k_{pMMapp}	apparent rate constant for propagation reactions involving C_M and V_M
k_{pSI}	true rate constant for propagation reactions involving C_S and V_I
k_{pSIapp}	apparent rate constant for propagation reactions involving C_S and V_I
k_{pSM}	true rate constant for propagation reactions involving C_S and V_M
k_{pSMapp}	apparent rate constant for propagation reactions involving C_S and V_M
k_0	rate constant for intermediate formation, $L \cdot mol^{-1}s^{-1}$
k_{-0}	rate constant for intermediate dissociation, s^{-1}
K_0	k_0/k_{-0}, equilibrium constant for intermediate formation, $L \cdot mol^{-1}$
k_1	ionization rate constant to form active species with monomeric gegenion, s^{-1}
k_{-1}	deactivation rate constant for active species with monomeric gegenion, s^{-1}
K_1	k_1/k_{-1}, equilibrium constant for active species with monomeric gegenion
k_2	ionization rate constant to form active species with dimeric gegenion, $L \cdot mol^{-1}s^{-1}$
k_{-2}	deactivation rate constant for active species with dimeric gegenion, s^{-1}

K_2	k_2/ k_{-2}, equilibrium constant for active species with dimeric gegenion, $L \cdot mol^{-1}$
LA	Lewis Acid
MeOIM	4-(2-methoxyisopropyl)styrene
M_{IB}	molar mass of isobutylene
M_{IM}	molar mass of inimer
$\bar{M}_n$	number average molecular weight
$\bar{M}_{n,theo}$	theoretical number average molecular weight
M_w	weight average molecular weight
MWD	molecular weight distribution
N_{C_I}	number of C_I end groups that has not been studied in MC molecule assembly
$p(i)$	probability of polymer chain with length i
$P_n^* LA$	polymer/Lewis acid intermediate with chain of length n
$P_n^+ LA^-$	active growing chain of length n, with monomeric Lewis acid gegenion
$P_n^+ LA_2^-$	active growing chain of length n, with dimeric Lewis acid gegenion
$r_0, r_1 \ldots r_9$	uniformly distributed random numbers between 0 and 1
SCVP	self-condensing vinyl polymerization
SCVCP	self-condensing vinyl copolymerization
$S(i)$	segments with length i
t_0	beginning time of the batch
t_M	time when a C_I group or C_S group reacts with a V_M group to start a new segment
t_S	time when a C_I group or C_M group reacts with a V_I group
t_{S2}	time when a C_S group reacts with a V_I group
t_f	batch end time
V_I	vinyl group on inimer and polymer
V_M	vinyl group on isobutylene

Nomenclature for Chapter 5

B_{kin}	average branching level determined from kinetic calculations and measured molecular weight
C_I	chloride-capped groups from the inimer or polymer
$C_I^{(i)}$	chloride-capped groups from the inimer or polymer in simulation (i)
C_M	chloride-capped groups on a chain end formed after propagation with monomer
$C_M^{(i)}$	chloride-capped groups on a chain end formed after propagation with monomer in simulation (i)
C_S	chloride-capped groups along the side of a chain, produced after propagation with an inimer vinyl group
$C_S^{(i)}$	chloride-capped groups along the side of a chain, produced after propagation with an inimer vinyl group in simulation (i)
IB	isobutylene
$IB^{(i)}$	isobutylene in simulation (i)
$[IB]_{exp}$	experimental measurements of the concentration of IB
IM	inimer, a small molecule that functions as both initiator and monomer
$IM^{(i)}$	inimer, a small molecule that functions as both initiator and monomer in simulation (i)
J	objective function value
k_{pII}	true rate constant for propagation reactions involving C_I and V_I
k_{pIIapp}	apparent rate constant for propagation reactions involving C_I and V_I
k^*_{pIIapp}	average rate constant defined in Table 5.4.
k_{pIM}	true rate constant for propagation reactions involving C_I and V_M
k_{pIMapp}	apparent rate constant for propagation reactions involving C_I and V_M
k^*_{pIMapp}	average rate constant defined in Table 5.4
k_{pMI}	true rate constant for propagation reactions involving C_M and V_I
k_{pMIapp}	apparent rate constant for propagation reactions involving C_M and V_I
k^*_{pMIapp}	average rate constant defined in Table 5.4
k_{pMM}	true rate constant for propagation reactions involving C_M and V_M
k_{pMMapp}	apparent rate constant for propagation reactions involving C_M and V_M
k^*_{pMMapp}	average rate constant defined in Table 5.4
k_{pSI}	true rate constant for propagation reactions involving C_S and V_I
k_{pSIapp}	apparent rate constant for propagation reactions involving C_S and V_I
k^*_{pSIapp}	average rate constant defined in Table 5.4
k_{pSM}	true rate constant for propagation reactions involving C_S and V_M
k_{pSMapp}	apparent rate constant for propagation reactions involving C_S and V_M
k^*_{pSMapp}	average rate constant defined in Table 5.4
$k_{p?}$	an unknown value that is related to k_{pIIapp}
k_0	rate constant for intermediate formation, $L \cdot mol^{-1}s^{-1}$
k_{-0}	rate constant for intermediate dissociation, s^{-1}
K_0	k_0/k_{-0}, equilibrium constant for intermediate formation, $L \cdot mol^{-1}$

k_1	ionization rate constant to form active species with monomeric gegenion, s^{-1}
k_{-1}	deactivation rate constant for active species with monomeric gegenion, s^{-1}
K_1	k_1/k_{-1}, equilibrium constant for active species with monomeric gegenion
k_2	ionization rate constant to form active species with dimeric gegenion, $L \cdot mol^{-1}s^{-1}$
k_{-2}	deactivation rate constant for active species with dimeric gegenion, s^{-1}
K_2	k_2/k_{-2}, equilibrium constant for active species with dimeric gegenion, $L \cdot mol^{-1}$
LA	Lewis Acid
MeOIM	4-(2-methoxyisopropyl)styrene
M_{IB}	molar mass of isobutylene
M_{IM}	molar mass of inimer
$\bar{M}_n$	number average molecular weight
$\bar{M}_{n_{exp}}$	experimental measurements of the number average molecular weight
$\bar{M}_{n,theo}$	theoretical number average molecular weight
$\bar{M}_w$	weight average molecular weight
MWD	molecular weight distribution
n	number of IB units in an internal or dangling segment
$n_T; m_T$	total number of IB and IM units in a polymer molecule
$P^{(3)}(n_T)$	polymer chains with n IB and IM units in total in simulation 3
$P^{(4)}$	polymer concentrations in simulation 4
P_n^*LA	polymer/Lewis acid intermediate with chain of length n
$P_n^+LA^-$	active growing chain of length n, with monomeric Lewis acid gegenion
$P_n^+LA_2^-$	active growing chain of length n, with dimeric Lewis acid gegenion
SCVP	self-condensing vinyl polymerization
SCVCP	self-condensing vinyl copolymerization
$S_D^{(2)}(n)$	dangling segment with length n in simulation 2
$S_I^{(2)}(n)$	internal segment with length n in simulation 2
s_{IB}^2	pooled variance estimates for the isobutylene concentration
$s_{\bar{M}_n}^2$	pooled variance estimates for the number average molecular weight
V_I	vinyl group on inimer and polymer
$V_I^{(i)}$	vinyl group on inimer and polymer in simulation (i)
V_M	vinyl group on isobutylene
$V_M^{(i)}$	vinyl group on isobutylene and polymer in simulation (i)

Chapter 1

Introduction

In this thesis, four mathematical models are developed to describe the living carbocationic copolymerization of inimer and isobutylene in batch reactors to produce *arborescent* polyisobutylene. Carbocationic polymerization is a chain-growth reaction where the active center is a carbenium ion[1] (shown in Figure 1.1). Because of the high reactivity of the carbocations, carbocationic polymerizations have been traditionally considered uncontrollable. They were treated in the same way as free radical polymerizations where the molecular weight was determined by the rates of side reactions, like chain transfer and termination, relative to the rate of propagation.[1] It was not until 1974 that living conditions were achieved experimentally in carbocationic polymerization.[2]

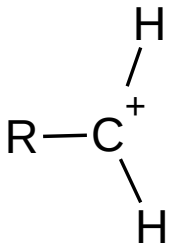

Figure 1.1 Carbenium ion

The annual production of polymers produced by carbocationic polymerization is relatively small, at around 2% of the total polymer market worldwide provided.[3] However, carbocationic polymerization is used for some important applications where other types of polymerization (*e.g.*, free radical, condensation, anionic) cannot be used.[1,4] Among these polymer products, butyl rubber, which is a copolymer of isobutylene and isoprene (Figure 1.2a), is the highest-volume prod-

uct.[3] Butyl rubbers have many desirable physical properties, like low air permeability, making them widely used as inner tubes for all kinds of vehicles.[1,5] Also, butyl rubbers also have broad damping properties that can be used to reduce vibration on machines.[1,5] Besides the excellent physical properties, butyl rubbers also have outstanding chemical stability and biocompatibility.[1,4]

Even though the polyisobutylene-based products have excellent properties for a variety of applications, their annual production is still relatively small comparing with other polymer products. The main reason is the undesirable operating conditions for carbocationic polymerization. Most carbocationic polymerizations are conducted at very low temperatures between -80 to -100 °C. Higher temperatures would cause low reactivity and molecular weight, because the rate of depropagation increases faster than the rate of propagation when the temperature increases.[1]

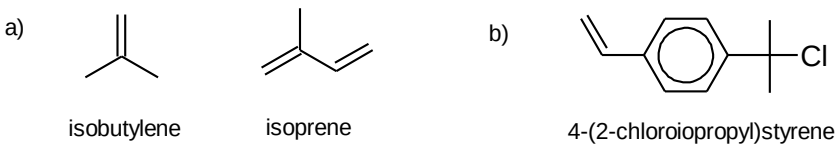

Figure 1.2 a) Isobutylene molecule and isoprene molecule; b) the inimer molecule 4-(2-chloro-isopropyl)styrene has a vinyl group that can undergo propagation reactions and a chloride that can be removed to initiate cationic polymerization

1.1 Arborescent Polymers

Recently, researchers have been paying attention to hyperbranched, dendritic or arborescent polymers.[6-8] These highly branched polymers have unique physical properties compared to their linear counterparts, making them good candidates for use in many specialized areas, *e.g.* biomaterials, gene and drug delivery and coatings.[6-10] One way to produce hyperbranched or arborescent polymers is by using inimer molecules like that shown in Figure 1.2b. Inimers have both the function of an initiator and a monomer. Because of this structure each inimer molecule has the potential to form a T-shaped branch on a polymer chain. By adding inimer into the recipe, it is quite easy to obtain arborescent polymers in a single batch reactor.[11]

In this thesis, mathematical models are developed to describe the formation of *arborescent* polyisobutylene (*arb*PIB) in a batch reactor.[11,12] This *arb*PIB and its derivatives are very promising biomaterials that can be used for human implantation, due to their outstanding properties, like tensile strength, permeability and biocompatibility. Some of the properties, like strength and permeability to liquid, are largely decided by its branching level and molecular weight distribution. In general, higher branching levels cause lower viscosity and lower hardness; higher molecules weight causes higher viscosity and more stiffness. In order to know how the initial concentration of inimer used in the recipe will influence on the polymer branching level and molecular weight over time, performing a large number of experiments would be necessary. However, this *arb*PIB material is synthesized in special reactors at low temperatures near -80℃, which makes experiments difficult and time-consuming for experimenters.

1.2 Mathematical Models And Parameter Estimation

In order to save time and energy required for performing experiments, and also to understand the mechanism of the reactions better, researchers have built mathematical models to describe a wide variety of polymerization systems.[13,14] A good mechanistic model can be used to explain the results of experiments that have been conducted and can be used to predict what will happen using new operating conditions. Reliable values of kinetic parameters are required to obtain good predictions. In many cases when researchers have a sound understanding of the important chemical phenomena, they can derive appropriate model equations, but they do not have accurate values of the required kinetic parameters. In this situation, parameter estimation using experimental data can help modelers to obtain accurate estimates of some or all of their model parameters.

The goal of the research in this thesis is to build fundamental models that can explain what is happening during the carbocationic copolymerization of the inimer and isobutylene in Figure 1.1. In this copolymerization system, there are six different propagation rate constants, which arise due to the three different types of active chain ends and two different types of vinyl groups in this system (which will be explained in Chapter 2). These models should: i) account for the effects of all six different types of propagation reactions; ii) predict concentration changes of inimer, isobutylene and polymer molecules over time; iii) predict values of average branching level, and number and weight average molecular weight (*i.e.* M_n and M_w); iv) predict the overall molecular weight distribution (MWD) of *arb*PIB and detailed information about MWDs of molecules with different numbers of branches; v) contain reliable parameter values that can be used in future modeling studies. In Chapters 2 to 5 of this thesis, four different mathematical models are developed to accomplish these goals.

In the Chapter 2, a relatively simple PREDICI model is introduced that tracks a large number of polymeric species with different levels of branching and different numbers of end

groups. The idea behind this model is simple, trying to include all possible reactions that could happen in the system between different types of molecules. Because of the very large number of reactions and species in the system, I applied several simplifying assumptions to make the size of the model manageable. Nevertheless, there are still over 1000 reaction steps and over 100 polymer species remaining in the model. This PREDICI model can only be applied to polymerization systems with very low branching level (below 5 branches per molecule on average). This model can predict concentration changes of inimer, isobutylene and polymers chains with different numbers of branches. Also, it can predict the values of M_n and M_w. An important feature of this model is that it can predict the MWD of the whole system, and also MWDs of polymers with different numbers of branches. Parameter estimation is performed by fitting limited available data with low branching levels. Although use of this model is only accurate for systems with low branching levels, it inspired the development of three additional models that are valid for high branching levels.

In order to build a model that can be applied for higher branching levels, I developed a Monte Carlo (MC) model using the traditional MC method developed by Gillespie[15], which is described in Chapter 3. The ideas behind this model are not complex and the implementation in Matlab is quite straightforward. Since the reaction mechanism in this MC model focuses on reactions between individual molecules, the model requires significantly long computing times (several days on my laptop computer) to achieve reliable results for typical batch runs. Thus, this MC model can achieve all the goals that were listed above, except that it is unsuitable for parameter estimation, due to the excessive computational effort.

To address the long computation-time issue of the traditional MC method, we developed an advanced MC model with the help of Dr. Piet Iedema described in Chapter 4. This model combines the idea of dynamic material balances and random processes, making it much faster (*e.g.*, by a factor of ~200) than the traditional MC model. However, the ideas required to develop

and implement this model are complicated. Like the traditional MC model, the advanced MC model can also provide information about each individual molecule in the system at the end of the batch. Even if it is more efficient, it is still too slow to be used for parameter estimation.

To address the issue of long computing time for parameter estimation, a good idea came to my mind after reading a paper by Zargar et al.[16] As a result, I developed a relatively simple model in PREDICI (shown in Chapter 5) that consists of three parallel systems: one that tracks the end groups, one that tracks the internal and dangling segments in the branched polymer molecules and on that tracks the concentration of polymer molecules and unreacted inimer and monomer. This model significantly shortens the computing time from hours to seconds, making it useful for parameter estimation. Because of the much faster calculations, much information about the details of the polymerizing system is neglected as compensation. This model can predict the value of M_n and the average branching level, but not M_w and MWD. Overall conclusions and recommended future work are summarized in Chapter 6.

1.3 Reference

1 J. E. Puskas, G. Kaszas. Carbocationic polymerization. Encyclopedia of polymer science and technology, V5. WileyInterscience; **2003**. P. 382

2 D. C. Pepper. *Makromol. Chem.* **1974,** 17, 1077

3 J.-P. Vairon, N. Spassky, in K. Matyjaszewski, ed., *Cationic Polymerization: Mechanisms, Synthesis, and Application* (Plastics Engineering 35), Marcel Dekker, Inc., New York, **1996**, p. 683

4 J. Feldthusen, B. Iván, A. H. E. Müller. *Macromolecules.* **1998**, 31, 578

5 T. C. Chung, W. Janvikul, R. Bernard, R. Hu, C. L. Li, S. L. Liu, G. J. Jiang. *Polymer.* **1995**, 36, 3565

6 C. Gao, D. Yan. *Prog. Polym. Sci.* **2004**, 29, 183

7 Y. Zhou, W. Huang, J. Liu, X. Zhu, D. Yan, *Adv. Mater.* **2010**, 22, 4567

8 M. Seiler, *Fluid Phase Equilibria*. **2006**, 241, 155

9 M. Irfan, M. Seiler, *Ind. Eng. Chem. Res.* **2010**, 49, 1169

10 S. Chen, X. Zhang, X. Cheng, R. Zhuo, Z. Gu, *Biomacromolecules*. **2008**, 9, 2578

11 J. E. Puskas, L. M. Dos Santos, G. Kaszas, K. Kulbaba, *J. Polym. Sci. Part A: Polym. Chem.* **2009**, 47, 1148

12 L. M. Dos Santos, *Synthesis of arborescent model polymer structures by living carbocationic polymerization for structure property studies*, Ph.D. thesis, University of Akron, Akron, USA, **2009**.

13 C. Kiparissides. *Chem. Eng. Sci.* **1996**, 51, 1637;

14 J. M. Asua, ed. *Polymer Reaction Engineering*. Blackwell Publishing, **2007**

15 D. T. Gillespie, *Journal of Physical Chemistry.* **1977**, 81(25), 2340

16 A. Zargar, K. Chang, L. J. Taite, F.J. Schork, *Macromol. React. Eng*. **2011**, 5, 373

Chapter 2

Mathematical Modeling of Arborescent Polyisobutylene Production in Batch Reactor

Yutian R. Zhao[1], Kimberley B. McAuley[1], Judit E. Puskas[2], Lucas M. Dos Santos[2], Alejandra Alvarez[3]

[1]Department of Chemical Engineering, Queen's University, Kingston, ON, Canada
[2]Department of Chemical & Biomolecular Engineering, University of Akron, Akron, OH USA
[3]Department of Polymer Science, University of Akron, Akron, OH USA

2.1 Abstract

A novel model describes copolymerization of isobutylene and inimer via living carbocationic polymerization. Six different propagation rate constants and two types of equilibrium reactions are considered. Simplifying assumptions are made to enable implementation in PREDICI, so that MWD could be predicted for molecules with different branching levels. Four apparent rate constants were estimated from experimental data with <5 branches per molecule. Model predictions provide a good fit to data, and simulation results show that polymers with high branching levels and ≥15 inimer units contribute significantly to the MWD, even though their concentrations are very low.

This chapter was published as:

Zhao YR, McAuley KB, Puskas JE, Dos Santos LM, Alvarez A. Mathematical modeling of arborescent polyisobutylene production in batch reactors. *Macromol. Theory Simul.* 2013; 22: 155-173.

2.2 Introduction

Hyperbranched polymers and their synthesis and applications have gained considerable attention in recent years, especially for biomedical applications such as drug and gene delivery.[1-5] Since Fréchet et al. discovered self-condensing vinyl polymerization (SCVP)[6], the process of synthesizing hyperbranched polymers has been greatly simplified. Their novel method uses inimer (IM) molecules that act as both initiator and monomer. Typical IM molecules (see first reactant in Figure 2.1) contain an initiating group (*e.g.*, a group that can produce a free radical or a cation) and a vinyl group that can polymerize.[7]

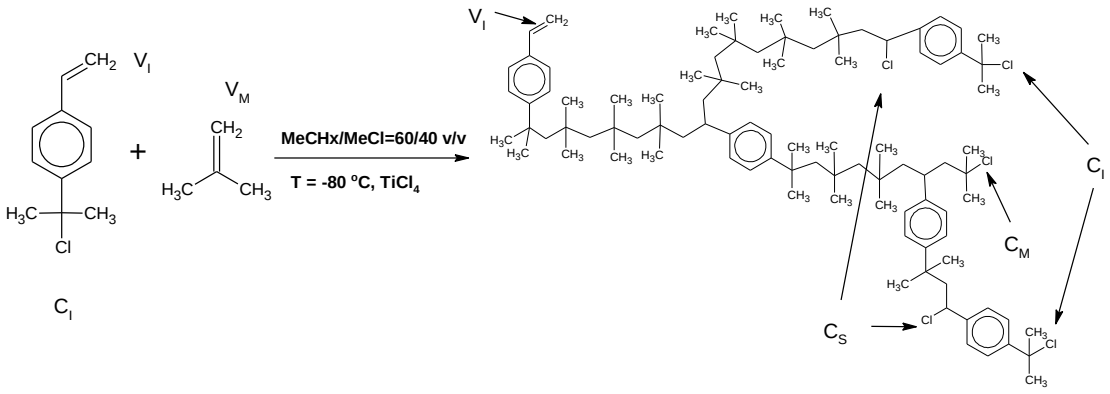

Figure 2.1 Synthetic strategy for production of *arb*PIB.[7] This scheme involves two types of vinyl groups, V_I and V_M and three types of cations arising from C_I, C_S and C_M

Homopolymerization of IM results in compact highly branched polymer molecules, whereas copolymerization of IM and vinyl monomers results in hyperbranched polymer with a tree-like 3-dimensional structure with relatively long polymer chains between branching points.[8] *Arborescent* polyisobutylene (*arb*PIB) is produced via carbocationic copolymerization of IM molecules and isobutylene monomer.[7-11] Puskas et al. used a small amount of the IM 4-(2-hydroxyisopropyl)styrene (0.03 to 0.26 mole percent) and a larger amount of isobutylene (99.97

to 99.74 mole percent) to synthesize high molecular weight *arb*PIB through a "one-pot" living-type polymerization.[9] In this living polymerization, tertiary chloride groups on dormant polymer chains are removed by a Lewis acid to produce active carbocations. The carbocations can then react with a few vinyl groups before the active chain ends are capped by chloride, returning the polymer to its dormant state. A simplified reaction scheme and an example of a simple hyper-branched product molecule are shown in Figure 2.1. This reaction scheme involves two types of vinyl groups, V_I, from the IM, and V_M, from the monomer. There are three different types of chloride groups (C_I, C_S and C_M) that can uncap to produce three different types of carbocations, where C_I is the chloride on the IM, C_S is the chloride produced after consumption of an IM vinyl group V_I, and C_M is the chloride produced after consumption of the monomer.

This one-pot synthetic strategy greatly reduces the labor required to make *arb*PIB compared with earlier multi-step processes.[12-15] Such a simple process for producing hyperbranched polymers makes it attractive for industrial production.[16]

Compared to linear PIB, branched PIB has several properties that are desirable in some biomedical and industrial applications, including lower viscosity and less shear sensitivity for high molecular weight polymers.[17] Recently, Lim et al. showed that a material with an *arb*PIB core has outstanding biocompatibility and biostability, making it a candidate for human implantation and drug delivery applications.[18] They also showed that the encrustation of *arb*PIB is comparable to or better than that of medical-grade silicone rubber in a rabbit model.[19]

The physical properties of *arb*PIB depend on the molecular weight distribution (MWD) and on *B*, the average number of branches per molecule. Two methods have been developed to measure *B*. One method determines branching by link destruction, B_{LD}, which can be calculated from:[7]

$$B_{LD} = M_n^{total}/M_n^{arms} \tag{2.1}$$

where M_n^{total} is the number average molecular weight of the *arb*PIB sample before link destruction and M_n^{arms} is the number average molecular weight of the arms, measured after link destruction. Figure 2.2 shows the method used by Puskas et al. to destroy the links.

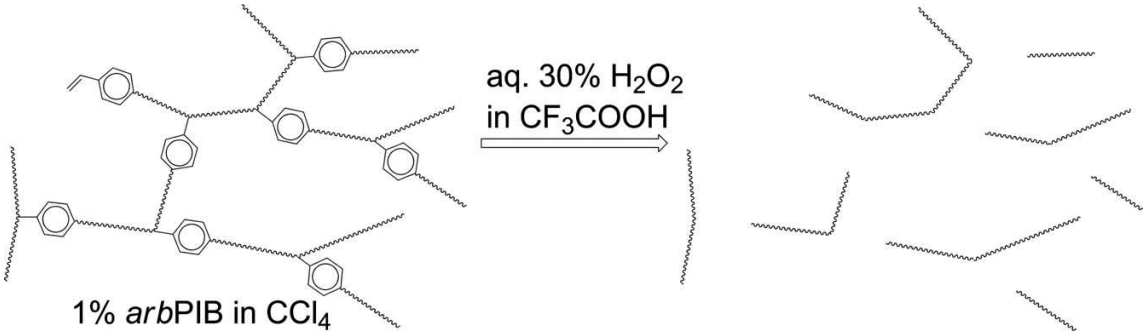

Figure 2.2 Aromatic link destruction reaction[22]

Using the second method, in which branching levels are estimated based on kinetics, B_{kin} is determined from:

$$B_{kin} = M_n/M_{n,theo} - 1 \tag{2.2}$$

$$M_{n,theo} = M_{IM} + \frac{[IB]_0 - [IB]}{[IM]_0 - [IM]} M_{IB} \approx \frac{[IB]_0 - [IB]}{[IM]_0} M_{IB}$$

where $M_{n,theo}$ is the molecular weight that would be obtained if IM were consumed as initiator only (*i.e.*, C_I groups are consumed and V_I does not react), which would lead to linear PIB without branches. After nearly all of the IM has been consumed, $M_{n,theo}$ can be approximated using the expression on the right. Values of B determined by B_{LD} and B_{kin} show good agreement.[7,20-22] In situations, like those simulated in this article, where end groups of type C_I are all consumed early in the batch reaction, B_{LD} and B_{kin} are related by $B_{LD} = B_{kin} + 1$.

2.2.1 Mathematical Modeling of Branched Polymer Production

Several types of branched polymers, especially polyolefins, have received considerable research attention due to their important industrial applications. Two different modeling approaches have been used. The first approach uses Monte Carlo simulations where individual polymer molecules are simulated using probabilities of different types of reaction events[23-30] and the second involves dynamic material balances on different types of branched species[31-36].

For example, Tobita and Iedema et al. developed effective Monte Carlo methods for modeling branching during olefin polymerization[23-25,29,30] and Matyjaszewski et al.[26,27] and Armes et al.[28] used Monte Carlo simulations to study the copolymerization of vinyl and divinyl monomers by atom transfer radical polymerization. The main benefit of Monte Carlo method is that it is possible to obtain very detailed structural information about branching and molecular weight.[24] The main disadvantage is the considerable computational effort required due to the large number of molecules that must be simulated to obtain accurate results.

Other researchers have used dynamic material balances to build models for long-chain branching of polymers. For example, Hutchinson used PREDICI, a commercial software package that applies a discrete Galerkin technique, to calculate the MWDs and long-chain-branching (LCB) due to chain-transfer to polymer for free radical ethylene polymerization in a continuous stirred tank reactor (CSTR).[32] Iedema et al. used PREDICI and method of moments to model free radical polymerization with LCBs, incorporating additional reactions to account for branching via terminal double bonds[31], along with chain transfer to chain transfer agent and termination by combination[33]. Several research groups have developed models to describe branching resulting from divinyl comonomers using controlled radical polymerization.[34-36] The main benefit of using a dynamic material balance approach is that it is relatively easy to derive balance equations for branched species of interest. The main disadvantage is the large number of species that must be tracked (and equations that must be solved) for systems with high branching levels, especially

when predictions of detailed structural information are required. Although researchers have developed mathematical models for many different polymerization systems involving branching, very little modeling work has been performed for systems involving IM.

2.2.2 Models for Branched Polymer Systems Involving IM

He et al. used Monte Carlo methods to simulate batch homopolymerization (SCVP) of IM by themselves[37] and in the presence of multifunctional initiators to produce multi-arm (star) polymers[38]. Sensitivity analysis was performed using different rate constants for reactions involving C_I and C_S active sites to predict MWD and degree of branching. Copolymerization of IM and vinyl monomers[39] was also modeled. A single rate constant value was assumed for polymerization of IM vinyl groups of type V_I and monomer vinyl groups V_M, and all end groups (of types C_M, C_I and C_S) were assumed to have the same reactivity. This model was aimed at understanding the influence of IM during living radical copolymerizations, but no attempt was made to estimate model parameters or to match results from any experiments.

Traditional material balance models have also been developed for dendritic polymer formation using IM. Müller et al. and Yan et al. produced a series of articles concerned with IM homopolymerization (SCVP) and copolymerization, which they call self-condensing vinyl copolymerization (SCVCP).[40-44] They made several simplifying assumptions about equal reactivity of end groups and vinyl groups to develop analytical expressions for average molecular weights and degree of branching. For IM homopolymerization (SCVP), they also predicted the MWD. Müller et al. performed dynamic material balances on vinyl groups and the two different types of reactive end group (C_I and C_S)[40], initially assuming different values for apparent propagation rate constants that correspond to the two types of reactive end groups. They then compared their simulation results with experimental data for carbocationic polymerization of the IM 3-(1-chloroethyl)-ethenylbenzene[6] and fitted an overall value of the apparent rate constant, assuming equal reactivi-

ty of carbocations. Using this fitted rate constant, they were able to obtain good predictions of M_w, but predicted polydispersities were much larger (*e.g.*, by orders of magnitude) compared to experimental polydispersities. Several possible reasons for the mismatch were suggested including steric hindrance, intramolecular loop formation and side reactions (chain transfer and termination) that were not considered in the model.[40]

In their copolymerization (SCVCP) models, Litvinenko and Müller used the same apparent propagation rate constant, regardless of the type of vinyl group or end-group in two articles.[42,44] In a more advanced model, they considered a different activity for end groups of type C_M than for C_I and C_S.[43] Simulation results were compared with experimental data for atom transfer radical copolymerization of styrene with the IM p-chloromethylstyrene.[43] The apparent reactivity ratio was tuned by hand to obtain improved predictions of M_n and M_w, but no systematic parameter estimation was performed. Later, Zhou et al.[45] extended the copolymerization model to study the influence of vinyl impurities without a reactive initiating group on IM homopolymerization. Their model assumes a single type of vinyl group, but accounts for two different types of end groups, which are assumed to have the same reactivity.

Cheng et al. also developed material balance equations for IM homopolymerization, which they solved using generating functions.[46,47] In their semi-batch reactor model, they assumed a single apparent propagation rate constant for all types of end groups[46], but in a subsequent batch reactor model, they accounted for different reactivities of end groups of type C_I and C_S[47]. They did not compare their simulation results with experimental data. Recently, Zargar et al.[48] used the method of moments to model the dendritic copolymerization of two vinyl monomers using a RAFT (reversible addition fragmentation chain transfer) agent as the IM. Zargar's model tracked the lengths of the linear segments that make up the branched polymer molecules, so that they could predict M_n, M_w and polydispersity for the segments, and the conversion of the two vinyl monomers. Reactive groups of type C_S were assumed to have the same reactivity as one

of the C_M groups. No attempt was made to compare simulation results with experimental data or to estimate any of the model parameters.

2.2.3 Mathematical Models for Linear Isobutylene Polymerization

De Freitas and Pinto[49] developed a dynamic model for cationic isobutylene polymerization in continuous precipitation reactors under nonliving conditions where the chain transfer and chain termination reactions are important. Puskas et al.[50,51] built several models based on the mechanism shown in Figure 2.3 for isobutylene homopolymerization under living conditions. In this mechanism, path A is dominant when the initial concentration of the Lewis acid (*i.e.*, $[TiCl_4]_0$) is lower than the initial concentration of initiator, $[I]_0$, while path B is dominant when $[TiCl_4]_0$ is higher than $[I]_0$. A detailed parameter estimability analysis was conducted and correlations among parameters were carefully analyzed.[51] Their models give a good fit of experimental data and provide good initial guesses for several parameters that appear in the current model. However, Faust et al.[52,53] published several articles that suggest that monomeric $TiCl_4$ is too weak to activate the initiation and propagation reactions. Thus, they assume that only path B exists in cationic PIB homopolymerization. In this article, we use the mechanism of Puskas et al. Experimental evidence indicates that the order of the propagation reaction is approximately first-order with respect to $[TiCl_4]_0$ when $[TiCl_4]_0$ is low (*e.g.*, $[TiCl_4]_0 = 0.25[I]_0$) and is nearly second-order when $[TiCl_4]_0$ is high (*e.g.* $[TiCl_4]_0 = 10[I]_0$).[54,55]

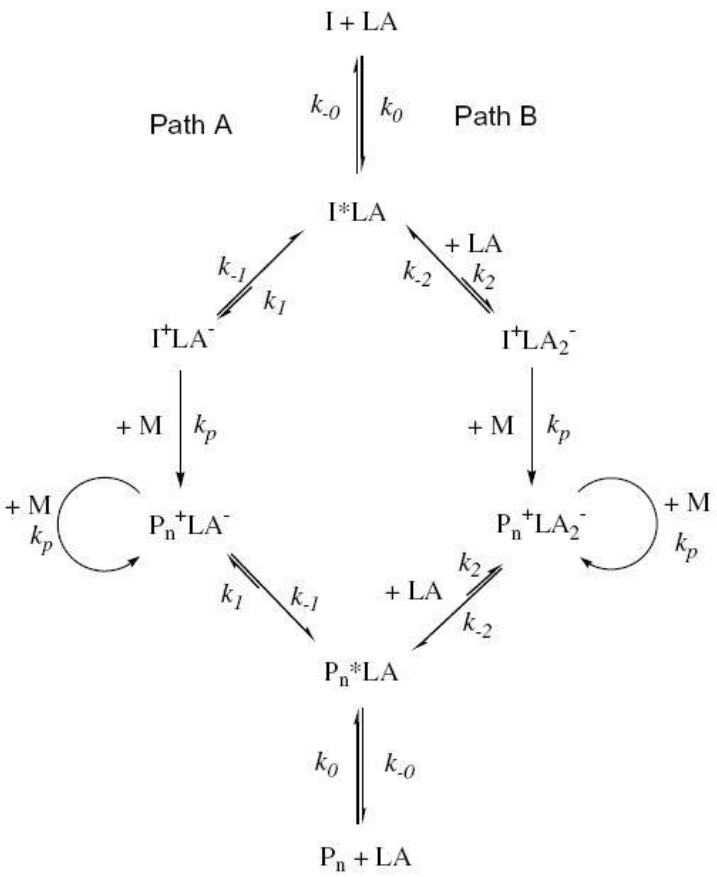

Figure 2.3 Comprehensive mechanism for living IB polymerization using $TiCl_4$ as the Lewis acid[51]

The reaction mechanism in Figure 2.3 can be rewritten as shown below to enable the development of rate expressions for the two paths:

$$A: \quad P_n + LA \underset{k_{-0}}{\overset{k_0}{\rightleftarrows}} P_n^* LA \underset{k_{-1}}{\overset{k_1}{\rightleftarrows}} P_n^+ LA^- \tag{2.3}$$

$$P_n^+ LA^- + IB \xrightarrow{kp_A} P_{n+1}^+ LA^-$$

$$B: \quad P_n + LA \underset{k_{-0}}{\overset{k_0}{\rightleftarrows}} P_n^* LA \underset{k_{-2}}{\overset{k_2 + LA}{\rightleftarrows}} P_n^+ LA_2^- \tag{2.4}$$

$$P_n^+ LA_2^- + IB \xrightarrow{kp_B} P_{n+1}^+ LA_2^-$$

where P_n is a polymer chain with n monomer units, LA is Lewis Acid, k_0, k_1 and k_2 are forward rate constants and k_{-0}, k_{-1} and, k_{-2} are rate constants for the corresponding reverse reactions. k_p is

the true propagation rate constant for the un-capped cation. The following expressions for equilibrium constants can be developed from these reactions:

$$K_0 = \frac{k_0}{k_{-0}} = \frac{[P_n^* LA]}{[P_n][LA]};\ \ K_1 = \frac{k_1}{k_{-1}} = \frac{[P_n^+ LA^-]}{[P_n^*][LA]};\ \ K_2 = \frac{k_2}{k_{-2}} = \frac{[P_n^+ LA_2^-]}{[P_n^* LA][LA]}$$

$$K_0 K_1 = \frac{[P_n^+ LA^-]}{[P_n][LA]};\ \ K_0 K_2 = \frac{[P_n^+ LA_2^-]}{[P_n][LA]^2} \tag{2.5}$$

Using these equilibrium constants, the overall polymerization rate expressions for the two paths are:

$$R_{pA} = k_p[P_n^+ LA^-][IB] = k_p K_0 K_1 [LA][P_n][IB] \tag{2.6}$$

$$R_{pB} = k_p[P_n^+ LA_2^-][IB] = k_p K_0 K_2 [LA]^2[P_n][IB] \tag{2.7}$$

Note that when both path A and path B are active, equations 2.6 and 2.7 are added together to determine the total rate of polymerization:

$$R_{pTot} = R_{pA} + R_{pB} = k_{app}[P_n][IB] \tag{2.8}$$

where k_{app}, the apparent propagation rate constant for IB homopolymerization, is related to the true propagation rate constant by:

$$k_{app} = k_p(K_0 K_1 [LA] + K_0 K_2 [LA]^2) \tag{2.9}$$

In summary, mathematical models have been developed for cationic IB homopolymerization and parameters have been estimated using experimental data. Although living copolymerizations involving IM have also been modeled, there are no existing models for arborescent copolymerization of IB and IM for which parameters have been estimated, so that model predictions can be compared effectively with the available data.

In this paper, we developed a new fundamental model for the copolymerization of IM and isobutylene in a batch reactor to produce arborescent polymers via carbocationic polymerization. Several assumptions are made so that this model can be implemented in PREDICI. Experimental data generated by Dos Santos et al.[10,21] are used for parameter estimation and model test-

ing. Using this model, detailed predictions of branching levels and MWD are obtained. Deviations between model predictions and the data are then used to suggest improved mechanisms and assumptions for developing more accurate and comprehensive models in the future.

2.3 Model Development

2.3.1 Mechanism and Notation

After examining the structure of highly branched PIB, it is apparent that there are three different kinds of chloride groups at ends and along the sides of the polymer molecules, as shown in Figure 2.1. The three types of chloride-capped ends (or side groups) are: i) chloride-capped groups from the IM, which are called C_I; ii) chloride-capped groups on a chain end formed after propagation with monomer, which are called C_M; iii) chloride-capped groups along the side of a chain, produced after propagation with an IM vinyl group, which are called C_S. Polymerization can occur when any of these different types of chloride groups is removed (by reaction with the Lewis acid) to produce a carbocation that can react with vinyl groups of type V_M or V_I. All chains in the system are usually in their dormant state (with *Cl* attached). Typically, a few monomer units can add to the chain ends during periods when the cations are uncapped.

In the notation used in this article, the branched molecule in Figure 2.1 is denoted by $P_5^{2I,2S}(10)$. The subscript 5 indicates that 5 IM molecules were consumed to make the molecule, and the 10 in brackets indicates that the molecule contains 10 monomer units. The *2I* superscript indicates that the molecule has two C_I end groups and the *2S* superscript indicates that the molecule has two C_S side groups. Since the number of IM units in the molecule is equal to the total number of chloride groups, an additional counter is not needed to track the C_M chloride ends. For $P_5^{2I,2S}(10)$, the number of C_M ends is 5 – 2 – 2 = 1. Figure 2.4 shows two unique examples of highly branched macromolecules that consist of 9 IM units and 18 monomer units with 2 C_I and 2 C_S chloride ends, but having different structures. We assume that these two molecules will have exactly the same rates of reaction with other species in the reaction mixture, even though their structures are slightly different. Note that $B_{\text{kin}} = 8$ for the branched molecules in Figure 2.4. This notation was adopted to make it clear that the number of monomer units (in brackets) is tracked

automatically by PREDICI. The index for the number of inimer units (*i.e.* the subscript) and the indices for the numbers of potential cations of different types (*i.e.*, the superscripts) are handled in PREDICI by defining different polymeric species.

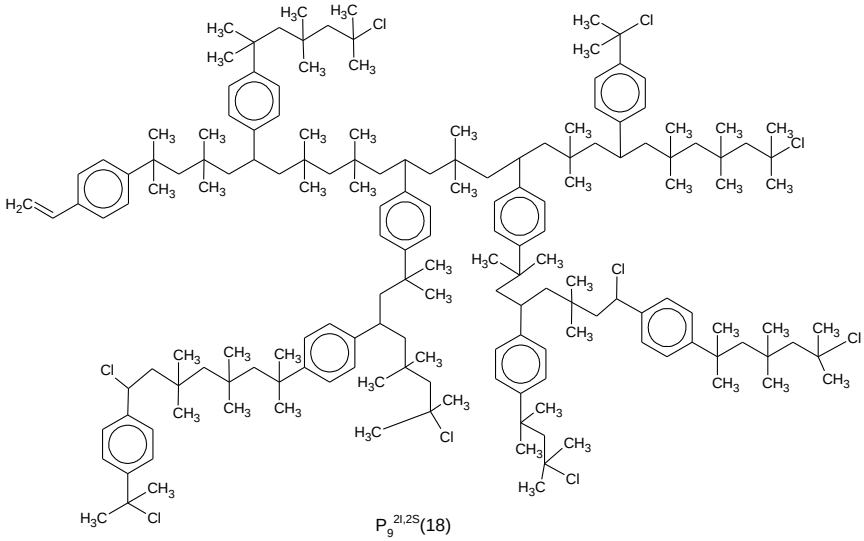

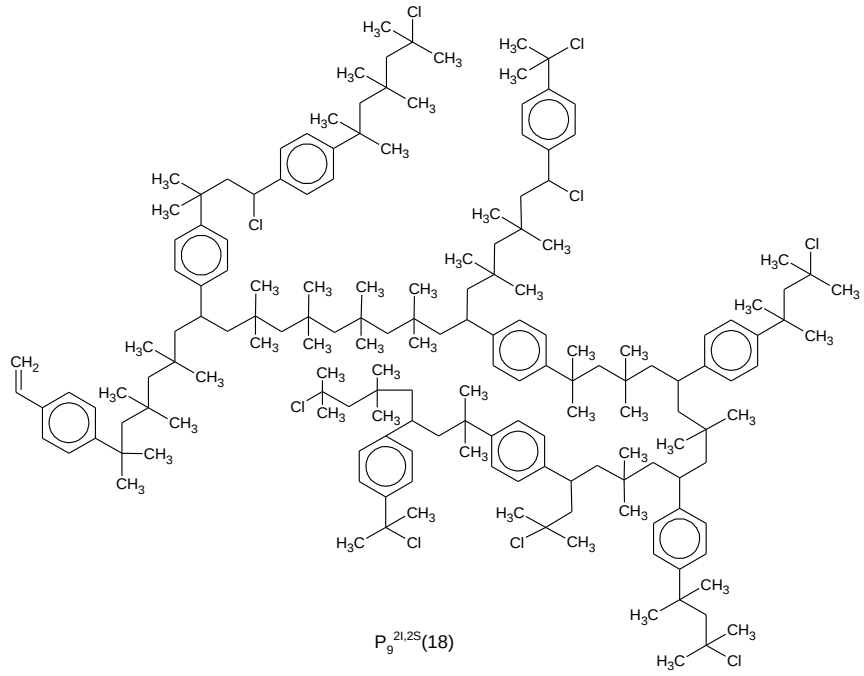

Figure 2.4 Two examples of $P_9^{2I,2S}(18)$ molecules that have 9 benzene groups from IM units, 18 isobutylene units, 2 chloride ends of type C_I from IM and 2 secondary chlorides of type C_S.

For the copolymerization of IM and isobutylene, many different reactions are possible between any two branched molecules. All of the possible reactions must be accounted for in reaction rate expressions. Reactions between the two types of vinyl groups (V_I and V_M) and different types of cations (arising from C_I, C_S and C_M) will have different true propagation rate constants. The rates of different types of reactions will also depend on the numbers of each type of potential cations on both reacting molecules, as well as the Lewis acid concentration (as shown for homopolymerization in equation 2.9). Here, molecules with specific structures are used as examples to write the corresponding propagation rate equations.

For propagation, there are six different true copolymerization rate constants of the form k_{pij}, where the subscript i indicates the type of cation, and j is the type of vinyl group (*i.e.*, k_{pIM}, k_{pMM}, k_{pSM}, k_{pII}, k_{pMI}, and k_{pSI}). Simple reactions involving these rate constants are shown in Figure 2.5. The bond that forms is shown in **bold** to make the diagrams easier to understand.

In general, all reactions between potential cations and the two types of vinyl groups can be summarized as shown in Table 2.1. General rate expressions for reactions between any two molecules are provided in Table 2.2. As shown in Tables 2.1 and 2.2, all reactions with vinyl groups of type V_M result in formation of a cation of type C_M, and reactions with V_I result in formation of a cation of type C_S. Groups of type C_I are present initially in the reactor (*i.e.*, on the IM) and are depleted over time. Note that when two polymer molecules react, any potential cation on the first molecule can react with the vinyl group of type V_I on the second molecule, or any cation on the second molecule can react with the vinyl group on the first molecule. The rate expressions in Table 2.2 account for both of these possibilities. For example, for the polymer + polymer reactions involving C_M type cations, the number of ways that two molecules can react is $i_1 - x_1 - y_1 + i_2 - x_2 - y_2$ because the first molecule contains $i_1 - x_1 - y_1$ potential cations of type C_M and the second molecule contains $i_2 - x_2 - y_2$.

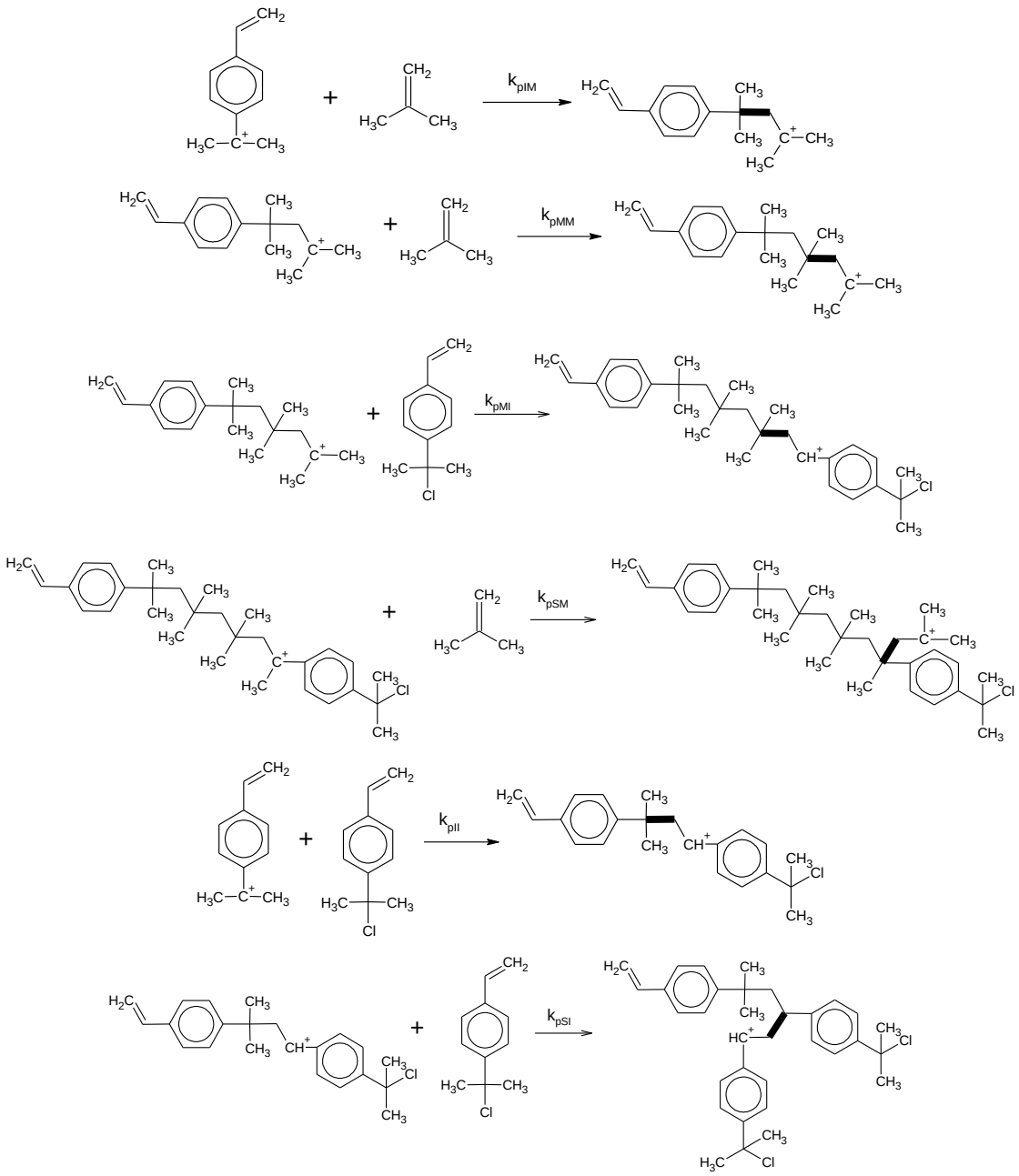

Figure 2.5 Six reactions corresponding to the different true propagation rate coefficients. The new bond that forms is shown in bold.

Table 2.1 Summary of typical reactions based on end groups

C_I react with V_I (IM)	$C_I + V_I \xrightarrow{k_{pIIapp}} C_S$
C_I react with V_M (IB)	$C_I + V_M \xrightarrow{k_{pIMapp}} C_M$
C_M react with V_I (IM)	$C_M + V_I \xrightarrow{k_{pMIapp}} C_S$
C_M react with V_M (IB)	$C_M + V_M \xrightarrow{k_{pMMapp}} C_M$
C_S react with V_I (IM)	$C_S + V_I \xrightarrow{k_{pSIapp}} C_S$
C_S react with V_M (IB)	$C_S + V_M \xrightarrow{k_{pSMapp}} C_M$

Table 2.2 Summary of reactions and rate expressions in terms of the apparent and true propagation rate constants assuming that all propagation reactions occur via both path A and path B. C_M, C_I and C_S in the second column indicate the type of cation that is participating in the reaction.

Polymer + IB	C_M	$P_i^{xI,yS}(m) + IB \xrightarrow{(i-x-y)k_{pMMapp}} P_i^{xI,yS}(m+1)$ $R_{pTot} = (i-x-y)k_{pMMapp}\left[P_i^{xI,yS}(m)\right][IB]$ $= (i-x-y)k_{pMM}(K_0K_1[LA] + K_0K_2[LA]^2)\left[P_i^{xI,yS}(m)\right][IB]$
	C_I	$P_i^{xI,yS}(m) + IB \xrightarrow{xk_{pIMapp}} P_i^{(x-1)I,yS}(m+1)$ $R_{pTot} = xk_{pIMapp}\left[P_i^{xI,yS}(m)\right][IB]$ $= xk_{pIM}(K_0K_1[LA] + K_0K_2[LA]^2)\left[P_i^{xI,yS}(m)\right][IB]$
	C_S	$P_i^{xI,yS}(m) + IB \xrightarrow{yk_{pSMapp}} P_i^{xI,(y-1)S}(m+1)$ $R_{pTot} = yk_{pSMapp}\left[P_i^{xI,yS}(m)\right][IB]$ $= yk_{pSM}(K_0K_1[LA] + K_0K_2[LA]^2)\left[P_i^{xI,yS}(m)\right][IB]$
Polymer + IM	C_M	$P_i^{xI,yS}(m) + IM \xrightarrow{(i-x-y)k_{pMIapp}} P_i^{(x+1)I,(y+1)S}(m)$ $R_{pTot} = (i-x-y)k_{pMIapp}\left[P_i^{xI,yS}(m)\right][IM]$ $= (i-x-y)k_{pMI}(K_0K_1[LA] + K_0K_2[LA]^2)\left[P_i^{xI,yS}(m)\right][IM]$
	C_I	$P_i^{xI,yS}(m) + IM \xrightarrow{xk_{pIIapp}} P_i^{xI,(y+1)S}(m)$ $R_{pTot} = xk_{pIIapp}\left[P_i^{xI,yS}(m)\right][IM]$ $= xk_{pII}(K_0K_1[LA] + K_0K_2[LA]^2)\left[P_i^{xI,yS}(m)\right][IM]$
	C_S	$P_i^{xI,yS}(m) + IM \xrightarrow{yk_{pSIapp}} P_i^{(x+1)I,yS}(m)$ $R_{pTot} = yk_{pSIapp}\left[P_i^{xI,yS}(m)\right][IM]$ $= yk_{pSI}(K_0K_1[LA] + K_0K_2[LA]^2)\left[P_i^{xI,yS}(m)\right][IM]$
IM + Polymer	C_I	$IM + P_i^{xI,yS}(m) \xrightarrow{k_{pIIapp}} P_i^{xI,(y+1)S}(m)$ $R_{pTot} = k_{pIIapp}\left[P_i^{xI,yS}(m)\right][IM]$ $= k_{pII}(K_0K_1[LA] + K_0K_2[LA]^2)[IM]\left[P_i^{xI,yS}(m)\right]$
Polymer + Polymer	C_M	$P_{i_1}^{x_1I,y_1S}(m_1) + P_{i_2}^{x_2I,y_2S}(m_2) \xrightarrow{(i_1-x_1-y_1+i_2-x_2-y_2)k_{pMIapp}} P_{i_1+i_2}^{(x_1+x_2)I,(y_1+y_2+1)S}(m_1+m_2)$ $R_{pTot} = (i_1-x_1-y_1+i_2-x_2-y_2)k_{pMIapp}\left[P_{i_1}^{x_1I,y_1S}(m_1)\right]\left[P_{i_2}^{x_2I,y_2S}(m_2)\right]$ $= (i_1-x_1-y_1+i_2-x_2-y_2)k_{pMI}(K_0K_1[LA] + K_0K_2[LA]^2)\left[P_{i_1}^{x_1I,y_1S}(m_1)\right]\left[P_{i_2}^{x_2I,y_2S}(m_2)\right]$
	C_I	$P_{i_1}^{x_1I,y_1S}(m_1) + P_{i_2}^{x_2I,y_2S}(m_2) \xrightarrow{(x_1+x_2)k_{pIIapp}} P_{i_1+i_2}^{(x_1+x_2-1)I,(y_1+y_2+1)S}(m_1+m_2)$ $R_{pTot} = (x_1+x_2)k_{pIIapp}\left[P_{i_1}^{x_1I,y_1S}(m_1)\right]\left[P_{i_2}^{x_2I,y_2S}(m_2)\right]$ $= (x_1+x_2)k_{pII}(K_0K_1[LA] + K_0K_2[LA]^2)\left[P_{i_1}^{x_1I,y_1S}(m_1)\right]\left[P_{i_2}^{x_2I,y_2S}(m_2)\right]$
	C_S	$P_{i_1}^{x_1I,y_1S}(m_1) + P_{i_2}^{x_2I,y_2S}(m_2) \xrightarrow{(y_1+y_2)k_{pSIapp}} P_{i_1+i_2}^{(x_1+x_2)I,(y_1+y_2)S}(m_1+m_2)$ $R_{pTot} = (y_1+y_2)k_{pSIapp}\left[P_{i_1}^{x_1I,y_1S}(m_1)\right]\left[P_{i_2}^{x_2I,y_2S}(m_2)\right]$ $= (y_1+y_2)k_{pSI}(K_0K_1[LA] + K_0K_2[LA]^2)\left[P_{i_1}^{x_1I,y_1S}(m_1)\right]\left[P_{i_2}^{x_2I,y_2S}(m_2)\right]$

2.3.2 Model Implementation in PREDICI

A model was developed and implemented in PREDICI that can track concentrations of IM, IB and polymer molecules that contain up to 15 IM units (*i.e.*, $i = 15$). When writing the pertinent reaction rate equations in PREDICI, the assumptions shown in Table 2.3 were made to keep the number of species and reactions to a manageable level. After making all of the assumptions in Table 2.3, the number of species implemented in PREDICI model is 122 and the number of reactions is 1430. Note that if assumptions 1-4 are not made, the number of species is 787 and the number of reactions is > 20000. Implementing a model that can account for molecules with up to 20 branches, using the assumptions in Table 2.3 would require 212 species and 4086 reactions.

Number and weight average molecular weights were calculated using the method of moments, by adding contributions from polymer molecules with different numbers of IM units and different numbers of C_S side groups:

$$M_n = \frac{\sum_{i=1}^{15}\sum_{y=0}^{i-1}\mu_{i,1}^{yS}}{\sum_{i=1}^{15}\sum_{y=0}^{i-1}\mu_{i,0}^{yS}} M_{IB} \tag{2.10}$$

$$M_w = \frac{\sum_{i=1}^{15}\sum_{y=0}^{i-1}\mu_{i,2}^{yS}}{\sum_{i=1}^{15}\sum_{y=0}^{i-1}\mu_{i,1}^{yS}} M_{IB} \tag{2.11}$$

where $\mu_{i,0}^{yS}$, $\mu_{i,1}^{yS}$ and $\mu_{i,2}^{yS}$ are zeroth, first and second moments of the chain length distribution for polymer species containing i IM units and y side groups of type C_S, respectively, and M_{IB} is the molar mass of isobutylene monomer. The complete MWD was also calculated using PREDICI.

Table 2.3 Assumptions for model development

1	Reactions between C_I end groups and IM can be neglected because $[IM]_0$ is low relative to $[IB]_0$, so that reactions involving k_{pII} can be neglected.
2	C_S end groups can only react with monomer vinyl groups. Reactions between C_S end groups and IM molecules can be neglected because IM molecules will typically initiate polymerization before their vinyl groups can be consumed by reaction. Reactions between C_S end groups and V_I groups on polymer molecules can be neglected due to steric hindrance. Because $[IM]_0$ is very low compared to $[IB]_0$, C_S groups will react with IB before they encounter the V_I groups on large molecules. Thus, reactions involving k_{pSI} can be neglected.
3	The C_I groups on the IM are all consumed very early in the reaction because the chloride end is designed to behave as an initiator for living carbocationic polymerization.[42] As a result, the only reaction that IM can undergo appreciably is reaction with IB to produce $P_1(1)$. Therefore, vinyl groups of type V_I can undergo propagation reactions only after they belong to oligomer or polymer molecules. Another consequence of this assumption is that there are no C_I groups on any polymer molecules so that reactions between polymer molecules and IM can be ignored. Note that this assumption means that there is no need to track the number of C_I groups in the model, (except for those on IM, which are consumed quickly).
4	Reactions that lead to 16 or more IM units in a molecule are neglected to keep the number of species and reactions manageable for implementation in PREDICI.
5	Puskas et al.[59] observed a penultimate effect during styrene/isobutylene copolymerization, indicating that the rate of IB addition to C_M may depend on whether the penultimate unit is IB or a styrene-like IM unit. Since $[IM]_0$ is so low compared to $[IB]_0$ in the recipes that will be simulated, this penultimate effect can be neglected with only a small effect on model predictions.
6	$[LA] \approx [LA]_0$ throughout the course of the batch reactions, because only a small fraction of the $TiCl_4$ is consumed to produce ions.[52]

2.3.2.1 Experimental Data and Parameter Estimation

The data in Table 2.4 were used for parameter estimation. These data are from a series of experiments conducted by Dos Santos[10,21] and were chosen because measured values of B_{kin} are relatively low (below 4.50). Other data with higher levels of branching (*e.g.*, with $B_{kin} = 10$) were not selected for parameter estimation because high branching levels are not consistent with the assumption that branched polymer molecules contain 15 or fewer IM units[7,11]. Note that the first three experiments in Table 2.4 are replicates that were conducted using the same reactor conditions. As shown in Table 2.4, $[TiCl_4]_0 >> [IM]_0$, which indicates that path B should be dominant. However, for all simulations the rate expressions from Table 2.2 that consider both paths A and B were used.

2.3.2.2 Initial Guesses and Uncertainties for Rate Constants

Based on the assumptions in Table 2.3, several true rate constants disappear from the model equations, so that the only rate and equilibrium constants that influence the rate of polymerization are k_{pIM}, k_{pMM}, k_{pMI}, k_{pSM}, $K_0K_1^I$, $K_0K_2^I$, $K_0K_1^M$, $K_0K_2^M$, $K_0K_1^S$ and $K_0K_2^S$. Table 2.5 shows initial values of the different parameters that were chosen for initial simulations. These values were selected based on the literature values in Table 2.6. Table 2.5 also shows reasonable upper and lower values for each parameter, between which the parameters could be adjusted without becoming physically unrealistic. Because there is no information in the literature about values of K_0K_1 and K_0K_2 for end groups of types C_S and C_I, the initial values and uncertainty ranges for these parameters are set at the same values as for C_M end groups.

Table 2.4 Experiments from Dos Santos[21] $[IB]_0$ = 1.74 M, $[TiCl_4]_0$ = 0.0313 M, T = -95 ℃ in Hx/MeCl (60/40). The inimer that initiated the polymerization was formed in situ from a precursor (MeOIM), as shown in Figure 3.1.

Sample	Time (min)	[IB] (mol/L)	Conversion (%)	M_n (kg/mol)	M_w (kg/mol)	PDI	B_{kin}
	10	1.434	17.6	57.7	75.0	1.3	2.8
06DNX001	20	0.877	49.6	93.0	139.5	1.5	1.2
$[IM]_0$ = 0.00114 M	40	0.388	77.7	185.8	315.9	1.7	1.8
	80	0.094	94.6	266.8	533.6	2.0	2.3
	10	1.169	32.8	61.2	85.7	1.4	1.2
06DNX010	20	0.783	55	97.7	156.3	1.6	1.1
$[IM]_0$ = 0.00114 M	40	0.226	87	208.1	353.8	1.7	1.8
	80	0.054	96.9	269.6	539.2	2.0	2.2
	15	1.056	39.3	73.9	103.5	1.4	1.2
06DNX030	30	0.566	67.5	133.4	213.4	1.6	1.3
$[IM]_0$ = 0.00114 M	80	0.078	95.5	224.1	493.0	2.2	1.7
	5	1.262	27.5	33.8	47.3	1.4	-
	10	0.987	43.3	48.8	68.3	1.4	-
	15	0.750	56.9	60.6	118.8	2.0	-
	21	0.524	69.9	84.4	135.9	1.6	-
06DNX090	30	0.233	86.6	109.7	193.1	1.8	-
$[IM]_0$ = 0.00227 M	40	0.0748	95.7	139.3	287.0	2.1	-
	60	0.019	98.9	172.4	379.3	2.2	-
	90	0.030	98.3	183.0	503.2	2.8	3.22
	120	0	100	191.4	620.1	3.2	-
	5	1.206	30.7	23.1	33.7	1.5	-
	10	0.907	47.9	34.0	51.3	1.5	-
	15	0.689	60.4	40.5	68.8	1.7	-
06DNX100	20	0.468	73.1	59.6	94.8	1.6	-
$[IM]_0$ = 0.00454 M	40	0.097	94.4	84.9	180.8	2.1	-
	60	0.071	95.9	92.9	242.5	2.6	-
	90	0.080	95.4	112.1	369.9	3.3	4.46

Table 2.5 Initial values, upper and lower values, and uncertainties of each parameter

Parameter	Initial	Lower	Upper	Unit
k_{pMM}	6.0×10^{8}	1×10^{8}	1×10^{9}	$L\cdot mol^{-1}\cdot s^{-1}$
k_{pMI}	1.2×10^{8}	1×10^{6}	1×10^{9}	$L\cdot mol^{-1}\cdot s^{-1}$
k_{pSM}	1×10^{9}	1×10^{7}	2×10^{9}	$L\cdot mol^{-1}\cdot s^{-1}$
k_{pIM}	6.0×10^{8}	1×10^{7}	1×10^{9}	$L\cdot mol^{-1}\cdot s^{-1}$
K_0K_1	5.6×10^{-9}	1×10^{-10}	1×10^{-7}	$L\cdot mol^{-1}$
K_0K_2	8.7×10^{-8}	1×10^{-9}	1×10^{-6}	$L^2\cdot mol^{-2}$

Table 2.6 Literature values for kinetic parameters from IB and styrene homopolymerization and copolymerization

	Value	Unit	Initiate system	Solvents	T/℃	Reference
k_{pIM} & k_{pMM} (k_{pIB})	$(6\pm2)\times10^{8}$	$L\cdot mol^{-1}\cdot sec^{-1}$	$RCl/TiCl_4$	CH_2Cl_2	-78	57
	(4.2-4.7) $\times10^{8}$	$L\cdot mol^{-1}\cdot sec^{-1}$	$TMPCl/TiCl_4$	Hx/MeCl 60/40	-80	58
	(3.6-5.7) $\times10^{8}$	$L\cdot mol^{-1}\cdot sec^{-1}$	$TMPCl/TiCl_4$	Hx/MeCl 60/40	-80	53
	(3-6) $\times10^{8}$	$L\cdot mol^{-1}\cdot sec^{-1}$	$TMPCl/TiCl_4$	Hx/MeCl 60/40	-80	52
	(0.3-1.0) $\times10^{9}$	$L\cdot mol^{-1}\cdot sec^{-1}$	H-[IB]n-Cl/TiCl4	Hx/MeCl 60/40	-80	
k_{pSt}	(1.3-7.7) $\times10^{9}$	$L\cdot mol^{-1}\cdot sec^{-1}$	--	$MeCH_X$/MeCl	-80 ~ -50	56
	8.4×10^{9}	$L\cdot mol^{-1}\cdot sec^{-1}$	--	CH_2Cl_2		
r_1	7.24	--	$TMPCl/TiCl_4$	$MeCH_X$/MeCl 40/60	-90	59
	0.3-9.79	--	--	--	--	
r_2	1.96	--	$TMPCl/TiCl_4$	$MeCH_X$/MeCl 40/60	-90	59
	0.17-6	--	--	--	--	
	1.40	--	Cumyl chloride/BCl_3	Methylene chloride	-78	60
K_0K_1	5.6×10^{-9}	$L^2\cdot mol^{-2}$	$TMPCl/TiCl_4$	Hx/MeCl 60/40	-80	50,51
K_0K_2	8.7×10^{-8}	$L^2\cdot mol^{-2}$	$TMPCl/TiCl_4$	Hx/MeCl 60/40	-80	51
	3.5×10^{-7}	$L^2\cdot mol^{-2}$	$TMPCl/TiCl_4$	Hx/MeCl 60/40	-80	50
	7.2×10^{-7}	$L^2\cdot mol^{-2}$	$TMPCl/TiCl_4$	Hx/MeCl 60/40	-80	53
	4.82 $\times10^{-7}$	$L^2\cdot mol^{-2}$	H-[IB]n-Cl/TiCl4	Hx/MeCl 60/40	-80	52

The data in Table 2.4 were collected using a hexane/MeCl solvent mixture with a ratio of 60/40 v/v, using IM and $TiCl_4$ as the initiating system at -95 ℃[10,21], which is different from some of the solvents and temperatures shown in Table 2.6. Solvent polarity can greatly influence rate and equilibrium constants for carbocationic polymerization[11], so that parameter values in Table 2.6 may be significantly different from values that would be appropriate for the experiments in Table 2.4. According to studies by Sipos et al.[53] and De et al.[56], temperature has only a small influence on propagation rate constants for carbocationic polymerization of isobutylene and styrene. For the different initiating systems shown in Table 2.6, researchers report similar values for k_{pMM}, which is the true homopolymerization rate constant for IB. Mayr et al.[57] used the diffusion clock method for determining true propagation rate constants in isobutylene homopolymerization. This method is based on competition at the propagating chain end between the monomer and a trapping agent whose reaction mechanism is known to be diffusion controlled. Faust's group[52,53,58] did a series of experiments and gradually narrowed the range of plausible k_p values for IB homopolymerization to 4.2-4.7 $\times 10^8$ $L \cdot mol^{-1} \cdot s^{-1}$, using conditions similar to those in Table 2.4. Thus, the value of k_{pMM} in Table 2.5 is well-known and a small uncertainty range is assigned.

The value of k_{pIM} is unknown, but can be assumed to be close to k_{pMM} due to the structure of the IM cation. However, due to the influence of the benzene ring, the exact value of k_{pIM} may different from k_{pMM}, which is accounted for by the larger uncertainty range specified for k_{pIM} in Table 2.5. No literature values could be found for k_{pMI} and k_{pSM}, due to the limited amount of research on copolymerization of IB and IM. However, the structure of the IM molecule near its vinyl group V_I is similar to the structure of styrene. As a result, literature values of k_{p12} and k_{p21} for IB (1) and styrene (2) copolymerization are shown in Table 2.6 as initial guesses for k_{pMI} and k_{pSM}, respectively, so that $k_{pMI} \approx k_{p12} = k_{pMM}/r_1$, $k_{pSM} \approx k_{p21} = k_{pSt}/r_2$. When calculating these rate constant values, k_{pSt} was set at 4×10^9 $L \cdot mol^{-1} \cdot s^{-1}$ because Faust et al.[56] has reported values ranging from 1.3×10^9 to 8.4×10^9 $L \cdot mol^{-1} \cdot s^{-1}$ using different temperatures and initiating systems. The re-

activity ratio values used to compute k_{pMI} and k_{pSM} were $r_1 = 5$ and $r_2 = 4$, which were selected from the range of plausible values reported by Puskas et al.[59] who reviewed reactivity ratios for IB/styrene copolymerization from different research groups. Since the true values for k_{p12} and k_{p21} may be significantly different than values for k_{pMI} and k_{pSM} due to steric hindrance, large uncertainty ranges for k_{pMI} and k_{pSM} are assigned in Table 2.5.

Puskas et al.[50,51] estimated the value of K_0K_1, obtaining wide confidence intervals, which are reflected in the uncertainty range shown in Table 2.5. K_0K_2 has been estimated by several researchers[50-53,58] and the large uncertainty range specified in Table 2.5 reflects the range of values that were obtained.

It is not possible to estimate all of the parameters in Table 2.5 uniquely from the available [IB], M_n, M_w and B_{kin} data in Table 2.4, because the true rate constants and equilibrium constants are multiplied together in the rate expressions in Table 2.2, leading to highly correlated effects of the parameters,[51] especially when experiments use the same value for $[TiCl_4]$. As a result, the parameters are lumped together into four apparent parameters for estimation, as shown in Table 2.7. The initial values, lower and upper bounds for the apparent parameters were calculated based on values in Table 2.5.

Table 2.7 The actual apparent rate constants for parameter estimation

Parameter	Initial	Lower	Upper	Unit
$k_{pMMapp} = k_{pMM}\times(K_0K_1[TiCl_4]_0+K_0K_2[TiCl_4]_0^2)$	0.158	4.11×10^{-4}	4.11	$L\cdot mol^{-1}\cdot s^{-1}$
$k_{pMIapp} = k_{pMI}\times(K_0K_1[TiCl_4]_0+K_0K_2[TiCl_4]_0^2)$	0.0316	4.11×10^{-6}	4.11	$L\cdot mol^{-1}\cdot s^{-1}$
$k_{pSMapp} = k_{pSM}\times(K_0K_1[TiCl_4]_0+K_0K_2[TiCl_4]_0^2)$	0.264	4.11×10^{-5}	4.11	$L\cdot mol^{-1}\cdot s^{-1}$
$k_{pIMapp} = k_{pIM}\times(K_0K_1[TiCl_4]_0+K_0K_2[TiCl_4]_0^2)$	0.158	4.11×10^{-5}	4.11	$L\cdot mol^{-1}\cdot s^{-1}$

where k'_{pMM}, k'_{pMI}, k'_{pIM} and k'_{pSM} are the corresponding apparent rate constants for k_{pMM}, k_{pMI}, k_{pIM} and k_{pSM}. $[TiCl_4]_0 = 0.0313$ M. The values obtained here are based on those in Table 2.5.

2.4 Simulation Results

It is sometimes difficult to determine whether all parameters that appear in a fundamental model should be estimated from the available data, or whether some parameters should be held at their literature values.[61] Estimating too many parameters using limited data leads to large uncertainty ranges for parameter estimates and can produce model predictions that are worse than if fewer parameters had been estimated. Estimating too few parameters gives poor predictions because of bias due to incorrect values for parameters that are not estimated.[62] In this article, statistical techniques developed by Yao et al.[63] and Wu et al.[64,65] are used to determine whether all four parameters in Table 2.7 can be estimated using the data in Table 2.4. Yao's sensitivity-based algorithm ranks parameters from the most estimable to the least estimable according to their effect on model predictions. After applying this algorithm, parameters with large initial uncertainty that have the most influence appear at the top of the list, while parameters having little effect on the model predictions appear near the bottom of the list.[66,67] An advantage of this method is that it also considers the correlated effects of different parameters. After determining the ranked list of parameters, Wu's mean-squared error criterion is used to determine the appropriate number of parameters to estimate from the ranked list, so that the most reliable predictions can be obtained.[64,65,68,69]

Estimability ranking results are shown in Table 2.8, with k_{pMIapp} listed as the most important parameter for estimation and k_{pSMapp} listed as the least influential parameter. k_{pSMapp} appears at the bottom of the list because it has a relatively small influence on the model predictions, compared with the other three parameters. Use of Wu's MSE criterion showed that all four of the apparent rate constants could be estimated together, using the data in Table 2.4. The resulting parameter estimates are shown in Table 2.8, along with their approximate 95% confidence intervals. Some parameters (*e.g.*, k_{pSMapp}) have relatively large confidence intervals, because of the limited number of runs and the limited amount of branching data used for parameter estimation. Parame-

ter estimation was repeated assuming that polymer molecules could only have up to 13 IM units rather than 15, giving similar parameter values to those shown in Table 2.8. Predictions using the model with 15 IM units were slightly better than those obtained using only 13 IM units.

Table 2.8 Parameter estimation results

Parameter	Initial	Final value	95% Confidence Interval	Unit
1 k_{pMIapp}	0.0316	0.195	$\pm$0.079	$L{\cdot}mol^{-1}{\cdot}s^{-1}$
2 k_{pMMapp}	0.158	2.126	$\pm$0.421	$L{\cdot}mol^{-1}{\cdot}s^{-1}$
3 k_{pIMapp}	0.158	3.99×10^{-4}	$\pm9.54\times10^{-5}$	$L{\cdot}mol^{-1}{\cdot}s^{-1}$
4 k_{pSMapp}	0.264	1.39×10^{-2}	$\pm7.06\times10^{-2}$	$L{\cdot}mol^{-1}{\cdot}s^{-1}$

A comparison between model predictions (using up to 15 IM units per molecule) and the experimental data in Table 2.4 are shown in Figures 2.6 and 2.7. Data from the replicate runs are plotted together in Figure 2.6 and experimental data with $[IM]_0$ = 0.00227 M and $[IM]_0$ = 0.00454 M are plotted together in Figure 2.7. In both Figure 2.6 and 2.7, the predicted IB consumption rate agrees well with the data, but the predicted consumption rate is slightly faster. In Figure 2.7a, the model predicts faster consumption of IB for the experiment with higher $[IM]_0$, which matches the trend of data. Simulation results for M_w in Figure 2.6b follow the correct upward trend, but are lower than the experimental data. Simulation results for M_n agree well with the experimental data. In Figure 2.7b the M_w predictions for run 06DNX100 agree well with the data, but the model predicts M_w values for run 06DNX090 that are lower than the data at long reaction times. The model predicts M_n values for 06DNX100 that are higher than the data at long times, but give relatively good M_n predictions for run 06DNX090. Note that the final polydispersity values predicted by the PREDICI model for the replicate runs are 1.8, which agrees well with the measured polydispersities of 2.0 to 2.2. However, predicted polydispersities of 2.1 for the more highly branched

polymers produced in runs 06DNX090 and 06DNX100 are lower than the measured values of 3.2 and 3.3, respectively.

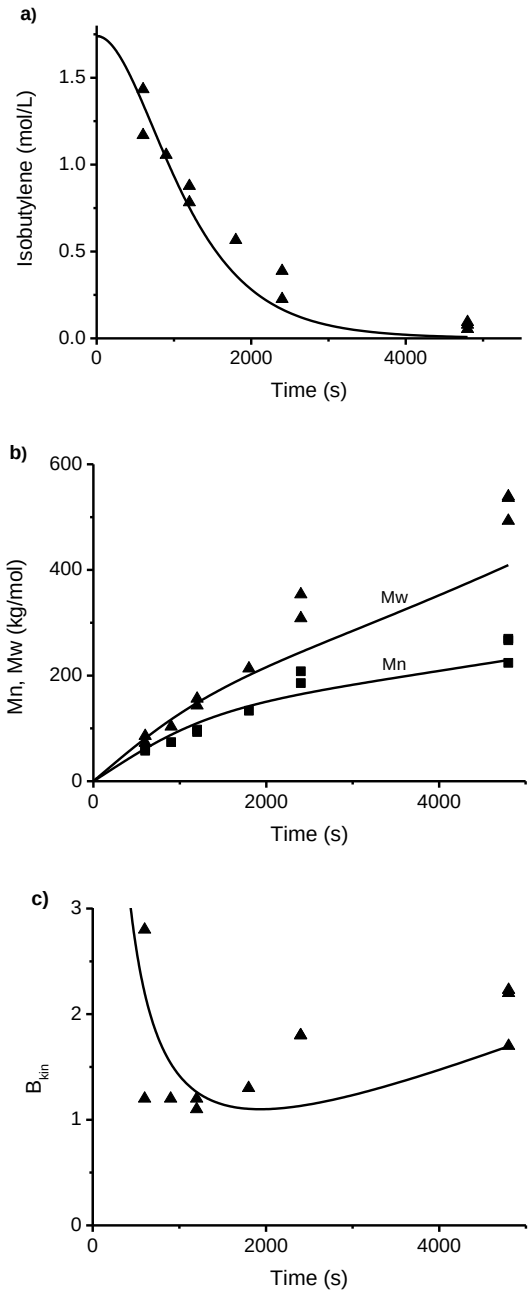

Figure 2.6 Comparison of experimental data from replicate experiments in Table 2.4 and model predictions using parameter values in Table 2.8. a) [IB] ▲data, ─ prediction; b) ■ M_n and▲ M_w data, ─ prediction c) B_{kin} ▲data, ─ prediction

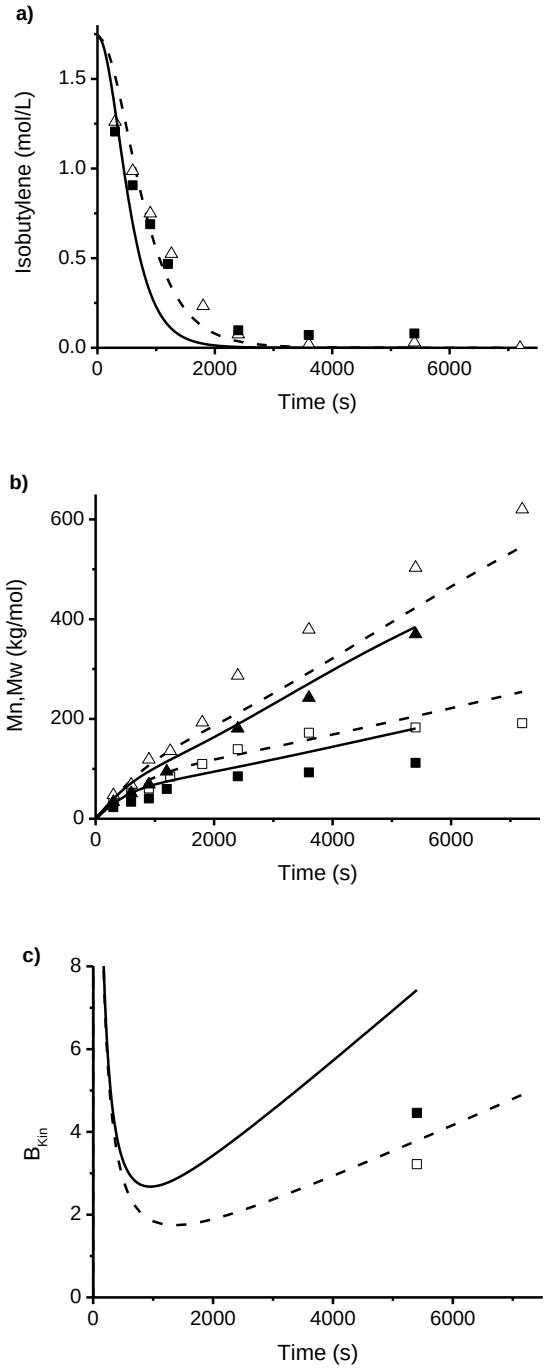

Figure 2.7 Comparison of experimental data from 06DNX090 and 06DNX100 in Table 2.4 and model predictions using parameter values in Table 2.8. a) [IB] 06DNX090 Δ data, - - - prediction; 06DNX100 ■ data, ─ prediction; b) 06DNX090 □ M_n, Δ M_w data, - - - prediction; 06DNX100 ■ M_n, ▲ M_w data, ─ prediction. c) B_{kin} 06DNX090 □ data, - - - prediction; 06DNX100 ■ data, ─ prediction

The simulated value of B_{kin} as obtained from equation 2.2 agrees well with the experimental data in Figure 2.6c, but is slightly higher than the experimental data in Figure 2.7c. In the experiments reported in Table 2.4, [IB] was measured over time, but [IM] was not, because [IM] is relatively low and the IM is consumed quickly. When calculating B_{kin} from the molecular weight data, Dos Santos and Puskas assumed instantaneous IM consumption and used the second expression in equation 2.2. For consistency, the same method for computing B_{kin} was used for the curves shown in Figures 2.6c and 2.7c, which may help to explain why some of calculated B_{kin} data values in Table 2.4 are higher at 10 min. than the corresponding values at 20 min. When the model prediction for [IM] is used in the first expression in Equation 2.2, the B_{kin} curve starts from zero at low times because all initial chains are linear, rather than at the unrealistically high initial values shown in Figures 2.6 and 2.7.

Note that the estimated value of k_{pIMapp} in Table 2.8 is considerably smaller than the initial value. As a result, the model predicts slow IM consumption (see Figure 2.8a), which is very different from the fast consumption behaviour predicted using the initial guess for k_{pIMapp}, shown in Figure 2.8b. Usually, the apparent initiation rate constant for carbocationic initiators is similar to the apparent propagation rate constant,[51] so that all of the initiator or inimer is consumed quickly. The most problematic feature of the simulated response in Figure 2.8a, however, is that almost half of the IM is still present in the system at the end of the reaction. The IM remains unreacted because of the low value of k_{pIMapp} and assumptions 1 and 3 in Table 2.3. In the simulations, reactions between the C_I groups on the IM and V_I groups on IM and polymer molecules are neglected, so that C_I is only permitted to react with V_M groups on the monomer. After the monomer has been consumed, no further reactions to consume the IM occur in the simulations. Although assumptions 1 and 3 make sense when k_{pIMapp} is similar to k_{pMMapp}, these assumptions may not be valid when the parameter estimates in Table 2.8 are used. However, according to the study of Puskas et al.,[8] under similar experimental conditions, the initiation efficiency of IM was below 0.5 (*i.e.*, less

than half of the C_I groups were consumed, which is consistent with Figure 2.8a. Note that assumption 3 prevents consumption of V_I groups on the inimer, because the model was formulated assuming that all of the C_I groups would be consumed rapidly. If the C_I groups persist, then permitting inimer molecules to react via their V_I groups becomes more important to obtain good model predictions. The model could be extended to account for additional reactions involving IM, but the number of species and reactions that would need to be included in PREDICI would become prohibitive (*i.e.*, if assumptions 1 and 3 were relaxed, the number of polymer species tracked by the model would more than double and the number of reaction steps would be more than 4000 if up to 15 IM units were permitted in each polymer molecule.

Given the small amount of data used to fit the parameters in Table 2.8, it is not clear whether k_{pIMapp} should be smaller than the initial guess. Perhaps the parameter estimator selected the small value in an attempt to fit $B_{\text{kin}} = 2.8$, which was reported after 10 min. in one of the replicate experiments. Using a small value of k_{pIMapp}, which leads to slow initiation, also helps to increase polydispersity so that molecular weight behaviour could be better fitted by the model.

One of the advantages of this model is that it can give detailed information, such as concentration, M_n, M_w and MWD curves for single polymer species, *e.g.* for P_1 (the linear polymer) or P_{10}^{5S} (branched polymer containing 10 IM units with 5 unreacted C_S groups). Also, information about similar types of polymer species can be combined via simple calculations. Figure 2.9 shows the detailed simulation results for polymer species with different numbers of IM units, obtained from simulations using the conditions for 06DNX100 and the estimated parameter values in Table 2.8. Note that polymer molecules of type 1IM, which have only one IM unit, are linear chains. Polymer molecules of type 3IM are a combination of P_3^{SS}, P_3^{S} and P_3. Figure 2.9a shows that polymer of type 1IM has the highest concentration in the system and that polymer species with more than 3 IM units have very low concentrations. In Figures 2.9b and 9c, values

of M_n and M_w for different polymer species show that, as expected, polymer molecules with 15 IM units have the highest molecular weight.

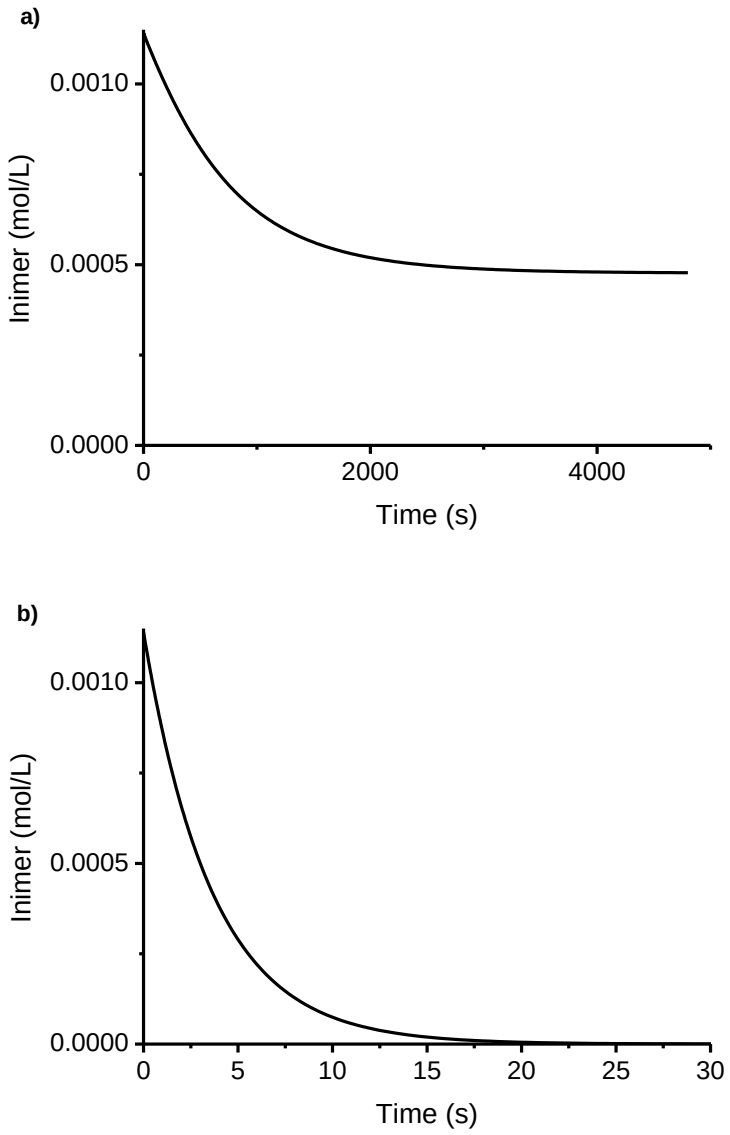

Figure 2.8 Predicted [IM] vs. time from the replicate runs, a) simulation results from using estimated value k_{pIMapp} in Table 2.8; b) simulation result from using initial value of k_{pIMapp} in Table 2.8, which we most believed. Note the different time scales for a) and b).

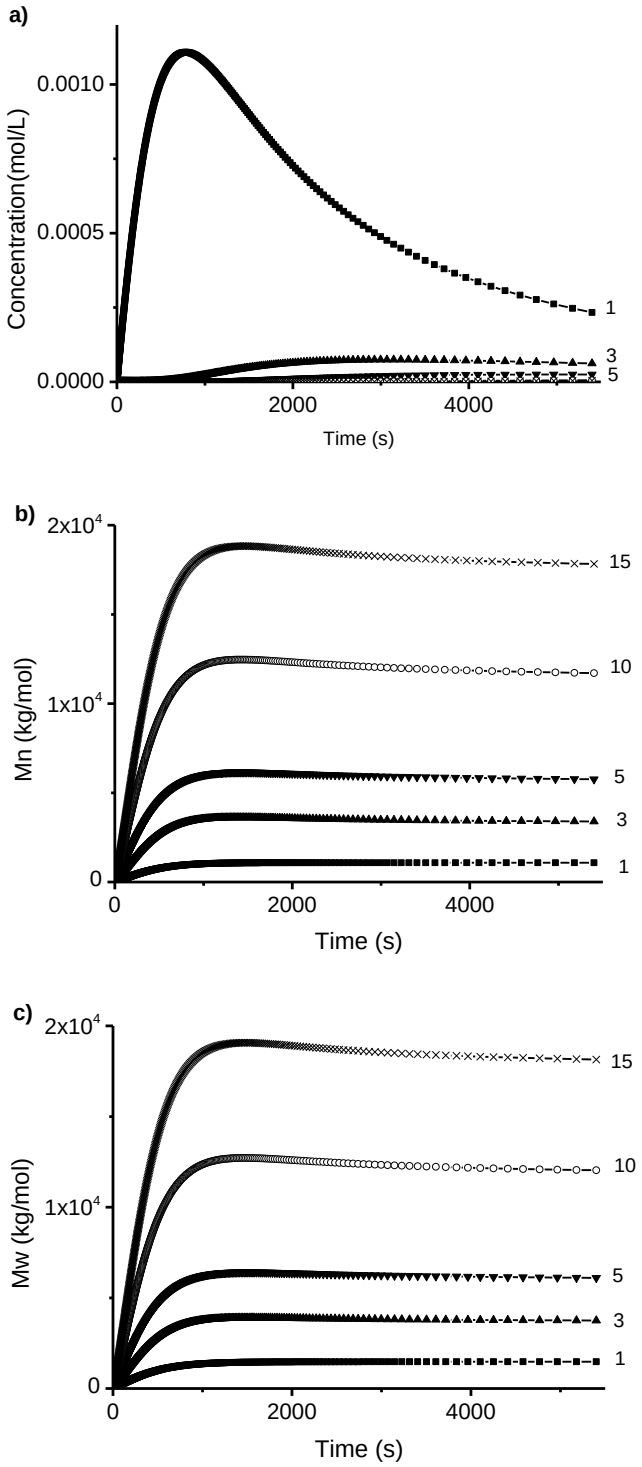

Figure 2.9 Detailed simulation results for polymer species with different numbers of IM units using the conditions for 06DNX100. a) Polymer concentrations vs. time; b) M_n vs. time; c) M_w vs. time. ■ 1 IM per molecule, ▲ 3 IM per molecule, ▼ 5 IM per molecule, ○ 10 IM per molecule and × 15 IM per molecule.

Figure 2.10 shows simulation results for the overall chain length distribution, which was determined by combining all polymer species together. Selected peaks corresponding to polymer molecules with different numbers of inimer units are also shown. In this predicted MWD curve, there are several distinct peaks, similar to experimental SEC results obtained by Dos Santos.[21] (The details are shown in Appendix 2.4.) The first peak in the overall distribution corresponds mainly to polymers with only 1 IM unit, and the second results mainly from a combination of polymers with 2 and 3 IM units. Polymers with more IM units produce overlapping peaks at higher chain lengths. The relative size of each individual peak decreases as the number of inimer units per molecule increases, up to 14 IM units (not shown). The reason that polymer species with 15 IM units do not follow this trend is that they are not permitted to react with other polymer molecules to form polymers with even higher branching levels. Figure 2.10 suggest that polymer molecules with 15 or more inimer units have a significant contribution to the overall MWD of the polymer, so that neglecting molecules with more than 15 inimer units is not valid, even for conditions that result in $B_{kin} \leq 5$.

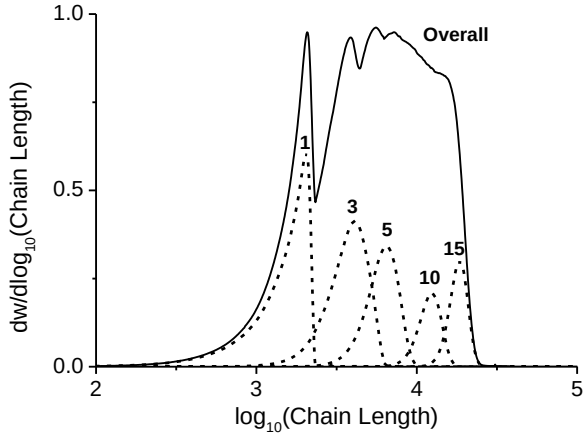

Figure 2.10 Simulation results for MWD using experimental conditions for run 06DNX100. The left-most peak of the overall MWD corresponds primarily to linear polymer with only one inimer unit. The second peak corresponds mainly to branched polymer with two or three inimer units. Note that area of the peaks decreases as the number of inimer units increases, except for peak 15.

2.5 Conclusion

A novel model was developed to describe copolymerization of isobutylene and an inimer via living carbocationic polymerization. Three different types of chloride end group (*i.e.* C_I, C_M and C_S) and two different types of vinyl groups (*i.e.* V_I and V_M) are considered, resulting in six different propagation rate constants. The model accounts for equilibrium reactions between carbocations and two types of counteranions, leading to two paths for propagation. Several simplifying assumptions were made so that the number of reactions (1430) and chemical species (122) could be kept to a manageable number for implementation using PREDICI. For example, the model only accounts for branched polymer molecules that contain up to 15 inimer units, and assumes that inimer is only consumed via reactions with isobutylene. Relaxing these assumptions leads to a much larger number of species and reactions that would need to be tracked. Literature values for different rate constants were used as initial parameter values and to determine reasonable upper and lower bounds for parameter estimation. A recently developed parameter ranking algorithm and mean-squared-error-based statistical criterion were used to determine that all of the apparent rate constants that appear in the model could be estimated using experimental data of Dos Santos and Puskas[10,21] where the average branching level is relatively low (*i.e.*, below five branches per molecule). The estimation results showed a good agreement with the experimental data; however, the estimated rate constant k_{pIMapp} for initiation reactions between inimer and isobutylene is considerably smaller than its initial value, leading to a significant portion of the inimer remaining unreacted at the end of the simulated batch experiments. Based on the simulation results, polymer species with a large number of inimer units (i.e, greater than 10) have very low concentrations, but are important in the system due to their high molecular weights, which contribute significantly to the weight average molecular weight and to the shape of the MWD. Unfortunately, the model predicts an unrealistically high concentration of molecules with 15 inimer units because molecules with 15 inimer units were not permitted to undergo further branching

reactions and therefore accumulated over time. This result indicates that the assumption of 15 or fewer inimer units per molecule was not valid, even for the experimental conditions (leading to 5 or fewer branches per molecule) used to fit the data.

Simulation results reveal that several important issues will need to be considered in future models. For example, the assumption that inimer can only react with isobutylene monomer should be relaxed so that more of the inimer will be consumed during typical simulations. Relaxing this assumption in the current model would lead to 665 additional species and more than 20,000 additional reactions. Also, the number of inimer units permitted in each polymer molecule should be increased substantially beyond 15, so that accurate simulation results can be obtained, especially for experimental conditions that lead to more highly branched polymer, including inimer homopolymerization. Increasing the maximum number of inimer units from 15 to 20 without relaxing any other assumptions would increase the number of reactions from 1430 to 4086 and the number of species from 122 to 212. In addition, some side reactions should be considered in the model. According to a very early study on IB homopolymerization by Kennedy et al.,[70] the solvent methyl chloride could play the role of initiator. Reactions between carbocations and the vinyl group on the same polymer molecule may also need to be considered to obtain accurate model predictions, especially when branching levels and vinyl group conversion are high. If these side reactions are considered, reactions between different polymer chains will occur at a lower rate influencing MWD and branching levels. Finally, the current model assumes equal reactivity for end groups of the same type, regardless of the size of the molecule on which they appear. Accounting for steric hindrance and mobility effects due to molecular size could result in improved model predictions.[40]

As simplifying assumptions are relaxed and more complex reaction mechanisms are considered, the number of polymer species, chemical reactions and model parameters will increase. Fortunately, additional experimental data (*e.g.*, with higher branching levels) are available for

parameter estimation under these conditions, [7,8,10,11,21] which will permit estimation of additional parameters. Since the number of reaction steps and polymer species is already prohibitive for detailed simulations using PREDICI, the mechanism will need to be expanded judiciously or different approaches such as Monte Carlo simulations may be required.

2.6 Reference

1 Y. Zhou, W. Huang, J. Liu, X. Zhu, D. Yan, *Adv. Mater.* **2010**, 22, 4567

2 M. Seiler, *Fluid Phase Equilibria*. **2006**, 241, 155

3 C. Gao, D. Yan. *Prog. Polym. Sci.* **2004**, 29, 183

4 M. Irfan, M. Seiler, *Ind. Eng. Chem. Res.* **2010**, 49, 1169

5 S. Chen, X. Zhang, X. Cheng, R. Zhuo, Z. Gu, *Biomacromolecules*. **2008**, 9, 2578

6 J. M. J. Fréchet, M. Henmi, I. Gitsov, S. Aoshima, M. R. Leduc, R. B. Grubbs, *Science.* **1995**, 269, 1080.

7 C. Paulo, J.E. Puskas, *Macromolecules.* **2001**, 34, 734.

8 J. E. Puskas, Y. Kwon. *Polym. Adv. Technol.* **2006**, 17, 615

9 J. E. Puskas, M. Grasmuller, *Macromol. Chem. Macromol. Symp.* **1998**, 132, 117

10 J. E. Puskas,; L. M. Dos Santos, G. Kaszas, K. Kulbaba, *J. Polym. Sci. Part A: Polym. Chem.* **2009**, 47, 1148

11 E. A. Foreman, J. E. Puskas, G. Kaszas, *J. Polym. Sci. Part A: Polym. Chem.* **2007**, 45, 5847

12 H. Frauenrath, *Prog. Polym. Sci.* **2005**, 30, 325

13 M. Higuchi, S. Shiki, K. Yamamoto, *Organic letters.* **2000**, 2 (20), 3079

14 H. Ritter, G. Draheim, *Macromol. Chem. Phys.* **1995**, 196, 2211.

15 M. Gauthier, *J. Polym. Sci., Part A: Polym. Chem*. **2007**, 45, 3803.

16 G. Langstein, O. Nuyken, W. Obrecht, J.E. Puskas, K. Weiss, *US 6,156,859*, **2000**

17 J.E. Puskas. G. Kaszas, *Prog. Polym. Sci.* **2000**, 25, 403

18 G. T. Lim, J.E. Puskas, D. H. Reneker, A. Jakli, W. E. Horton, Jr. *Biomacromolecules.* **2011**, 12, 1795

19 J. E. Puskas, E. A. Foreman-Orlowski, G. T. Lim, S. E. Porosky, M.M. Evancho-Chapman, S.P. Schmidt, M.E. Fray, M. Piatek, P. Prowans, K. Lovejoy, *Biomaterials*. **2010**, 31, 2477.

20 J. E. Puskas, W. Burchard, A. J. Heidenreich, L. M. Dos Santos, *J Polym Sci A: Polym Chem.* **2012**, 50, 70

21 L. M. Dos Santos, *Synthesis of arborescent model polymer structures by living carbocationic polymerization for structure property studies*, Ph.D. thesis, University of Akron, Akron, USA, **2009**.

22 L. M. Dos Santos, E. Foreman, M. Sen, J. E. Puskas, *Polymer Preprints*. **2007**, 48, 350.

23 H. Tobita, *J. Polym. Sci., Part B: Polym. Phys.* **1993**, 31, 1363

24 H. Tobita, *J. Polym. Sci., Part B: Polym. Phys.* **2001**, 39, 391

25 H. Tobita, *Macromol. Theory Simul*. **1996**, 5, 1167

26 H. Gao, P. Polanowski, K. Matyjaszewski, *Macromolecules.* **2009**, 42, 5925

27 P. Polanowski, J. K. Jeszka, W. Li, K. Matyjaszewski, *Polymer.* **2011**, 52, 5092

28 I. Bannister, N. C. Billingham, S. P. Armes, *Soft Matter.* **2009**, 5, 3495

29 P. D. Iedema, H. C. J. Hoefsloot, *Macromolecules*. **2006**, 39, 3081

30 P. D. Iedema, M. Wulkow, H. C. J. Hoefsloot, *Polymer*. **2007**, 48, 1770

31 P. D. Iedema, S. Grcev, H. C. J. Hoefsloot, *Macromolecules*. **2003**, 36, 458

32 R. A. Hutchinson, *Macromol. Theory Simul*. **2001**, 10, 144

33 D. M. Kim, P. D. Iedema, *Chemical Engineering Science.* **2008**, 63, 2035

34 R. Wang, Y. Luo, B. Li, S. Zhu, *Macromolecules*. **2009**, 42, 85

35 D. Wang, X. Li, W. Wang, X. Gong, B. Li, S. Zhu, *Macromolecules*. **2012**, 45, 28

36 J. Poly, D. J. Wilson, M. Destarac, D. Taton, *J. Polym. Sci. Part A: Polym. Chem*. **2009**, 47, 5313

37 X. He, J. Tang, *Polym. Sci., Part A: Polym. Chem*. **2008**, 46, 4486

38 X. He, H. Liang, C. Pan, *Polymer* **2003**, 44, 6697

39 X. He, H. Liang, C. Pan, *Macromol. Theory Simul*. **2001**, 10, 196

40 A. H. E. Müller, D. Yan, M. Wulkow, *Macromolecules.* **1997**, 30, 7015.

41 D. Yan, A. H. E. Müller, K. Matyjaszewski, *Macromolecules.* **1997**, 30, 7024.

42 G. I. Litvinenko, P. F. W. Simon, A. H. E. Müller, *Macromolecules.* **1999**, 32, 2410

43 G. I. Litvinenko, P. F. W. Simon, A. H. E. Müller, *Macromolecules.* **2001**, 34, 2418

44 G. I. Litvinenko, A. H. E. Müller, *Macromolecules.* **2002**, 35, 4577

45 Z. Zhou, D. Yan, *Macromolecules.* **2008**, 41, 4429

46 K. C. Cheng, T. H. Chuang, J. S. Chang, W. Guo, W. F. Su, *Macromolecules* **2005**, 38, 8252

47 K. C. Cheng, Y. Y. Su, T. H. Chuang, W. Guo, W. F. Su, *Macromolecules.* **2010**, 43, 8965

48 A. Zargar, K. Chang, L. J. Taite, F.J. Schork, *Macromol. React. Eng*. **2011**, 5, 373

49 M. F. De Freitas, J. C. Painto, *J. Appl. Polym. Sci*. **1996**, 60, 1109

50 J. E. Puskas, H. Peng, *Polym. React. Eng*. **1999**, 7(4), 553

51 J. E. Puskas, S. Shaikh, K. Z. Yao, K. B. McAuley, G. Kaszas, *European Polymer Journal.* **2005**, 41, 1

52 H. Schlaad, Y. Kwon, L. Sipos, R. Faust, B. Charleux, *Macromolecules.* **2000**, 33, 8225

53 L. Sipos, P. De, R. Faust, *Macromolecules*. **2003**, 36, 8282-8290

54 G. Kaszas, J. E. Puskas, *Polymer Reaction Engineering.* **1994**, 2(3), 251

55 J. E. Puskas, M. G. Lanzendorfer, *Macromolecules.* **1998**, 31, 8684

56 P. De, R. Faust, H. Schimmel, A. Ofial, H. Mayr, *Macromolecules.* **2004**, 37, 4422

57 M. Roth, H. Mayr, *Macromolecules.* **1996**, 29, 6104-6109

58 P. De, R. Faust *Macromolecules*. **2005**, 38, 9897-9900

59 J. E. Puskas, S. W. P. Chain, K. B. McAuley, G. Kaszas, S. Shaikh, *J. Polym. Sci. Part A: Polym. Chem.* **2007**, 45, 1778-1787

60 J. E. Puskas, G. Kaszas, J. P. Kennedy, T. Kelen, F. Tudos, *J. Macromol. Sci. Chem.* **1982-83**, A(18), 1315

61 K. A. P. McLean, K. B. McAuley, *Can. J. Chem. Eng*. **2012**,9,351

62 S. Wu, K. B. McAuley, T. J. Harris, *Can. J. Chem. Eng*. **2011**, 1, 148

63 K. Z. Yao, B. M. Shaw, B. Kou, K. B. McAuley, D. W. Bacon, *Polymer Reaction Engineering*. **2003**, 11(3), 563-588

64 S. Wu, K. B. McAuley, T. J. Harris, *Can. J. Chem. Eng*. **2011**, 89, 325

65 S. Wu, K. A. P. McLean, T. J. Harris, K. B. McAuley, *Int. J. Adv. Mechatronic Sys.* **2011**, 3, 188

66 B. Kou, K. B. McAuley, C. C. Hsu, D. W. Bacon, K. Z. Yao, *Ind. Eng. Chem. Res.* **2005**, 44, 2428

67 D. E. Thompson, K. B. McAuley, P. J. McLellan, *Macromol. React. Eng.* **2010**, 4, 73

68 J. D. Woloszyn, K. B. McAuley, *Macromol. React. Eng.* **2011**, 5, 453

69 H. Karimi, M. A. Schaffer, K. B. McAuley, *Macromol. React. Eng.* **2012**,6,93

70 J. P. Kennedy, R. M. Thomas, *J. Polym. Sci.* **1960**, 45, (145), 227.

Appendix 2.1 Examples of Reaction Steps Implemented in PREDICI

Initiation $IM + IB \xrightarrow{k_{pIMapp}} P_1(1)$

Propagation

$P_1(n) + IB \xrightarrow{k_{pMMapp}} P_1(n+1)$ $\quad$ $P_1(n) + P_1(m) \xrightarrow{2\times k_{pMIapp}} P_2^S(n+m)$

$P_2^S(n) + IB \xrightarrow{k_{pMMapp}} P_2^S(n+1)$ $\quad$ $P_2^S(n) + IB \xrightarrow{k_{pSMapp}} P_2\ (n+1)$

$P_2(n) + IB \xrightarrow{2\times k_{pMM}} P_2(n+1)$ $\quad$ $P_2(n) + P_1(m) \xrightarrow{3\times k_{pMIapp}} P_3^S(n+m)$

$P_2(n) + P_2(m) \xrightarrow{4\times k_{pMIapp}} P_4^S(n+m)$ $\quad$ $P_2^S(n) + P_1(m) \xrightarrow{2\times k_{pMIapp}} P_3^{2S}(n+m)$

$P_2^S(n) + P_2(m) \xrightarrow{3\times k_{pMIapp}} P_3^{2S}(n+m)$ $\quad$ $P_2^S(n) + P_2^S(m) \xrightarrow{2\times k_{pMIapp}} P_4^{3S}(n+m)$

In all, 1430 steps were implemented into PREDICI. Note that the reactions involving polymers with more than 3 IM units are not listed here. Reactions between C_I end groups and V_I vinyl groups as well as C_S end groups and V_I vinyl groups are neglected due to simplifying assumptions in Table 2.3. The detailed explanations about these reactions are described in section 2.3 Model Development.

Appendix 2.2 Calculation of Mw from Different Polymer Species

Assume we have X different polymer samples 1, 2, 3,…, X and each of them has its own M_n and M_w. Then we would like to combine them and calculate the overall average M_n and M_w. In the blend, the total concentrations for different samples are denoted as $[S_1]$, $[S_2]$…$[S_X]$.

First, I will show the definition of M_n and M_w.

$$\textit{Since} \quad n_i = \frac{[P_i]}{\sum_{i=1}^{\infty}[P_i]} \quad \textit{and} \quad w_i = \frac{n_i[P_i]}{\sum_{i=1}^{\infty} n_i[P_i]}$$

$$\therefore M_n = \sum_{i=1}^{\infty} n_i m_i = \frac{\sum_{i=1}^{\infty}[P_i]m_i}{\sum_{i=1}^{\infty}[P_i]} \qquad \text{(A2.2.1)}$$

$$\textit{which gives} \quad M_n \sum_{i=1}^{\infty}[P_i] = \sum_{i=1}^{\infty}[P_i]m_i \qquad \text{(A2.2.2)}$$

$$\textit{Similarly,}\ M_w = \sum_{i=1}^{\infty} w_i m_i = \frac{\sum_{i=1}^{\infty} n_i m_i^2}{\sum_{i=1}^{\infty} n_i m_i} = \frac{\sum_{i=1}^{\infty}[P_i]m_i^2}{\sum_{i=1}^{\infty}[P_i]m_i} \qquad \text{(A2.2.3)}$$

$$\textit{which gives} \quad M_w \sum_{i=1}^{\infty}[P_i]m_i = \sum_{i=1}^{\infty}[P_i]m_i^2 \qquad \text{(A2.2.4)}$$

$$\text{For the jth polymer sample, } [S_j] = \sum_{i=1}^{\infty}[P_i]_j \qquad \text{(A2.2.5)}$$

where n_i is the number fraction of molecules of length i, w_i is the weight fraction of polymer with chain length i, m_i is the molecular weight of polymer chain with i repeat units; P_i is a polymer molecule with i repeat units; $[P_i]$ is the concentration of polymer chains with i repeat units; $[P_i]_j$ means the concentration of polymer chains with i repeat units from sample j in the overall mixture; S_j is the j th sample and $[S_j]$ is the concentration of sample j in the overall mixture.

After we mix all the samples together, we use the definition to calculate the overall M_n.

$$M_n = \frac{\sum_{i=1}^{\infty}[P_i]_1 m_{i1} + \sum_{i=1}^{\infty}[P_i]_2 m_{i2} + \sum_{i=1}^{\infty}[P_i]_3 m_{i3} + \cdots + \sum_{i=1}^{\infty}[P_i]_X m_{iX}}{\sum_{i=1}^{\infty}[P_i]_1 + \sum_{i=1}^{\infty}[P_i]_2 + \sum_{i=1}^{\infty}[P_i]_3 + \cdots + \sum_{i=1}^{\infty}[P_i]_X} \qquad \text{(A2.2.6)}$$

After substituting using equation (A2.2.2), we get

$$M_n = \frac{M_{n1}\sum_{i=1}^{\infty}[P_i]_1 + M_{n2}\sum_{i=1}^{\infty}[P_i]_2 + M_{n3}\sum_{i=1}^{\infty}[P_i]_3 + \cdots + M_{nX}\sum_{i=1}^{\infty}[P_i]_X}{\sum_{i=1}^{\infty}[P_i]_1 + \sum_{i=1}^{\infty}[P_i]_2 + \sum_{i=1}^{\infty}[P_i]_3 + \cdots + \sum_{i=1}^{\infty}[P_i]_X} \qquad \text{(A2.2.7)}$$

Substituting using equation (A2.2.5) gives,

$$M_n = \frac{M_{n1}[S_1] + M_{n2}[S_2] + M_{n3}[S_3] + \ldots + M_{nX}[S_X]}{[S_1] + [S_2] + [S_3] + \ldots + [S_X]} \qquad \text{(A2.2.8)}$$

$$\therefore M_n = \frac{\sum_{j=1}^{X} M_{nj}[S_j]}{\sum_{j=1}^{X}[S_j]} \qquad \text{(A2.2.9)}$$

Similarly, we use the definition of M_w in equation A2.2.2 to obtain the following expression that accounts for the different samples.

$$M_w = \frac{\sum_{i=1}^{\infty}[P_i]_1 m_{i1}^2 + \sum_{i=1}^{\infty}[P_i]_2 m_{i2}^2 + \sum_{i=1}^{\infty}[P_i]_3 m_{i3}^2 + \cdots + \sum_{i=1}^{\infty}[P_i]_X m_{iX}^2}{\sum_{i=1}^{\infty}[P_i]_1 m_{i1} + \sum_{i=1}^{\infty}[P_i]_2 m_{i2} + \sum_{i=1}^{\infty}[P_i]_3 m_{i3} + \cdots + \sum_{i=1}^{\infty}[P_i]_X m_{iX}} \quad \text{(A.2.2.10)}$$

Substituting using equations (A2.2.2) and (A2.2.4) gives

$$M_w = \frac{M_{w1}\sum_{i=1}^{\infty}[P_i]_1 m_{i1} + M_{w2}\sum_{i=1}^{\infty}[P_i]_2 m_{i2} + M_{w3}\sum_{i=1}^{\infty}[P_i]_3 m_{i3} + \cdots + M_{wX}\sum_{i=1}^{\infty}[P_i]_X m_{iX}}{M_{n1}\sum_{i=1}^{\infty}[P_i]_1 + M_{n2}\sum_{i=1}^{\infty}[P_i]_2 + M_{n3}\sum_{i=1}^{\infty}[P_i]_3 + \cdots + M_{nX}\sum_{i=1}^{\infty}[P_i]_X} \quad \text{(A.2.2.11)}$$

Substituting again using equation (A2.2.2) gives

$$M_w = \frac{M_{w1}M_{n1}\sum_{i=1}^{\infty}[P_i]_1 + M_{w2}M_{n2}\sum_{i=1}^{\infty}[P_i]_2 + M_{w3}M_{n3}\sum_{i=1}^{\infty}[P_i]_3 + \cdots + M_{wX}M_{nX}\sum_{i=1}^{\infty}[P_i]_X}{M_{n1}\sum_{i=1}^{\infty}[P_i]_1 + M_{n2}\sum_{i=1}^{\infty}[P_i]_2 + M_{n3}\sum_{i=1}^{\infty}[P_i]_3 + \cdots + M_{nX}\sum_{i=1}^{\infty}[P_i]_X} \quad \text{(A2.2.12)}$$

A further substitution using equation (A2.2.5) gives

$$M_w = \frac{M_{w1}M_{n1}[S_1] + M_{w2}M_{n2}[S_2] + M_{w3}M_{n3}[S_3] + \cdots + M_{wX}M_{nX}[S_X]}{M_{n1}[S_1] + M_{n2}[S_2] + M_{n3}[S_3] + \cdots + M_{nX}[S_X]} \quad \text{(A2.2.13)}$$

$$\therefore M_w = \frac{\sum_{j=1}^{X} M_{nj}M_{wj}[S_j]}{\sum_{j=1}^{X} M_{nj}[S_j]} \quad \text{(A2.2.14)}$$

Thus, we can calculate the overall M_n and M_w using equations A2.2.9 and A2.2.14.

Appendix 2.3 Scaling Factor Used in PREDICI

PREDICI calculates the weighted residual sum of squares using equation:

$$SSE = \sum_{j=1}^{r}\sum_{i=1}^{n_j} \varepsilon_{i,j}^2 = \sum_{j=1}^{r}\sum_{i=1}^{n_j} (m_{i,j} - s_{i,j})^2 / w_{i,j}^2 \quad \text{(A2.3.1)}$$

$$w_{i,j} = \max(scale_j, m_{i,j}) > 0 \quad \text{(A2.3.2)}$$

where r is the number of responses; n_j is the number of data points for each response; $m_{i,j}$ is the measurement of experimental data point for the j^{th} response and the i^{th} data points and $s_{i,j}$ is the corresponding simulation results; $w_{i,j}$ is the weighting factor, which is determined by equation A2.3.2.

PREDICI gives the resulting total residual r_{rel}, which is defined as:

$$r_{rel} = \frac{1}{\sqrt{N}} \sqrt{SSE} \quad \text{(A2.3.3)}$$

where $N = \sum_{j=1}^{r} n_j$, *i.e.* the total number of data points used in parameter estimation.

The objective function used by us can be expressed as:

$$J = \sum_{j=1}^{r}\sum_{i=1}^{n_j} (m_{i,j} - s_{i,j})^2 / s_{p,j}^2 \quad \text{(A2.3.4)}$$

where $s_{p,j}^2$ is the measurement uncertainty (pure error variance) value of the j^{th} response, which we obtain from pooled variance estimates from the replicate experiments.

In order to obtain the desired objective function, we need to use some tricks to let the weighting factor in equation A2.3.2 be related to the pure error variance. The weighting factor used automatically in PREDICI is the maximum between the scaling factor and the measured value. Since we do not want the measured value to be selected, all of the pure error variance estimates were multiplied with a same factor (*e.g.* a^2) to produce weighting factors $scale = a\sqrt{s_{p,j}^2}$

that are larger than all of the corresponding measurements. Using these scaling factors, the corresponding objective function is:

$$SSE = \sum_{j=1}^{r}\sum_{i=1}^{n_j} \varepsilon_{i,j}^2 = \sum_{j=1}^{r}\sum_{i=1}^{n_j} (m_{i,j} - s_{i,j})^2 / a^2 \cdot s_{p,j}^2 \qquad \text{(A2.3.5)}$$

Combining equation A2.3.3 to A2.3.5, we can get the expression of the objective function as shown below:

$$J = a^2 \cdot N \cdot r_{rel}^2 \qquad \text{(A2.3.6)}$$

Using large values for each of the scaling factors in data files does not affect the parameter estimation results, but allows information about the relative uncertainty in each measured data type to be included in PREDICI's parameter estimation routine.

Appendix 2.4 Simulation results compared with SEC results

Figure 2.11 shows the simulation results for MWD with the initial condition $[IM]_0$ = 0.00114 M and $[IB]_0$ = 1.74 M and the estimated parameter values in Table 2.8. Figure 2.12 shows the corresponding SEC results from Dos Santos's thesis obtained using a variety of detectors[21]. We can see similar multi-peak curves from the SEC results. The trend is similar to our simulation results.

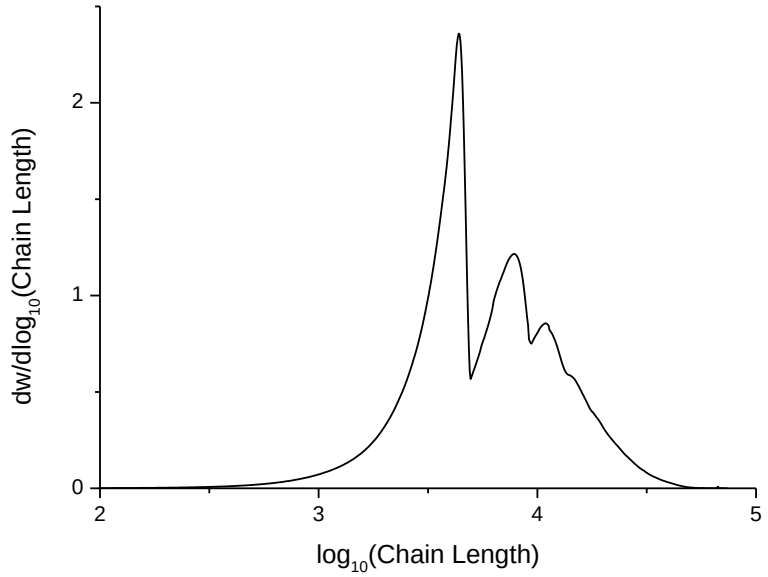

Figure 2.11 Simulation results for MWD using experimental conditions for run 06DNX001, 06DNX010 and 06DNX030.

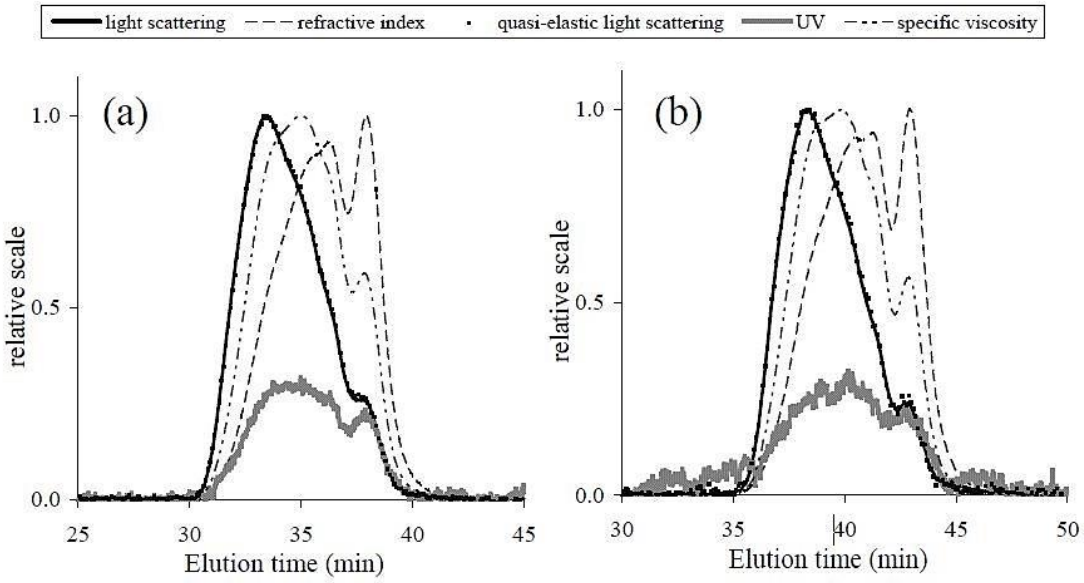

Figure 2.12 SEC traces of selected *arb*PIB samples obtained from Dos Santos[21]. (a) 06DNX001; (b) 06DNX010

Chapter 3

Monte Carlo Model for Arborescent Polyisobutylene Production in Batch Reactor

Yutian R. Zhao[1], Kimberley B. McAuley[1], Judit E. Puskas[2]

[1]Department of Chemical Engineering, Queen's University, Kingston, ON, Canada
[2]Department of Chemical & Biomolecular Engineering, University of Akron, Akron, OH USA

3.1 Abstract

A Monte Carlo (MC) model is developed to predict MWD and branching during the production of *arborescent* polyisobutylene. The model describes self-condensing vinyl copolymerization (SCVCP) of isobutylene and inimer via living carbocationic polymerization. Six different propagation rate constants are required to account for two types of vinyl groups and three types of carbocations in the system. MC model predictions are better than predictions from a previous PREDICI material balance model because fewer simplifying assumptions are required. The MC model predictions reveal that reactions that were previously neglected have an important influence on polymer properties.

This chapter was published as:

Zhao YR, McAuley KB, Puskas JE. Monte Carlo model for arborescent polyisobutylene production in the batch reactor. *Macromol. Theory Simul.* 2013; 22: 365-376.

3.2 Introduction

Polyisobutylene (PIB) with an arborescent or tree-like structure can be produced via living carbocationic polymerization of isobutylene and an inimer as shown in Figure 3.1. This arborescent material has been used as a core to produce block copolymers with polystyrene end blocks. The resulting thermoplastic elastomer has outstanding biocompatibility, biostability and mechanical properties and is a promising candidate for human implantation.[1- 7] By comparing with medical-grade silicone rubber, the encrustation of *arborescent* PIB is comparable or even better, making it a promising material for breast implants.[8]

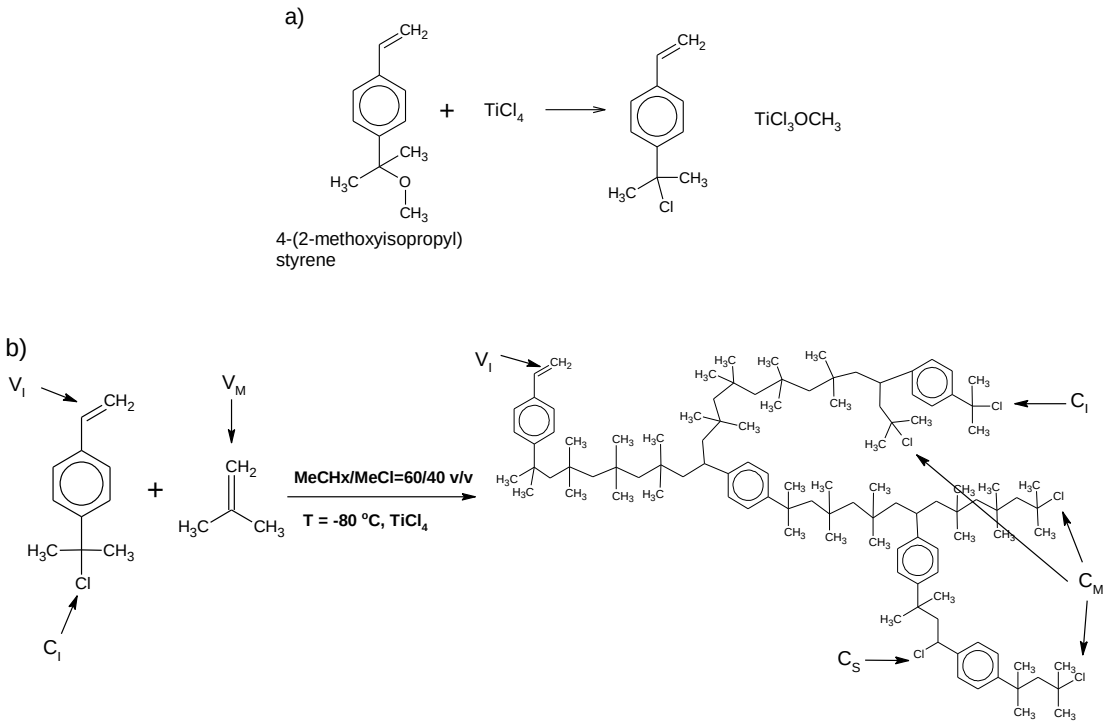

Figure 3.1 Reaction scheme to produce *arborescent* polyisobutylene. Step a) is the exchange reaction that generates IM from MeOIM.[13] Step b) is the overall reaction scheme to produce an *arb*PIB molecule from several IM and isobutylene molecules.[15]

The *arborescent* PIB core can be produced through a "one-pot" copolymerization of inimer (IM) molecules and isobutylene (IB) monomer.[4,9-12] A simplified reaction scheme for producing the *arborescent* PIB is shown in Figure 3.1. A more detailed reaction mechanism can be found elsewhere.[13-15] When 4-(2-methoxyisopropyl)styrene (MeOIM) is used to produce *arborescent* PIB, the first step (Figure 3.1a) in this process is an exchange reaction that converts the MeOIM to a chlorinated inimer molecule, which is called IM throughout this article. This reaction is often conducted using a large excess of Lewis acid ($TiCl_4$) to ensure complete conversion.[13] The resulting IM can initiate polymerization when the chloride group is removed by further reaction with Lewis acid. Other types of initiation (*e.g.*, proton initiation with trace amounts of water) can be neglected when a proton trap (*e.g.*, 2,6-di-tert-butylpyridine) is included in the polymerization recipe.[13]

As shown in Figure 3.1b, there are two types of vinyl groups (V_I from the inimer and V_M from the monomer) and three types of chloride end groups (C_I, C_S and C_M) that can be uncapped by Lewis acid to produce carbocations for chain propagation. C_I groups are the chloride groups associated with the IM; C_S groups are chloride groups formed after the consumption of a V_I group; C_M groups are chloride groups formed after the consumption of V_M groups.[15] The number of possible combinations between different chloride end groups and different vinyl groups is 6, which leads to 6 true propagation rate constants, *i.e.*, k_{pII}, k_{pIM}, k_{pMI}, k_{pMM}, k_{pSI}, k_{pSM}, where the first subscript after k_p represents the type of chloride end group and the second is the type of vinyl group that is consumed. In this living polymerization, when any chloride end group is uncapped by Lewis acid to produce a carbocation, several propagation steps may occur before the carbocation returns to its dormant state by capping with chloride.[16] An interesting feature of this polymerization is that every polymer molecule that is produced has exactly one V_I group, assuming that intra-molecular reactions do not occur.

After the experiment, the branching level of the arborescent polymer is calculated by B_{kin}:[13]

$$B_{kin} = M_n/M_{n,theo} - 1 \tag{3.1}$$

$$M_{n,theo} = M_{IM} + \frac{[IB]_0 - [IB]}{[IM]_0 - [IM]} M_{IB}$$

where $M_{n,theo}$ is the molecular weight that would be obtained if IM were consumed as initiator only (*i.e.*, C_I groups are consumed and V_I does not react), which would lead to linear PIB without branches.

The concept of "one-pot" living homopolymerization of IM molecules was first introduced by Fréchet et al. in 1995, which they named self-condensing vinyl polymerization (SCVP).[17] Later, self-condensing vinyl copolymerization (SCVCP) of inimers and vinyl monomers was performed experimentally.[2-4,8-14]

Several research groups have developed mathematical models for SCVP and SCVCP systems. These models can be classified into two different categories: i) models based on dynamic material balances,[18-25] and ii) models based on Monte Carlo (MC) simulations.[26-28] The main advantage of the dynamic material balance approach is that it is relatively straightforward to develop individual material balance equations. The main disadvantage is the large number of polymer species that need to be tracked and material balances that need to be solved when detailed information about the branching level is of interest.[15] For MC simulations, the great advantage is that detailed structural information about polymer molecules can be obtained, but a considerable computational effort is required to generate accurate results.

Müller et al. and Yan et al.[18-22] produced a series of articles that use material balances methods to model SCVP and SCVCP. In their model development, several simplifying assumptions about equal reactivities of all or some end groups and vinyl groups were made to derive analytical expressions for average molecular weights and average branching level.

Cheng et al.[23,24] used material balance equations to develop models for SCVP, which they solved using generating functions. Equal reactivities for some of the end groups were also assumed in their models. Recently, Zargar et al.[25] developed a model for SCVCP, using the method of moments to keep track of the lengths of linear segments that make up the branched polymer molecules. Using this method, information about M_n, M_w and polydispersity for the segments can be obtained, as can the conversion of the two vinyl monomers. However, the molecular weight distribution (MWD) for the overall polymer molecules cannot be predicted. In their model, the C_S end groups were assumed to have the same reactivity as the C_M groups.

In our previous work,[15] a PREDICI material balance model was built for the *arborescent* PIB system in Figure 3.1, which is a type of SCVCP. This was the first SCVCP model to be developed without applying equal reactivity assumptions. This model consists of dynamic material balances on polymer species containing different numbers of inimer units and chloride end groups. Two paths (path A and path B in Figure 3.2) were considered for chain propagation.[16,28] Based on the restrictive set of assumptions in Table 3.1, only four lumped parameters, whose estimated values are shown in Table 3.2, were required to conduct the simulations. Simulations that permit up to 15 IM molecules per polymer molecule required balances on 122 species and required 1430 reaction steps in PREDICI. The simulation results agreed reasonably well with available data corresponding to low average branching levels (~2 branches per molecule) but worse predictions of M_w, M_n and branching were obtained for polymers with higher branching levels.[15]

He et al.[26] built homopolymerization models for inimers in the presence of multifunctional initiator, using MC methods, in which different rate constants were considered for C_I and C_S types of active sites, when predicting MWD and degree of branching. They also developed a three-dimensional MC bond fluctuation lattice model to study steric effects and intramolecular cyclization during inimer homopolymerization.[27] In addition, He et al.[28] used MC methods to simulate SCVCP. In the development of this model, He et al., assumed that a single rate constant

value is appropriate for reactions between different end groups and different types of vinyl groups. To our knowledge, the models by He et al. are the only MC models available in the literature for SCVP or SCVCP systems.

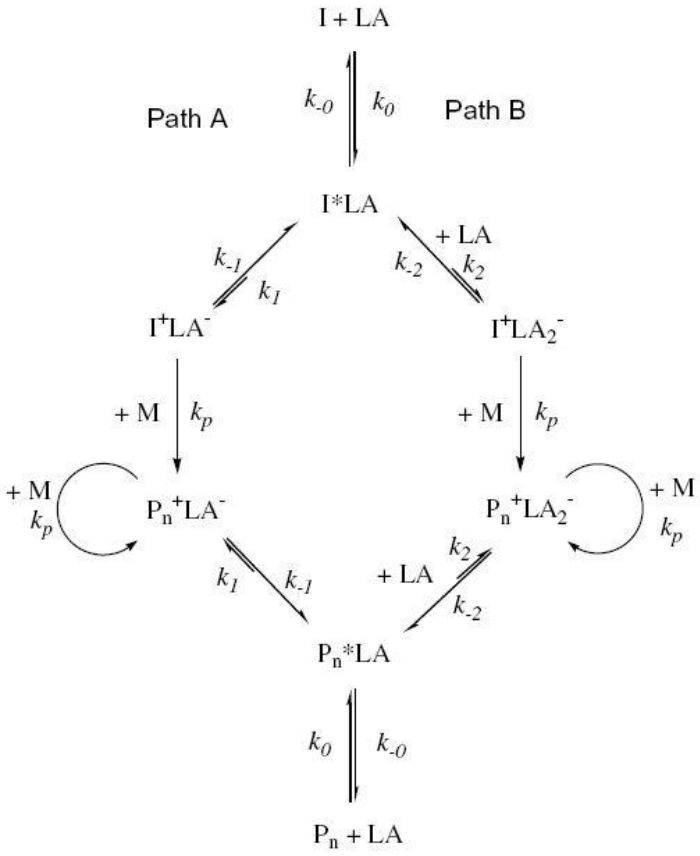

Figure 3.2 Comprehensive mechanism for living IB polymerization using $TiCl_4$ as the Lewis acid[16]

Table 3.1 Assumptions for PREDICI material balance model development[15]

1	Reactions between C_I end groups and IM can be neglected because $[IM]_0$ is low relative to $[IB]_0$, so that reactions involving k_{pII} can be neglected.
2	C_S end groups can only react with monomer vinyl groups. Reactions between C_S end groups and IM molecules can be neglected because IM molecules will typically initiate polymerization before their vinyl groups can be consumed by reaction. Reactions between C_S end groups and V_I groups on polymer molecules can be neglected due to steric hindrance. Because $[IM]_0$ is very low compared to $[IB]_0$, C_S groups will react with IB before they encounter the V_I groups on large molecules. Thus, reactions involving k_{pSI} can be neglected.
3	The C_I groups on the IM are all consumed very early in the reaction because the chloride end is designed to behave as an initiator for living carbocationic polymerization. As a result, the only reaction that IM can undergo appreciably is an initiation reaction with IB. Therefore, vinyl groups of type V_I can undergo propagation reactions only after they belong to oligomer or polymer molecules. Another consequence of this assumption is that there are no C_I groups on any polymer molecules so that reactions between polymer molecules and IM can be ignored. Note that this assumption means that there is no need to track the number of C_I groups in the model, (except for those on IM, which are consumed quickly).
4	Reactions that lead to 16 or more IM units in a molecule are neglected to keep the number of species and reactions manageable for implementation in PREDICI.
5	Puskas et al.[29] observed a penultimate effect during styrene/isobutylene copolymerization, indicating that the rate of IB addition to C_M may depend on whether the penultimate unit is IB or a styrene-like IM unit. Since $[IM]_0$ was low compared to $[IB]_0$ in the recipes simulated using the PREDICI model, this penultimate effect could be neglected with only a small effect on model predictions.
6	$[LA] \approx [LA]_0$ throughout the course of the batch reactions simulated using PREDICI, because only a small fraction of the $TiCl_4$ was consumed to produce ions.[30] Also, $[LA]_0$ is sufficiently large so that the MeOIM is converted instantaneously to IM at the beginning of the batch.

Table 3.2 Parameter estimation results for four lumped parameters.[15]

Parameter	Estimate	Units
$k_{pMIapp} = k_{pMI}\times(K_0K_1[TiCl_4]_0+K_0K_2[TiCl_4]_0^2)$	0.195	$L\cdot mol^{-1}\cdot s^{-1}$
$k_{pMMapp} = k_{pMM}\times(K_0K_1[TiCl_4]_0+K_0K_2[TiCl_4]_0^2)$	2.126	$L\cdot mol^{-1}\cdot s^{-1}$
$k_{pIMapp} = k_{pIM}\times(K_0K_1[TiCl_4]_0+K_0K_2[TiCl_4]_0^2)$	3.99×10^{-4}	$L\cdot mol^{-1}\cdot s^{-1}$
$k_{pSMapp} = k_{pSM}\times(K_0K_1[TiCl_4]_0+K_0K_2[TiCl_4]_0^2)$	1.39×10^{-2}	$L\cdot mol^{-1}\cdot s^{-1}$

where $K_0 = \frac{k_0}{k_{-0}} = \frac{[P_n^*LA]}{[P_n][LA]}$; $K_1 = \frac{k_1}{k_{-1}} = \frac{[P_n^+LA^-]}{[P_n^*LA]}$; $K_2 = \frac{k_2}{k_{-2}} = \frac{[P_n^+LA_2^-]}{[P_n^*LA][LA]}$.

However, MC simulations have been used for many other types of polymerization reactors.[31-34] MC methods for chemical reactions were first developed in the 1970s by Gillespie[35] and are now commonly used for polymerization models. Soares and Hamielec[36] used a simple free radical polymerization system (involving only initiation, propagation and termination) to illustrate how MC calculations are typically performed. The modeler must first specify the number of molecules of each different species in the reaction system, which is related to the species concentrations C_j in a small volume V:

$$N_j = C_j V N_A \tag{3.2}$$

where N_A is *Avogadro's* number. The initial number of molecules influences the accuracy of MC simulations.[35] All rate constants used in MC simulations are typically specified in units of s^{-1}, whereas many rate constants, like k_p, used in material balance models can have units like $L\cdot mol^{-1}\cdot s^{-1}$. The MC rate constant for propagation is related to the usual rate constant by:

$$k_p^{MC} = \frac{k_p}{VN_A} = \frac{k_p}{N_j}C_j \tag{3.3}$$

In the example of Soares and Hamielec, the MC reaction rate expressions are:

$$R_i^{MC} = k_i^{MC}N_iN_m;$$

$$R_p^{MC} = k_p^{MC}N_pN_m;$$

$$R_t^{MC} = k_t^{MC} N_{p1} N_{p2};$$

$$R_{total}^{MC} = R_i^{MC} + R_p^{MC} + R_t^{MC} \tag{3.4}$$

where N_i, N_m and N_p are the number of initiator, monomer and polymer molecules, respectively, within the chosen volume.

Assuming that one of the reactions occurs after a time period Δt, the corresponding probability of the *j*th reaction is related to the rates for all of the possible reactions by:

$$p_j = \frac{R_j^{MC}}{R_i^{MC} + R_p^{MC} + R_t^{MC}} = \frac{R_j^{MC}}{R_{total}^{MC}} \tag{3.5}$$

where *j* can be *i*, *p* or *t*. The length of the time step Δt between successive reactions is calculated from:

$$\Delta t = \frac{ln1/r_1}{R_{total}^{MC}} \tag{3.6}$$

where r_1 is a random number between 0 and 1 selected from a uniform distribution.[35] Note that for systems with a larger sample volume (with more initial molecules), the denominator R_{total}^{MC} becomes larger, so that the time between reactions tends to become smaller.

A second uniform random number r_2 is generated to decide which of the reactions will happen, based on their relative rates. Initiation is selected if $0 < r_2 \leq R_i^{MC}/R_{total}^{MC}$. Propagation is selected if $R_i^{MC}/R_{total}^{MC} < r_2 \leq (R_i^{MC} + R_p^{MC})/R_{total}^{MC}$ and termination is selected if $(R_i^{MC} + R_p^{MC})/R_{total}^{MC} < r_2 < 1$. After the reaction type is selected, changes are made to the number of species in the small reaction volume and the time is updated from *t* to $t + \Delta t$. The process is repeated by selecting r_1 and r_2 for the next time step. The simulation stops when the reaction time reaches the final end time or when the desired final conversion is reached.

To our knowledge, no researchers have built a model for SCVCP that accounts for all six propagation rate constants (*i.e.*, without applying equal reactivity assumptions for different types of ends and vinyl groups) using either a material balance or MC approach. In this paper, a MC

model is developed for SCVCP of IM and IB with six different propagation rate constants. This MC model is able to predict dynamic changes in concentrations of IM and IB, as well as detailed information about branching and MWD. Simulation results are presented after a description of the MC model development. Comparisons are made with predictions from our previous PREDICI material balance model that incorporated the restrictive assumptions in Table 3.1. Recommendations are made regarding development of future MC models that may have reduced computation times.

3.3 Model Development

As shown in Figure 3.1, there are three types of end groups (C_I, C_M and C_S) and two types of vinyl groups (V_I and V_M), which lead to six true propagation rate constants that are related to six apparent rate constants k_{pIIapp}, k_{pIMapp}, k_{pMIapp}, k_{pMMapp}, k_{pSIapp} and k_{pSMapp}, respectively. Expressions and estimated values for the four apparent rate constants k_{pIMapp}, k_{pMIapp}, k_{pMMapp} and k_{pSMapp} used in our previous PREDICI model are shown in Table 3.2. Analogous expressions for k_{pIIapp} and k_{pSIapp} are:

$$k_{pIIapp} = k_{pII} \times (K_0 K_1 [TiCl]_0 + K_0 K_2 [TiCl]_0^2) \tag{3.7}$$

$$k_{pSIapp} = k_{pSI} \times (K_0 K_1 [TiCl]_0 + K_0 K_2 [TiCl]_0^2) \tag{3.8}$$

Here, the same notation as in our previous work is used to track polymer chains with different numbers of inimer and monomer units and different numbers of end groups of different types. For example $P_{18}^{3I,6S}(108)$ refers to a polymer molecule containing 18 IM units and 108 monomer units. The *3I* superscript indicates that the polymer molecule has three C_I end groups and the *6S* superscript indicates that the molecule has six C_S groups. Since the number of IM units in the arborescent polymer molecule is always equal to the total number of different chloride end groups, it is not necessary to use a separate counter to track the C_M ends. For a polymer of the type $P_{18}^{3I,6S}(108)$, the number of C_M ends is 18-3-6=9.

All six possible reactions between the three different potential cations and two different vinyl groups are summarized in Table 3.3. Also, all possible reactions that can happen between different types of species in the polymerization system are listed in Table 3.4.

Table 3.3 Summary of six possible propagation reactions and corresponding reaction rates between end groups and vinyl groups during copolymerization of IM and IB

	Reaction	Rate Expression
1	$C_I + V_I \xrightarrow{k_{pIIapp}} C_S$	$R_1^{MC} = k_{pIIapp}^{MC} N_{C_I} N_{V_I}$
2	$C_I + V_M \xrightarrow{k_{pIMapp}} C_M$	$R_2^{MC} = k_{pIMapp}^{MC} N_{C_I} N_{V_M}$
3	$C_M + V_I \xrightarrow{k_{pMIapp}} C_S$	$R_3^{MC} = k_{pMIapp}^{MC} N_{C_M} N_{V_I}$
4	$C_M + V_M \xrightarrow{k_{pMMapp}} C_M$	$R_4^{MC} = k_{pMMapp}^{MC} N_{C_M} N_{V_M}$
5	$C_S + V_I \xrightarrow{k_{pSIapp}} C_S$	$R_5^{MC} = k_{pSIapp}^{MC} N_{C_S} N_{V_I}$
6	$C_S + V_M \xrightarrow{k_{pSMapp}} C_M$	$R_6^{MC} = k_{pSMapp}^{MC} N_{C_S} N_{V_M}$

Table 3.4 Summary of reactions and rate expressions for reactions between different types of molecules during copolymerization of IM and IB. C_M, C_I and C_S in the second column indicate the type of cation that is participating in the reaction.[15]

IM + IB	C_I	$IM + IB \xrightarrow{k_{IMapp}^{MC}} P_1^{0I,0S}(1)$ $R_{pTot} = k_{IMapp}^{MC}[IM][IB]$
IM + IM	C_I	$IM + IM \xrightarrow{k_{IIapp}^{MC}} P_2^{1I,1S}(0)$ $R_{pTot} = k_{IIapp}^{MC}[IM]^2$
Polymer + IB	C_M	$P_i^{xI,yS}(m) + IB \xrightarrow{(i-x-y)k_{pMMapp}^{MC}} P_i^{xI,yS}(m+1)$ $R_{pTot} = (i-x-y)k_{pMMapp}^{MC}\left[P_i^{xI,yS}(m)\right][IB]$
	C_I	$P_i^{xI,yS}(m) + IB \xrightarrow{xk_{pIMapp}^{MC}} P_i^{(x-1)I,yS}(m+1)$ $R_{pTot} = xk_{pIMapp}^{MC}\left[P_i^{xI,yS}(m)\right][IB]$
	C_S	$P_i^{xI,yS}(m) + IB \xrightarrow{yk_{pSMapp}^{MC}} P_i^{xI,(y-1)S}(m+1)$ $R_{pTot} = yk_{pSMapp}^{MC}\left[P_i^{xI,yS}(m)\right][IB]$
Polymer + IM	C_M	$P_i^{xI,yS}(m) + IM \xrightarrow{(i-x-y)k_{pMIapp}^{MC}} P_i^{(x+1)I,(y+1)S}(m)$ $R_{pTot} = (i-x-y)k_{pMIapp}^{MC}\left[P_i^{xI,yS}(m)\right][IM]$
	C_I	$P_i^{xI,yS}(m) + IM \xrightarrow{xk_{pIIapp}^{MC}} P_i^{xI,(y+1)S}(m)$ $R_{pTot} = xk_{pIIapp}^{MC}\left[P_i^{xI,yS}(m)\right][IM]$
	C_S	$P_i^{xI,yS}(m) + IM \xrightarrow{yk_{pSIapp}^{MC}} P_i^{(x+1)I,yS}(m)$ $R_{pTot} = yk_{pSIapp}^{MC}\left[P_i^{xI,yS}(m)\right][IM]$
IM + Polymer	C_I	$IM + P_i^{xI,yS}(m) \xrightarrow{k_{pIIapp}^{MC}} P_i^{xI,(y+1)S}(m)$ $R_{pTot} = k_{pIIapp}^{MC}\left[P_i^{xI,yS}(m)\right][IM]$
Polymer + Polymer	C_M	$P_{i_1}^{x_1I,y_1S}(m_1) + P_{i_2}^{x_2I,y_2S}(m_2) \xrightarrow{(i_1-x_1-y_1+i_2-x_2-y_2)k_{pMIapp}^{MC}} P_{i_1+i_2}^{(x_1+x_2)I,(y_1+y_2+1)S}(m_1+m_2)$ $R_{pTot} = (i_1-x_1-y_1+i_2-x_2-y_2)k_{pMIapp}^{MC}\left[P_{i_1}^{x_1I,y_1S}(m_1)\right]\left[P_{i_2}^{x_2I,y_2S}(m_2)\right]$
	C_I	$P_{i_1}^{x_1I,y_1S}(m_1) + P_{i_2}^{x_2I,y_2S}(m_2) \xrightarrow{(x_1+x_2)k_{pIIapp}^{MC}} P_{i_1+i_2}^{(x_1+x_2-1)I,(y_1+y_2+1)S}(m_1+m_2)$ $R_{pTot} = (x_1+x_2)k_{pIIapp}^{MC}\left[P_{i_1}^{x_1I,y_1S}(m_1)\right]\left[P_{i_2}^{x_2I,y_2S}(m_2)\right]$
	C_S	$P_{i_1}^{x_1I,y_1S}(m_1) + P_{i_2}^{x_2I,y_2S}(m_2) \xrightarrow{(y_1+y_2)k_{pSIapp}^{MC}} P_{i_1+i_2}^{(x_1+x_2)I,(y_1+y_2)S}(m_1+m_2)$ $R_{pTot} = (y_1+y_2)k_{pSIapp}^{MC}\left[P_{i_1}^{x_1I,y_1S}(m_1)\right]\left[P_{i_2}^{x_2I,y_2S}(m_2)\right]$

3.3.1 Monte Carlo Model Development

First, a small reaction volume is selected and the corresponding number of molecules of each type that are contained within this volume is computed using equation 3.2. Since the copolymerization of IM and IB is performed in a solvent, any small changes in volume due to polymerization are neglected. Equation 3.6 and random number r_1 are used to determine the time interval Δt between reactions where R_{total}^{MC} is the sum of six reaction rates shown in Table 3.3.

Next, the type of reaction that occurs is calculated using random number r_2. The *j*th reaction is selected if:

$$\frac{\sum_{i=1}^{j-1} R_i^{MC}}{R_{total}^{MC}} < r_2 \leq \frac{\sum_{i=1}^{j} R_i^{MC}}{R_{total}^{MC}} \tag{3.9}$$

The next step is to randomly select a corresponding end group and vinyl group on molecules from the reacting mixture and to update the numbers of end groups and molecules of each type. To keep track of the required information for the arborescent system, a large $5 \times m$ matrix is constructed, where *m* is the initial number of inimer units in the system, as shown in Table 3.5. Each column of the matrix represents a single molecule with a V_I vinyl group (*i.e.*, either an IM molecule or a polymer molecule). As reactions proceed and V_I groups are consumed, the number of columns is reduced to match the number of V_I groups in the system. The first row of the matrix counts the number of inimer units in each molecule (and is initially a row with all values equal to 1). The second row counts the number of IB units in each molecule (and is initially a row with all values equal to 0). The remaining rows keep track of the number of different chloride end groups on each molecule. As a result, each column contains all the pertinent information about a single IM or polymer molecule in the small volume *V*.

Table 3.5 special matrix for counting IM and polymers

#	1	2	3	…	*m*-1	*m*	
IM	1	1	1	…	1	1	
IB	0	0	0	…	0	0	
C_I	1	1	1	…	1	1	
C_M	0	0	0	…	0	0	
C_S	0	0	0	…	0	0	5×*m*

To find the total number of C_I, C_M and C_S end groups and V_I vinyl groups in the small reaction volume, appropriate values from the matrix are added together or, to save computing time, counter variables C_{Itot}, C_{Mtot}, C_{Stot} and V_{Itot} can be used to track the total number of C_I, C_M and C_S end groups and V_I vinyl groups, respectively. Since r_2 determines which type of reaction occurs during the time step, the type of chloride end group and the type of vinyl group that will participate are known in each reaction step. For example, assume that the 3rd reaction from Table 3.3 is selected. The MC code then selects which polymer molecule the C_M end group belongs to using the following criterion, based on uniform random number r_3.

$$\frac{\sum_{i=1}^{c-1} C_{Mi}}{C_{Mtot}} < r_3 \leq \frac{\sum_{i=1}^{c} C_{Mi}}{C_{Mtot}} \tag{3.10}$$

where c is the number of the column that corresponds to the selected molecule and C_{Mi} is the number of C_M groups on the molecule whose information is stored in the ith column. In this way, the number of C_M end groups on each molecule influences the probability of the molecule being selected. For cases where reactions involve C_I or C_S end groups, the appropriate reacting molecule (in the cth) column is determined by finding c so that:

$$\frac{\sum_{i=1}^{c-1} C_{Ii}}{C_{Itot}} < r_3 \leq \frac{\sum_{i=1}^{c} C_{Ii}}{C_{Itot}} \tag{3.11}$$

and

$$\frac{\sum_{i=1}^{c-1} C_{Si}}{C_{Stot}} < r_3 \leq \frac{\sum_{i=1}^{c} C_{Si}}{C_{Stot}} \tag{3.12}$$

respectively. If the selected reaction involves consumption of a V_I group, a uniformly distributed random number r_4 is used to determine the column l that corresponds to the molecule with the V_I group that is consumed:

$$\frac{\sum_{i=1}^{l-1} V_{Ii}}{V_{Itot}} < r_4 \leq \frac{\sum_{i=1}^{l} V_{Ii}}{V_{Itot}} \tag{3.14}$$

If $c = l$, a new value of the random number r_4 must be selected, because loop formation is not considered in this MC model.

After the reacting molecules are decided, changes are recorded in the corresponding columns in Table 3.5, according to the reactions in Table 3.4. If the reaction involves two molecules with V_I groups (*i.e.*, either polymer or IM molecules) then one column is updated to reflect the structure of the new molecule and the other column is removed from the matrix. If a reaction involving a V_M vinyl group is selected, the number of columns does not change, but the total number of monomers in the small volume is reduced by one.

After each single reaction is finished, the reaction time is updated to t+Δt, obtained from equation 3.6, and random numbers are generated for the reaction at the next time step. This process is repeated until the whole simulation is terminated when $t + \Delta t$ reaches the specified end time or the desired conversion is reached.

At the end of the simulation, the resulting matrix, which contains information about all of the polymer molecules in the small volume V can be used to calculate the overall M_n, M_w, and MWD. Additionally, MWD can also be determined for different classes of polymer molecules that may be of interest (*e.g.*, molecules with different numbers of branch points).

3.4 Results

When MC simulations are undertaken, the results depend on the values of the random numbers that are generated. If a very small reaction volume, *V*, and small corresponding number of initial molecules is selected, then noticeably different results can be obtained for different random number sequences. When a larger number of initial molecules is used, the results tend to be more reliable and are less sensitive to the particular random number sequences generated. However, simulating more molecules leads to shorter time steps and to longer computational times.[35]

Figure 3.3a compares the MWD calculated from two different MC simulations with different initial numbers of IM molecules (50000 and 1500000, respectively), but the same starting recipe. Results from our previous PREDICI model are also shown.[15] The parameter values used are provided in Table 3.2 and the initial condition is $[\mathrm{IM}]_0 = 0.00454\, mol\, L^{-1}, [\mathrm{IB}]_0 = 1.74\, mol\, L^{-1}$. Note that the limitation of 15 branches per molecule was applied in the PREDICI model but was not applied in the MC simulations. The remaining assumptions are identical in both methods (see Table 3.1). Figure 3.3a clearly shows that using the larger initial number of IM molecules (corresponding to a reference volume that is 30 times bigger) provides a much smoother MWD than when only 50000 initial IM molecules are used. Unfortunately, running the simulation with 1500000 initial IM molecules took more than 2 weeks of computation time on a personal computer operating by Windows XP with Intel Core i5 2.4GHz and 2.92GB of RAM using a 32-bit 2010b version of Matlab. The corresponding simulation with 50000 initial IM molecules took approximately 20 minutes. Note that we did not optimize the implementation of the MC code in Matlab, and that there may be more efficient ways to perform the MC simulations that would result in shorter simulation times. One minor coding change that we investigated was to replace disappearing columns in the matrix in Table 3.5 with zeros rather than shrinking the matrix dimension as the simulation proceeds. This alternative increased the overall simulation times for the results shown in Figure 3.3a. Figure 3.3a shows that the largest molecules in the reaction

mixture have chain lengths of approximately 10^5, which is considerable smaller than the number of monomer units used in the MC simulations (*e.g.*, 1.9×10^7 initial IB molecules are present in the small reference volume for the case when 50000 initial IM molecules are considered).

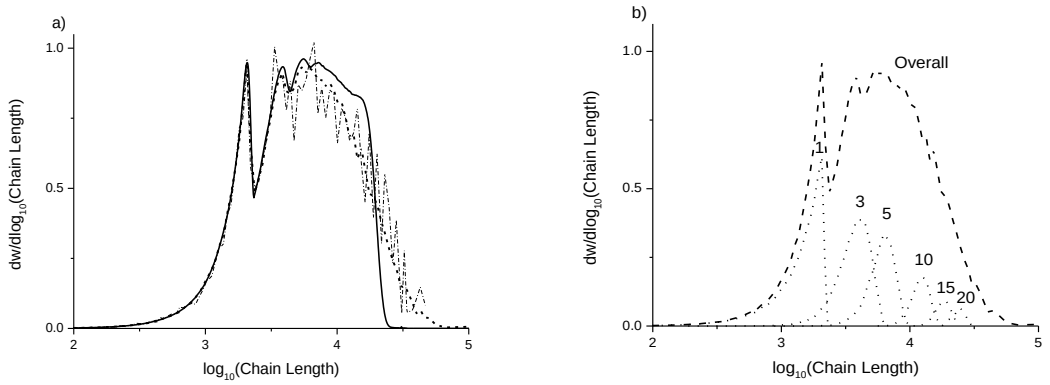

Figure 3.3 a) Comparison of predicted chainlength distributions obtained using different initial numbers of IM molecules – · – 50000, - - - 1500000 and ── PREDICI predictions; b) individual MWD curves for polymer molecules with different numbers of IM units from MC simulation with 1500000 initial IM molecules.

Note that the shapes of the MWD curves generated by the MC simulations are similar to the results from the PREDICI model, except for a discrepancy in the higher molecular weight tail, which is due to the limitation of only 15 branches per molecule that was applied in the PREDICI simulation to make the model tractable. The distinct lower-molecular weight peak located near DP = 2000, which appears in all three simulations, corresponds primarily to linear polymer molecules that contain only one IM molecule.[15] Figure 3.3b shows individual MWD curves for polymer molecules with different numbers of IM units. Notice that molecules with 20 inimer units (corresponding to B_{kin}=19) have a noticeable influence on the MWD, even though the average branching level is B_{kin}=7.4. The current MC model is a significant advance over our previous

PREDICI model because it will permit simulation of experimental data sets with measured values of B_{kin} up to 32.[12]

If only average properties are of interest, like M_n, M_w, overall branching levels and monomer concentrations (see Figure 3.4), then relatively accurate results can be obtained with a much smaller number of initial molecules. For example, we found that using only 10000 initial IM molecules provides relatively reliable results for these properties using these same experimental settings (not shown in this paper), requiring only 1.5 minutes for each simulation. (see Appendix 3.1) Long simulation times are only required when detailed information about the MWD or branching distribution is of interest.

Figure 3.4 compares predictions of average properties (*i.e.*, IM and IB concentration, M_n, M_w and B_{kin}) obtained from the MC model with those from our previous PREDICI model.[15] These comparisons show excellent agreement, except for M_w predictions at longer times where branching levels are highest. This discrepancy occurs because the PREDICI model under-predicts the M_w due to the upper limit of 15 branches that was assumed.

A great advantage of this MC model is that the assumptions 1-4 in Table 3.1 can be relaxed, which means that k_{pIIapp} and k_{pSIapp}, which were set to zero in the PREDICI model, can be included in the current MC model. Since no researchers have reported values for k_{pIIapp} and k_{pSIapp} and very few have performed SCVP experiments using this type of inimer, it is difficult to assign reasonable values for k_{pIIapp} and k_{pSIapp}. Dos Santos and Puskas[13,37] reported several SCVP experiments using MeOIM inimer, which we use here to obtain rough values for k_{pIIapp} and k_{pSIapp}. However, in their experiments, a low initial $TiCl_4$ concentration relative to the inimer concentration ([MeOIM] = 0.094 $mol\ l^{-1}$ and $[TiCl_4]_0$ = 0.06 $mol\ l^{-1}$) was used to prevent initial high reaction rates and an associated temperature spike. As a result, the expected rate constant values for k_{pIIapp} and k_{pSIapp} that we estimate from Dos Santos's SCVP polymerization may be smaller than their corresponding values using the experimental copolymerization settings simulated in Figures 3.3

and 3.4. Nevertheless, using these rough values ($k_{pIIapp} \approx 0.0075$ $L{\cdot}mol^{-1}{\cdot}s^{-1}$ and $k_{pSIapp} \approx 0.0001$ $L{\cdot}mol^{-1}{\cdot}s^{-1}$) is more realistic than setting values to zero or picking values randomly. These parameters values were obtained by manually adjusting k_{pIIapp} and k_{pSIapp} until a simple PREDICI inimer homopolymerization model (simulations shown in Appendix 3.2) gave a good match to conversion vs. time data obtained in the first stage of the IM homopolymerization, before additional $TiCl_4$ was added to the reacting mixture.

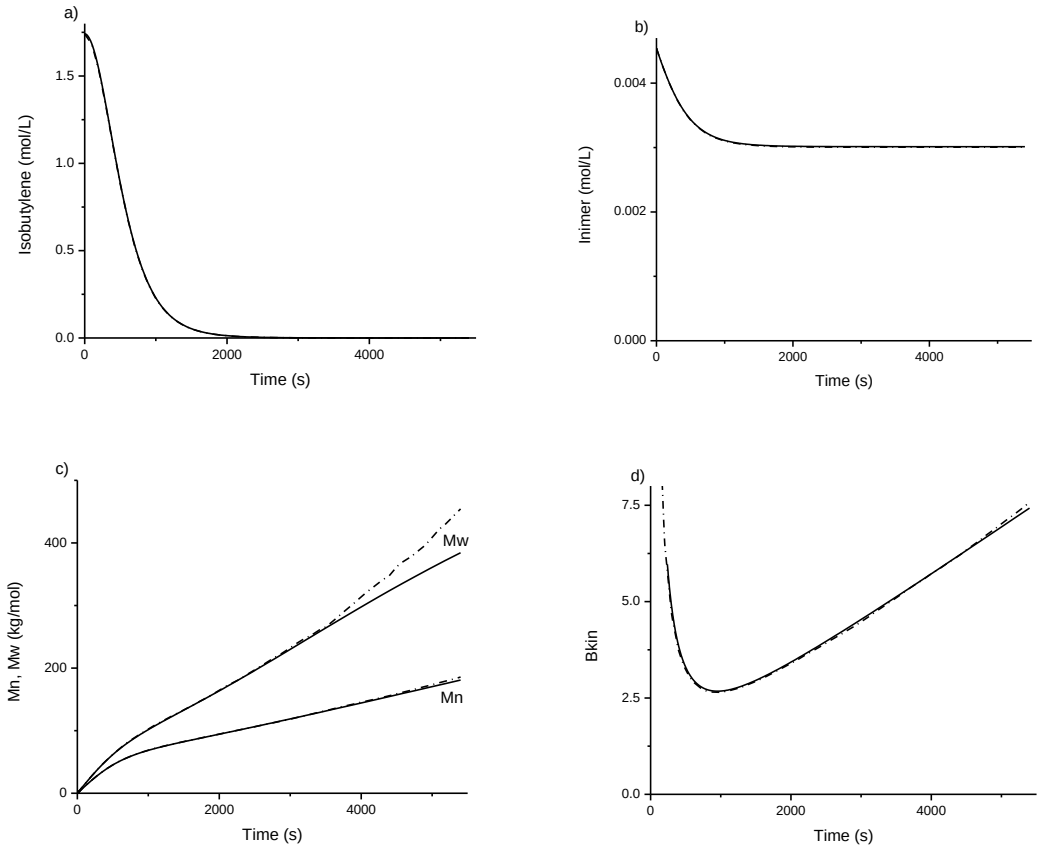

Figure 3.4 . Comparison between MC and PREDICI model predictions for simulations with $[IM]_0$ = 0.00454 M. The MC simulations used 50000 IM and 19162996 IB molecules initially – · – MC, ––– PREDICI. The MC results are difficult to see in a) because they overlap with the PREDICI results.

Figure 3.5 compares the results of MC simulations using all 6 propagation parameters with our previous results that used only the 4 parameters that were included in the PREDICI model (see Figure 3.4). There is a clear difference between the simulations conducted with and without the additional parameters, which lead to additional reactions 2, 4, 6, 7, 8, 9, 11 and 12 in Table 3.4**.** Large deviations were obtained for all of the variables shown in Figure 3.5, except for [IB]. Figure 3.5a shows that the isobutylene monomer was consumed at almost the same rate in both models. As expected, the IM is consumed faster in the model with all 6 parameters, particularly at longer reaction times due to the additional reactions that IM can participate in. For M_n, M_w and B_{kin}, the predicted results from the improved six-parameter model are lower than from the model with only 4 parameters. This interesting phenomenon is caused by the small but non-zero values of k_{pIIapp} and k_{pSIapp}. After 2000 s, there are very few IB molecules left in the system. As k_{pMIapp} is relatively high and single IM molecules are allowed to react with polymer chains, a large portion of the highly reactive C_M end groups are converted into less reactive C_S end groups via reaction 3. These C_S groups react much more slowly with V_I than C_M groups do. As a result, the overall rate of growth in degree of polymerization and branching is decreased, resulting in lower molecular weights and branching levels.

Although k_{pIIapp} and k_{pSIapp} were assigned relatively low values in the improved MC model, the deviations shown in Figure 3.5 indicate that these two parameters and the corresponding reactions may play an important role in the development of molecular weight and branching. The estimates that we used for k_{pIIapp} and k_{pSIapp} are highly uncertain and the estimates used for k_{pMMapp}, k_{pMIapp}, k_{pIMapp} and k_{pSMapp} (see Table 3.2) are inaccurate because they were obtained by assuming that $k_{pIIapp} = k_{pSIapp} = 0$ and that no molecules with > 15 IM units exist in the batch reactor. As a result, further parameter estimation studies are recommended so that reliable predictions of experimental data can be obtained, especially for *arborescent* PIB production with high branching levels.[9,12]

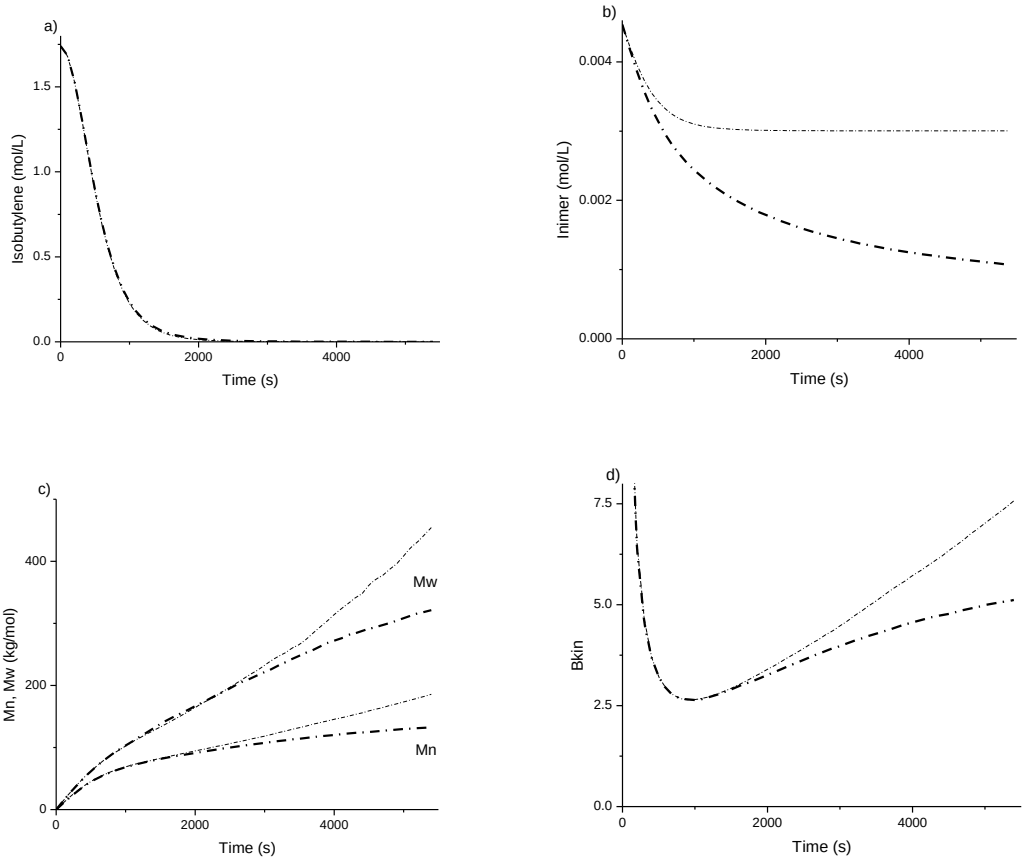

Figure 3.5 Comparison between MC model with only 4 parameters and MC model with all 6 parameters when $[IM]_0$ = 0.00454 M. Note that 50000 IM and 19162996 IB molecules are used initially in the MC simulations. The thinner dash-dot lines correspond to MC simulations with only 4 parameters and the thicker dash-dot lines correspond to MC model with 6 parameters. In a) the results are overlaid so that the thinner line cannot be seen.

Inimer homopolymerization can also be simulated by this MC model by assigning a zero initial value for the number of IB molecules. In the resulting SCVP system, there are only two types of chloride end groups (C_I and C_S) and one kind of vinyl group (V_I). As a result, there are only two different propagation rate constants (*i.e.*, k_{pIIapp} and k_{pSIapp}). Simulations shown in Figure 3.6 where conducted using k_{pIIapp} = 0.0075 $L{\cdot}mol^{-1}{\cdot}s^{-1}$ and k_{pSIapp} = 0.0001 $L{\cdot}mol^{-1}{\cdot}s^{-1}$, which are the same values used to generate Figure 3.5, used 2000000 initial IM molecules, requiring a simu-

lation time of several days. Even though the values assigned for apparent propagation rate constants may be low, the predicted consumption rate of IM is fast, with nearly all of the IM consumed within the first 10 minutes. As is common in condensation polymerizations, growth in the weight and number average molecular weight is slow at the beginning and then M_w increases rapidly when the conversion of IM is very high. As there is no monomer in the SCVP system other than the IM, the value of B_{kin} = 132.08 is the same as the average number of IM units per polymer chain, minus one. The final simulated polydispersity is 9.9. The chain length distribution shown in Figure 3.6d is quite jagged, indicating that a larger number of initial IM molecules and a longer simulation time would be required to obtain an accurate MWD curve.

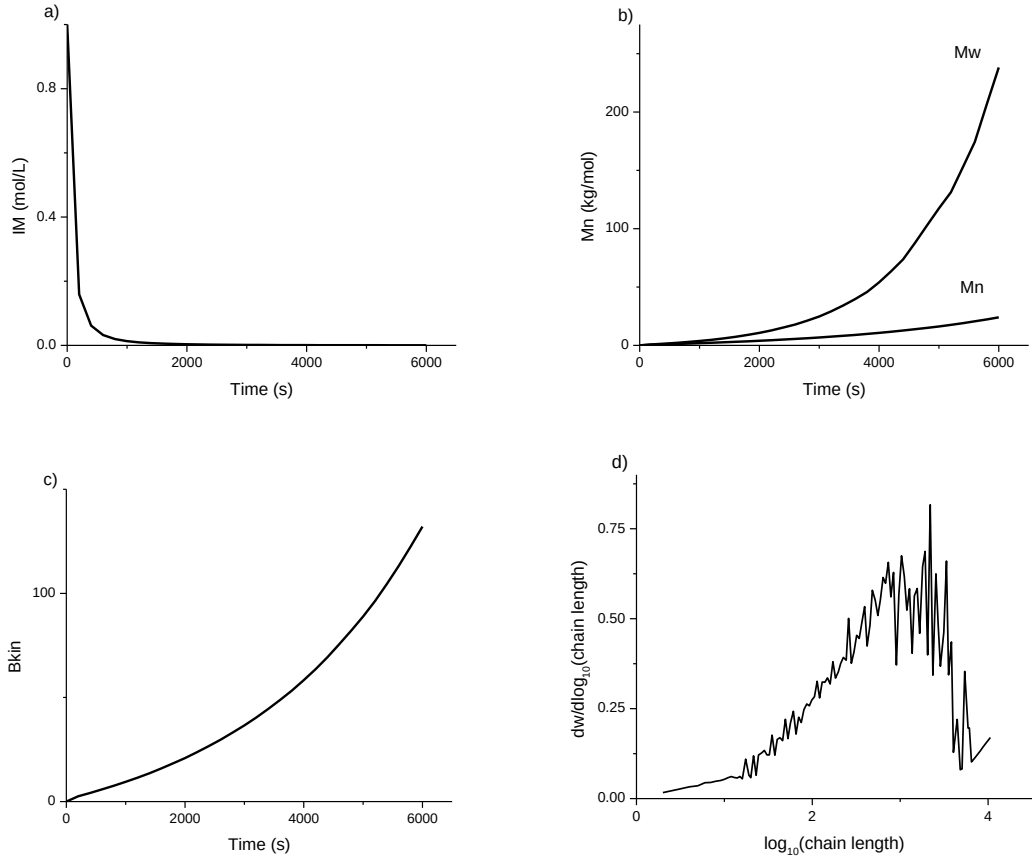

Figure 3.6 SCVP results with $[IM]_0$ = 1 M and 2000000 initial IM units

3.5 Conclusions

A MC model was developed to describe the arborescent copolymerization of isobutylene and inimer via carbocationic polymerization. Unlike previous self-condensing vinyl copolymerization models, the current model accommodates six different apparent propagation rate constants with different values. These rate constants are required to account for the two types of vinyl groups and three types of carbocations that appear in this copolymerization system. Simulation results that correspond to experimental conditions studied by Dos Santos,[13] reveal that a large initial number of IM and IB molecules (*e.g.*, 1500000 IM molecules and 574889868 IB molecules) must be simulated to obtain relatively smooth MWD curves. If only average properties (*e.g.*, M_n, M_w and average branching levels) are of interest, a much smaller initial number of IM and IB molecules is required (*e.g.*, 10000 IM molecules and 3832599 IB molecules) to obtain reliable simulation results.

Simulation results from this MC model were verified by comparing with results from a previous PREDICI material balance model. Simulation results confirm that the PREDICI model becomes inaccurate as branching levels increase, due to simplifying assumptions that were required to keep the material balance model tractable. The MC model is much more powerful than the PREDICI material balance model, because it can simulate copolymerization recipes that result in high branching levels (*i.e.*, when some molecules have > 15 branches) and also because the model can simulate inimer homopolymerization. Inimer homopolymerization simulations conducted using the model confirm that the molecular weight behavior is similar to that encountered during condensation polymerizations, with a slow initial rise in degree of polymerization, followed by a dramatic increase at long reaction times where conversion is high. Systematic parameter estimation will be required so that accurate simulation results can be obtained and model predictions can be tested using experimental data with high branching levels.[9,12] Unfortunately, long computation times encountered using this MC model would make computation times for parame-

ter estimation prohibitively long unless powerful computers are used. Alternative MC models that use conditional MC techniques and more advanced material balance models should be developed in future to enable parameter estimation and to provide accurate predictions using less computational effort.

3.6 Reference

1 C. Götz, G. T. Lim, J. E. Puskas, V. Altstädt, *Journal of the Mechanical Behavior of Biomedical Materials*, **2012**, 10, 206

2 J. E. Puskas, Y. H. Chen, *Biomacromolecules.* **2004**, 5(4), 1141

3 J. E. Puskas, Y. H. Chen, Y. Dahman, D. Padavan, *J. Polym. Sci. A.*, **2004**, 42(13), 3091

4 J. E. Puskas, M. Grasmüller, *Macromol. Chem. Macromol. Symp.* **1998**, 132, 117

5 J. E. Puskas, C. Paulo, P. Antony *US 6,747,*098, **2004**.

6 G.T. Lim, J.E. Puskas, D. H. Reneker, A. Jakli, W. E. Horton, Jr. *Biomacromolecules.* **2011**, 12, 1795

7 G. T. Lim, S. A. Valente, C. R. Hart-Spicer, M. M. Evancho-Chapman, J. E. Puskas, W. I. Horne, S.P. Schmidt. *Journal of the mechanical behavior of biomedical materials*. **2013**, 21, 47

8 J. E. Puskas, E. A. Foreman-Orlowski, G. T. Lim, S. E. Porosky, M.M. Evancho-Chapman, S.P. Schmidt, M.E. Fray, M. Piatek, P. Prowans, K. Lovejoy, *Biomaterials*. **2010**, 31, 2477

9 C. Paulo, J. E. Puskas, *Macromolecules.* **2001**, 34, 734

10 J. E. Puskas, Y. Kwon. *Polym. Adv. Technol.* **2006**, 17, 615

11 J. E. Puskas, L. M. Dos Santos, G. Kaszas, K. Kulbaba, *J. Polym. Sci. Part A: Polym. Chem.* **2009**, 47, 1148

12 E. A. Foreman, J. E. Puskas, G. Kaszas, *J. Polym. Sci. Part A: Polym. Chem.* **2007**, 45, 5847

13 L. M. Dos Santos, Ph.D. thesis, University of Akron, Akron, USA, May, **2009**

14 C. Paulo, Ph.D. thesis, the University of Western Ontario, London, Canada, August, **2000**

15 Y. R. Zhao, K. B. McAuley, J. E. Puskas, L. M. Dos Santos, A. Alvarez. *Macromol. Theory Simul.* **2013**, 22, 155

16 J. E. Puskas, S. Shaikh, K. Z. Yao, K. B. McAuley, G. Kaszas, *European Polymer Journal*.

2005, 41, 1

17 J. M. J. Fréchet, M. Henmi, I. Gitsov, S. Aoshima, M. R. Leduc, R. B. Grubbs, *Science.* **1995**, 269, 1080

18 A. H. E. Müller, D. Yan, M. Wulkow, *Macromolecules.* **1997**, 30, 7015

19 D. Yan, A. H. E. Müller, K. Matyjaszewski, *Macromolecules.* **1997**, 30, 7024

20 G. I. Litvinenko, P. F. W. Simon, A. H. E. Müller, *Macromolecules.* **1999**, 32, 2410

21 G. I. Litvinenko, P. F. W. Simon, A. H. E. Müller, *Macromolecules.* **2001**, 34, 2418

22 G. I. Litvinenko, A. H. E. Müller, *Macromolecules.* **2002**, 35, 4577

23 K. C. Cheng, T. H. Chuang, J. S. Chang, W. Guo, W. F. Su, *Macromolecules* **2005**, 38, 8252

24 K. C. Cheng, Y. Y. Su, T. H. Chuang, W. Guo, W. F. Su, *Macromolecules.* **2010**, 43, 8965

25 A. Zargar, K. Chang, L. J. Taite, F.J. Schork, *Macromol. React. Eng*. **2011**, 5, 373

26 X. He, H. Liang, C. Pan, *Polymer* **2003**, 44, 6697

27 X. He, J. Tang, *J. Polym. Sci. Part A: Polym. Chem*. **2008**, 46, 4486-4494

28 X. He, H. Liang, C. Pan, *Macromol. Theory Simul*. **2001**, 10, 196

29 J. E. Puskas, H. Peng, *Polym. React. Eng*. **1999**, 7(4), 553

30 J. E. Puskas, S. W. P. Chain, K. B. McAuley, G. Kaszas, S. Shaikh, *J. Polym. Sci. Part A: Polym. Chem.* **2007**, 45, 1778-1787

31 He, H. Zhang, J. Chen, Y. Yang, *Macromolecules*. **1997**, 30, 8010

32 L. Nie, W. Yang, H. Zhang, S. Fu, *Polymer*. **2005**, 46, 3175

33 M. A. Al-Harthi, J. K. Masihullah, S. H. Abbasi, J. B. P. Soares, *Macromol. Theory Simul*. **2009**, 18, 307

34 M. Al-Harthi, M. J. Khan, S. H. Abbasi, J. B. P. Soares, *Macromol. React. Eng.* **2009**, 3, 148

35 D. T. Gillespie, *Journal of Physical Chemistry.* **1977**, 81(25), 2340

36 J. B. P. Soares, A. E. Hamielec, *Macromol. React. Eng.* **2007**, 1. 53

37 L. M. Dos Santos, J. E. Puskas. *Polymer Preprints*, **2008**, *49*, 87

Appendix 3.1 MC Simulation with Only 10000 Initial IM Molecules

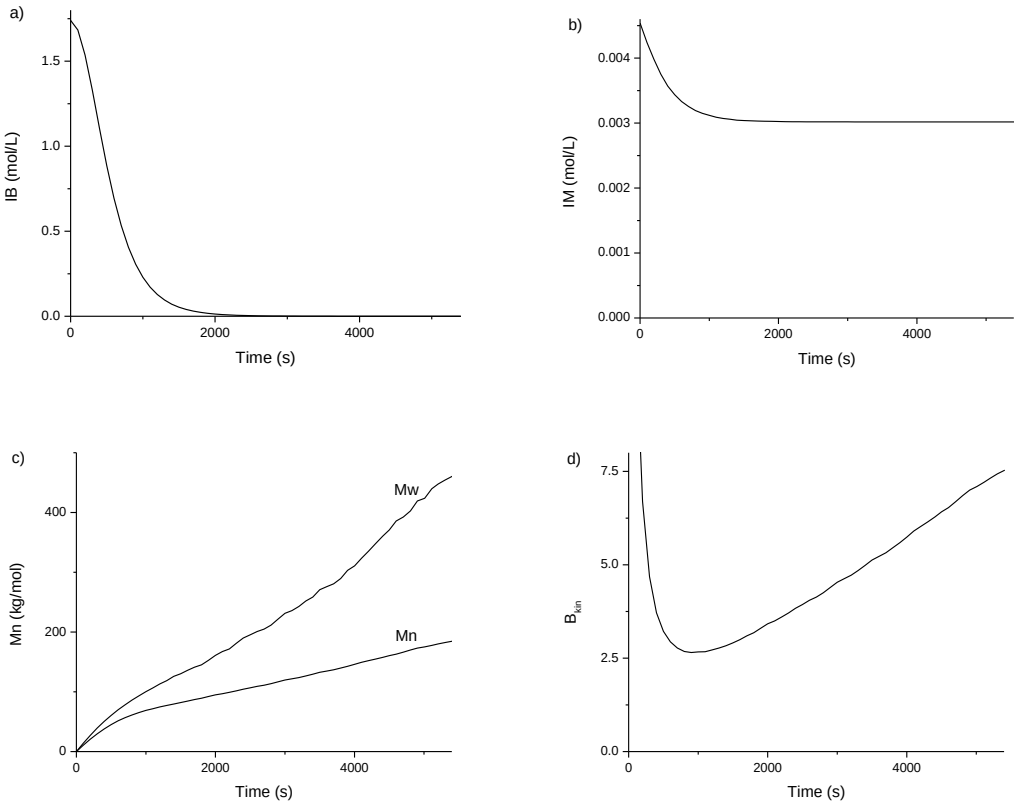

Figure 3.7 MC predictions for simulations with $[IM]_0$ = 0.00454 M. The MC simulations used 10000 IM and 3832599 IB molecules initially. These figures agree well with the MC simulations in Figure 3.4 for less computing time.

Appendix 3.2 Simple PREDICI Simulation for k_{pIIapp} And k_{pSIapp}

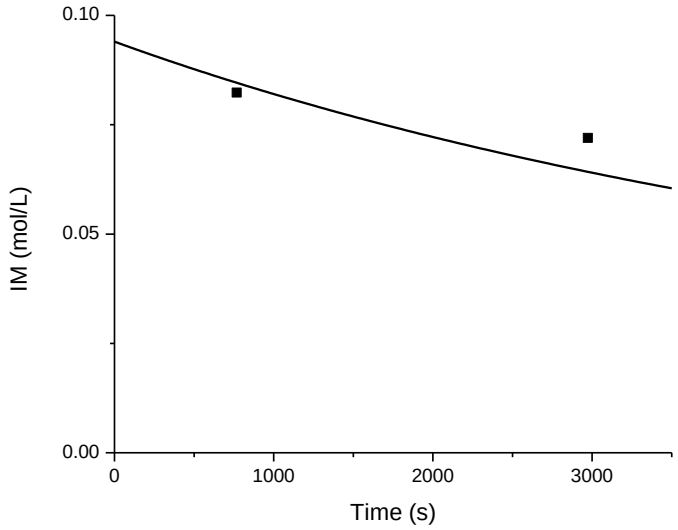

Figure 3.8 PREDICI rough simulation results for k_{pIIapp} = 0.00075 $Lmol^{-1}s^{-1}$ and k_{pSIapp} = 0.00001 $Lmol^{-1}s^{-1}$ with experimental data. ── simulation results; ■ is the experimental data.

Figure 3.8 shows that rough estimates of $k_{pIIapp} = 0.00075\, L \cdot mol^{-1} \cdot s^{-1}$ and $k_{pSIapp} = 0.00001\, L \cdot mol^{-1} \cdot s^{-1}$ can do a reasonable job of matching the homopolymerization data of Dos Santos et al.[37] when we assume that all of the MeOIM initially in the reactor was converted to IM. Note, however, that this assumption is not valid because there was initially insufficient $TiCl_4$ in the batch reactor to completely convert the MeOIM into active IM.[13,37] As a result, the estimated values of k_{pIIapp} and k_{pSIapp} above are likely much too small. If we assume, somewhat arbitrarily, that about 10% of the MeOIM was converted to IM, then the following values are more appropriate: $k_{pIIapp} = 0.0075\ \ L \cdot mol^{-1} \cdot s^{-1}$ and $k_{pSIapp} = 0.0001\ L \cdot mol^{-1} \cdot s^{-1}$. These values were used as rough order-of-magnitude values for the simulations in this chapter and as starting values for the parameter estimation study in Chapter 5.

Appendix 3.3 Matlab Code for MC Model with Six Parameters

Here is the Matlab code used to generate the Figures 3.5 and 3.6. This MC model contains all six parameters.

```
function [] = SCVCP(IM,IB)
   tic;  %calculate the computing time for one simulation

   %reaction time and condition:
   t = 0;              %initial time of the batch
   ti = 300;           %time interval for average properties in the sum_mat shown later
   tf = 5400;          %end time of the batch
   ml = 1.74           %concentration of IB
   const = IB/ml;      %Used for calculate of kpMC=kp*Cj/Nj

   %counters for reaction species and other properties:
   VmTot = IB;
   CiTot = IM;
   CmTot = 0;
   CsTot = 0;
   column = IM;
   pol_sum = 0;
   Mn_sum = 0;
   Mw_sum = 0;
   Br_sum = 0;

   % rate constants:
   % Estimated values from parallel PREDICI model
%     kpII = 3.32E-2/const;
%     kpIM = 4.46E-4/const;
%     kpMI = 5.19E-1/const;
%     kpMM = 2.27/const;
%     kpSI = 6.45E-3/const;
%     kpSM = 4.11E-5/const;

   % Estimated values from lengthy PREDICI model
   kpII = 0.0075/const;
   kpIM = 0.000399/const;
   kpMI = 0.195/const;
   kpMM = 2.126/const;
   kpSI = 0.0001/const;
   kpSM = 0.0139/const;

   % Beautiful matrix that keep the information of IM and polymers:
   matIM = ones(1,IM);
   matIB = zeros(1,IM);
   matCi = ones(1,IM);
   matCm = zeros(1,IM);
   matCs = zeros(1,IM);
   mat = [matIM; matIB; matCi; matCm; matCs];
   sum_mat = zeros(1,6);
   row = 0;

   %%%%%%%%%%%%%%%%%%%%%%%%%%%%%%%%%%%%%%%%%%%%%%%%%%%%%%%%%%%%%%%%%%%%%%%%
```

```
%reaction starts and continues in this while loop:
%%%%%%%%%%%%%%%%%%%%%%%%%%%%%%%%%%%%%%%%%%%%%%%%%%%%%%%
while ((t <= tf) && (column > 5))

    %MC reaction rates
    re1 = kpIM*CiTot*VmTot;   %Ci+Vm
    re2 = kpMM*CmTot*VmTot;   %Cm+Vm
    re3 = kpMI*CmTot*column;  %Cm+Vi
    re4 = kpSM*CsTot*VmTot;   %Cs+Vm
    re5 = kpSI*CsTot*column;  %Cs+Vi
    re6 = kpII*CiTot*column;  %Ci+Vi
    reTot = re1+re2+re3+re4+re5+re6;   %total reaction speed

    % possibilities for choosing from different reactions
    p1 = re1/reTot;
    p2 = (re1+re2)/reTot;
    p3 = (re1+re2+re3)/reTot;
    p4 = (re1+re2+re3+re4)/reTot;
    p5 = (re1+re2+re3+re4+re5)/reTot;
    p6 = 1;

    % Obtaining polymer properties at different time points
    if t > ti
        ti = ti + 300;              %increase time interval
        display(t);                 %the actual time for each time point
        row = row + 1;          %increase one row in sum_mat for average information

        % update the concentrations of different end groups and vinyl groups
        IB_Con = VmTot/const;
        Vi_Con = column/const;
        Ci_Con = CiTot/const;
        Cm_Con = CmTot/const;
        Cs_Con = CsTot/const;

        % set to zero for calculations of polymer chains, Mn, Mw and Br
        pol_sum = 0;
        Mn_sum = 0;
        Mw_sum = 0;
        Br_sum = 0;

        %Calculate Mn & Mw
        for col = 1 : column
            if (mat(1,col) ~= 1) | (mat(2,col) ~= 0)      %find polymer chains from the matrix
                pol_sum = pol_sum + 1;
                Mn_sum = Mn_sum + mat(1,col)*0.1805 + mat(2,col)*0.056;
                Mw_sum = Mw_sum + (mat(1,col)*0.1805 + mat(2,col)*0.056)^2;
                Br_sum = Br_sum + mat(1,col);
            end
        end
        Mn = Mn_sum/pol_sum;         %Mn for polymers
        Mw = Mw_sum/Mn_sum;       %Mw for polymers
        IM_Con = (column - pol_sum)/const;
        %Mntheory = 0.056*(IB - VmTot)/IM + 0.1805; % This is the approximate way of calculation in
1st paper
        %Bkin = Mn/Mntheory -1;
```

```
    Bkin = Br_sum/pol_sum -1;    %accurate calculation also used in parallel PREDICI model
    sum_mat(row,1) = t;
    sum_mat(row,2) = IB_Con;
    sum_mat(row,3) = IM_Con;
    sum_mat(row,4) = Mn;
    sum_mat(row,5) = Mw;
    sum_mat(row,6) = Bkin;
end

%%%%%%%%%%%%%%%%%%%%%%%%%%%%%%%%%%%%%%%%%%%%%%%%%%%%%%%%%%%%%%%%%%%%%%%%%%%%
%Reaction happens from here
%%%%%%%%%%%%%%%%%%%%%%%%%%%%%%%%%%%%%%%%%%%%%%%%%%%%%%%%%%%%%%%%%%%%%%%%%%%%

%calculation for the time interval deciding the next reaction happen
r1 = rand;                    %random number
tau = log(1/r1)/reTot;      %delta t
t = t + tau;                   %the time when next reaction happen

%using random r2 to decide which reaction to happen after the delta t
r2 = rand;

%%%%%%%%%%%%%%%%%%%%%%%%%%%%%%%%%%%%%%%%%%%%%%%%%%%%%%%%%%%%%%%%%%%%%%%%%%%%
%1.Ci+Vm
%%%%%%%%%%%%%%%%%%%%%%%%%%%%%%%%%%%%%%%%%%%%%%%%%%%%%%%%%%%%%%%%%%%%%%%%%%%%
if (0 < r2) & (r2 <= p1)
    r3 = rand;      %select the molecule having this Ci group
    j = 0;
    sum = 0;        %sum of the Ci on polymer molecules

    for i = 1:column,
        j = j + 1;
        sum  = sum + mat(3,j);
        if sum > r3*CiTot
            break;
        end
    end

    mat(2,j) = mat(2,j) + 1;      %number of IB plus 1
    mat(3,j) = mat(3,j) - 1;      %number of Ci group minus 1
    mat(4,j) = mat(4,j) + 1;      %number of Cm group plus 1
    CiTot = CiTot - 1;             %total number of Ci minus 1
    CmTot = CmTot + 1;            %total number of Cm plus 1
    VmTot = VmTot - 1;            %total number of Vm minus 1

%%%%%%%%%%%%%%%%%%%%%%%%%%%%%%%%%%%%%%%%%%%%%%%%%%%%%%%%%%%%%%%%%%%%%%%%%%%%
%2.Cm+Vm
%%%%%%%%%%%%%%%%%%%%%%%%%%%%%%%%%%%%%%%%%%%%%%%%%%%%%%%%%%%%%%%%%%%%%%%%%%%%
elseif ( p1 < r2) & (r2 <= p2)
    r3 = rand;      %select the molecule having this Cm group
    j = 0;
    sum = 0;        %sum of the Cm on polymer molecules

    for i = 1:column,
        j = j + 1;
        sum  = sum + mat(4,j);
```

```
        if sum > r3*CmTot
            break;
        end
    end

    mat(2,j) = mat(2,j) + 1;     %number of IB plus 1
    VmTot = VmTot - 1;        %total number of Vm minus 1

%%%%%%%%%%%%%%%%%%%%%%%%%%%%%%%%%%%%%%%%%%%%%%%%%%%%%%%%%%%%%%%%%%%%%%%
%3.Cm+Vi
%%%%%%%%%%%%%%%%%%%%%%%%%%%%%%%%%%%%%%%%%%%%%%%%%%%%%%%%%%%%%%%%%%%%%%%
elseif (p2 < r2) & (r2 <= p3)
    r3 = rand;     %select the molecule having this Cm group
    j = 0;
    sum = 0;       %sum of the Cm on polymer molecules

    for i = 1:column,
        j = j + 1;
        sum  = sum + mat(4,j);
        if sum > r3*CmTot
            break;
        end
    end

    r4 = rand;                %select the molecule having this Vi group
    l = ceil(r4*column);
    while (l == j)           %avoid the molecule to react with itself
        r4 = rand;
        l = ceil(r4*column);
    end

    mat(1,j) = mat(1,j) + mat(1,l);        %IM
    mat(2,j) = mat(2,j) + mat(2,l);        %IB
    mat(3,j) = mat(3,j) + mat(3,l);        %Ci
    mat(4,j) = mat(4,j) + mat(4,l) - 1;   %number of Cm group minus 1
    mat(5,j) = mat(5,j) + mat(5,l) + 1;   %number of Cs group plus 1
    mat(:,l) = [];                          %delete the lth molecule
    CmTot = CmTot - 1;                   %Cm - 1
    CsTot = CsTot + 1;                    %Cs + 1

%%%%%%%%%%%%%%%%%%%%%%%%%%%%%%%%%%%%%%%%%%%%%%%%%%%%%%%%%%%%%%%%%%%%%%%
%4.Cs+Vm
%%%%%%%%%%%%%%%%%%%%%%%%%%%%%%%%%%%%%%%%%%%%%%%%%%%%%%%%%%%%%%%%%%%%%%%
elseif (p3 < r2) & (r2 <= p4)
    r3 = rand;     %select the molecule having this Cs group
    j = 0;
    sum = 0;       %sum of the Cs on polymer molecules

    for i = 1:column,
        j = j + 1;
        sum  = sum + mat(5,j);
        if sum > r3*CsTot
            break;
        end
    end
```

```
    mat(2,j) = mat(2,j) + 1;       %IB + 1
    mat(4,j) = mat(4,j) + 1;       %Cm + 1
    mat(5,j) = mat(5,j) - 1;       %Cs - 1
    CmTot = CmTot + 1;
    CsTot = CsTot - 1;
    VmTot = VmTot - 1;

%%%%%%%%%%%%%%%%%%%%%%%%%%%%%%%%%%%%%%%%%%%%%%%%%%%%%%%%%%%%%%%%%%%%%%%
%5.Cs+Vi
%%%%%%%%%%%%%%%%%%%%%%%%%%%%%%%%%%%%%%%%%%%%%%%%%%%%%%%%%%%%%%%%%%%%%%%
elseif (p4 < r2) & (r2 <= p5)
    r3 = rand;     %select the molecule having this Cs group
    j = 0;
    sum = 0;       %sum of the Cs on polymer molecules

    for i = 1:column,
        j = j + 1;
        sum  = sum + mat(5,j);
        if sum > r3*CsTot
            break;
        end
    end

    r4 = rand;           %select the molecule having this Vi group
    l = ceil(r4*column);
    while (l == j)      %avoid the molecule to react with itself
        r4 = rand;
        l = ceil(r4*column);
    end

    mat(1,j) = mat(1,j) + mat(1,l);   %IM
    mat(2,j) = mat(2,j) + mat(2,l);   %IB
    mat(3,j) = mat(3,j) + mat(3,l);   %Ci
    mat(4,j) = mat(4,j) + mat(4,l);   %number of Cm group minus 1
    mat(5,j) = mat(5,j) + mat(5,l);   %number of Cs group plus 1
    mat(:,l) = [];                        %delete the lth molecule

%%%%%%%%%%%%%%%%%%%%%%%%%%%%%%%%%%%%%%%%%%%%%%%%%%%%%%%%%%%%%%%%%%%%%%%
%6.Ci+Vi
%%%%%%%%%%%%%%%%%%%%%%%%%%%%%%%%%%%%%%%%%%%%%%%%%%%%%%%%%%%%%%%%%%%%%%%
elseif (p5 < r2) & (r2 <= p6)
    r3 = rand;     %select the molecule having this Ci group
    j = 0;
    sum = 0;       %sum of the Ci on polymer molecules

    for i = 1:column,
        j = j + 1;
        sum  = sum + mat(3,j);
        if sum > r3*CiTot
            break;
        end
    end

    r4 = rand;           %select the molecule having this Vi group
```

```
        l = ceil(r4*column);
        while (l == j)      %avoid the molecule to react with itself
            r4 = rand;
            l = ceil(r4*column);
        end

        mat(1,j) = mat(1,j) + mat(1,l);        %IM
        mat(2,j) = mat(2,j) + mat(2,l);        %IB
        mat(3,j) = mat(3,j) + mat(3,l) - 1;    %Ci
        mat(4,j) = mat(4,j) + mat(4,l);        %number of Cm group minus 1
        mat(5,j) = mat(5,j) + mat(5,l) + 1;    %number of Cs group plus 1
        mat(:,l) = [];                          %delete the lth molecule
        CiTot = CiTot - 1;
        CsTot = CsTot + 1;
    end
    column = size(mat,2);                      %update the number of columns in the matrix
end

%%%%%%%%%%%%%%%%%%%%%%%%%%%%%%%%%%%%%%%%%%%%%%%%%%%%%%%%%%%%%%%%%%%%%%%%%%%%%%%
%Reaction stops and calculate the properties at the end of batch
%%%%%%%%%%%%%%%%%%%%%%%%%%%%%%%%%%%%%%%%%%%%%%%%%%%%%%%%%%%%%%%%%%%%%%%%%%%%%%%

display(t);           %end time of the batch
row = row + 1;    %add a row in sum_mat for polymer information at the end of batch

%update concentrations of different end groups and vinyl groups
IB_Con = VmTot/const;
Vi_Con = column/const;
Ci_Con = CiTot/const;
Cm_Con = CmTot/const;
Cs_Con = CsTot/const;
Vi = column;

%add a new row in matrix to store total chain length IB+IM
mat = [mat; zeros(1,column)];
for col = 1 : column
    mat(6,col) = mat(1,col) + mat(2,col);
end

%delete IMs in the matrix
col = 1;
while (col <= column)
    if mat(6,col) == 1
        mat(:,col) = [];
        column = column - 1;
    else
        col = col + 1;
    end
end

%Calculate Mn & Mw
Mn_sum = 0;
Mw_sum = 0;
Br_sum = 0;
for col = 1 : column      %here column is just polymers
```

```
    Mn_sum = Mn_sum + mat(1,col)*0.1805 + mat(2,col)*0.056;
    Mw_sum = Mw_sum + (mat(1,col)*0.1805 + mat(2,col)*0.056)^2;
    Br_sum = Br_sum + mat(1,col);
  end
  Mn = Mn_sum/column;          %Mn for polymers
  Mw = Mw_sum/Mn_sum;      %Mw for polymers
  IM_Con = (Vi - column)/const;
  %Mntheory = 0.056*(IB - VmTot)/IM + 0.1805;
  %Bkin = Mn/Mntheory -1;
  Bkin = Br_sum/column - 1;
  sum_mat(row,1) = t;
  sum_mat(row,2) = IB_Con;
  sum_mat(row,3) = IM_Con;
  sum_mat(row,4) = Mn;
  sum_mat(row,5) = Mw;
  sum_mat(row,6) = Bkin;

  % reorder all the polymer molecules from the smallest to the largest
  for i = 1 : column
    min_value = mat(6,i);
    min_col = i;
    for j = i : column
      if  min_value > mat(6,j)
        min_value = mat(6,j);
        min_col = j;
      end
    end
    temp = mat(:,i);
    mat(:,i) = mat(:,min_col);
    mat(:,min_col) = temp;
  end

  % Build GPC histogram
  col = 1;                    %column number of polymer matrix
  range = 0.03;               %size of the bin
  GPC_log = zeros(1,5);       %GPC results
  GPC_row = 1;                %the row in GPC results matrix
  for value = 0 : range : 6   %put polymer chains into different bins
    sum = 0;                  %sum the number of units (IB+IM) in each bin
    count = 0;                %count the number of polymers in each bin
    while (col <= column) && (log10(mat(6,col)) > value) && (log10(mat(6,col)) <= (value +

range))
      sum  = sum + mat(6,col);
      count = count + 1;
      col = col + 1;
    end
    if sum ~= 0
      GPC_log(GPC_row,1) = value;          %current value of the lower side of the bin
      GPC_log(GPC_row,2) = sum/count;   %average chain size
      GPC_log(GPC_row,3) = log(10)*sum*GPC_log(GPC_row,2);  %wlog(r)
      GPC_log(GPC_row,4) = sum;            %w(r)
      GPC_log(GPC_row,5) = count;          %n(r)
      GPC_row = GPC_row + 1;               %add a row for next bin information
    end
```

```
    end

    %%%%%%%%%%%%%%%%%%%%%%%%%%%%%%%%%%%%%%%%%%%%%%%%%%%%%%%%%%%%%%%%%%%%%%%
    %output results into Excel
    %%%%%%%%%%%%%%%%%%%%%%%%%%%%%%%%%%%%%%%%%%%%%%%%%%%%%%%%%%%%%%%%%%%%%%%

    mat = mat';
    xlswrite('C:\Users\zhaoyu\Desktop\Thesis_Appendix.xlsx',mat,'test','A1');
    xlswrite('C:\Users\zhaoyu\Desktop\Thesis_Appendix.xlsx',GPC_log,'test','H1');
    xlswrite('C:\Users\zhaoyu\Desktop\Thesis_Appendix.xlsx',sum_mat,'test','P1');

    toc
end
```

Appendix 3.4 Matlab Code for MC Model with Four Parameters

Here is the Matlab code used to generate the Figures 3.3 to 3.5. This MC model applied the assumptions that k_{pIIapp} and k_{pSIapp} are neglected from the model.

```
function [] = SCVCP_as(IM,IB)
   tic;  %calculate the computing time for one simulation

   % reaction time and condition:
   t = 0;              %initial time of the batch
   ti = 300;           %time interval for average properties in the sum_mat shown later
   tf = 5400;          %end time of the batch
   ml = 1.74           %concentration of IB
   const = IB/ml;    %Used for calculate of kpMC=kp*Cj/Nj

   % counters for reaction species and other properties:
   VmTot = IB;
   CiTot = IM;
   CmTot = 0;
   CsTot = 0;

   pol_sum = 0;
   Mn_sum = 0;
   Mw_sum = 0;

   % rate constants:
   %Estimated values from lengthy PREDICI model
   kpIM = 0.000399/const;
   kpMM = 2.126/const;
   kpMI = 0.195/const;
   kpSM = 0.0139/const;

   % beautiful matrix that keep the information of IM and polymers
   % this is a little different from the one with 6 parameters
   % here are two matrix are used to take down the information
   % one matrix for IM and one matrix for polymers
   matIM = ones(1,IM);
   matIB = zeros(1,IM);
   matCi = ones(1,IM);
   matCm = zeros(1,IM);
   matCs = zeros(1,IM);
   mat = [matIM; matIB; matCi; matCm; matCs];  % a matrix for IM
   polymer = [];                                    % a matrix just for polymer
   sum_mat = zeros(1,6);
   row = 0;


   %%%%%%%%%%%%%%%%%%%%%%%%%%%%%%%%%%%%%%%%%%%%%%%%%%%%%%%%%%%%%%%%%%%%%%%%%%%%%%%%
   % reaction starts and continues in this while loop:
   %%%%%%%%%%%%%%%%%%%%%%%%%%%%%%%%%%%%%%%%%%%%%%%%%%%%%%%%%%%%%%%%%%%%%%%%%%%%%%%%
   while (t <= tf)
      inimer = size(mat,2);          %count the number of IM
      column = size(polymer,2);   %count the number of polymer
```

```
% MC reaction rates
re1 = kpIM*inimer*VmTot;     %Ci+Vm
re2 = kpMM*CmTot*VmTot;  %Cm+Vm
re3 = kpMI*CmTot*column;    %Cm+Vi
re4 = kpSM*CsTot*VmTot;     %Cs+Vm
reTot = re1+re2+re3+re4;        %total reaction speed

% possibilities for choosing from different reactions
p1 = re1/reTot;
p2 = (re1+re2)/reTot;
p3 = (re1+re2+re3)/reTot;
p4 = 1;

% Obtaining polymer properties at different time points
if t > ti
   ti = ti + 300;          %increase time interval
   display(t);             %the actual time for each time point
   row = row + 1;       %increase one row in sum_mat for average information

   % update the concentrations of different end groups and vinyl groups
   IB_Con = VmTot/const;
   %Vi_Con = (column + inimer)/const;
   Ci_Con = CiTot/const;
   Cm_Con = CmTot/const;
   Cs_Con = CsTot/const;

   % set to zero for calculations of polymer chains, Mn, Mw and Br
   pol_sum = 0;
   Mn_sum = 0;
   Mw_sum = 0;

   %Calculate Mn & Mw
   for col = 1 : column
      pol_sum = pol_sum + 1;
      Mn_sum = Mn_sum + polymer(1,col)*0.1805 + polymer(2,col)*0.056;
      Mw_sum = Mw_sum + (polymer(1,col)*0.1805 + polymer(2,col)*0.056)^2;
   end
   Mn = Mn_sum/pol_sum;        %Mn for polymers
   Mw = Mw_sum/Mn_sum;       %Mw for polymers
   inimer = size(mat,2);
   IM_Con = inimer/const;
   Mntheory = 0.056*(IB - VmTot)/IM + 0.1805;
   Bkin = Mn/Mntheory -1;
   sum_mat(row,1) = t;
   sum_mat(row,2) = IB_Con;
   sum_mat(row,3) = IM_Con;
   sum_mat(row,4) = Mn;
   sum_mat(row,5) = Mw;
   sum_mat(row,6) = Bkin;
end

%%%%%%%%%%%%%%%%%%%%%%%%%%%%%%%%%%%%%%%%%%%%%%%%%%%%%%%%%%%%%%%%%%%%%%%%%%%%
%Reaction happens from here
%%%%%%%%%%%%%%%%%%%%%%%%%%%%%%%%%%%%%%%%%%%%%%%%%%%%%%%%%%%%%%%%%%%%%%%%%%%%
```

```
%calculation for the time interval deciding the next reaction happen
r1 = rand;                    %random number
tau = log(1/r1)/reTot;    %delta t
t = t + tau;                   %the time when next reaction happen

%using random r2 to decide which reaction to happen after the deltat
r2 = rand;

%%%%%%%%%%%%%%%%%%%%%%%%%%%%%%%%%%%%%%%%%%%%%%%%%%%%%%%%%%%%%%%%%%%%%%%
%1.Ci+Vm
%%%%%%%%%%%%%%%%%%%%%%%%%%%%%%%%%%%%%%%%%%%%%%%%%%%%%%%%%%%%%%%%%%%%%%%
if (0 <= r2) & (r2 <= p1)
   column = column + 1;                %add a new column to store a new polymer
   polymer(:,column) = [1;1;0;1;0];   %form a new polymer
   mat(:,1) = [];                          %delete the IM from Matrix
   VmTot = VmTot - 1;                 %total number of Vm minus 1
   CiTot = CiTot - 1;
   CmTot = CmTot + 1;

%%%%%%%%%%%%%%%%%%%%%%%%%%%%%%%%%%%%%%%%%%%%%%%%%%%%%%%%%%%%%%%%%%%%%%%
%2.Cm+Vm
%%%%%%%%%%%%%%%%%%%%%%%%%%%%%%%%%%%%%%%%%%%%%%%%%%%%%%%%%%%%%%%%%%%%%%%
elseif ( p1 < r2) & (r2 <= p2)
   r3 = rand;          %select the molecule having this Cm group
   j = 0;
   sum = 0;            %sum of the Cm on polymer molecules

   for i = 1:column,
      j = j + 1;
      sum  = sum + polymer(4,j);
      if sum > r3*CmTot
         break;
      end
   end

   polymer(2,j) = polymer(2,j) + 1;  %number of IB plus 1
   VmTot = VmTot - 1;                %total number of Vm nimus 1

%%%%%%%%%%%%%%%%%%%%%%%%%%%%%%%%%%%%%%%%%%%%%%%%%%%%%%%%%%%%%%%%%%%%%%%
%3.Cm+Vi
%%%%%%%%%%%%%%%%%%%%%%%%%%%%%%%%%%%%%%%%%%%%%%%%%%%%%%%%%%%%%%%%%%%%%%%
elseif (p2 < r2) & (r2 <= p3)
   r3 = rand;          %select the molecule having this Cm group
   j = 0;
   sum = 0;            %sum of the Cm on polymer molecules

   for i = 1:column,
      j = j + 1;
      sum  = sum + polymer(4,j);
      if sum > r3*CmTot
         break;
      end
   end
```

```
        r4 = rand;                                  %select the molecule having this Vi gorup
        l = ceil(r4*column);
        while ((l == j) & (polymer(1,l) == 0))      %avoid the molecule to react with itself
            r4 = rand;
            l = ceil(r4*column);
        end

        polymer(1,j) = polymer(1,j) + polymer(1,l);       %IM
        polymer(2,j) = polymer(2,j) + polymer(2,l);       %IB
        %polymer(3,j) = polymer(3,j) + polymer(3,l);      %Ci
        polymer(4,j) = polymer(4,j) + polymer(4,l) - 1;   %number of Cm group minus 1
        polymer(5,j) = polymer(5,j) + polymer(5,l) + 1;   %number of Cs group plus 1
        polymer(:,l) = [];                                  %delete the lth molecule
        CmTot = CmTot - 1;                                 %Cm - 1
        CsTot = CsTot + 1;                                  %Cs + 1
        column = column - 1;                               %delete one polymer

    %%%%%%%%%%%%%%%%%%%%%%%%%%%%%%%%%%%%%%%%%%%%%%%%%%%%%%%%%%%%%%%%%%%%%%%
    %4.Cs+Vm
    %%%%%%%%%%%%%%%%%%%%%%%%%%%%%%%%%%%%%%%%%%%%%%%%%%%%%%%%%%%%%%%%%%%%%%%
    elseif (p3 < r2) & (r2 <= p4)
        r3 = rand;          %select the molecule having this Cm group
        j = 0;
        sum = 0;            %sum of the Cs on polymer molecules

        for i = 1:column,
            j = j + 1;
            sum  = sum + polymer(5,j);
            if sum > r3*CsTot
                break;
            end
        end

        polymer(2,j) = polymer(2,j) + 1;       %IB + 1
        polymer(4,j) = polymer(4,j) + 1;       %Cm + 1
        polymer(5,j) = polymer(5,j) - 1;       %Cs - 1
        CmTot = CmTot + 1;
        CsTot = CsTot - 1;
        VmTot = VmTot - 1;
    end
end

%%%%%%%%%%%%%%%%%%%%%%%%%%%%%%%%%%%%%%%%%%%%%%%%%%%%%%%%%%%%%%%%%%%%%%%
%Reaction stops and calculate the properties at the end of batch
%%%%%%%%%%%%%%%%%%%%%%%%%%%%%%%%%%%%%%%%%%%%%%%%%%%%%%%%%%%%%%%%%%%%%%%

display(t);             %end time of the batch
row = row + 1;      %add a row in sum_mat for polymer information at the end of batch

%update concentrations of different end groups and vinyl groups
%Vi = column + inimer;            %number of total Vi
IB_Con = VmTot/const;
%Vi_Con = Vi/const;
Ci_Con = CiTot/const;
Cm_Con = CmTot/const;
```

```
Cs_Con = CsTot/const;

%add a new row in matrix to store total chain length IB+IM
column = size(polymer,2);
polymer = [polymer; zeros(1,column)];
for col = 1 : column
   polymer(6,col) = polymer(1,col) + polymer(2,col);
end

%Calculate Mn & Mw
Mn_sum = 0;
Mw_sum = 0;
for col = 1 : column              %here column is just polymers
   Mn_sum = Mn_sum + polymer(1,col)*0.1805 + polymer(2,col)*0.056;
   Mw_sum = Mw_sum + (polymer(1,col)*0.1805 + polymer(2,col)*0.056)^2;
end
Mn = Mn_sum/column;         %Mn for polymers
Mw = Mw_sum/Mn_sum;         %Mw for polymers
inimer = size(mat,2);
IM_Con = inimer/const;
Mntheory = 0.056*(IB - VmTot)/IM + 0.1805;
Bkin = Mn/Mntheory -1;
sum_mat(row,1) = t;
sum_mat(row,2) = IB_Con;
sum_mat(row,3) = IM_Con;
sum_mat(row,4) = Mn;
sum_mat(row,5) = Mw;
sum_mat(row,6) = Bkin;

% reorder all the polymer molecules from the smallest to the largest
for i = 1 : column
   min_col = i;
   for j = i : column
      if  min_value > polymer(6,j)
         min_value = polymer(6,j);
         min_col = j;
      end
   end
   temp = polymer(:,i);
   polymer(:,i) = polymer(:,min_col);
   polymer(:,min_col) = temp;
end


% Build GPC histogram
range = 0.03;                %size of the bin
col = 1;                     %column number of polymer matrix
GPC_log = zeros(1,5);        %GPC results
GPC_row = 1;                 %the row in GPC results matrix
for value = 0 : range : 6    %put polymer chains into different bins
   sum = 0;                  %sum the number of units (IB+IM) in each bin
   count = 0;                %count the number of polymers in each bin
   while (col <= column) && (log10(polymer(6,col)) >= value)
&& (log10(polymer(6,col)) < (value + range))
      sum  = sum + polymer(6,col);
```

```
            count = count + 1;
            col = col + 1;
        end
        if sum ~= 0
            GPC_log(1,GPC_row) = value;
            GPC_log(2,GPC_row) = sum/count;       %average chain size
            GPC_log(3,GPC_row) = log(10)*sum*GPC_log(2,GPC_row);  %wlog(r)
            GPC_log(4,GPC_row) = sum;              %w(r)
            GPC_log(5,GPC_row) = count;            %n(r)
            GPC_row = GPC_row + 1;
        end
    end

%%%%%%%%%%%%%%%%%%%%%%%%%%%%%%%%%%%%%%%%%%%%%%%%%%%%%%%%%%%%%%%%%%%%%%%%%%%
%output results into Excel
%%%%%%%%%%%%%%%%%%%%%%%%%%%%%%%%%%%%%%%%%%%%%%%%%%%%%%%%%%%%%%%%%%%%%%%%%%%
    mat = mat';
    polymer = polymer';
    %xlswrite('C:\Documents and Settings\Zhaoyu\Desktop\SCVCP.xlsx',mat,'510^4(300)','A1');
    xlswrite('C:\Users\zhaoyu\Desktop\Thesis_Appendix.xlsx',polymer,'5e4 as','A1');
    xlswrite('C:\Users\zhaoyu\Desktop\Thesis_Appendix.xlsx',GPC_log,'5e4 as','P1');
    xlswrite('C:\Users\zhaoyu\Desktop\Thesis_Appendix.xlsx',sum_mat,'5e4 as','W1');

    toc
end
```

Chapter 4

Advanced Monte Carlo for Arborescent Polyisobutylene Production in Batch Reactor

Yutian R. Zhao[1], Kimberley B. McAuley[1], Piet D. Iedema[2], Judit E. Puskas[3]

[1]Department of Chemical Engineering, Queen's University, Kingston, ON, Canada
[2]Department of Chemical Engineering, University of Amsterdam, The Netherlands
[3]Department of Chemical & Biomolecular Engineering, University of Akron, Akron, OH USA

4.1 Abstract

An advanced Monte Carlo (MC) model is developed to predict the molecular weight distribution and branching level for *arborescent* polyisobutylene (*arb*PIB) produced in a batch reactor via carbocationic copolymerization of isobutylene and an inimer. This new MC model uses differential equations and random numbers to determine the detailed structure of dendritic polymer molecules. Results agree with those from a traditional MC model for the same system, but the proposed model requires considerably less computational effort. The proposed MC model is also used to obtain information about polymer segments between branch points and dangling polymer segments.

This chapter was published as:

Zhao YR, McAuley KB, Iedema PD, Puskas JE. Advanced Monte Carlo model for arborescent polyisobutylene production in batch reactor. *Macromol. Theory Simul.* 2014; 23: 383-400.

4.2 Introduction

Because of their unique chemical and physical properties, synthesis of arborescent polymers has been studied by many researchers.[1-5] The discovery of self-condensing vinyl polymerization (SCVP) by Fréchet et al.[6] greatly simplified the process of synthesizing arborescent polymers. SCVP uses inimers (*i.e.*, molecules that act both as initiator and monomer) to create the arborescent structure. Figure 4.1 shows a typical inimer (IM) molecule, which has a vinyl group that can polymerize and a chloride group that can be removed to initiate carbocationic polymerization. By copolymerizing this IM with isobutylene (IB), Puskas et al.[7-11] developed a simple method to produce polyisobutylene (PIB) with an arborescent or tree-like structure and used this new material as a core to produce block copolymers with polystyrene end blocks. This block copolymer has excellent mechanical properties, biocompatibility and biostability, making it a very promising material for human implantation,[7, 12-17] especially for breast implants.[18]

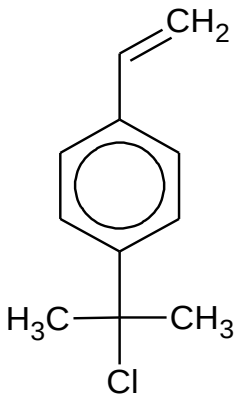

Figure 4.1 Typical structure of an inimer

Figure 4.2 shows a simplified reaction scheme for the "one-pot" living copolymerization of IM and IB developed by Puskas et al.[7-11, 19-22] The first step is an exchange reaction that converts 4-(2-methoxyisopropyl)styrene (MeOIM) to IM. A large excess of $TiCl_4$, which is a Lewis

acid (LA), is often used in the experiments to ensure that this exchange reaction goes to completion and that there is sufficient LA to initiate the living carbocationic polymerization. A proton trap (*e.g.* 2,6-di-tert-butylpyridine) is used in the polymerization to remove other sources of initiation (*e.g.*, proton initiation due to trace amounts of water).[19] The second step is a reaction between IM and IB molecules to form arborescent polymer molecules. Step two involves two different types of vinyl groups (V_I from IM and V_M from IB) and three different kinds of chloride end groups (C_I, C_M and C_S) that can produce carbocations. C_I chloride groups come directly from the IM; C_M chloride groups are formed by consuming V_M groups; C_S chloride groups are formed by consuming V_I groups.[21] As a result, six true propagation rate constants are associated with the different possible combinations of vinyl groups and chloride end groups. These 6 true propagation rate constants are $k_{pII}, k_{pIM}, k_{pMI}, k_{pMM}, k_{pSI}\ and\ k_{pSM}$, where the first letter after k_p refers to the type of chloride group that forms the carbocation and the second letter is related to the type of vinyl groups that is being consumed. One important property of the polymer molecules produced by this scheme is that each polymer chain has exactly one V_I vinyl group, assuming that intramolecular reactions do not occur.

The average branching level for the polymer chains that are produced is:[19, 22]

$$B_{kin} = \frac{\bar{M}_n}{\bar{M}_{n,theo}} - 1 \tag{4.1}$$

$$\bar{M}_{n,theo} = M_{IM} + \frac{[IB]_0 - [IB]}{[IM]_0 - [IM]} M_{IB} \tag{4.2}$$

where $\bar{M}_n$, is the number average molecular weight for all polymers and $\bar{M}_{n,theo}$ is a theoretical molecular weight that would be obtained if IM were consumed as initiator only (*i.e.*, if none of the V_I groups could react and only linear PIB was produced).

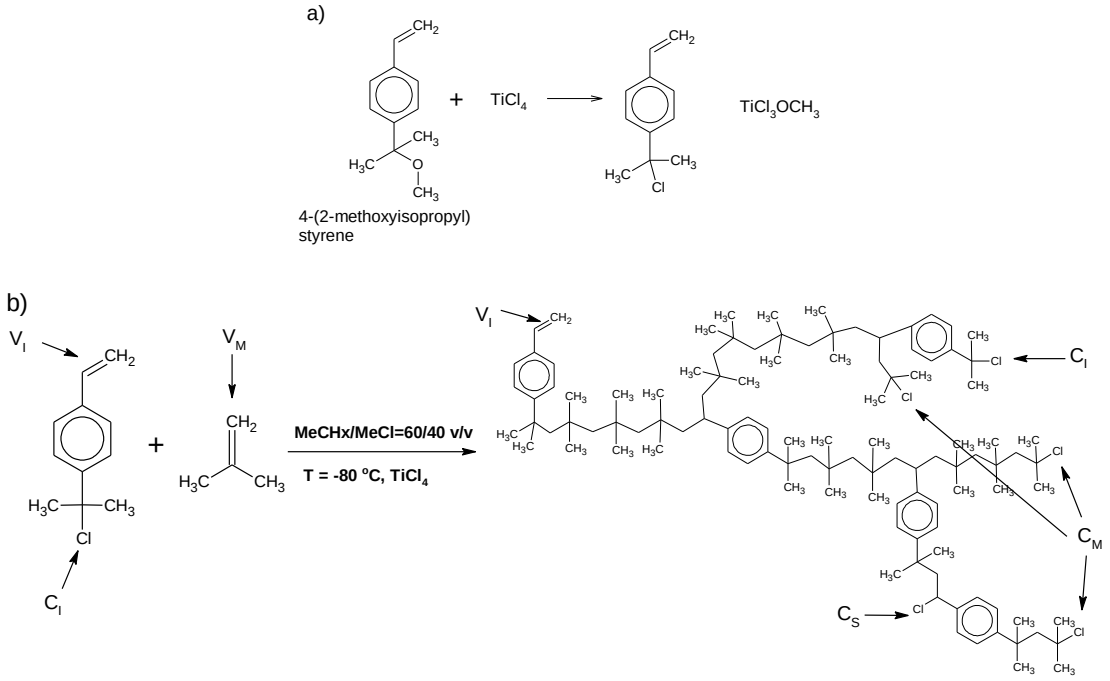

Figure 4.2 a) Exchange reaction that converts 4-(2-methoxyisopropyl)styrene to IM;[19] b) a simplified reaction scheme for the "one-pot" living copolymerization of IM and IB[21]

Puskas et al.,[23-26] have shown that there are two paths whereby the LA can cap and uncap the chloride end groups (see Figure 4.3). Path A involves only one LA molecule, while path B requires two. Both paths can exist in the system at the same time, however, when the LA concentration is low, path A dominates and when the LA concentration is high, path B dominates. In this living polymerization, several propagation steps may occur after any chloride end group is removed and then the carbocation returns to its dormant state through capping with a chloride. Based on Figure 4.3, there are three different equilibrium constants (K_0, K_1 and K_2) that influence the overall rate of propagation. Table 4.1 shows how the six apparent propagation rate constants ($k_{pIIapp}, k_{pIMapp}, k_{pMIapp}, k_{pMMapp}, k_{pSIapp}\ and\ k_{pSMapp}$) that determine the rate of arborescent polymer formation are related to the corresponding true propagation rate constants and the equilibrium constants. The model developed in this paper will predict the polymerization rate and

the type of polymer molecules that form using values of these six apparent propagation rate constants shown in Table 4.1 and the overall reactions shown in Table 4.2.

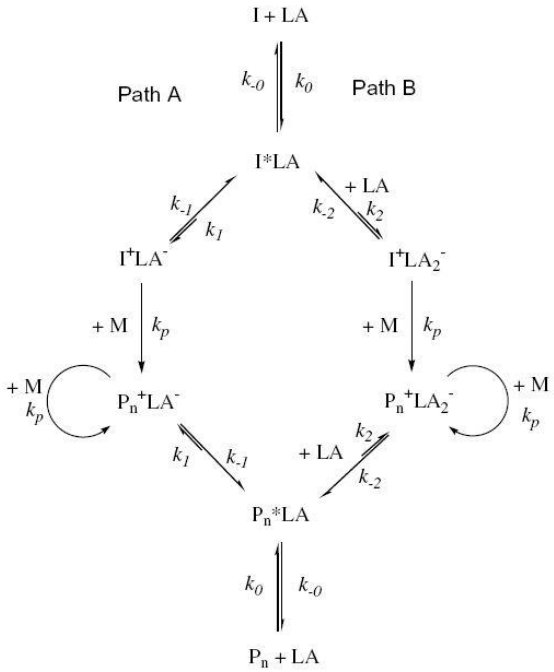

Figure 4.3 Two different paths for carbocationic polymerization using different amount of Lewis acid coinitiator. Path A is dominant when LA concentration is lower than the concentration of initiator; Path B is dominant when LA concentration is much higher than the concentration of initiator. Note I is initiator and M is monomer.[26]

Table 4.1 Six apparent propagation rate constants and their estimated values.[21,22]

Parameter	**Estimate**	**Units**
$k_{pIIapp} = k_{pII} \times (K_0K_1[TiCl_4]_0 + K_0K_2[TiCl_4]_0^2)$	7.5×10^{-3}	$L{\cdot}mol^{-1}{\cdot}s^{-1}$
$k_{pIMapp} = k_{pIM} \times (K_0K_1[TiCl_4]_0 + K_0K_2[TiCl_4]_0^2)$	3.99×10^{-4}	$L{\cdot}mol^{-1}{\cdot}s^{-1}$
$k_{pMIapp} = k_{pMI} \times (K_0K_1[TiCl_4]_0 + K_0K_2[TiCl_4]_0^2)$	0.195	$L{\cdot}mol^{-1}{\cdot}s^{-1}$
$k_{pMMapp} = k_{pMM} \times (K_0K_1[TiCl_4]_0 + K_0K_2[TiCl_4]_0^2)$	2.126	$L{\cdot}mol^{-1}{\cdot}s^{-1}$
$k_{pSIapp} = k_{pSI} \times (K_0K_1[TiCl_4]_0 + K_0K_2[TiCl_4]_0^2)$	1.0×10^{-4}	$L{\cdot}mol^{-1}{\cdot}s^{-1}$
$k_{pSMapp} = k_{pSM} \times (K_0K_1[TiCl_4]_0 + K_0K_2[TiCl_4]_0^2)$	1.39×10^{-2}	$L{\cdot}mol^{-1}{\cdot}s^{-1}$

where $K_0 = \frac{k_0}{k_{-0}} = \frac{[P_n^*LA]}{[P_n][LA]}$; $K_1 = \frac{k_1}{k_{-1}} = \frac{[P_n^+LA^-]}{[P_n^*LA]}$; $K_2 = \frac{k_2}{k_{-2}} = \frac{[P_n^+LA_2^-]}{[P_n^*LA][LA]}$

Table 4.2 Summary of six possible propagation reactions between end groups and vinyl groups during copolymerization of IM and IB

	Reactions
1	$C_I + V_I \xrightarrow{k_{pIIapp}} C_S$
2	$C_I + V_M \xrightarrow{k_{pIMapp}} C_M$
3	$C_M + V_I \xrightarrow{k_{pMIapp}} C_S$
4	$C_M + V_M \xrightarrow{k_{pMMapp}} C_M$
5	$C_S + V_I \xrightarrow{k_{pSIapp}} C_S$
6	$C_S + V_M \xrightarrow{k_{pSMapp}} C_M$

Several research groups have developed mathematical models for SCVP and SCVCP systems. These models can be classified mainly into two different types: (1) dynamic material balance models [21,27-34] and (2) Monte Carlo (MC) models.[22,35-37] These two areas are complementary in that each has advantages that the other does not. For example, it is relatively straightforward to build individual material balance equations, especially using automated tools like PREDICI[38] but not as easy to formulate and implement models using MC methods. However, MC models can provide very detailed information about the structure of polymer molecules, but dynamic material balance models may not be able to provide such detailed information unless a prohibitive number of differential equations is used.[21, 22]

Müller et al. and Yan et al.[27-31] wrote a series of articles focusing on SCVP and SCVCP systems using material balance methods. In order to develop analytical expressions for average molecular weight and degree of branching, they made several simplifying assumptions about equal reactivity of end groups and vinyl groups. They noted that their SCVP models provide reasonable values for $\bar{M}_w$, but unrealistically high value for degree of branching.[27] Cheng et al.[32,33] developed more complicated material balance models for SCVP systems in batch and semi-batch

reactors, and solved them using generating functions. They also assumed equal reactivities for all or some of the end groups to make the models tractable. Zargar et al.[34] applied the method of moments to model a SCVCP system. Their model keeps track of the length of linear segments that make up the branched-polymer molecules. Although information about $\bar{M}_w$ and $\bar{M}_n$ can be predicted for the segments, the molecular weight distribution (MWD) for polymer molecules cannot be predicted by their model. In the meantime, they assumed equal reactivities for C_S and C_M groups.

In our previous work,[21] we built a SCVCP material balance model for *arborescent* PIB production in batch reactors using PREDICI. This model was the first to be developed without applying equal reactivity assumptions for different types of vinyl groups and end groups. A large number of dynamic material balances were required to track different polymer species with different numbers and types of chloride end groups. Both path A and path B (shown in Figure 4.3) were considered. Some restrictive assumptions (shown in Table 4.3) were made to keep the model to a manageable size. As a result, only four apparent rate constants (k_{pIMapp}, k_{pMIapp}, k_{pMMapp} and k_{pSMapp}) were used in the model. Values of these parameters were estimated using experimental data and are reported in Table 4.1.[19,21,22] Simulation results agreed well with experimental data corresponding to low average branching levels (about 2 branches per polymer chain), but were worse for polymers having higher branching levels.[21]

Table 4.3 Assumptions from our previous PREDICI model[21]

1	Reactions between C_I end groups and IM can be neglected because $[IM]_0$ is low relative to $[IB]_0$, so that reactions involving k_{pII} can be neglected.
2	C_S end groups can only react with monomer vinyl groups. Reactions between C_S end groups and IM molecules can be neglected because IM molecules will typically initiate polymerization before their vinyl groups can be consumed by reaction. Reactions between C_S end groups and V_I groups on polymer molecules can be neglected due to steric hindrance. Because $[IM]_0$ is very low compared to $[IB]_0$, C_S groups will react with IB before they encounter the V_I groups on large molecules. Thus, reactions involving k_{pSI} can be neglected.
3	The C_I groups on the IM are all consumed very early in the reaction because the chloride end is designed to behave as an initiator for living carbocationic polymerization. As a result, the only reaction that IM can undergo appreciably is an initiation reaction with IB. Therefore, vinyl groups of type V_I can undergo propagation reactions only after they belong to oligomer or polymer molecules. Another consequence of this assumption is that there are no C_I groups on any polymer molecules so that reactions between polymer molecules and IM can be ignored. Note that this assumption means that there is no need to track the number of C_I groups in the model, (except for those on IM, which are consumed quickly).
4	Reactions that lead to 16 or more IM units in a molecule are neglected to keep the number of species and reactions manageable for implementation in PREDICI.
5	Puskas et al.[49] observed a penultimate effect during styrene/isobutylene copolymerization, indicating that the rate of IB addition to C_M may depend on whether the penultimate unit is IB or a styrene-like IM unit. Since $[IM]_0$ was low compared to $[IB]_0$ in the recipes simulated using the PREDICI model, this penultimate effect could be neglected with only a small effect on model predictions.
6	$[LA] \approx [LA]_0$ throughout the course of the batch reactions simulated using PREDICI, because only a small fraction of the $TiCl_4$ was consumed to produce ions.[50] Also, $[LA]_0$ is sufficiently large so that the MeOIM is converted instantaneously to IM at the beginning of the batch.

Several Monte Carlo methods have been developed for SCVP and SCVCP systems. He et al. developed SCVP models that account for multifunctional initiators[35] and that focus on steric effects and intramolecular cyclization[36]. In their related SCVCP model,[37] they made equal reactivity assumptions for the two types of vinyl groups and for the different types of end groups. Recently, we developed a MC model for *arborescent* PIB production in batch reactors that accounts for all six apparent propagation rate constants shown in Table 4.1 (*i.e.*, no equal reactivity assumptions for vinyl groups or carbocations were needed).[22] Restrictive assumptions 1 to 4 from Table 4.3 were not required in this model. As a result, more realistic results were obtained at higher branching levels than was possible using the earlier PREDICI material-balance model. In addition, IM homopolymerization can also be simulated, which was not possible using the PREDICI model due to assumption 1, 2 and 4 in Table 4.3. Unfortunately, the MC model required long computation times to obtain reliable results, making this model unsuitable for use in parameter estimation.

Most MC polymerization models use traditional MC techniques,[22,39-42] first developed by Gillespie[43]. In this method, a small reference volume containing an initial number of molecules of different types is selected and used to follow individual chemical reactions over the course of the batch. A short period of time Δt corresponding to the time of the next reaction step is calculated using a random number from an exponential distribution, with properties determined by the various rate constants and number of reactant molecules. Random numbers are generated to select the type of reaction that occurs at each time step and then simulation proceeds slowly from the initial time to the final time of interest. More accurate (representative) results are obtained when a larger reference volume is selected, at the cost of shorter times between reactions and higher computational requirements. Traditional MC models for SCVP and SCVCP have been developed by He et al.[35-37] and by our research group[22]. The main problem with these models is the long computation times required to obtain accurate MWD and branching information.

Iedema et al.[44-46] developed an alternative type of MC algorithm, called conditional MC, based on a simplification of the full MC method invented by Tobita[47,48]. In conditional MC and full MC, the modeler imagines looking back from the final time for the batch, and uses probabilities to construct individual polymer molecules one-by-one using the entire reactor volume. The chain assembly process stops when a sufficient number of polymer chains have been created to obtain reliable distribution results. Iedema's conditional MC is an improvement over Tobita's full MC method because ordinary-differential-equation material balances are solved for some species, so that fewer stochastic calculations are required, thereby saving computational effort.[45] One reason that Iedema's conditional MC methods have not enjoyed widespread use is that they are more difficult to implement and understand than traditional MC algorithms.[22]

In this paper, an advanced MC model is developed for the *arborescent* PIB system. Like the conditional MC methods of Iedema et al., the proposed MC method uses material balance differential equations along with stochastic calculations to compute detailed molecular weight and branching information for individual molecules. First, some structural properties of *arborescent* PIB chains are discussed and the proposed MC algorithm is developed. Simulation results and the computational effort required to obtain accurate results are compared with results from our traditional MC model.[22] Benefits and difficulties arising from the use of the proposed MC method are highlighted.

4.3 Model Development

The basic idea in the proposed method is to imagine assembling a series of polymer chains, one by one, using information from dynamic material balances and MC simulation. The approach is very different from that used in typical Gillespie-style MC simulations wherein reactions between the various molecules are determined, one by one, starting at time zero and stepping forward to the end of the batch.[22,43] Instead, in the proposed method, it is helpful to think about looking back, from the end time of the batch, at what happened during the batch to create the individual polymer molecules. The proposed assembly process for a polymer molecule begins by thinking about the single vinyl group that appears on each polymer molecule. This vinyl group (of type V_I) was originally associated with an inimer molecule at the start of the batch. The first step in the assembly process is to figure out what happened to the chloride end group on this IM molecule (*i.e.* C_I) during the batch. Was it converted to a C_M or C_S group via reaction with a V_M or a V_I group? The answer depends on the concentrations of species in the reaction mixture at the time when the reaction occurred. This information is supplied by material balances and random numbers. The description below and in Tables 4.4 to 4.9 shows how the fate of this initial C_I group and other chloride groups in the molecule is determined. Material balances and random numbers are also used to decide how many branches the particular molecule has, the lengths of the *internal segments* between branches, and the lengths of the *dangling segments* on the polymer chains.

Table 4.2 shows the reactions between vinyl groups and end groups that influence the development of molecular weight and branching in the PIB polymer. The first five rows in Table 4.4 contain dynamic material balances on these groups, which can be solved using the initial concentrations $[IB]_0 = [V_M]_0$ and $[IM]_0 = [V_I]_0 = [C_I]_0$. Note that initial conditions for $[C_M]_0$ and $[C_S]_0$ are typically zero for batch reactor operation.

Table 4.4 Dynamic material balances and initial conditions (IC) used in advanced MC calculations.

Species	Material balances	IC (M)	
V_I	$\frac{d[V_I]}{dt} = -k_{pII}[C_I][V_I] - k_{pMI}[C_M][V_I] - k_{pSI}[C_S][V_I]$	$[IM]_0$	4.4.1
V_M	$\frac{d[V_M]}{dt} = -k_{pIM}[C_I][V_M] - k_{pMM}[C_M][V_M] - k_{pSM}[C_S][V_M]$	$[IB]_0$	4.4.2
C_I	$\frac{d[C_I]}{dt} = -k_{pII}[C_I][V_I] - k_{pIM}[C_I][V_M]$	$[IM]_0$	4.4.3
C_M	$\frac{d[C_M]}{dt} = k_{pIM}[C_I][V_M] - k_{pMI}[C_M][V_I] + k_{pSM}[C_S][V_M]$	0	4.4.4
C_S	$\frac{d[C_S]}{dt} = k_{pII}[C_I][V_I] + k_{pMI}[C_M][V_I] - k_{pSM}[C_S][V_M]$	0	4.4.5
$C_{HI\rightarrow M}$	$\frac{d[C_{HI\rightarrow M}]}{dt} = k_{pIM}[C_I][V_M]$	0	4.4.6
$C_{HI\rightarrow S}$	$\frac{d[C_{HI\rightarrow S}]}{dt} = k_{pII}[C_I][V_I]$	0	4.4.7
C_{HM}	$\frac{d[C_{HM}]}{dt} = -k_{pMI}[C_{HM}][V_I]$	1	4.4.8
C_{HS}	$\frac{d[C_{HS}]}{dt} = -k_{pSI}[C_{HS}][V_I] - k_{pSM}[C_{HS}][V_M]$	1	4.4.9
$C_{HS\rightarrow M}$	$\frac{d[C_{HS\rightarrow M}]}{dt} = k_{pSM}[C_{HS}][V_M]$	0	4.4.10
$C_{HS\rightarrow S}$	$\frac{d[C_{HS\rightarrow S}]}{dt} = k_{pSI}[C_{HS}][V_I]$	0	4.4.11

Table 4.4 contains additional material balances on hypothetical counter species (not required to solve material balances 4.4.1 to 4.4.5) that are solved to aid in the assembly of random polymer molecules, as described in the algorithm in Table 4.5. Details concerning the random numbers are provided in Table 4.6 (shown in Simulation Results section). For example, $C_{HI\rightarrow M}$ in equation 4.4.6 is a counter for the total number of moles (per liter) of C_I groups that have been converted to C_M at a particular time in the batch. Figure 4.6 is a plot of $C_{HI\rightarrow M}$ vs. time, which was obtained using $[IM]_0 = 0.00454\ mol \cdot L^{-1}$, $[IB]_0 = 1.74\ mol \cdot L^{-1}$and the parameter values

in Table 4.1, using a final time for the batch of t_f = 5400 s. This figure shows that 75% of the reactions where a C_I group was converted to a C_M group (by Reaction 2 in Table 4.2) had occurred by about 528 seconds. The additional hypothetical counter species will be described later in this section.

The two types of segments that appear within typical *arborescent* PIB molecules are (1) *internal segments* that are sequences of PIB homopolymer between two IM units, and (2) *dangling segments* that start at an IM unit and end with an unreacted C_M group. Figure 4.4 uses the molecule from Figure 4.2 to illustrate the two types of segments. The vinyl group of type V_I on this molecule corresponds to the IM unit labeled 1. This PIB molecule has four internal segments (of lengths 3, 4, 2 and 0, respectively), which appear between the various IM units, and three dangling segments (of lengths 1, 3 and 1, respectively) that have terminal C_M groups.

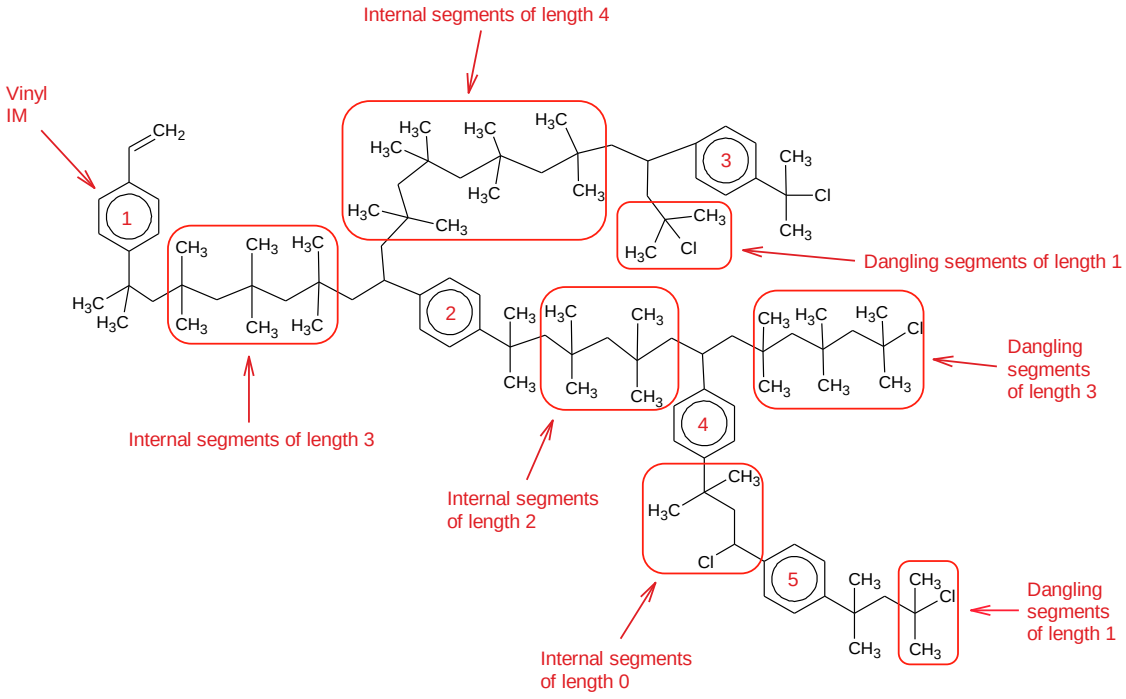

Figure 4.4 Detailed illustration of dangling segments and internal segments.

Table 4.5 Algorithm for assembling a random polymer molecule using information available at the end of the batch.

1	Pick a random V_I group from the final reaction mixture, which is attached to a polymer chain. Consider the C_I group from the corresponding inimer molecule. This C_I group must have been consumed at some time during the batch because the V_I group is on a polymer molecule and not an unreacted inimer. Set the number of additional C_I groups that need further study to $N_{C_I} = 0$, for the moment, because we are not currently aware of any additional inimer units on the polymer molecule. Use random number, r_0, the solution of the ODEs in Table 4.4 and the criteria at the top of Table 4.6 to find out what happened to this C_I group. The possibilities are that: (1) it reacted with a V_M group or (2) it reacted with a V_I group. Note that r_0 and all of the other random numbers used in this algorithm are uniformly distributed between 0 and 1. ***Go to step 2 for option (1) and step 9 for option (2)***
2	The C_I group reacted with a V_M group to start an IB segment. Use random number r_2 to find the time t_M when this reaction happened. Use random number r_4 to decide what the IB segment looks like at the end of the batch. It can be either (1) an internal segment or (2) a dangling segment. ***Go to step 3 for option (1) and step 8 for option (2)***
3	Use random number r_4 from the previous step to decide the time t_S when the IB segment reacted with a V_I group to end the internal segment. Increment N_{C_I}, the number of C_I groups that have not been studied, by 1, because we are aware of an additional C_I group whose fate must be determined. Use random number r_5 to find the length of the internal segment. ***Go to step 4***
4	The reaction in the previous step formed a C_S group. Use random number r_7 to decide what happened to it. The possibilities are that: (1) it remained unreacted to the end of the batch, (2) it reacted with a V_M group, or (3) it reacted with a V_I group. ***Go to step 10 for option (1), step 5 for option (2) and step 7 for option (3)***
5	The C_S group reacted with a V_M group to start a new IB segment. Use random number r_8 to decide the time t_M when this happened. ***Go to step 6***
6	A new IB segment started to grow. Use random number r_4 to decide what the IB segment is, either (1) an internal segment or (2) a dangling segment at the end of the batch. ***Go to step 3 for option (1) and step 8 for option (2)***
7	The C_S group reacted with a V_I group. Use random number r_9 to decide the time t_{S2} when this happened. Augment N_{C_I} the number of unstudied C_I group by one. ***Go to step 4***
8	The C_M group continued to react with V_M groups until the end of batch to form a dangling segment. Use random number r_6 to determine the length of this dangling segment. ***Go to step 10***
9	The C_I group reacted with a V_I group. Use random number r_3 to find time t_S when this reaction happened. Augment N_{C_I} the number of unstudied C_I group by one. ***Go to step 4***
10	Check if $N_{C_I} = 0$. ***If yes, go to step 12. If no, go to step 11***
11	There are still some C_I groups that have not been studied yet. Pick one of them and decide what happened to it during the batch using random number r_1. There are three possible outcomes for this C_I group, since it is not the C_I groups on the initial IM: (1) it remained unreacted until the end; (2) it reacted with a V_M group sometime during the batch; or (3) it reacted with a V_I group sometime during the batch. Reduce$N_{C_I}$the number of unstudied C_I groups by one. ***Go to step 10 for option (1), step 2 for option (2) and step 9 for option (3)***
12	Since all end groups studied remain unreacted at the end of the batch, the process of assembling the polymer molecule is finished. If additional polymer molecules need to be studied, go to step 1. Otherwise stop.

Table 4.6 Random numbers, Criteria and Outcomes used in the MC algorithm in Table 4.5

Random number	Range of values	Outcomes
Determining the fate of the first C_I group		
r_0	$\left(0 \ , \ \frac{\frac{[C_{HI\to M}(t_f)]}{[C_I(t_0)]}}{1-\frac{[C_I(t_f)]}{[C_I(t_0)]}}\right)$	(1) C_I group on initial IM reacted with a V_M group to form a C_M group
	$\left(\frac{\frac{[C_{HI\to M}(t_f)]}{[C_I(t_0)]}}{1-[C_I(t_f)]/[C_I(t_0)]} \ , \ 1\right)$	(2) C_I group on initial IM reacted with a V_I group to form a C_S group during the batch
Determining the fate of the subsequent C_I groups		
r_1	$\left(0 \ , \ \frac{[C_I(t_f)]}{[C_I(0)]}\right)$	(1) C_I group remains unreacted until the end
	$\left(\frac{[C_I(t_f)]}{[C_I(0)]} \ , \ \frac{[C_I(t_f)]}{[C_I(0)]}+\frac{[C_{HI\to M}(t_f)]}{[C_I(0)]}\right)$	(2) C_I group reacted with a V_M group to form a C_M group
	$\left(\frac{[C_I(t_f)]}{[C_I(0)]}+\frac{[C_{HI\to M}(t_f)]}{[C_I(0)]} \ , \ 1\right)$	(3) C_I group reacted with a V_I group to form a C_S group during the batch
Determining time t_M when a C_I group reacted with a V_M group		
r_2	Find time t_M as shown in **Figure 4.6**, so that $\frac{[C_{HI\to M}(t_M)]}{[C_{HI\to M}(t_f)]}=r_2$	This is the time when the C_I group reacted with a V_M group
Determining time t_S when a C_I group reacted with a V_I group		
r_3	Find time t_S so that $\frac{[C_{HI\to S}(t_S)]}{[C_{HI\to S}(t_f)]}=r_3$	This is the time when the C_I group reacted with a V_I group
Determining the fate of a segment		
r_4	$\left(0 \ , \ \frac{[C_{HM}(t_M)]-[C_{HM}(t_f)]}{[C_{HM}(t_M)]}\right)$	(1) An internal segment formed
	$\left(\frac{[C_{HM}(t_M)]-[C_{HM}(t_f)]}{[C_{HM}(t_M)]} \ , \ 1\right)$	(2) A dangling segment remains at the end of the batch
Determining the end time of an internal segment		
r_4	Find time t_S so that $\frac{[C_{HM}(t_S)]-[C_{HM}(t_f)]}{[C_{HM}(t_M)]}=r_4$	This is the time when the C_M group reacted with the V_I group
Determining the length of an internal segment		
r_5	Find the chain length l so that $\sum_{i=1}^{l-1}p(i)\le r_5<\sum_{i=1}^{l}p(i)$ where $p(i)$ is obtained from a probability table (see Table 4.7**)**	The length of the internal segment is l
Determining the length of a dangling segment		
r_6	Find the chain length l so that $\sum_{i=1}^{l-1}p(i)\le r_6<\sum_{i=1}^{l}p(i)$ where $p(i)$ is obtained from Table 4.9	The length of dangling segment is l
Determining the fate of a C_S group		
r_7	$\left(0 \ , \ \frac{[C_{HS}(t_f)]}{[C_{HS}(t_S)]}\right)$	(1) C_S group remains unreacted at the end of the batch
	$\left(\frac{[C_{HS}(t_f)]}{[C_{HS}(t_S)]} \ , \ \frac{[C_{HS}(t_f)]}{[C_{HS}(t_S)]}+\frac{[C_{HS\to M}(t_f)]-[C_{HS\to M}(t_S)]}{[C_{HS}(t_S)]}\right)$	(2) C_S group reacted with a V_M group to form a C_M group
	$\left(\frac{[C_{HS}(t_f)]}{[C_{HS}(t_S)]}+\frac{[C_{HS\to M}(t_f)]-[C_{HS\to M}(t_S)]}{[C_{HS}(t_S)]} \ , \ 1\right)$	(3) C_S group reacted with a V_I group to form another C_S group
Determining time t_M when a C_S group reacted with a V_M group		
r_8	Find time t_M so that $\frac{[C_{HS\to M}(t_M)]-[C_{HS\to M}(t_S)]}{[C_{HS\to M}(t_f)]-[C_{HS\to M}(t_S)]}=r_8$	This is the time when the C_S group reacted with a V_M group
Determining time t_{S2} when a C_S group reacted with a V_I group		
r_9	Find time t_{S2} so that $\frac{[C_{HS\to S}(t_{S2})]-[C_{HS\to S}(t_S)]}{[C_{HS\to S}(t_f)]-[C_{HS\to S}(t_S)]}=r_9$	This is the time when the C_S group reacted with a V_I group

Consider assembling the polymer molecule in Figure 4.4, which is constructed schematically in Figure 4.5 using the proposed MC algorithm outlined in Table 4.5. The assembly of the molecule proceeds via seven stages (A, B, C …G) as shown in Figure 4.5.

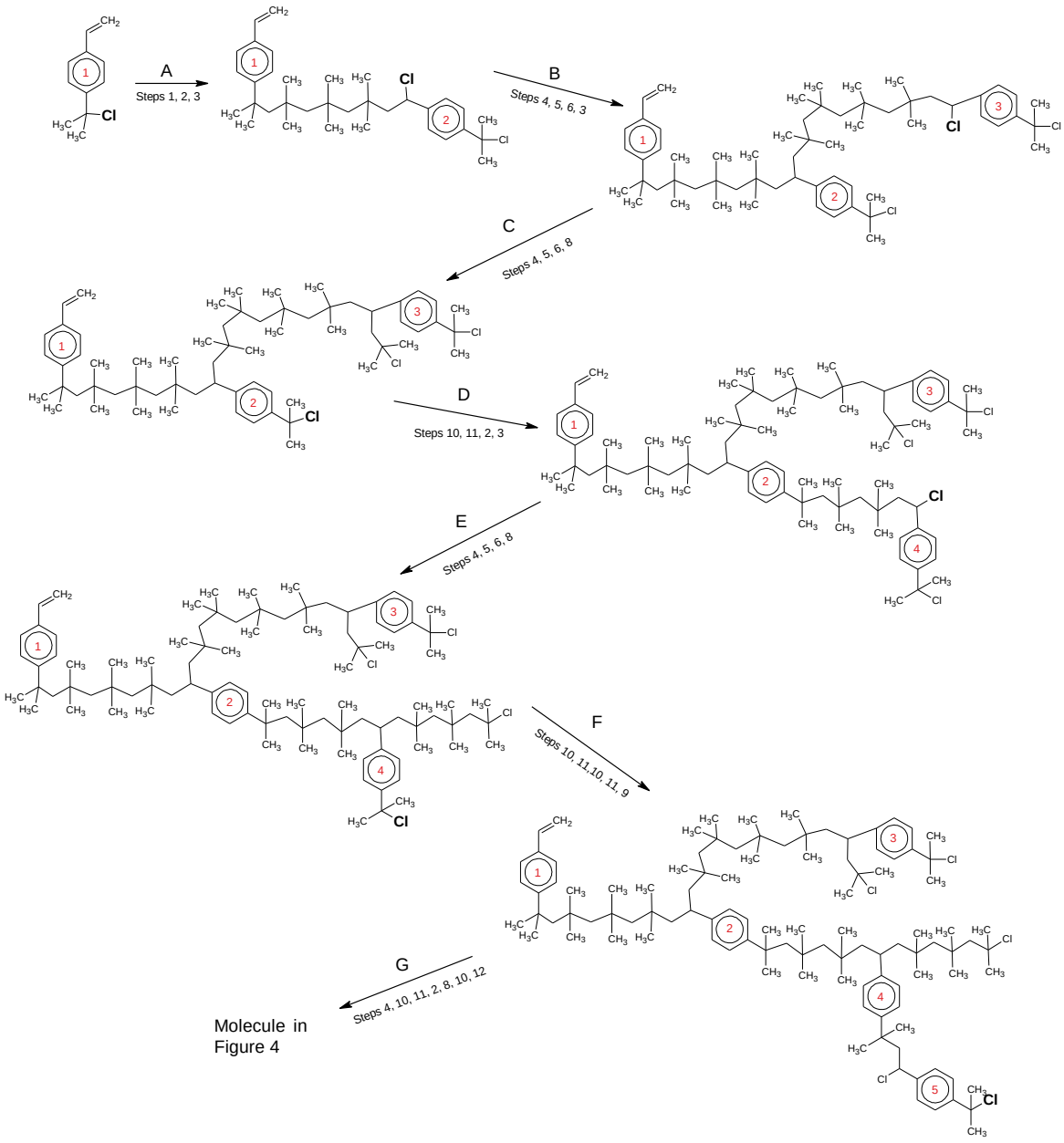

Figure 4.5 Detailed process for assembling the polymer molecule shown in Figure 4.4. The **Cl** groups that uncaps to initiate the next segment is shown in bold

In stage A, the internal segment between IM(1) and IM(2) is constructed. In stage B, a second internal segment is constructed between IM(2) and IM(3). In stage C, a dangling segment is constructed at the side of IM(3). Stage D is the construction of the internal segment between IM(2) and IM(4). Stage E is the construction of a dangling segment at the side of IM(4). Stage F is the construction of an internal segment of length zero between IM(4) and IM(5), and stage G is the construction of a dangling segment from IM(5) to complete the molecule. Each of these stages requires several steps from Table 4.5. Stage A starts by thinking about the C_I group that corresponds to IM(1). This C_I group must have reacted with a V_M group (via reaction 2 in Table 4.3) at some time during the batch to initiate the formation of the corresponding internal segment between IM(1) and IM(2). Starting at step 1 in Table 4.5, the random number r_0 must have had a value between 0 and $\frac{[C_{HI\rightarrow M}(t_f)]}{[C_I(t_0)]} \Big/ \left(1-\frac{[C_I(t_f)]}{[C_I(t_0)]}\right)$ so that option (1) was chosen. Note that $\frac{[C_{HI\rightarrow M}(t_f)]}{[C_I(t_0)]}$ is the fraction of C_I groups that were consumed to form V_M groups during the whole batch and $\frac{[C_I(t_f)]}{[C_I(t_0)]}$ is the fraction of C_I groups that remain unreacted at the end of the batch, so $\frac{[C_{HI\rightarrow M}(t_f)]}{[C_I(t_0)]} \Big/ \left(1-\frac{[C_I(t_f)]}{[C_I(t_0)]}\right)$ is the probability that a C_I group that reacted was converted to a C_M group.

In step 2, the time t_M when the reaction happened is determined using random number r_2. Figure 4.6 shows how a r_2 value of 0.75 would be converted into the corresponding time $t_M = 528$ s. Because the segment between IM(1) and IM(2) on the molecule in Figure 4.4 is an internal segment, random number r_4 must have been between 0 and $\frac{[C_{HM}(t_M)]-[C_{HM}(t_f)]}{[C_{HM}(t_M)]}$. Note that $[C_{HM}]$ is a hypothetical species concentration shown in Figure 4.7b (shown in Simulation Results section) computed using equation 4.4.8 in Table 4.4. $[C_{HM}]$ is used to determine the fraction of the segments initiated at time t_M that became internal segments by the end of the batch, using the

ratio $\frac{[C_{HM}(t_M)]-[C_{HM}(t_f)]}{[C_{HM}(t_M)]}$. For example, using t_M=528 s, this fraction would be $\frac{0.636-0.053}{0.636} = 0.917$ indicating that 91.7% of C_M groups formed at 528 s would become internal segments. Since C_{HM} is a hypothetical species that is only used to compute ratios, its initial value of 1.0 was selected arbitrarily.

In step 3, r_4 is also used to determine the time t_S when growth of the internal segment ceased (due to Reaction 3). Random number r_5 is then used to decide the number of IB units l in the internal segment, as shown in Table 4.6. Note that $p(i)$ is the probability that an internal segment born at time t_M and stopped at time t_S contains i IB units. Table 4.7 is an example of a probability look-up table for internal segments that start at $t_M = 2520$ s and stop at different values of t_S. For example, an internal segment that started to grow at 2520 s and ended at 2880 s would have a 3.119% probability of having only one IB unit and a 10.752% probability of having two IB units for the recipe with $[IB]_0 = 1.74$ M and $[IM]_0 = 0.00454$ M. Table 4.7 was constructed using t_S values at 180-second intervals throughout the batch. The entries were determined using a PREDICI simulation that considers propagation of the internal segments:

$$S(i) + V_M \xrightarrow{k_{pMMapp}} S(i+1) \tag{4.3}$$

Reactions 1 to 6 in Table 4.2 were also included in these PREDICI simulations to provide the time-varying concentration of V_M groups. Note that the sum of the entries in each column of Table 4.7 is one. Implementation details for the PREDICI simulations are shown in appendix 4.1. An alternative way of generating the probability information in Table 4.7 is to use Matlab to solve the ODEs shown in Table 4.8 (along with ODEs 4.4.1 to 4.4.5 in Table 4.4). Because the longest segments in the probability tables like Table 4.7 contain up to 2500 repeat units, we selected 3000 as the longest possible chain length for the segments that should be considered when solving the differential equations. The probability results are generated by starting simulations at different times, *e.g.* $t_M = 0, 180, 360 \ldots 5220$ s, and providing output results every 180 s until the

end of the batch ($t_f = 5400$ s), using $[S(1)]_0 = 1, [S(2)]_0 = [S(3)]_0 = \cdots = [S(3000)]_0 = 0$ as initial conditions along with appropriate initial values for V_I, V_M, C_I, C_M and C_S. Because $[S(1)]_0$ was set arbitrarily at 1 mol/L, the sum of the concentrations for the segments with different lengths will always add to one, and the predicted values of $S(1), S(2), \ldots, S(3000)$ at different end times of interest match the probability values required in Table 4.7, and other analogous tables.

Table 4.7 Probabilities of lengths of internal segments that are born at t_M = 2520 s and that end at different times t_S. The probability values were obtained using the parameter values in Table 4.1 for a batch with $[IB]_0$=1.74 M, $[IM]_0$=0.00454 M and t_f = 5400 s. Similar tables are required for different values of t_M.

	End Time t_S							
# of IB units	2520 s	2700 s	2880 s	3060 s	…	5040 s	5220 s	5400 s
1	1	0.13575	0.03119	0.01030	…	0.00018	0.00016	0.00014
2	0	0.27008	0.10752	0.04679	…	0.00151	0.00135	0.00127
3	0	0.26989	0.18607	0.10665	…	0.00648	0.00590	0.00562
4	0	0.18047	0.21546	0.16264	…	0.01858	0.01716	0.01655
5	0	0.09070	0.1877	0.18663	…	0.04008	0.03754	0.03657
⋮	⋮	⋮	⋮	⋮	⋮	⋮	⋮	⋮

Table 4.8 ODEs for different chain lengths that are solved by an alternative way using Matlab.

$\frac{d[S(1)]}{dt} = -k_{pMMapp}[S(1)][V_M]$	(4.8.1)
$\frac{d[S(2)]}{dt} = k_{pMMapp}[S(1)][V_M] - k_{pMMapp}[S(2)][V_M]$	(4.8.2)
⋮	⋮
$\frac{d[S(2999)]}{dt} = k_{pMMapp}[S(2998)][V_M] - k_{pMMapp}[S(2999)][V_M]$	(4.8.2999)
$\frac{d[S(3000)]}{dt} = k_{pMMapp}[S(2999)][V_M]$	(4.8.3000)

Note that 31 different tables that are analogous to Table 4.7 were constructed for different values of t_M at 180-second intervals. This discretization interval was selected because it provides sufficiently accurate results for linear interpolation when values of t_M and t_S that are not shown in the tables are obtained from r_2 and r_4. For example, imagine that r_2 and r_4 resulted in $t_M = 2610$ s and $t_S = 2898$ s, respectively. Determining $l = 3$ for the internal segment between IM(1) and IM(2) would require the generation of random number r_5 followed by linear interpolation in Table 4.7 and in the corresponding table with $t_M = 2700$ s (not shown). If t_M were exactly 2520 s and t_S were exactly 2880 s, then Table 4.7 could be used to determine that a value of $r_5 = 0.35$ would result in $l = 4$ because 0.35 is between $0.03119 + 0.10752 + 0.18607 = 0.32478$ and $0.32478 + 0.21546 = 0.54024$. Similarly, if t_M were 2520 s and t_S were 3060 s, $r_5 = 0.35$ would result in $l = 5$. Interpolating to obtain l when $t_M = 2520$ s and $t_S = 2898$ s gives:

$$l = 4 + \frac{2898 - 2880}{3060 - 2880}(5 - 4) = 4.1 \tag{4.4}$$

Similarly the corresponding table with $t_M = 2700$ s (not shown) using $t_S = 2898$ s results in $l = 2.1$. A final interpolation between results obtained using the two tables gives:

$$l_{final} = 4.1 + \frac{2610 - 2520}{2700 - 2520}(2.1 - 4.1) = 3.1 \approx 3 \tag{4.5}$$

Next, the algorithm is used to grow the internal segment between IM(2) and IM(3) according to the steps shown for stage B in Figure 4.5. In step 4, the fate of the C_S group that formed at the end of the internal segment is determined using r_7. Note that the C_I group on IM(2) will be studied later, so the counter N_{C_I} is increased from 0 to 1 as a reminder. For the molecule in Figure 4.5, the newly formed C_S from IM(2) reacted with a V_M group via reaction 6 to start a new segment (between IM(2) and IM(3)). For this to happen, r_7 would need to be tween$\frac{[C_{HS}(t_f)]}{[C_{HS}(t_S)]}$ and $\frac{[C_{HS}(t_f)]}{[C_{HS}(t_S)]} + \frac{[C_{HS\to M}(t_f)] - [C_{HS\to M}(t_S)]}{[C_{HS}(t_S)]}$, where $[C_{HS}]$ and $[C_{HS\to M}]$ are concentrations of hypothetical species that are calculated using equations 4.4.9 and 4.4.10 and are shown in Figures 4.7c and 4.7d.

Next, step 5 in Table 4.5 and random number r_8 are used to determine the time t_M when the C_S group was consumed. In step 6, a new random number of type r_4 is used to decide whether the segment is an internal segment or a dangling segment at the end of the batch. For the molecule in Figure 4.5, this is an internal segment, so its length ($l = 4$) is determined using a random number of type r_5. Since an additional inimer appears at the end of the segment, N_{C_I} is incremented to 2 in step 3.

In stage C, the algorithm focuses on the C_S group beside IM(3). In step 4, a random number of type r_7 is used to determine that the corresponding C_S group reacted with a V_M group to start a new segment. In step 5, the corresponding time t_M is determined and in steps 6 and 8, the segment is discovered to be a dangling segment of length 1. Table 4.9 is a probability look-up table for all dangling segments where the sum of the probabilities in each column equals one. Dangling segments that are born at low times tend to be longer than dangling segments that are born near the final batch time. For example, Table 4.9 shows that a dangling segment born late in the batch at $t_M = 5040$ s has a 79.507% probability of being one unit long and a 18.225% probability of being two units long when the batch ends at $t_f = 5400$ s using the initial recipe $[IB]_0$=1.74 M and $[IM]_0$=0.00454 M. Note that Table 4.9 is a collection of the probability values in the right-most columns of tables like Table 4.7.

Table 4.9 Probabilities for dangling segments born at different times with time interval 180 s.

	Starting time t_M						
# of IB units	0 s	180 s	360 s	…	5040 s	5220 s	5400 s
1	0.00000	0.00000	0.00000		0.79507	0.89778	1
2	0.00000	0.00000	0.00000		0.18225	0.09677	0
3	0.00000	0.00000	0.00000		0.02098	0.00527	0
⋮	⋮	⋮	⋮	⋮	⋮	⋮	⋮

Next, the algorithm proceeds to stage D. In step 10, it checks the value of N_{C_I}, which is 2 because the C_I groups associated with IM(2) and IM(3) have not been studied. In step 11, it is determined that the C_I group on IM(2) reacted with a V_M to start a new segment, which eventually turned out to be the internal segment of length 2 between IM(2) and IM(4). Proceeding further through the algorithm leads to discovery of the presence of IM(4) and IM(5), as well as the types and lengths of all of the remaining segments. Information about the current molecule is stored (*i.e.*, the number of IB units in the molecule, the number of IM units and any information about the internal and dangling segments that could be of interest to the modeler). Then, if desired, additional polymer chains can be selected randomly from the final reaction mixture and their structures can be discovered using the algorithm in Table 4.5. Note that this algorithm selects and assembles random polymer molecules from the number chain-length distribution, because each molecule in the batch is equally likely to be assembled. This approach is different from that used by Iedema et al.[45] and Tobita[47] to assemble polymers in free radical polymerization, where polymer molecules are selected randomly from the weight chain-length distribution. As such, a larger number of molecules may need to be assembled to obtain accurate information about the high-molecular weight tail.

Note that the differential equations in Table 4.4 and the entries in the probability tables (like Table 4.7 and Table 4.9) only need to be solved once, before the first molecule is assembled. Assembly of additional molecules only requires the generation of additional random numbers as described in Tables 4.5 and 4.6. The proposed MC algorithm to assemble the molecules using the probability tables was coded in Matlab (2012b 64 bit) on a Windows 7 laptop computer with Intel Core i5 2.4GHz and 4 GB of RAM.

4.4 Simulation Results

The ODEs in Table 4.4 were solved using Matlab and the results are shown in Figure 4.6, 4.7 and 4.8 for a batch reactor containing $[IB]_0 = 1.74\ M$, $[IM]_0 = 0.00454\ M$ with a final time of 5400 s. Results shown in Figure 4.8 match those obtained using traditional MC methods,[22] but were easier to obtain because no random numbers were required. Figure 4.8a shows that the IB monomer was consumed very quickly, while 41% of the inimer vinyl groups remain unreacted at the end of the batch. Figure 4.8b shows the concentration of three different end groups. Because of the low propagation rate constants for C_I groups in Table 4.1, a large number of C_I groups are predicted to remain at the end of the batch. Note that rate constant k_{pIMapp} was estimated using laboratory data from Dos Santos[19] using a PREDICI model that used the assumptions in Table 4.3. Because assumptions 1 to 4 are unrealistic, this estimate for k_{pIMapp} may be too low. Also, the value for k_{pIIapp}, which was obtained using a very simple PREDICI model, may be inaccurate.[22] In future, it will be important to find a better way to estimate all six of the rate constants in Table 4.1.

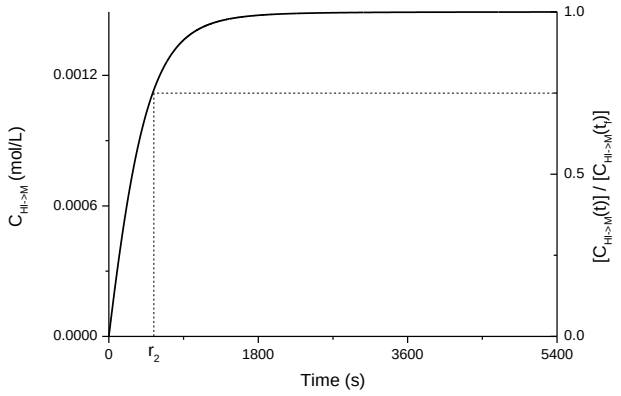

Figure 4.6 Fraction of the total C_I end groups that are eventually converted to C_M groups (via reaction 2 in Table 4.2) at any time during a batch with $[IB]_0$ = 1.74 M and $[IM]_0$ = 0.00454 M that ends at t_f = 5400 s. The values of r_2 and t_M shown on the plot indicate that 75% of the reactions of this type have occurred by a time of 528 s.

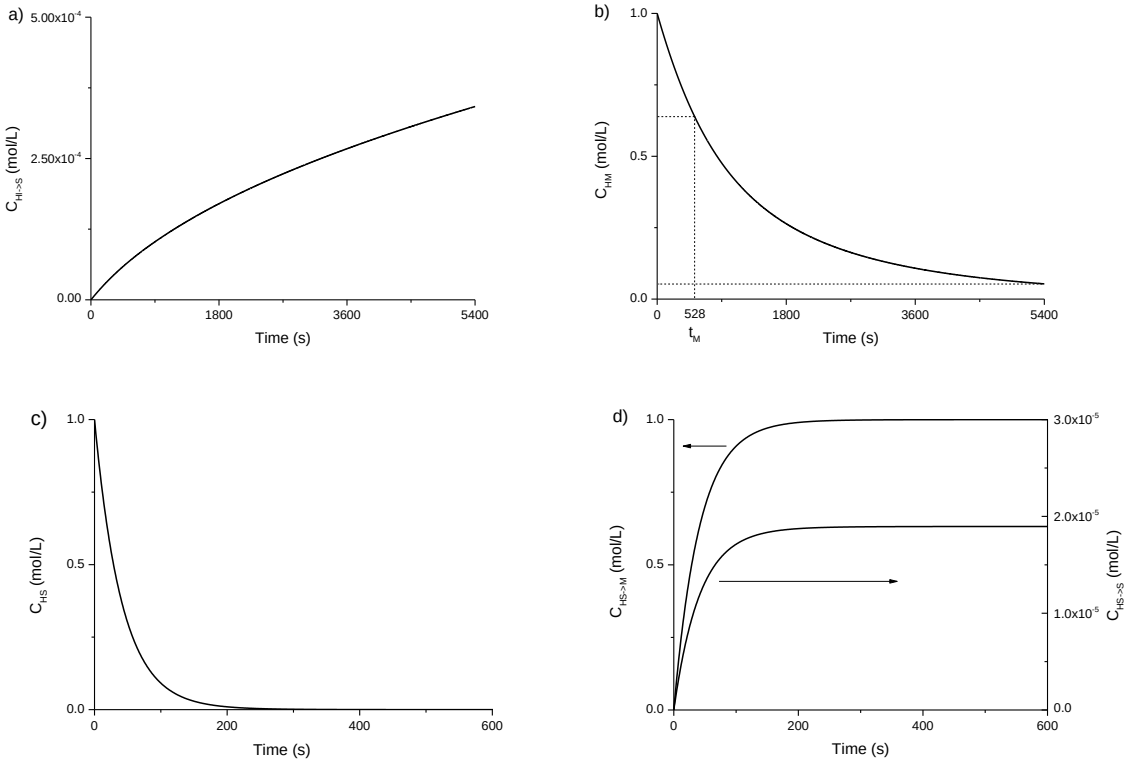

Figure 4.7 Model predictions for hypothetical species from Table 4.4, a) $C_{HI \rightarrow S}$; b) C_{HM}; c) C_{HS}; d) $C_{HS \rightarrow M}$ and $C_{HS \rightarrow S}$ obtained by starting with $[IB]_0 = 1.74$ M and $[IM]_0 = 0.00454$ M. Note that only the first 600 seconds of the simulated results are shown in c) and d).

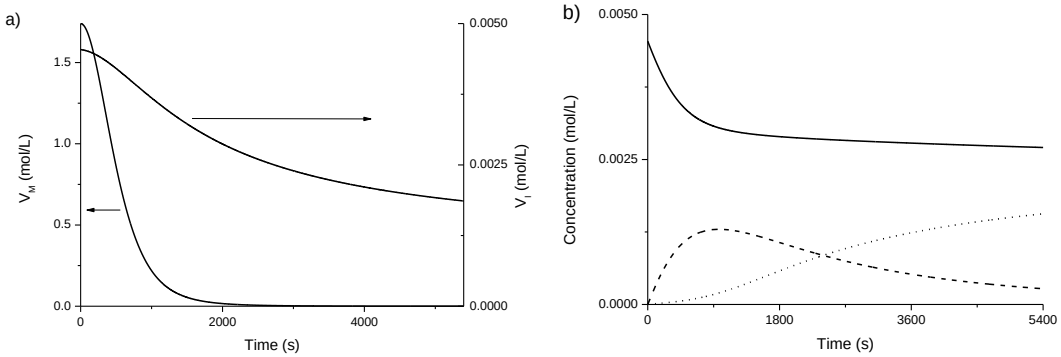

Figure 4.8 Predicted concentrations of vinyl groups and end groups obtained by solving ODEs in Table 4.4, a) V_I and V_M vinyl groups; b) ── is C_I groups; - - - is C_M groups; ····· is C_S groups, starting with $[IB]_0 = 1.74$ M and $[IM]_0 = 0.00454$ M.

As shown in Figure 4.8b, the concentration of C_M groups increases from zero at the start of the batch, reaches a maximum and then falls as fewer V_M groups are available in the reactor. The concentration of C_S groups increases throughout the batch, because after about 2000 s, the only vinyl groups that are available are V_I groups.

Figure 4.9 shows MWD results obtained using the proposed MC algorithm in Tables 4.5 to 4.8. Results are shown for three different numbers of random polymer chains (*i.e.*, 1×10^4, 1×10^5 and 2×10^5). As expected the MWD becomes smoother as additional polymer chains are simulated. The MWD obtained using only 1×10^4 chains is more jagged than those obtained using 1×10^5 and 2×10^5 chains, which are quite similar. The time required to generate the probability tables (*e.g.*, Tables 4.7 and 4.8) using PREDICI was approximately one day using a discretization interval of 180 s. Generating this same information by repeatedly solving the ODEs in Table 4.8 for internal and dangling segments that formed at a variety of times required only about 5 minutes in total. Similar probability results were obtained using PREDICI and Matlab. When numerical solution of the ODEs in Table 4.8 was used, there was no requirement to import probability results from PREDICI into Matlab via Excel, which required 140 s when PREDICI was used. Assembling 1×10^4 random chains in Matlab (using the probability tables generated using either method) required only 3.5 min. Assembling 1×10^5 polymer chains required approximately 15 min. and assembling 2×10^5 polymer chains required approximately 29 min, indicating that the time to assemble the molecules is approximately proportional to the number of polymer chains assembled. Because of the adequate accuracy and relatively short computation time, we used 1×10^5 polymer chains to generate the results in the remaining figures (*i.e.*, Figure 4.10 to Figure 4.12) in this article. In Figure 4.9 for the curve with 1×10^5 polymer chains, the $\bar{M}_n$ is 130.7 kg mol^{-1}, the $\bar{M}_w$ is 317.9 kg mol^{-1}, resulting in a polydispersity of 2.43. The bimodal

shape of the predicted MWD curve is consistent with the experimental data.[19] The first peak is mostly associated with linear chains, as explained in our previous articles.[21,22]

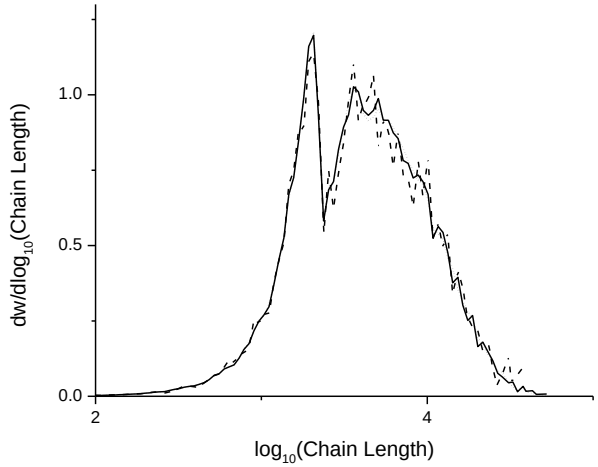

Figure 4.9 MWDs obtained using different number of random polymer chains and discretization intervals of 180 s in Tables 4.7 and 4.8, for a batch with $[IB]_0$ = 1.74 M and $[IM]_0$ = 0.00454 M and t_f = 5400 s. - - - is a distribution with 1×10^4 polymer chains; ── is a distribution with 1×10^5 polymer chains; ⋯⋯ is a distribution with 2×10^5 polymer chains.

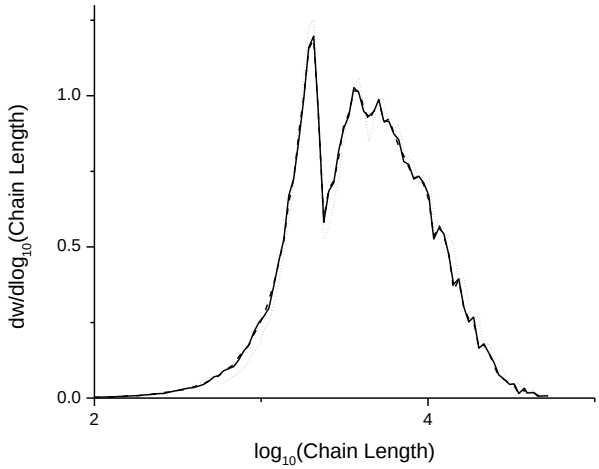

Figure 4.10 MWDs with different time intervals in Tables 4.7 and 4.8, using $[IB]_0$ = 1.74 M and $[IM]_0$ = 0.00454 M and t_f = 5400 s and 1×10^5 polymer chains. - - - is a distribution with 60 s discretization intervals; ── is a distribution with 180 s intervals; ⋯⋯ is a distribution with 600 s intervals.

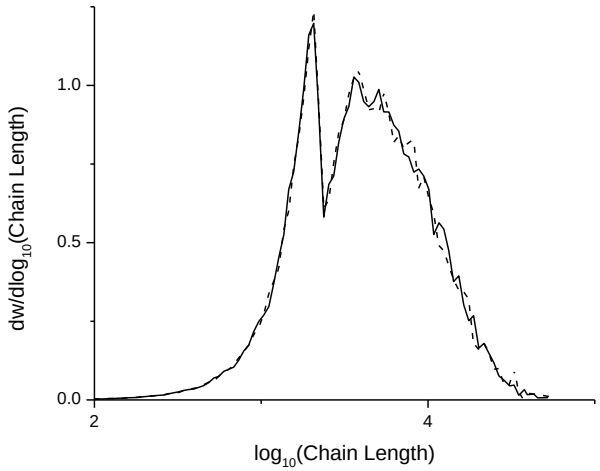

Figure 4.11 MWDs for results from traditional MC and advanced MC for a batch with $[IB]_0$ = 1.74 M and $[IM]_0$ = 0.00454 M and t_f = 5400 s. ── is advanced MC and there are 1×10^5 polymer chains, using 180 s intervals in Tables 4.7 and 4.8; - - - is from a traditional MC simulation that results in 0.99313×10^5 polymer chains.

The discretization interval selected to construct probability tables (like Table 4.7 and Table 4.9) also plays an important role on the accuracy of the results. In Figure 4.10, MWD results are compared using three different time intervals (*i.e.* 60 s, 180 s and 600 s). Results obtained using an interval of 180 s are nearly identical to those obtained using 60 s. Results obtained using the coarsest discretization (600 s) are noticeably different. Note that there is a huge difference in the computing times (using PREDICI) that were required to construct the probability tables. It took about half a day to construct tables using a 600 s discretization interval, about a day for a 180 s discretization interval and more than two days for the 60 s discretization interval. Also, it took longer for Matlab to import the larger tables containing information corresponding to the shorter time intervals. As a result, to ensure good accuracy and reasonable computation times, we selected the 180 s interval to obtain the results shown in Figure 4.9, Figure 4.11 and Figure 4.12.

Results from the proposed MC simulation and our previous traditional MC simulation are shown in Figure 4.11, with $[IB]_0 = 1.74\ M$ and $[IM]_0 = 0.00454\ M$.[22] There are only very minor discrepancies in the results obtained using these two methods. We anticipate that these minor discrepancies would disappear if more molecules were assembled and shorter discretization intervals were used for the MC simulations and if a larger initial volume (or initial number of IB and IM molecules) were used in the traditional MC simulations. Note that 6×10^5 initial IM molecules and 229955947 IB molecules (resulting in 99313 polymer chains) were used to obtain the traditional MC results in Figure 4.11, so that the number of polymer chains considered is approximately equal for the two types of MC results shown. The overall computational effort required to obtain the two MWD curves in Figure 4.11 is quite different. It took about a day to perform all of the PREDICI and Matlab calculations required for the advanced MC simulation. The corresponding traditional MC computation required considerably greater computational effort. The traditional MC simulation proceeded for eight days before the laptop ran out of working memory and the simulation stopped. To overcome this problem, fewer initial molecules were used (1×10^5 IM and 38325991 IB) to simulate the MWD six times. The results from the six MWDs were then combined to produce the dashed line in Figure 4.11. We acknowledge that the combined results from the six simulations will be slightly less accurate than if all of the molecules had been simulated using the longer simulation. We also acknowledge that a more powerful computer with more memory or parallel computing could have been used to perform the calculations. Regardless, the six sets of traditional MC MWD simulations required 10.7 hours each on the laptop computer described above, resulting in a total computing time of 2.7 days. A much longer computing time (~ two weeks) would be expected if the memory overload problem had not been encountered and the traditional MC calculations had been performed successfully using all 6×10^5 initial IM molecules and 229955947 initial IB molecules. One benefit of the proposed MC meth-

od is that computation times increase approximately linearly with the number of molecules simulated (after the probability tables have been constructed) whereas using traditional MC methods, computation times increase exponentially with the number of molecules simulated.

Another benefit of the proposed MC method is that it can readily generate MWD information for the dangling segments and internal segments, as shown in Figure 4.12. At the final time, the sample of 1×10^5 random polymer molecules contained a total of 36236 dangling segments and 308953 internal segments (segments with length zero are not included), indicating that there are approximately 9 times as many internal segments as dangling segments. Longer reaction times would lead to an even larger number of internal segments and to higher branching levels and average molecular weights.

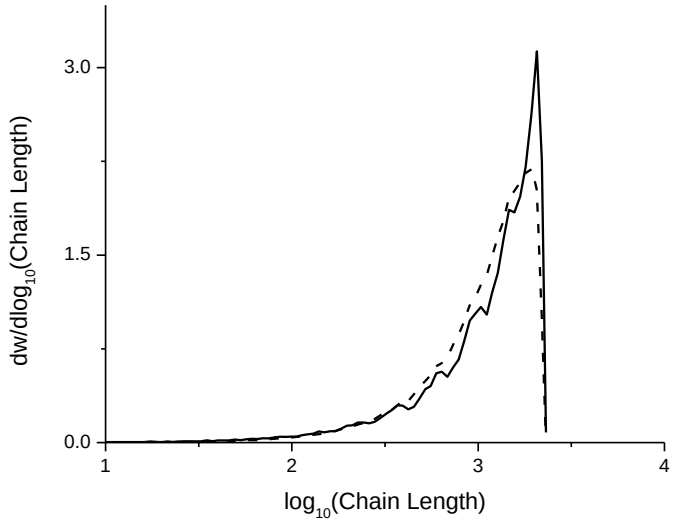

Figure 4.12 MWDs results for dangling segments and internal segments from advanced MC with $[IB]_0$ = 1.74 M and $[IM]_0$ = 0.00454 M and t_f = 5400 s and 1×10^5 polymer chains. ── are dangling segments (36236 pieces); - - - are internal segments (308953 pieces). Note internal segment with length 0 is not considered here.

Although the proposed MC method resulted in much faster computing times than the traditional MC method, it would still not be practical to use it for parameter estimation. In future, it will be beneficial to find an accurate and simple method to obtain improved parameter estimates for the six rate constants used to generate the simulation results in this article.

4.5 Conclusion

An advanced MC model was developed to describe the copolymerization of IB and inimer via carbocationic polymerization to form arborescent polymers. Like our previous traditional MC model,[22] this new MC model considers all six apparent propagation rate constants, which arise from the two types of vinyl groups and three types of chloride end groups. Simulation results obtained using the proposed MC model are consistent with those obtained using a traditional MC algorithm. However, the proposed MC model can readily be used to obtain additional information, such as MWDs of internal and dangling segments. The proposed MC method is much more computationally efficient (by a factor of approximately 200 for a typical batch reactor simulation when Matlab is used for all of the calculations) than the traditional MC method, requiring less computational time and memory. Unfortunately, the proposed MC method was considerably more complicated to formulate, implement and explain than the traditional MC technique.

The parameter values used to conduct the MC simulations were estimated using a previous PREDICI model with simplifying assumptions that were shown to be invalid.[21,22] In future, the parameters should be re-estimated using a more complex model with valid assumptions. Although the computational effort for the proposed MC model is considerably lower than for the traditional MC model, the computation times required to achieve accurate results may still be too onerous to use the proposed model for parameter estimation. In future, a revised material balance model will be formulated so that the parameters can be estimated reliably.

4.6 Reference

1 Y. Zhou, W. Huang, J. Liu, X. Zhu, D. Yan, *Adv. Mater.* **2010**, 22, 4567

2 M. Seiler, *Fluid Phase Equilibria*. **2006**, 241, 155

3 C. Gao, D. Yan. *Prog. Polym. Sci.* **2004**, 29, 183

4 M. Irfan, M. Seiler, *Ind. Eng. Chem. Res.* **2010**, 49, 1169

5 S. Chen, X. Zhang, X. Cheng, R. Zhuo, Z. Gu, *Biomacromolecules*. **2008**, 9, 2578

6 J. M. J. Fréchet, M. Henmi, I. Gitsov, S. Aoshima, M. R. Leduc, R. B. Grubbs, *Science.* **1995**, 269, 1080.

7 J. E. Puskas, M. Grasmüller, *Makromol. Chem. Macromol. Symp.* **1998**, 132, 117

8 C. Paulo, J. E. Puskas, *Macromolecules.* **2001**, 34, 734

9 J. E. Puskas, Y. Kwon, *Polym. Adv. Technol.* **2006**, 17, 615

10 J. E. Puskas, L. M. Dos Santos, G. Kaszas, K. Kulbaba, *J. Polym. Sci., Part A: Polym. Chem.* **2009**, 47, 1148

11 E. A. Foreman, J. E. Puskas, G. Kaszas, *J. Polym. Sci., Part A: Polym. Chem.* **2007**, 45, 5847

12 C. Götz, G. T. Lim, J. E. Puskas, V. Altstädt, *Journal of the Mechanical Behavior of Biomedical Materials*, **2012**, 10, 206

13 J. E. Puskas, Y. H. Chen, *Biomacromolecules.* **2004**, 5(4), 1141

14 J. E. Puskas, Y. H. Chen, Y. Dahman, D. Padavan, *J. Polym. Sci. A.*, **2004**, 42(13), 3091

15 J. E. Puskas, C. Paulo, P. Antony *US 6,747,*098, **2004**.

16 G.T. Lim, J.E. Puskas, D. H. Reneker, A. Jakli, W. E. Horton, Jr. *Biomacromolecules.* **2011**, 12, 1795

17 G. T. Lim, S. A. Valente, C. R. Hart-Spicer, M. M. Evancho-Chapman, J. E. Puskas, W. I. Horne, S.P. Schmidt. *Journal of the mechanical behavior of biomedical materials*. **2013**,

21, 47

18 J. E. Puskas, E. A. Foreman-Orlowski, G. T. Lim, S. E. Porosky, M.M. Evancho-Chapman, S.P. Schmidt, M.E. Fray, M. Piatek, P. Prowans, K. Lovejoy, *Biomaterials*. **2010**, 31, 2477

19 L. M. Dos Santos, Ph.D. thesis, University of Akron, Akron, USA, May, **2009**

20 C. Paulo, Ph.D. thesis, the University of Western Ontario, London, Canada, August, **2000**

21 Y. R. Zhao, K. B. McAuley, J. E. Puskas, L. M. Dos Santos, A. Alvarez. *Macromol. Theory Simul.* **2013**, 22, 155

22 Y. R. Zhao, K. B. McAuley, J. E. Puskas. *Macromol. Theory Simul.* **2013**, 22, 365

23 G. Kaszas, J. E. Puskas, *Polymer Reaction Engineering.* **1994**, 2(3), 251

24 J. E. Puskas, M. G. Lanzendorfer, *Macromolecules.* **1998**, 31, 8684

25 J. E. Puskas, H. Peng, *Polym. React. Eng*. **1999**, 7(4), 553

26 J. E. Puskas, S. Shaikh, K. Z. Yao, K. B. McAuley, G. Kaszas, *European Polymer Journal*. **2005**, 41, 1

27 A. H. E. Müller, D. Yan, M. Wulkow, *Macromolecules.* **1997**, 30, 7015

28 D. Yan, A. H. E. Müller, K. Matyjaszewski, *Macromolecules.* **1997**, 30, 7024

29 G. I. Litvinenko, P. F. W. Simon, A. H. E. Müller, *Macromolecules.* **1999**, 32, 2410

30 G. I. Litvinenko, P. F. W. Simon, A. H. E. Müller, *Macromolecules.* **2001**, 34, 2418

31 G. I. Litvinenko, A. H. E. Müller, *Macromolecules.* **2002**, 35, 4577

32 K. C. Cheng, T. H. Chuang, J. S. Chang, W. Guo, W. F. Su, *Macromolecules* **2005**, 38, 8252

33 K. C. Cheng, Y. Y. Su, T. H. Chuang, W. Guo, W. F. Su, *Macromolecules.* **2010**, 43, 8965

34 A. Zargar, K. Chang, L. J. Taite, F.J. Schork, *Macromol. React. Eng*. **2011**, 5, 373

35 X. He, H. Liang, C. Pan, *Polymer* **2003**, 44, 6697

36 X. He, J. Tang, *J. Polym. Sci. Part A: Polym. Chem*. **2008**, 46, 4486-4494

37 X. He, H. Liang, C. Pan, *Macromol. Theory Simul*. **2001**, 10, 196

38 M. Wulkow. *Macromol. React. Eng.* **2008**, 2, 461

39 J. B. P. Soares, A. E. Hamielec, *Macromol. React. Eng.* **2007**, 1, 53

40 J. He, H. Zhang, J. Chen, Y. Yang. *Macromolecules.* **1997**, 30, 8010

41 L. Nie, W. Yang, H. Zhang, S. Fu. *Polymer.* **2005**, 46, 3175

42 M. Al-Harthi, M. J. Khan, S. H. Abbasi, J. B. P. Soares. *Macromol. React. Eng.* **2009**, 3, 148

43 D. T. Gillespie, *Journal of Physical Chemistry.* **1977**, 81(25), 2340

44 P. D. Iedema, M. Wulkow, H. C. J. Hoefsloot. *Polymer*. **2007**, 48, 1770

45 P. D. Iedema, H. C. J. Hoefsloot. *Macromolecules*. **2006**, 39, 3081

46 P. D. Iedema, H. C. J. Hoefsloot. *Macromol. Theory Simul.* **2001**, 10, 855

47 H. Tobita. *J. Polym. Sci., Part B: Polym. Phys*. **2001**, 39, 391

48 H. Tobita. *J. Polym. Sci., Part B: Polym. Phys*. **1993**, 31, 1363

49 J. E. Puskas, S. W. P. Chain, K. B. McAuley, G. Kaszas, S. Shaikh, *J. Polym. Sci. Part A: Polym. Chem.* **2007**, 45, 1778-1787

50 H. Schlaad, Y. Kwon, L. Sipos, R. Faust, B. Charleux, *Macromolecules.* **2000**, 33, 8225

Appendix 4.1 Implementation Details in PREDICI for Internal Segments

PREDICI was used to solve some differential equations to generate the probability results in Tables 4.7 and 4.9. These simulations require PREDICI to track dangling segments that are born at different times (*i.e.* t = 0, 1, 2…90 min.). Figure 4.13 shows the reaction mechanism as it was implemented in PREDICI. In this simulation, I wanted to arbitrarily set the initial concentration of dangling segments born at time zero containing one monomer unit. (*i.e.* L0(1)) to 1.0 mol/L. However, PREDICI does not seem to allow the user to set concentrations for polymer chains with specific chain lengths. To solve this implementation problem, I used a standard PREDICI reaction wherein fake monomer can be converted into polymer:

$$M(0) \xrightarrow{k_{ph}} L0(1) \tag{A4.1.1}$$

The rate constant k_{ph} (h for hypothetical) was set at a very high value ($10^{10}\ s^{-1}$), so that the required L0(1) would appear nearly instantly at time zero.

Similarly, I needed L1(1) to appear in the batch reactor instantly at time = 1 min. To do so, I generated the L1(1) (and also L2(1)…L90(1)) nearly instantaneously at time zero. However, L1(1) was not permitted to start propagating until t = 1 min. by setting the rate constant kp1.fun (shown in Figure 4.14) to zero before t = 1 min. and to k_{pMM} after 1 min. In a similar fashion dangling chains of type L2(1) were permitted to start propagating at t = 2 min. and chains of type L89(1) were permitted to start propagating after t = 89 min.

To generate the internal segments, we just need to change the end-of-batch time to different time points and use the same reactions in PREDICI shown in Figure 4.13 and 4.14.

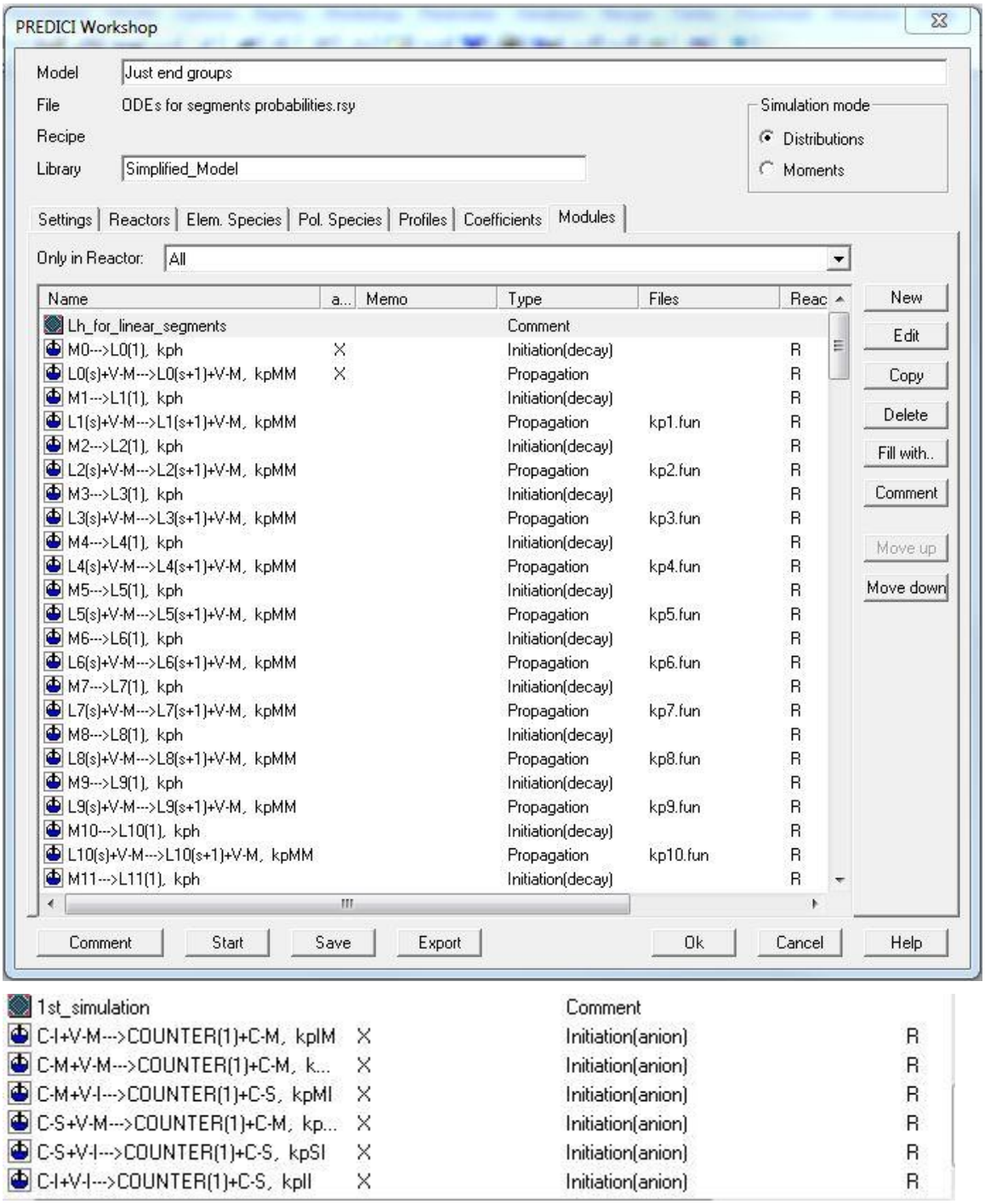

Figure 4.13 Captured photo from PREDICI. L0 is the concentration of segments that start growing at $t = 0$; L1 is the concentration of the segments that start growing at $t = 1$ min.; L2,L3… are linear segments that are born at different time. M0, M1… are the corresponding initiator that initiates the linear segments.

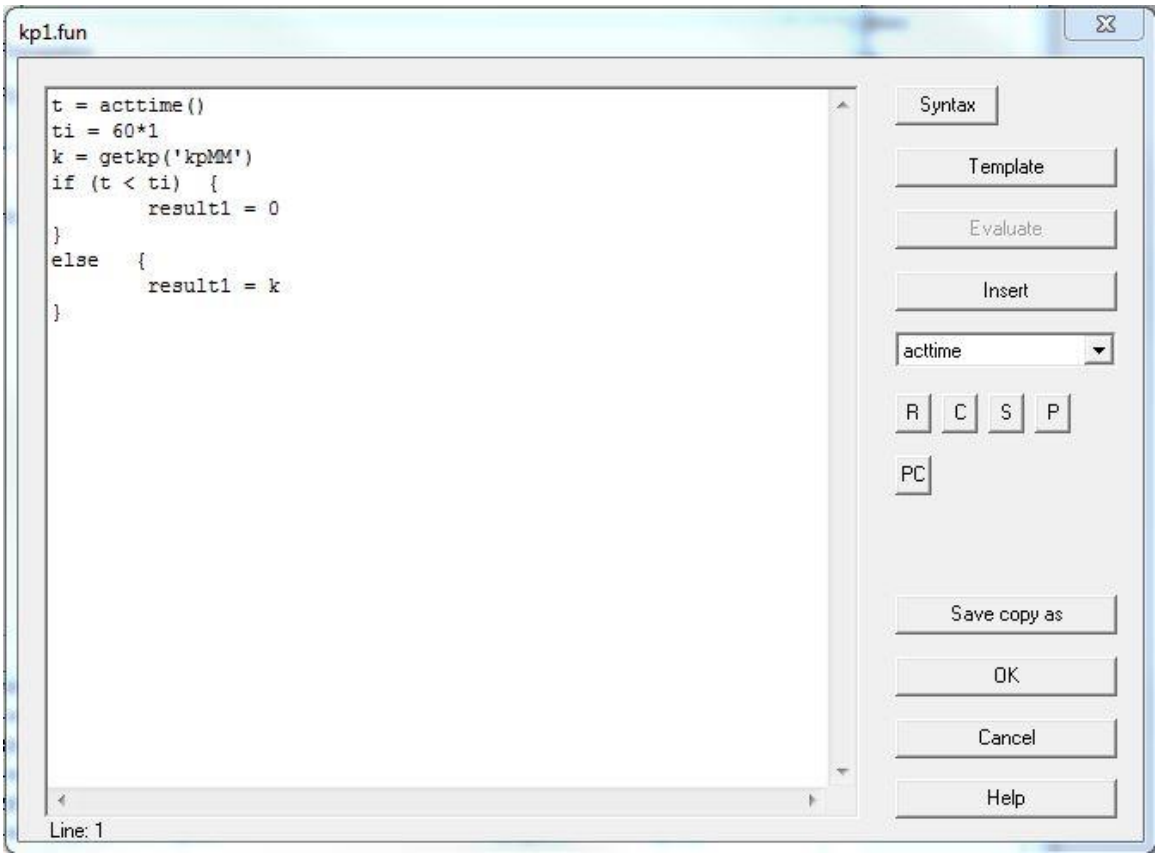

Figure 4.14 PREDICI file for kp1.fun that controls the birth time of L1(1).

Appendix 4.2 Matlab Code for Advanced MC Model with 3 Minutes Interval

```
function [] = Con_MC_3_min(polymer)
    tic %calculate the computing time of each simulations

    t_end = 5400;                %end of batch reaction
    macro = [0 0 0 0];           %matrix used to store polymers
    internal_segments = [0];     %matrix used to store internal segments
    internal_counter = 1;         %count the number of internal segments
    dangling_segments = [0];     %matrix used to store dangling segments
    dangling_counter = 1;        %count the number of dangling segments

    %import the table containing concentrations of different species over time
    res = xlsread('C:\Users\zhaoyu\Desktop\Con_MC_ode_4th_paper.xlsx','ODE','A1:L5401');
    [row column] = size(res)
    num = 1;              %counter of polymer chains that have been assembled

    %import table containing dangling segment
    dangling = xlsread('C:\Users\zhaoyu\Desktop\Con_MC_dtable_4th_paper.xlsx','dangling','A2:AE4501');

    %import tables containing internal segments starting from different tM
    %tM=0,3,6…90
    internal(1).a = xlsread('C:\Users\zhaoyu\Desktop\Con_MC_itable_4th_paper.xlsx','0','A2:AE4101');
    internal(2).a = xlsread('C:\Users\zhaoyu\Desktop\Con_MC_itable_4th_paper.xlsx','3','A2:AD3501');
    internal(3).a = xlsread('C:\Users\zhaoyu\Desktop\Con_MC_itable_4th_paper.xlsx','6','A2:AC3001');
    internal(4).a = xlsread('C:\Users\zhaoyu\Desktop\Con_MC_itable_4th_paper.xlsx','9','A2:AB2501');
    internal(5).a = xlsread('C:\Users\zhaoyu\Desktop\Con_MC_itable_4th_paper.xlsx','12','A2:AA2001');
    internal(6).a = xlsread('C:\Users\zhaoyu\Desktop\Con_MC_itable_4th_paper.xlsx','15','A2:Z2001');
    internal(7).a = xlsread('C:\Users\zhaoyu\Desktop\Con_MC_itable_4th_paper.xlsx','18','A2:Y2001');
    internal(8).a = xlsread('C:\Users\zhaoyu\Desktop\Con_MC_itable_4th_paper.xlsx','21','A2:X2001');
    internal(9).a = xlsread('C:\Users\zhaoyu\Desktop\Con_MC_itable_4th_paper.xlsx','24','A2:W2001');
    internal(10).a = xlsread('C:\Users\zhaoyu\Desktop\Con_MC_itable_4th_paper.xlsx','27','A2:V2001');
    internal(11).a = xlsread('C:\Users\zhaoyu\Desktop\Con_MC_itable_4th_paper.xlsx','30','A2:U1001');
    internal(12).a = xlsread('C:\Users\zhaoyu\Desktop\Con_MC_itable_4th_paper.xlsx','33','A2:T1001');
    internal(13).a = xlsread('C:\Users\zhaoyu\Desktop\Con_MC_itable_4th_paper.xlsx','36','A2:S1001');
    internal(14).a = xlsread('C:\Users\zhaoyu\Desktop\Con_MC_itable_4th_paper.xlsx','39','A2:R1001');
    internal(15).a = xlsread('C:\Users\zhaoyu\Desktop\Con_MC_itable_4th_paper.xlsx','42','A2:Q1001');
    internal(16).a = xlsread('C:\Users\zhaoyu\Desktop\Con_MC_itable_4th_paper.xlsx','45','A2:P1001');
    internal(17).a = xlsread('C:\Users\zhaoyu\Desktop\Con_MC_itable_4th_paper.xlsx','48','A2:O1001');
    internal(18).a = xlsread('C:\Users\zhaoyu\Desktop\Con_MC_itable_4th_paper.xlsx','51','A2:N1001');
    internal(19).a = xlsread('C:\Users\zhaoyu\Desktop\Con_MC_itable_4th_paper.xlsx','54','A2:M1001');
    internal(20).a = xlsread('C:\Users\zhaoyu\Desktop\Con_MC_itable_4th_paper.xlsx','57','A2:L1001');
    internal(21).a = xlsread('C:\Users\zhaoyu\Desktop\Con_MC_itable_4th_paper.xlsx','60','A2:K1001');
    internal(22).a = xlsread('C:\Users\zhaoyu\Desktop\Con_MC_itable_4th_paper.xlsx','63','A2:J1001');
    internal(23).a = xlsread('C:\Users\zhaoyu\Desktop\Con_MC_itable_4th_paper.xlsx','66','A2:I1001');
    internal(24).a = xlsread('C:\Users\zhaoyu\Desktop\Con_MC_itable_4th_paper.xlsx','69','A2:H1001');
    internal(25).a = xlsread('C:\Users\zhaoyu\Desktop\Con_MC_itable_4th_paper.xlsx','72','A2:G1001');
    internal(26).a = xlsread('C:\Users\zhaoyu\Desktop\Con_MC_itable_4th_paper.xlsx','75','A2:F1001');
    internal(27).a = xlsread('C:\Users\zhaoyu\Desktop\Con_MC_itable_4th_paper.xlsx','78','A2:E1001');
    internal(28).a = xlsread('C:\Users\zhaoyu\Desktop\Con_MC_itable_4th_paper.xlsx','81','A2:D1001');
    internal(29).a = xlsread('C:\Users\zhaoyu\Desktop\Con_MC_itable_4th_paper.xlsx','84','A2:C1001');
    internal(30).a = xlsread('C:\Users\zhaoyu\Desktop\Con_MC_itable_4th_paper.xlsx','87','A2:B1001');
    internal(31).a =
xlsread('C:\Users\zhaoyu\Desktop\Con_MC_itable_4th_paper.xlsx','90','A2:A1001');%tM=90

    %column numbers of different species in the table of concentrations
    col_time = 1;
    col_Ci = 2;
    col_Cm = 3;
    col_Cs = 4;
    col_Vi = 5;
    col_Vm = 6;
    col_Ci_m = 7;
```

```
col_Ci_s = 8;
col_CHM = 9;
col_CHS = 10;
col_CHS_M = 11;
col_CHS_S = 12;

%%%%%%%%%%%%%%%%%%%%%%%%%%%%%%%%%%%%%%%%%%%%%%%%%%%%%%%%%%%%%%%%%%%%%%%%%%%%
%start to construct polymer chains
%%%%%%%%%%%%%%%%%%%%%%%%%%%%%%%%%%%%%%%%%%%%%%%%%%%%%%%%%%%%%%%%%%%%%%%%%%%%

while num <= polymer %assemble certain number of polymer chains
    t = 0;
    num = num + 1;  %count the number of polymers
    numIB = 0;      %counter for IB segment
    numIM = 1;      %counter for IM segment
    remain_Ci = 1;  %NCi in the paper

    while (remain_Ci > 0)  %Construct each single linear chains

        t = 0;
        remain_Ci = remain_Ci - 1;

        %%%%%%%%%%%%%%%%%%%%%%%%%%%%%%%%%%%%%%%%%%%%%%%%%%%%%%%%%%%%%%%%%%%%%%%%%%%%
        %Selet a Vi vinyl group
        %%%%%%%%%%%%%%%%%%%%%%%%%%%%%%%%%%%%%%%%%%%%%%%%%%%%%%%%%%%%%%%%%%%%%%%%%%%%

        r1 = rand;  %Here r0 and r1 are combined into r1

        %1 Ci react nothing remain Ci to the end
        if r1 <= res(row,col_Ci)/res(1,col_Ci)

            %if it is a IM instead of polymer, do not count it
            if numIM == 1
                num = num - 1;
            end

            t = t_end;

        %2 Ci react with Vm to form a Cm group
        elseif  res(row,col_Ci)/res(1,col_Ci)< r1 & r1 <= ((res(row,col_Ci)/res(1,col_Ci) + ...
                res(row,col_Ci_m)/res(1,col_Ci)))

            endgroup = 1;  %change end group to Cm

            r2 = rand;

            %find reaction time tm
            for k = 1 : row
                if res(k,col_Ci_m) > r2*res(row,col_Ci_m)
                    break
                end
            end
            t = res(k,col_time);

            while (t < t_end)

                %2.1 Cm end group
                if endgroup == 1  % use number 1 to represent Cm

                    r4 = rand;

                    %2.1.1 Cm react with Vi to form a internal segment
                    if r4 < ((res(round(t+1),col_CHM) - res(row,col_CHM))/res(round(t+1),col_CHM))
```

```
remain_Ci = remain_Ci + 1;   %NCi plus 1
endgroup = 2; %change end group to Cs

t_start = t;
CHM_t = (1-r4)*(res(round(t+1),col_CHM));     %concentration at t_end_segment

%find corresponding ending time ts when the internal segment was ended
for k = round(t+1) : row
   if res(k,col_CHM) < CHM_t
      break
   end
end

if k == 5401 %do not count the t = t_end here, it causes problem
   t_end_segment = res(k,col_time)-1;   %end time of internal segment
else
   t_end_segment = res(k,col_time);
end

t = res(k,col_time);                        %update reaction time

col_start = floor(t_start/180);             %corespoinding starting column
col_end = floor(t_end_segment/180);  %corespoinding end column
distance = (col_end-col_start);             %distance between two columns

%%%%%%%%%%%%%%%%%%%%%%%%%%%%%%%%%%%%%%%%%%%%%%%%%%%%%%%%%%%%%%%%%%%%%%%%%%%%
%the birth time is of a segment in between time column a and b (b=a+3min)
%the end time is in between time column c and d (d=c+3min)
%the 1st interpolation use the same ts, but different tm
%the 2nd interpolation use the same tm and ts
%%%%%%%%%%%%%%%%%%%%%%%%%%%%%%%%%%%%%%%%%%%%%%%%%%%%%%%%%%%%%%%%%%%%%%%%%%%%
%1st interpolation cacluates the chain born at a ended in ts (between c & d),
%using table 4.7 to get length1
%1st interpolation cacluates the chain born at b ended in ts (between c & d),
%using table similar to 4.7 to get length2
%%%%%%%%%%%%%%%%%%%%%%%%%%%%%%%%%%%%%%%%%%%%%%%%%%%%%%%%%%%%%%%%%%%%%%%%%%%%
%2nd interpolation calculates the chain born at tm (between a & b) ended at
%ts using length1 and length 2 from the 1st interpolation
%%%%%%%%%%%%%%%%%%%%%%%%%%%%%%%%%%%%%%%%%%%%%%%%%%%%%%%%%%%%%%%%%%%%%%%%%%%%
%Note lengthac is the length of segment that was born at a and ended at c.
%Similar explanations are applied to lengthad, lengthbc and lengthbd.
%%%%%%%%%%%%%%%%%%%%%%%%%%%%%%%%%%%%%%%%%%%%%%%%%%%%%%%%%%%%%%%%%%%%%%%%%%%%

r5 = rand;
length1 = 1;   %length of chain from the 1st table
length2 = 1;   %length of chain from the 2nd table
lengthac = 1;  %together with ad for linear interpolation
lengthad = 1;
lengthbc = 1;  %together with bd for linear interpolation
lengthbd = 1;
P = 0;
P1 = 0;
P2 = 0;
pac = 0;
pad = 0;
pbc = 0;
pbd = 0;

%use two tables when col_start and col_end are not in between the same time interval
if distance ~= 0

   while r5 > pac     %1st interpolation
      pac = pac + internal(col_start+1).a(lengthac,distance+1);
      lengthac = lengthac + 1;
```

```
        end

        while r5 > pad     %1st interpolation
            pad = pad + internal(col_start+1).a(lengthad,distance+2);
            lengthad = lengthad + 1;
        end

        length1 = (t_end_segment-col_end*180)*(lengthac-lengthad)/(-180)+lengthac;

        while r5 > pbc     %1st interpolation from a table with tM + 3
            pbc = pbc + internal(col_start+2).a(lengthbc,distance);
            lengthbc = lengthbc + 1;
        end

        while r5 > pbd     %1st interception 1 from a table with tM + 3
            pbd = pbd + internal(col_start+2).a(lengthbd,distance+1);
            lengthbd = lengthbd + 1;
        end

        length2 = (t_end_segment-col_end*180)*(lengthbc-lengthbd)/(-180)+lengthbc;

        %2nd interpolation
        length = (t_start-col_start*180)*(length1-length2)/(-180)+length1;

    %col_start and col_end are in between the same time interval (one table is enough)
    else
        length = 1;
        while r5 > P     %find the length
            P = P + internal(col_start+1).a(length,2);
            length = length + 1;
        end
        %just one interpolation
        length = (t_end_segment-t_start)*length/180;
    end

    length = round(length);
    numIB = numIB + length;
    numIM = numIM + 1;
    internal_segments(internal_counter,1) = length;
    internal_counter = internal_counter + 1;


%2.1.2 Cm reacts with Vm until the end to form dangling segment
else

    col_t = 1;          %time in dangling table
    while (t > col_t*180)
        col_t = col_t + 1;
    end

    r6 = rand;
    length1 = 1;
    length2 = 1;
    sum1 = 0;
    sum2 = 0;

    while (sum1 < r6)  %for length of dangling segment
        sum1 = sum1 + dangling(length1,col_t);
        length1 = length1 + 1;
    end

    while (sum2 < r6)
        sum2 = sum2 + dangling(length2,col_t+1);
        length2 = length2 + 1;
```

```
                    end

                    %linear interpolation
                    length = (t-(col_t-1)*180)*(length1-length2)/(-180)+length1;
                    length = round(length);
                    numIB = numIB + length;
                    t = t_end;
                    dangling_segments(dangling_counter,1) = length;
                    dangling_counter = dangling_counter + 1;
                end

            %2.2 Cs end group
            elseif endgroup == 2 %Cs end group

                r7 = rand;
                %2.2.1 Cs group remains unreacted until the end
                if r7 <= res(row,col_CHS)/res(round(t+1),col_CHS)

                    t = t_end;

                %2.2.2 Cs group react with Vm at sometime
                elseif res(row,col_CHS)/res(round(t+1),col_CHS) < r7 & r7 <=
((res(row,col_CHS)+res(row,col_CHS_M) - res(round(t+1),col_CHS_M))/res(round(t+1),col_CHS))

                    r8 = rand;

                    %find corresponding reaction time tm
                    for k = round(t+1) : row
                        if res(k,col_CHS_M) > r8*(res(row,col_CHS_M)-res(round(t+1),col_CHS_M)) +
res(round(t+1),col_CHS_M)
                            break
                        end
                    end
                    t = res(k,col_time);

                    endgroup = 1; % change end group to Cm

                %2.2.3 Cs group react with Vi at sometime
                elseif ((res(row,col_CHS)+res(row,col_CHS_M)-res(round(t+1),col_CHS_M)) /
res(round(t+1),col_CHS)) < r7

                    r9 = rand;

                    %find corresponding reaction time ts2
                    for k = round(t+1) : row
                        if res(k,col_CHS_S) > r9*(res(row,col_CHS_S)-res(round(t+1),col_CHS_S)) +
res(round(t+1),col_CHS_S)
                            break
                        end
                    end
                    t = res(k,col_time);

                    numIM = numIM + 1;
                    remain_Ci = remain_Ci + 1;

                end
            end
        end


    %3 Ci react with Vi to form a Cs group
    else

        endgroup = 2;  %change end group to Cs
```

```
numIM = numIM + 1;
remain_Ci = remain_Ci + 1;

r3 = rand;

%find corresponding reaction time ts when this happens
for k = 1 : row
   if res(k,col_Ci_s) > r3*res(row,col_Ci_s)
      break
   end
end
t = res(k,col_time);


while (t < t_end)

   %3.1 Cm end group
   if endgroup == 1  %Cm end group

      r4 = rand;
      %3.1.1 Cm react with Vi to form a internal segment
      if r4 <= ((res(round(t+1),col_CHM) - res(row,col_CHM))/res(round(t+1),col_CHM)

         remain_Ci = remain_Ci + 1;
         endgroup = 2; %change end group to Cs

         t_start = t;
         CHM_t = (1-r4)*(res(round(t+1),col_CHM));  %concentration at t_end_segment use
r4 to find the end time

         %find corresponding ending time ts when this ends
         for k = round(t+1) : row
            if res(k,col_CHM) < CHM_t
               break
            end
         end

         if k == 5401
            t_end_segment = res(k,col_time)-1;   %end time of internal segment
         else
            t_end_segment = res(k,col_time);
         end

         t = res(k,col_time);                    %update reaction time

         col_start = floor(t_start/180);         %corespoinding starting column
         col_end = floor(t_end_segment/180);     %corespoinding end column
         distance = (col_end-col_start);         %distance between two columns

         r5 = rand;
         length1 = 1;
         length2 = 1;
         lengthac = 1;
         lengthad = 1;
         lengthbc = 1;
         lengthbd = 1;
         P = 0;
         P1 = 0;
         P2 = 0;
         pac = 0;
         pad = 0;
         pbc = 0;
         pbd = 0;
```

```
    if distance ~= 0    %see the same part in section 2
       while r5 > pac     %1st interpolation
          pac = pac + internal(col_start+1).a(lengthac,distance+1);
          lengthac = lengthac + 1;
       end

       while r5 > pad     %1st interpolation
          pad = pad + internal(col_start+1).a(lengthad,distance+2);
          lengthad = lengthad + 1;
       end

       length1 = (t_end_segment-col_end*180)*(lengthac-lengthad)/(-180)+lengthac;

       while r5 > pbc     %1st interpolation
          pbc = pbc + internal(col_start+2).a(lengthbc,distance);
          lengthbc = lengthbc + 1;
       end

       while r5 > pbd     %1st interpolation
          pbd = pbd + internal(col_start+2).a(lengthbd,distance+1);
          lengthbd = lengthbd + 1;
       end

       length2 = (t_end_segment-col_end*180)*(lengthbc-lengthbd)/(-180)+lengthbc;

       %2nd interpolation
       length = (t_start-col_start*180)*(length1-length2)/(-180)+length1;

    else
       length = 1;
       while r5 > P     %interpolation
            P = P + internal(col_start+1).a(length,2);
            length = length + 1;
       end
       length = (t_end_segment-t_start)*length/180;
    end

    length = round(length);
    numIB = numIB + length;
    numIM = numIM + 1;
    internal_segments(internal_counter,1) = length;
    internal_counter = internal_counter + 1;


%3.1.2 Cm reacts with Vm until the end to form dangling segment
else

    col_t = 1;          %time in dangling table
    while (t > col_t*180)
       col_t = col_t + 1;
    end

    r6 = rand;
    length1 = 1;
    length2 = 1;
    sum1 = 0;
    sum2 = 0;

    %linear interpolation
    while (sum1 < r6)  %for chain length
       sum1 = sum1 + dangling(length1,col_t);
       length1 = length1 + 1;
    end
```

```
                while (sum2 < r6)
                    sum2 = sum2 + dangling(length2,col_t+1);
                    length2 = length2 + 1;
                end

                length = (t-(col_t-1)*180)*(length1-length2)/(-180)+length1;
                length = round(length);
                numIB = numIB + length;
                t = t_end;
                dangling_segments(dangling_counter,1) = length;
                dangling_counter = dangling_counter + 1;
            end

        %3.2 Cs end group
        elseif endgroup == 2 %Cs end group

            r7 = rand;
            %2.2.1 Cs group remains unreacted until the end
            if r7 <= res(row,col_CHS)/res(round(t+1),col_CHS)

                t = t_end;

            %2.2.2 Cs group react with Vm at sometime
            elseif res(row,col_CHS)/res(round(t+1),col_CHS) < r7 & r7 <= (res(row,col_CHS) +
res(row,col_CHS_M) - res(round(t+1),col_CHS_M))/res(round(t+1),col_CHS)

                r8 = rand;

                %find corresponding reaction time tm when this happens
                for k = round(t+1) : row
                    if res(k,col_CHS_M) > r8*(res(row,col_CHS_M) - res(round(t+1),col_CHS_M)) +
res(round(t+1),col_CHS_M)
                        break
                    end
                end
                t = res(k,col_time);
                endgroup = 1;

            %3.2.3 Cs group react with Vi at sometime
            elseif ((res(row,col_CHS)+res(row,col_CHS_M)-
res(round(t+1),col_CHS_M))/res(round(t+1),col_CHS)) < r7

                r9 = rand;

                %find corresponding reaction time ts2 when this happens
                for k = round(t+1) : row
                    if res(k,col_CHS_S) > r9*(res(row,col_CHS_S) - res(round(t+1),col_CHS_S)) +
res(round(t+1),col_CHS_S)
                        break
                    end
                end

                t = res(k,col_time);
                numIM = numIM + 1;
                remain_Ci = remain_Ci + 1;

            end
        end
    end
  end
end

%%%%%%%%%%%%%%%%%%%%%%%%%%%%%%%%%%%%%%%%%%%%%%%%
%After assemble one polymer molecule
```

```
        %store polymer information into matrix
        %%%%%%%%%%%%%%%%%%%%%%%%%%%%%%%%%%%%%%%%
        if numIM ~= 1 | numIB ~= 0
            Mn = numIB*0.056 + numIM*0.1805;
            Mw = (numIB*0.056 + numIM*0.1805)^2;
            macro(num,:) = [numIM, numIB, Mn, Mw];
        end

    end

    %%%%%%%%%%%%%%%%%%%%%%%%%%%%%%%%%%%%%%%%%%%%%%%%%%%%%%
    %output results into Excel
    %%%%%%%%%%%%%%%%%%%%%%%%%%%%%%%%%%%%%%%%%%%%%%%%%%%%%%
    xlswrite('C:\Users\zhaoyu\Desktop\3min_4th_paper_results.xlsx',macro,'Polymer','A1');
    xlswrite('C:\Users\zhaoyu\Desktop\3min_4th_paper_results.xlsx',internal_segments,'Internal','A1');
    xlswrite('C:\Users\zhaoyu\Desktop\3min_4th_paper_results.xlsx',dangling_segments,'Dangling','A1');

    toc
end
```

Chapter 5

Parallel Models for Arborescent Polyisobutylene Synthesized in Batch Reactor

Yutian R. Zhao[1], Kimberley B. McAuley[1], Judit E. Puskas[2]

[1]Department of Chemical Engineering, Queen's University, Kingston, ON, Canada
[2]Department of Chemical & Biomolecular Engineering, University of Akron, Akron, OH USA

5.1 Abstract

A mathematical model is developed for estimating kinetic parameters that influence the production of *arborescent* polyisobutylene (*arb*PIB) via carbocationic copolymerization of inimer and isobutylene. Six different propagation rate constants arise due to the two types of vinyl groups and three types of carbocations. These six parameters are estimated using parallel simulation systems in PREDICI that track i) functional groups, ii) internal and dangling segments in the polymer and iii) concentrations of inimer and polymer molecules. Parameter estimates obtained using the proposed model result in a better fit to literature data than was obtained using a previous model that neglected two types of propagations reactions. Predictions from the proposed model are consistent with Monte Carlo simulations for MWD of the internal and dangling segments.

This chapter has been submitted for publication in the AIChE Journal.

5.2 Introduction

Fréchet et al. invented self-condensing vinyl polymerization (SCVP) about two decades ago, greatly simplifying the synthesis process for arborescent or hyperbranched polymers.[1] In their SCVP system, an "inimer"(IM) is used to initiate the polymerization and induce branching. An IM molecule typically has two types of active sites: i) an initiating site that can start propagation; and ii) a vinyl group that can be polymerized to form a branching point. The inimer used in the current study is 4-(2-chloroisopropyl) styrene, shown in Figure 5.1a, which is produced *in situ* from 4-(2-methoxyisopropyl)styrene (MeOIM) and $TiCl_4$.[2,3] Since the invention of SCVP, considerable research has been performed on related topics including: synthesizing polymers via self-condensing vinyl copolymerization (SCVCP),[2-9] developing different kinds of IM molecules and arborescent polymers[10-12] and building mathematical models for SCVP and SCVCP systems.[13-26] Puskas et al.[27-29] developed a promising biomaterial via living block copolymerization of styrene on an *arborescent* polyisobutylene (*arb*PIB) core. This *arb*PIB core was synthesized through a "one-pot" living carbocationic copolymerization of isobutylene (IB) and IM molecules.[13] A simplified reaction scheme is shown in Figure 5.1b. This biomaterial can be used for human implantation (*e.g.*, for breast implants) and has higher biocompatibility, better strength and less permeability to liquids than silicone materials.[28,29]

In Puskas's "one-pot" living cationic polymerization, shown in Figure 5.1b, there are two types of vinyl groups V_I, V_M and three types of chloride end groups C_I, C_M, C_S as shown in Figure 5.1b. V_I is the vinyl group on IM, while V_M is the vinyl group on the IB monomer. A C_I end group is an unreacted chloride group on IM, a C_M end group forms after addition of a V_M group, and a C_S end group forms after the reaction of a V_I group. As a result, there are six different propagation rate constants, which are $k_{pII}, k_{pIM}, k_{pMI}, k_{pMM}, k_{pSI}\ and\ k_{pSM}$, where the first subscript after k_p represents the type of end group that is uncapped for reaction, and the second subscript

represents the type of vinyl group that is consumed. Table 5.1 summarizes all six reactions between different end groups and vinyl groups. The rate constants above the arrows in Table 5.1 are apparent rate constants that depend on equilibrium constants for capping and uncapping of chloride end groups and the corresponding true rate constants, as shown in Table 5.2. The expressions in Table 5.2 were developed using Puskas's two-path reaction scheme for carbocationic polymerization, which is shown in Figure 5.2 for a homopolymerization process.

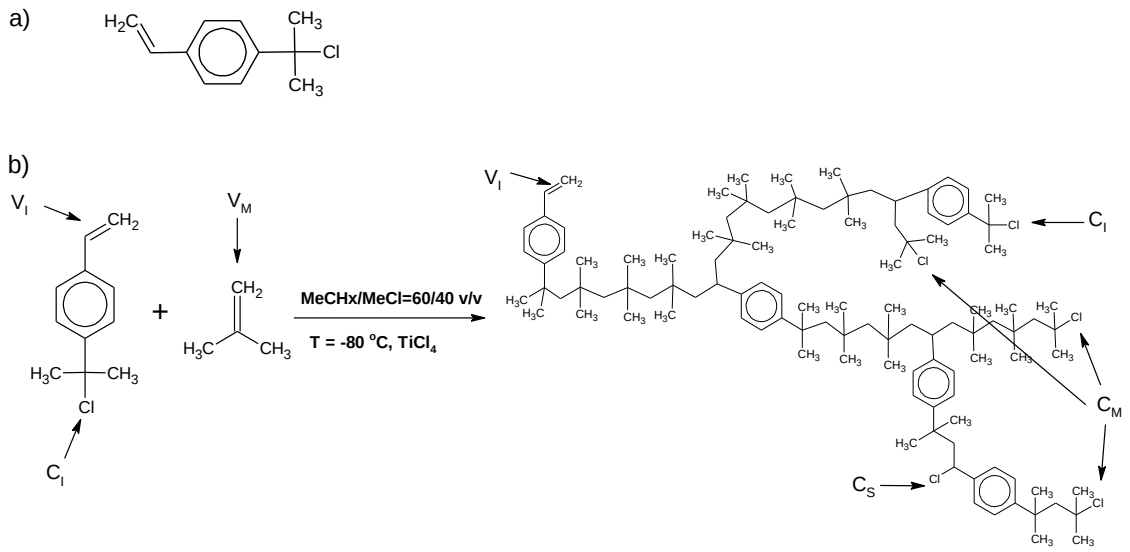

Figure 5.1 a) Typical structure of an inimer; b) a simplified reaction scheme for the "one-pot" living copolymerization of IM and IB.[13]

In living carbocationic polymerization, there is a fast equilibrium between capped and uncapped chloride end groups, which occurs due to the presence of a Lewis acid (LA). Note that $TiCl_4$ is the LA used in the reaction scheme shown in Figure 5.1b. According to Puskas et al.,[30-33] there are two paths for uncapping the chloride end groups. Path A is dominant when there is only a small amount of LA in the system, while path B is dominant when there is a large excess of LA in the system. Values of apparent rate constants $k_{pIMapp}, k_{pMIapp}, k_{pMMapp}$ and k_{pSMapp} in Table 5.2 were estimated using our previous PREDICI model, which is only valid at very low

branching levels using the experimental data of Dos Santos.[3,13] Values for k_{pIIapp} and k_{pSIapp}, which were excluded from our previous model via simplifying assumptions, are reasonable nominal values that we used in Monte Carlo models to simulate detailed branching and molecular weight information.[14,15]

Table 5.1 Summary of six possible propagation reactions between end groups and vinyl groups using apparent propagation rate constants during copolymerization of IM and IB.

	Reactions
1	$C_I + V_I \xrightarrow{k_{pIIapp}} C_S$
2	$C_I + V_M \xrightarrow{k_{pIMapp}} C_M$
3	$C_M + V_I \xrightarrow{k_{pMIapp}} C_S$
4	$C_M + V_M \xrightarrow{k_{pMMapp}} C_M$
5	$C_S + V_I \xrightarrow{k_{pSIapp}} C_S$
6	$C_S + V_M \xrightarrow{k_{pSMapp}} C_M$

Table 5.2 Six apparent propagation rate constants and their estimated values.[13-15]

Parameter	**Estimate**	**Units**
$k_{pIIapp} = k_{pII} \times (K_0K_1[TiCl_4]_0 + K_0K_2[TiCl_4]_0^2)$	7.5×10^{-3}	$L{\cdot}mol^{-1}{\cdot}s^{-1}$
$k_{pIMapp} = k_{pIM} \times (K_0K_1[TiCl_4]_0 + K_0K_2[TiCl_4]_0^2)$	3.99×10^{-4}	$L{\cdot}mol^{-1}{\cdot}s^{-1}$
$k_{pMIapp} = k_{pMI} \times (K_0K_1[TiCl_4]_0 + K_0K_2[TiCl_4]_0^2)$	0.195	$L{\cdot}mol^{-1}{\cdot}s^{-1}$
$k_{pMMapp} = k_{pMM} \times (K_0K_1[TiCl_4]_0 + K_0K_2[TiCl_4]_0^2)$	2.126	$L{\cdot}mol^{-1}{\cdot}s^{-1}$
$k_{pSIapp} = k_{pSI} \times (K_0K_1[TiCl_4]_0 + K_0K_2[TiCl_4]_0^2)$	1.0×10^{-4}	$L{\cdot}mol^{-1}{\cdot}s^{-1}$
$k_{pSMapp} = k_{pSM} \times (K_0K_1[TiCl_4]_0 + K_0K_2[TiCl_4]_0^2)$	1.39×10^{-2}	$L{\cdot}mol^{-1}{\cdot}s^{-1}$

where $K_0 = \frac{k_0}{k_{-0}} = \frac{[P_n^*LA]}{[P_n][LA]}$; $K_1 = \frac{k_1}{k_{-1}} = \frac{[P_n^+LA^-]}{[P_n^*LA]}$; $K_2 = \frac{k_2}{k_{-2}} = \frac{[P_n^+LA_2^-]}{[P_n^*LA][LA]}$

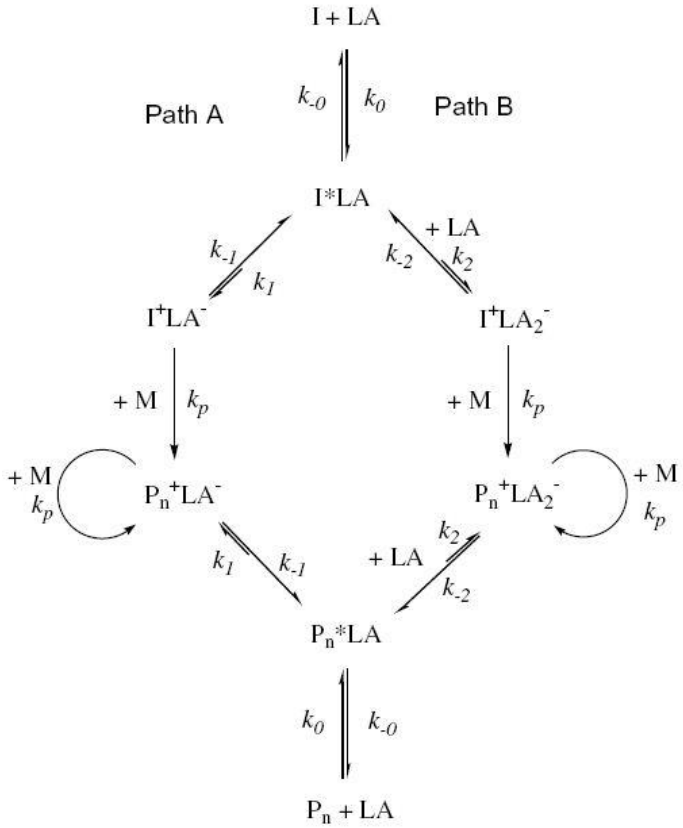

Figure 5.2 Two different paths for carbocationic polymerization using different amount of Lewis acid co-initiator. Path A is dominant when LA concentration is lower than that of the initiator; Path B is dominant when LA concentration is higher than that of the initiator. Note I is initiator and M is monomer.[33]

The average branching level in *arb*PIB can be calculated from:[3]

$$B_{kin} = \frac{\overline{M}_n}{\overline{M}_{n,theo}} - 1 \tag{5.1}$$

$$\overline{M}_{n,theo} = M_{IM} + \frac{[IB]_0 - [IB]}{[IM]_0 - [IM]} M_{IB} \tag{5.2}$$

where $\overline{M}_n$ is the number average molecular weight and $\overline{M}_{n,theo}$ is the theoretical number average molecular weight, calculated for the situation where vinyl groups on IM are unable to react so that only linear IB chains are produced.

Puskas et al. showed that the physical properties of this *arb*PIB biomaterial are largely decided by its molecular weight distribution and branching level.[5,34] Thus, building a model that can accurately predict these properties will be beneficial for designing future experiments to achieve targeted properties. Several research groups have built models for SCVP and SCVCP systems.[13-26] Many of these models rely on simplifying assumptions that may influence the accuracy of the model predictions.[16-26] SCVP and SCVCP models can be classified into two categories: i) models that are based on dynamic material balance equations and ii) models that are based on Monte Carlo (MC) simulations.

Müller et al. and Yan et al.[22-26] developed a series of models for SCVP and SCVCP systems using dynamic material balance equations. Their SCVP model[22,23] resulted in analytical expressions for molecular weight distribution and branching level for inimer homopolymerization in a batch reactor. To develop analytical expressions for average molecular weights and branching levels during SCVCP (*i.e.* copolymerization of inimer and a vinyl monomer), they assumed that different types of propagation rate constants are equal. This assumption may not be valid for copolymerization of 4-(2-chloroisopropyl)styrene and IB, based on the chemical structures of the three carbocations involved.[13]

Cheng et al.[20,21] developed two SCVP models using dynamic material balances, which were solved using generating functions. Their first model assumed that the same value could be used for two different propagation rate constants (*i.e.*, k_{pIIapp} and k_{pSIapp}). In their second model, this assumption was relaxed.

Only a few research groups have performed MC simulations of SCVP or SCVCP systems. He et al.[17] built a MC model for a SCVP system using a multifunctional initiator in addition to the inimer. In their SCVCP model,[19] equal reactivity assumptions were made for different types of end groups and different types of vinyl groups, which may lead to inaccurate predictions.

Our previous research on modeling of *arborescent* PIB used a combination of material balance models and MC models.[13-15] First, we built a dynamic material balance model using PREDICI, which tracks polymer chains according to the number of inimer units and monomer units they contain, as well as the number of end-groups of different types.[13] Because of the prohibitive number of polymer species that needed to be tracked, several assumptions (shown in Table 5.3) were applied to keep the number of species and reactions manageable (*i.e.*, 122 different species and 1430 reaction steps in PREDICI). This model should only be used for predicting molecular weight distribution and branching levels when the average number of branches per molecule is small (*i.e.*, <5) so that very few branched molecules contain more than 15 branches. To our knowledge, this was the first SCVCP model in the literature that has been used for estimating a variety of model parameters that correspond to different types of end groups. Parameters k_{pIMapp}, k_{pMIapp}, k_{pMMapp} and k_{pSMapp} were estimated, providing a good fit of the experimental data (see Table 5.2).[3] Note that parameters k_{pIIapp} and k_{pSIapp} could not be estimated because the simplifying assumptions in Table 5.3 remove these parameters from the model. In situations involving longer reaction times and higher branching levels, the influence of these neglected parameters will become more important. One of the objectives of the current modeling work is to develop an improved PREDICI model that can be used to estimate k_{pIIapp} and k_{pSIapp} and to obtain improved estimates of k_{pIMapp}, k_{pMIapp}, k_{pMMapp} and k_{pSMapp}. This new model should give more reliable predictions of product properties for highly branched *arborescent* PIB.

Table 5.3 Assumptions from our previous PREDICI model.[13]

1	Reactions between C_I end groups and IM can be neglected because $[IM]_0$ is low relative to $[IB]_0$, so that reactions involving k_{pIIapp} can be neglected.
2	C_S end groups can only react with monomer vinyl groups. Reactions between C_S end groups and IM molecules can be neglected because IM molecules will typically initiate polymerization before their vinyl groups can be consumed by reaction. Reactions between C_S end groups and V_I groups on polymer molecules can be neglected due to steric hindrance. Because $[IM]_0$ is very low compared to $[IB]_0$, C_S groups will react with IB before they encounter the V_I groups on large molecules. Thus, reactions involving k_{pSIapp} can be neglected.
3	The C_I groups on the IM are all consumed very early in the reaction because the chloride end is designed to behave as an initiator for living carbocationic polymerization. As a result, the only reaction that IM can undergo appreciably is an initiation reaction with IB. Therefore, vinyl groups of type V_I can undergo propagation reactions only after they belong to oligomer or polymer molecules. Another consequence of this assumption is that there are no C_I groups on any polymer molecules so that reactions between polymer molecules and IM can be ignored. Note that this assumption means that there is no need to track the number of C_I groups in the model, (except for those on IM, which are consumed quickly).
4	Reactions that lead to 16 or more IM units in a molecule are neglected to keep the number of species and reactions manageable for implementation in PREDICI.
5	Puskas et al.[35] observed a penultimate effect during styrene/isobutylene copolymerization, indicating that the rate of IB addition to C_M may depend on whether the penultimate unit is IB or a styrene-like IM unit. Since $[IM]_0$ was low compared to $[IB]_0$ in the recipes simulated using the PREDICI model, this penultimate effect could be neglected with only a small effect on model predictions.
6	$[LA] \approx [LA]_0$ throughout the course of the batch reactions simulated using PREDICI, because only a small fraction of the $TiCl_4$ was consumed to produce ions.[36] Also, $[LA]_0$ is sufficiently large so that the MeOIM is converted instantaneously to IM at the beginning of the batch.

More recently, we developed models that use two different kinds of MC algorithms to account for the influence of all six apparent propagation rate constants on the detailed branching and MWD of the arborescent polymer.[14,15] In these MC models, assumptions 1, 2, 3 and 4 in Table 5.3 are not required. Our first MC model uses a traditional approach, first developed by Gillespie,[37] to track reactions and reaction times for a small sample of molecules in the batch reactor, starting at time zero and proceeding to the end of the batch. This methodology is relatively easy to develop, but requires long simulation times to achieve accurate MWD results. Our second MC model uses an advanced algorithm that combines dynamic material balances on small molecules and end-groups with advanced MC calculations to construct individual molecules.[15] This advanced MC algorithm is much more complicated than the simpler Gillespie approach, but results in an algorithm that is hundreds of times faster than the traditional MC algorithm. However, even this advanced MC algorithm is too computationally demanding for practical use in a parameter estimation scheme. As a result, our simulations obtained using both MC models relied on poorly estimated values of k_{pIMapp}, k_{pMIapp}, k_{pMMapp} and k_{pSMapp} obtained from our PREDICI model and educated guesses for k_{pIIapp} and k_{pSIapp}.

The objective of the research described in the current article is to build an advanced PREDICI model that can provide accurate predictions for $\overline{M}_n$ and B_{kin}, even when branching levels are higher than 15 branches per molecule. Using the approach from our earlier PREDICI model (even with the restrictive assumptions in Table 5.3) accounting for molecules with up to 20 branches would require > 200 species and >4000 reactions in PREDICI, which could not be practically implemented. As a result a different strategy is used. The development of this advanced PREDICI model is described below, followed by a parameter estimation study and simulation results.

5.3 Model Development

This advanced PREDICI model focuses on internal and dangling chain segments and overall measured characteristics (*i.e.*, $\overline{M}_n$ and IB concentration). Although detailed MWD information for the overall polymer chains will not be predicted, this advanced PREDICI model is more convenient and more accurate for parameter estimation than our previous PREDICI model that relied on assumptions 1 to 4 in Table 5.3.

The basic idea of the proposed model is to simulate several parallel polymerization systems at the same time. This idea was inspired by Zargar et al.[16] who developed two parallel models to aid in the understanding of a branched RAFT copolymerization. Our 1st simulation focuses on end groups; the 2nd simulation concentrates on internal segments and dangling segments in the branched polymer molecules; the 3rd simulation determines the number average chain length of the polymer; the 4th simulation tracks the concentrations of small molecules and polymer chains, without paying attention to chain length. Note that the model predictions can be obtained by either simulating models 1, 2 and 3 together or 1, 2 and 4 together (which is the faster and easier alternative). Nonetheless, the derivation and results from the 3rd simulation are shown because of the interesting M_w and MWD predictions that arise. The reactions that are considered in each of the parallel simulations are summarized in Table 5.4. All of the symbols are defined in the notation. Six of the rate constants shown in Table 5.4 are the apparent rate constants that are listed in Table 5.2. However, additional rate constants that are required in the third and fourth simulations are pseudo rate constants, denoted by an asterisk. For example, k^*_{pIMapp} in the second reaction in simulation 3 is the average rate constant for reaction of an IB molecule with a polymer chain of any size n_T. The overall rate of this reaction depends on the average number and type of chloride end groups on polymer molecules. As shown in Table 5.5, k^*_{pIMapp} can be calculated at any time

using equation 5.5.1. This expression arises from the fact that the consumption rate of V_M in simulation 1 should be the same of the consumption rate of IB in simulation 3:

$$-k_{pIMapp}\left[C_I^{(1)}\right]\left[V_M^{(1)}\right] = -k_{pIMapp}\left[IM^{(3)}\right]\left[IB^{(3)}\right] - k^*_{pIMapp}\left[P^{(3)}(n_T)\right]\left[IB^{(3)}\right] \quad (5.3)$$

Since $\left[V_M^{(1)}\right] = \left[IB^{(3)}\right]$, equation 5.3 can be rearranged to give equation 5.5.1.

The key idea is that each pseudo rate constant must be updated over time so that all four parallel simulation systems will result in the same rates of consumption for isobutylene and the same rates of consumption for inimer. As a result, the following constraints need to be enforced at each time during the four simulations:

$$\left[V_M^{(1)}\right] = \left[V_M^{(2)}\right] = \left[IB^{(3)}\right] = \left[IB^{(4)}\right] \quad (5.4)$$

$$\left[V_I^{(1)}\right] = \left[V_I^{(2)}\right] = \left[IM^{(3)}\right] + \left[P^{(3)}(n_T)\right] = \left[IM^{(4)}\right] + \left[P^{(4)}\right] \quad (5.5)$$

where the superscripts refer to the simulation that the species belongs to. Equation 5.4 indicates that the concentration of V_M groups is the same as the concentration of IB molecules. Equation 5.5 indicates that the concentration of V_I groups is the same as the sum of the concentrations of polymer molecules and unreacted inimer, because each polymer molecule contains a single V_I group. Note that cyclization reactions are neglected in this model and in our previous models.[13-15] Enforcing these constraints results in the expressions for the pseudo rate constants in Table 5.5.

Table 5.4 Four parallel polymerization simulations that focus on different arborescent polymerization characteristics

	Simulation 1 **Chain Ends**	**Simulation 2** **Internal and Dangling Segments**	**Simulation 3** **Chain Length**	**Simulation 4** **Molecules**
1	$C_I^{(1)} + V_M^{(1)} \xrightarrow{k_{pIMapp}} C_M^{(1)}$	$C_I^{(2)} + V_M^{(2)} \xrightarrow{k_{pIMapp}} S_D^{(2)}(1)$	$IM^{(3)} + IB^{(3)} \xrightarrow{k_{pIMapp}} P^{(3)}(2)$ $P^{(3)}(n_T) + IB^{(3)} \xrightarrow{k^*_{pIMapp}} P^{(3)}(n_T+1)$	$IM^{(4)} + IB^{(4)} \xrightarrow{k_{pIMapp}} P^{(4)}$ $P^{(4)} + IB^{(4)} \xrightarrow{k^*_{pIMapp}} P^{(4)}$
2	$C_M^{(1)} + V_M^{(1)} \xrightarrow{k_{pMMapp}} C_M^{(1)}$	$S_D^{(2)}(n) + V_M^{(2)} \xrightarrow{k_{pMMapp}} S_D^{(2)}(n+1)$	$P^{(3)}(n_T) + IB^{(3)} \xrightarrow{k^*_{pMMapp}} P^{(3)}(n_T+1)$	$P^{(4)} + IB^{(4)} \xrightarrow{k^*_{pMM}app} P^{(4)}$
3	$C_M^{(1)} + V_I^{(1)} \xrightarrow{k_{pMIapp}} C_S^{(1)}$	$S_D^{(2)}(n) + V_I^{(2)} \xrightarrow{k_{pMIapp}} S_I^{(2)}(n) + C_S^{(2)}$	$P^{(3)}(n_T) + IM^{(3)} \xrightarrow{k^*_{pMIapp}} P^{(3)}(n_T+1)$ $P^{(3)}(n_T) + P^{(3)}(m_T) \xrightarrow{k^*_{pMIapp}} P^{(3)}(n_T+m_T)$	$P^{(4)} + IM^{(4)} \xrightarrow{k^*_{pMIapp}} P^{(4)}$ $P^{(4)} + P^{(4)} \xrightarrow{k^*_{pMIapp}} P^{(4)}$
4	$C_S^{(1)} + V_M^{(1)} \xrightarrow{k_{pSMapp}} C_M^{(1)}$	$C_S^{(2)} + V_M^{(2)} \xrightarrow{k_{pSMapp}} S_D^{(2)}(1)$	$P^{(3)}(n_T) + IB^{(3)} \xrightarrow{k^*_{pSMapp}} P^{(3)}(n_T+1)$	$P^{(4)} + IB^{(4)} \xrightarrow{k^*_{pSMapp}} P^{(4)}$
5	$C_S^{(1)} + V_I^{(1)} \xrightarrow{k_{pSIapp}} C_S^{(1)}$	$C_S^{(2)} + V_I^{(2)} \xrightarrow{k_{pSIapp}} C_S^{(2)} + S_I^{(2)}(0)$	$P^{(3)}(n_T) + IM^{(3)} \xrightarrow{k^*_{pSIapp}} P^{(3)}(n_T+1)$ $P^{(3)}(n_T) + P^{(3)}(m_T) \xrightarrow{k^*_{pSIapp}} P^{(3)}(n_T+m_T)$	$P^{(4)} + IM^{(4)} \xrightarrow{k^*_{pSIapp}} P^{(4)}$ $P^{(4)} + P^{(4)} \xrightarrow{k^*_{pSIapp}} P^{(4)}$
6	$C_I^{(1)} + V_I^{(1)} \xrightarrow{k_{pIIapp}} C_S^{(1)}$	$C_I^{(2)} + V_I^{(2)} \xrightarrow{k_{pIIapp}} C_S^{(2)} + S_I^{(2)}(0)$	$IM^{(3)} + IM^{(3)} \xrightarrow{k_{pIIapp}} P^{(3)}(2)$ $IM^{(3)} + P^{(3)}(n_T) \xrightarrow{k_{pIIapp}} P^{(3)}(n_T+1)$ (via V_I group on polymer) $P^{(3)}(n_T) + IM^{(3)} \xrightarrow{k^*_{pIIapp}} P^{(3)}(n_T+1)$ (via V_I group on inimer) $P^{(3)}(n_T) + P^{(3)}(m_T) \xrightarrow{k^*_{pIIapp}} P^{(3)}(n_T+m_T)$	$IM^{(4)} + IM^{(4)} \xrightarrow{k_{pIIapp}} P^{(4)}$ $IM^{(4)} + P^{(4)} \xrightarrow{k_{pIIapp}} P^{(4)}$ (via V_I group on polymer) $P^{(4)} + IM^{(4)} \xrightarrow{k^*_{pIIapp}} P^{(4)}$ (via V_I group on inimer) $P^{(4)} + P^{(4)} \xrightarrow{k^*_{pIIapp}} P^{(4)}$

Note that the apparent rate constants are applied in the coding. The number in the superscripted brackets after different species shows the simulation system the species belongs to.

Table 5.5 Pseudo rate constants derived using reactions in corresponding rows in Table 5.4 for Simulations 1, 3 and 4.

5.5.1	$k^*_{pIMapp} = \frac{[C_I^{(1)}] - [IM^{(3)}]}{\sum[P^{(3)}(n_T)]} k_{pIMapp} = \frac{[C_I^{(1)}] - [IM^{(4)}]}{[P^{(4)}]} k_{pIMapp}$
5.5.2	$k^*_{pMMapp} = \frac{[C_M^{(1)}]}{\sum[P^{(3)}(n_T)]} k_{pMMapp} = \frac{[C_M^{(1)}]}{[P^{(4)}]} k_{pMMapp}$
5.5.3	$k^*_{pMIapp} = \frac{[C_M^{(1)}]}{\sum[P^{(3)}(n_T)]} k_{pMIapp} = \frac{[C_M^{(1)}]}{[P^{(4)}]} k_{pMIapp}$
5.5.4	$k^*_{pSMapp} = \frac{[C_S^{(1)}]}{\sum[P^{(3)}(n_T)]} k_{pSMapp} = \frac{[C_S^{(1)}]}{[P^{(4)}]} k_{pSMapp}$
5.5.5	$k^*_{pSIapp} = \frac{[C_S^{(1)}]}{\sum[P^{(3)}(n_T)]} k_{pSIapp} = \frac{[C_S^{(1)}]}{[P^{(4)}]} k_{pSIapp}$
5.5.6	$k^*_{pIIapp} = \frac{[C_I^{(1)}] - [IM^{(3)}]}{\sum[P^{(3)}(n_T)]} k_{pIIapp} = \frac{[C_I^{(1)}] - [IM^{(4)}]}{[P^{(4)}]} k_{pIIapp}$

The 1st row in Table 5.4 is concerned with reactions involving C_I end groups on inimer or polymer molecules and the V_M group on a monomer. Simulation 1 keeps track of the resulting change in the type of end group (from C_I to C_M). Simulation 2 keeps track of the new dangling segment of length 1, $S_D^{(2)}(1)$, that arises from this type of reaction. The first row for Simulation 3 contains two reactions. The first tracks the creation of a new polymer molecule $P^{(3)}(2)$, which contains two units (one inimer and one monomer) when a C_I end from an inimer reacts with IB. The second tracks the growth of polymer molecules when a C_I end group from a polymer chain reacts with IB. In the 4th simulation, the first reaction in the first row tracks the increase in the number of polymer chains that occurs when IM reacts with IB. Note that the number of units in the polymer chains is not tracked in Simulation 4. The second reaction in Simulation 4 accounts for the IB that is consumed by reactions with C_I end groups on polymer chains. This reaction does not produce an additional polymer molecule.

The 2nd row in Table 5.4 describes chain propagation by adding monomer to a C_M end group. Simulation 1 keeps track of the consumption of V_M groups by this chain-growth reaction. Simulation 2 tracks the propagation of dangling segments. Simulation 3 tracks the increase in chain length for the whole polymer molecule. Simulation 4 shows that the concentration of polymer chains does not change, but that IB is consumed.

Similarly, the 3rd row accounts for the consumption of V_I groups on inimer and polymer molecules by reaction with C_M end groups which produces C_S end groups. Simulation 2 tracks the conversion of a dangling segment to an internal chain segment $S_I^{(2)}(n)$ when this type of reaction occurs. Simulation 3 is interesting, because it accounts for the joining of two polymer molecules that can happen due to this type of reaction. Simulation 4 is similar, except that it does not track chain lengths.

The 4th row accounts for the creation of a new dangling segment (*i.e.*, a branch) that occurs when a C_S end group reacts with IB. The 5th row is concerned with the consumption of V_I vinyl groups via C_S end groups. This type of reaction produces an internal segment of length zero. The 6th row in Table 5.4 describes the reaction between C_I end groups and V_I vinyl groups. This type of reaction also produces internal segments of length zero. Note that four different reactions are required in simulations 3 and 4 for this type of reaction, because it can occur between two IM molecules, between the C_I group on an IM and the V_I group on a polymer molecule, between the C_I group on a polymer molecule and the V_I group on an IM, or between two polymer molecules.

When developing simulation 3, we debated about the values that should be specified for some rate constants. For example, for the reaction involving two IM molecules in row 6, we initially believed that the rate constant should be $2k_{pIIapp}$ rather than k_{pIIapp} because this reaction can happen in two ways; both IM molecules have a V_I group and a C_I group. When the concentra-

tions of V_I groups predicted by simulation 3 did not match the results from simulation 1, we proved that the rate constant for this reaction should be k_{pIIapp} using the argument below. Consider the reactions:

$$C_I + V_I \xrightarrow{k_{pIIapp}} C_S \tag{5.6}$$

$$IM + IM \xrightarrow{k_{p?}} P \tag{5.7}$$

where $k_{p?}$ has an unknown value that is related to k_{pIIapp} so that these two reaction rates are consistent. Consider starting with 1 mol/L of IM (and nothing else) in the batch reactor. At time zero, reactions (5.6) and (5.7), which are really two ways of writing the same reaction, are the only reactions that can occur. Using these initial concentrations, the rate of consumption of V_I groups to form new polymer molecules by reaction (5.6) is:

$$k_{pIIapp}[C_I][V_I] = 1\frac{mol}{L} \cdot 1\frac{mol}{L} \cdot k_{pIIapp} \tag{5.8}$$

Similarly, the rate of formation of new polymer molecules via reaction (5.7) is:

$$k_{p?}[IM]^2 = \left[1\frac{mol}{L}\right]^2 k_{p?} \tag{5.9}$$

Equations 5.8 and 5.9 should have the same rate, as a result,

$$k_{p?} = k_{pIIapp} \tag{5.10}$$

and there is no need to multiply the apparent rate constants k^*_{pMIapp} by two in the 3rd row. Similar arguments apply for k^*_{pSIapp} in the 5th row and k^*_{pIIapp} in the 6th row of Table 5.4.

When first developing the proposed model, we developed only simulations 1, 2 and 3. Using simulation 3, we were able to match predicted values of $\bar{M}_n$ from our MC simulations[14,15], but not $\bar{M}_w$ and MWD. Simulation 3 gives MWD predictions that are considerably narrower than the MWDs predicted by the MC simulations (see Figure 5.3).

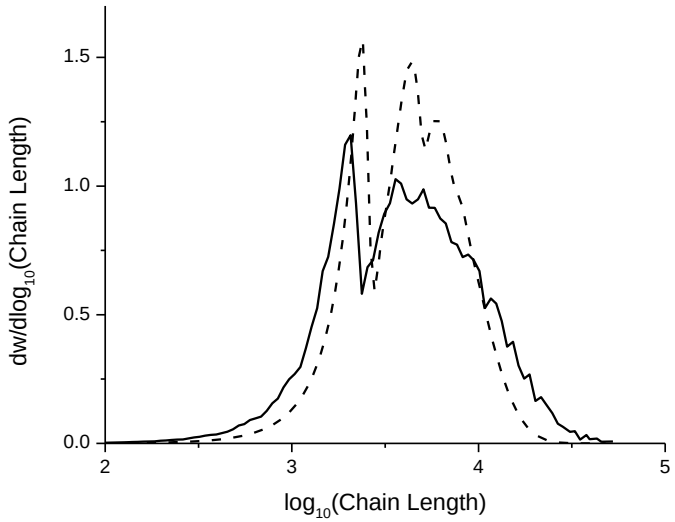

Figure 5.3 Comparison of the calculated MWD between simulation 3 using PREDICI and our previous advanced MC model[15] using the initial condition $[IM]_0$ = 0.00454 M and $[IB]_0$ = 1.74 M and the parameter values in Table 5.2. - - - is the MWD calculated by PREDICI; ─ is the MWD calculated by advanced MC with 10^5 polymer chains.

This discrepancy is caused by the implication that all polymer chains, regardless of their chain length, will have the same average reaction rate. For example, the final reaction for simulation 3 specifies that the reaction between two large chains:

$$P^{(3)}(1000) + P^{(3)}(500) \xrightarrow{k^*_{pIIapp}} P^{(3)}(1500) \tag{5.11}$$

will proceed, on average, at the same rate as a reaction between two small chains:

$$P^{(3)}(10) + P^{(3)}(5) \xrightarrow{k^*_{pIIapp}} P^{(3)}(15) \tag{5.12}$$

that react at the same time. However, for the current polymerization system, this assumption is not valid. Larger molecules tend to have more branches and therefore more end groups, so that reaction (5.11) tends to occur much more quickly than reaction (5.12). As a result, simulation 3 is able to accurately track the number of polymer molecules, but not the chain length distribution. As a result, we decided to add simulation 4 in Table 5.4, which only counts the number concen-

tration of polymer molecules in the system. The development of the number average molecular weight during the batch can be calculated from:

$$\bar{M}_n = \frac{[IM]_0^{(4)} - [IM]^{(4)}}{[P]^{(4)}} M_{IM} + \frac{[IB]_0^{(4)} - [IB]^{(4)}}{[P]^{(4)}} M_{IB} \tag{5.13}$$

It is preferable to compute $\bar{M}_n$ using equation 5.13 instead of the method of moments in simulation 3, because simulation 4 requires less computational effort than simulation 3, which may be beneficial during parameter estimation. In addition, simulation 4 does not produce any misleading information about $\bar{M}_w$ and MWD, which the modeler might be tempted to believe. Results from simulation 3 are included in the current article because they serve as a warning to other researchers who might try a similar modeling approach. Note that the bimodal MWD predicted by the MC simulation in Figure 5.3 is consistent with bimodal distributions observed experimentally[3,15]. The low-molecular-weight peak is primarily linear polymer and the higher-molecular-weight peak results from the branched polymer molecules.

The average number of branches per polymer molecule can be determined from:

$$B_{\text{kin}} = \frac{[IM]_0^{(4)} - [IM]^{(4)}}{[P]^{(4)}} - 1 \tag{5.14}$$

which is equivalent to equation 5.1. If there are only linear chains in the system, so that the number of inimer units consumed is equal to the number of polymer molecules, the value of B_{kin} is zero. Although our initial aim was to develop a simplified PREDICI model that would predict [IB], [IM], B_{kin}, $\bar{M}_n$, $\bar{M}_w$ and MWD values, the current model (simulations 1, 2 and 4) can only predict [IB], [IM], B_{kin} and $\bar{M}_n$. In the next section, we describe how the model predictions of [IB] and $\bar{M}_n$ can be used along with data provided by Dos Santos[3] to provide improved estimates of the model parameters.

5.4 Parameter Estimation and Simulation Results

5.4.1 Parameter Estimation

The experimental data of Dos Santos that were used in our previous parameter estimation study are used again here to estimate all six apparent rate constants.[3,13] Recall that only four apparent rate constants (k_{pIMapp}, k_{pMMapp}, k_{pMIapp} and k_{pSMapp}) were estimated in our previous study because k_{pIIapp} and k_{pSIapp} were eliminated due to simplifying assumptions 1 and 2 in Table 5.3. The initial values and uncertainty ranges for k_{pIMapp}, k_{pMMapp}, k_{pMIapp} and k_{pSMapp} shown in Table 5.6 are the same values that we used in our previous work. These values were obtained using information from the literature and our engineering judgment.[3,13,32,33,35,36,38-42] The lower and upper bounds shown were enforced during parameter estimation to ensure that estimated parameter values are physically realistic.[13] For the additional two parameters, k_{pIIapp} and k_{pSIapp}, which were not considered in our previous PREDICI model, we selected the rough initial guesses of 7.5×10^{-3} and 1×10^{-4} $L\cdot mol^{-1}\cdot s^{-1}$shown in Table 5.6 that were used in our previous MC simulation studies.[14,15] These values were calculated using inimer homopolymerization data.[3,43] A large range between the lower and upper bounds for these parameters is specified in Table 5.6 because we could not find any additional information in the literature about reasonable values for these two parameters. Note that the initial guesses are the same as the values for the lower bounds, because the inimer homopolymerization data were obtained using a lower concentration of Lewis acid (*i.e.*, $TiCl_4$) than in the copolymerization experiments that are simulated in the current article. This lower Lewis acid concentration should lead to lower values of the apparent rate constants (see Table 5.2) than the values that apply to the data sets used for parameter estimation.

Table 5.6 Initial values and lower and upper bounds used for estimation of six apparent rate constants

Parameter	Initial	Lower	Upper	Units
k_{pIIapp}	7.5×10^{-3}	7.5×10^{-3}	10	$L{\cdot}mol^{-1}{\cdot}s^{-1}$
k_{pIMapp}	1.58×10^{-1}	4.11×10^{-5}	4.11	$L{\cdot}mol^{-1}{\cdot}s^{-1}$
k_{pMIapp}	3.16×10^{-2}	4.11×10^{-6}	4.11	$L{\cdot}mol^{-1}{\cdot}s^{-1}$
k_{pMMapp}	4.58×10^{-1}	4.11×10^{-4}	4.11	$L{\cdot}mol^{-1}{\cdot}s^{-1}$
k_{pSIapp}	1×10^{-4}	1×10^{-4}	10	$L{\cdot}mol^{-1}{\cdot}s^{-1}$
k_{pSMapp}	2.64×10^{-4}	4.11×10^{-5}	4.11	$L{\cdot}mol^{-1}{\cdot}s^{-1}$

When developing fundamental models of polymerization reactors, it is important to determine whether all of the kinetic parameters in the model should be estimated, or whether only a subset of the parameters should be estimated from the available data.[33,44-52] Estimating too many parameters using limited data leads to large uncertainty ranges for the parameters and can produce worse predictions than when fewer parameters are estimated. On the other hand, estimating too few parameters can also give poor predictions, due to incorrect values that are assumed for the un-estimated parameters.[53-57] In this study, advanced statistical techniques are used to determine if all six parameters in Table 5.6 could be estimated reliably using the limited data collected by Dos Santos.[13,52-57] An orthogonalization method[52] is first used to rank all of the parameters from the most estimable to the least estimable, based on information about the influence of each parameter on predictions of the available data, uncertainties in the initial parameter values, and uncertainties in the different types of measurements. This algorithm also accounts for correlated effects of model parameters.[49,52] After the parameters are ranked, Wu's mean-squared error (MSE) criterion[55] is used to decide on the appropriate number of parameters to estimate to obtain the most reliable predictions using the available data. The final parameter estimates were obtained using the following weighted nonlinear least-squares objective function:

$$J = \sum \frac{([IB]_{exp} - [IB])^2}{s_{IB}^2} + \sum \frac{(\bar{M}_{nexp} - \bar{M}_n)^2}{s_{\bar{M}_n}^2} \tag{5.15}$$

where $[IB]_{exp}$ and $\bar{M}_{nexp}$ are the experimental measurements of the concentration of IB and the number average molecular weight, respectively. s_{IB}^2 =0.01485 $mol^2 \cdot L^{-2}$ and $s_{\bar{M}_n}^2$ =313.255 $kg^2 \cdot mol^{-2}$ are pooled variance estimates for the isobutylene concentration and number average molecular weight, respectively, determined from replicates experiments.[3] Note that objective function 5.15 contains fewer terms than the objective function used in our earlier parameter estimation study.[13] A term penalizing deviations between experimental data and the weight average molecular weight is not included in equation 5.15 because the current model, unlike our previous PREDICI model, cannot predict $\bar{M}_w$. Also, we decided to remove a term that penalizes deviations between "measured" branching level and predictions of B_{kin}. Our reason for removing the B_{kin} term from the objective function is that Dos Santos did not measure B_{kin} independently in the experiments used for parameter estimation.[3] Instead, the B_{kin} values that he reported were calculated from equation 5.1 using measured values of $\bar{M}_n$ and [IB], assuming that [IM] = 0 after the first few minutes of the reaction. Since measured values of $\bar{M}_n$ and [IB] from Dos Santos's experiments already appear in objective function 5.15, it is not appropriate to include an additional term that accounts for this same information in the pseudo-measurements, especially when the assumption that [IM]=0 may not be accurate. Note that Dos Santos did measure branching levels (via a link destruction technique) for some *arb*PIB experiments, obtaining good agreement with B_{kin} calculations.[3] These data are not used for parameter estimation because we could not find sufficient information about the details of the polymer synthesis (*e.g.*, the time at which the *arb*PIB was sampled from the batch reactor).

Parameter estimation was performed 20 times starting from different sets of initial guesses selected between the lower and upper values specified in Table 5.6. The first estimation was

started from the initial values specified in Table 5.6, which are the same initial values used in our previous modeling study.[13-15] Starting from these values, the estimability ranking method of Yao et al.[52] and Thompson et al.[49] was used to rank the six parameters from most estimable to least estimable. Parameters k_{pMMapp}, k_{pMIapp} and k_{pIMapp} are the top three most estimable parameters because there is a large fraction of IB units in the system (compared with IM), giving these parameters a large influence on the model predictions. Parameters k_{pSMapp}, k_{pIIapp} and k_{pSIapp} are the least estimable because they have less influence. Wu's critical ratio was then used to determine that the top three parameters on the ranked list should be estimated and that the remaining three parameters should be held at its initial value. Estimating the top three parameters gave J = 68.1, which is considerably better than J = 1349.3 obtained using the initial parameter guesses and only slightly better than J = 69.0, which is obtained when the objective function is computed using parameter values employed in our previous Monte Carlo simulations (see Table 5.2).[14,15] Using the values in Table 5.2 as initial guesses in the second estimation attempt resulted in a different parameter ranking, with parameter k_{pMMapp} appearing at the bottom of the list. This different ranking may have occurred because the value of k_{pMMapp} = 2.126 L mol^{-1}s^{-1} was already well-estimated during our previous parameter estimation study.[13] In this case, Wu's critical ratio determined that five parameters should be estimated, resulting in J = 29.2 at the converged parameter values, which is much better than the value obtained starting from the previous initial parameter values.

These results illustrate that initial parameter guesses can have a large influence on parameter ranking results and parameter estimates, as noted in previous parameter estimation studies for polymerization models.[53,58] The reasons that different results can be obtained when different initial guesses are used are that polymerization models are often nonlinear with respect to the model parameters and convergence to different local minima can occur. To test whether the pa-

rameter estimates corresponding to J = 29.2 are reliable, a further 18 attempts at parameter ranking, selection and estimation were performed by starting at random initial guesses between the lower and upper bounds specified in Table 5.6. From 8 of these 18 attempts, we found that all six parameters could be estimated from the available data, using Wu's critical ratio. In these 8 attempts, two gave the best value of the objective function of J = 28.9. Three of the 18 attempts resulted in selection of five parameters for estimation, two of the 18 attempts selected four parameters for estimation, four attempts selected three parameters for estimation and one attempt selected only two parameters for estimation. Additional details are provided elsewhere.[59] During some of the estimation attempts, especially when a larger number of parameters was being estimated, PREDICI gave warnings about correlation among the parameters and "too many reductions", indicating that the data set might not contain sufficient information to estimate all of the parameters. Note that the best six attempts at parameter estimation provided values of J between 28.9 and 29.3. These six estimation attempts provided similar estimates for k_{pIMapp}, k_{pMIapp}, k_{pMMapp} and k_{pSMapp}. However, the estimated values of k_{pIIapp} and k_{pSIapp} have more variability among these six estimations, suggesting that the data contain only limited information about these two parameters. Our difficulties in estimating these two parameters may be caused by the very low initial concentration of IM relative to IB (*i.e.*, $6.55 \times 10^{-4} \leq \frac{[IM]_0}{[IB]_0} \leq 2.61 \times 10^{-3}$ in the five experimental runs used for parameter estimation). The low concentrations of IM in the system and the lack of monitoring of [IM] during the experiments provide little information for accurate fitting of k_{pIIapp} and k_{pSIapp}. To better estimate these two parameters, it would be beneficial to obtain more experimental data from runs with higher [IM], which would lead to higher branching levels.

The best parameter values that were obtained, which correspond to J = 28.9 are provided in Table 5.7, along with approximate 95% confidence intervals. The estimates for the top three

parameters in Table 5.7 (shown in bold) are significantly different from zero, but the other parameter estimates are not. Also, the non-overlapping confidence intervals for k_{pIMapp}, k_{pMMapp} and k_{pMIapp} indicate that the values of these three propagation parameters are significantly different from each other, indicating that assumptions about equal reactivities of different types of end groups and vinyl groups made by other modelers are not valid for this IB and IM copolymerization system. These ranking and estimation results reveal that the parameters, k_{pIIapp} and k_{pSIapp}, which were neglected in our earlier model[12] do influence the model predictions. However, these two parameters are difficult to estimate accurately. Note that the estimated values of k_{pSMapp} shown in Table 5.7 is at the lower bound specified in Table 5.6. Decreasing the lower bound for k_{pSMapp} during parameter estimation does not result in a noticeable improvement in the value of *J*.

Table 5.7 Parameter ranking and estimation results for all six apparent rate constants

	Parameter	Initial	Final value	95% Confidence Interval	Unit
1	$\boldsymbol{k_{pIMapp}}$	8.00×10^{-3}	$\mathbf{4.46 \times 10^{-4}}$	$\mathbf{\pm 1.45 \times 10^{-4}}$	$\boldsymbol{L{\cdot}mol^{-1}{\cdot}s^{-1}}$
2	$\boldsymbol{k_{pMMapp}}$	1.47×10^{0}	$\mathbf{2.27 \times 10^{0}}$	$\mathbf{\pm 4.88 \times 10^{-1}}$	$\boldsymbol{L{\cdot}mol^{-1}{\cdot}s^{-1}}$
3	$\boldsymbol{k_{pMIapp}}$	1.14×10^{-4}	$\mathbf{5.19 \times 10^{-1}}$	$\mathbf{\pm 1.75 \times 10^{-1}}$	$\boldsymbol{L{\cdot}mol^{-1}{\cdot}s^{-1}}$
4	k_{pIIapp}	2.97×10^{-2}	3.32×10^{-2}	$\pm 1.55 \times 10^{-1}$	$L{\cdot}mol^{-1}{\cdot}s^{-1}$
5	k_{pSIapp}	6.26×10^{-1}	6.45×10^{-3}	$\pm 6.43 \times 10^{-2}$	$L{\cdot}mol^{-1}{\cdot}s^{-1}$
6	k_{pSMapp}	2.08×10^{-1}	4.11×10^{-5}	$\pm 3.04 \times 10^{-4}$	$L{\cdot}mol^{-1}{\cdot}s^{-1}$

5.4.2 Simulation Results

The proposed PREDICI model requires less than 10 seconds to simulate a typical experimental run (see Figure 5.4) using a Windows 7 laptop computer with Intel Core i5 2.4GHz and 4 GB of RAM. Figures 5.4 to 5.6 show comparisons between the experimental results (■ symbol) and simulation results obtained using the new estimated parameter values (solid lines) and old parameter values from Table 5.2 (dashed lines). Figure 5.4 contains replicate results obtained from three experimental runs. Note that no data are available for the inimer concentrations in Figures 5.4b, 5.5b and 5.6b and the polymer concentrations in Figures 5.4c, 5.5c and 5.6c. In Figures 5.4d, 5.5d and 5.6d, the experimental values of B_{kin} (shown using ▲) are calculated values from equation 5.1 using measurements for $\overline{M}_n$ and [IB], with [IM] assumed to be zero to match the assumption made by Dos Santos. Alternative values of B_{kin} shown using the open triangles (Δ) are computed using equation 5.1, with measured values of $\overline{M}_n$ and [IB] and the simulated value of [IM].

Figure 5.4 shows plots of [IB], [IM], [P], B_{kin}, $\bar{M}_n$, and $\bar{M}_w$ vs time for a recipe with $[IM]_0 = 0.00114$ M and $[IB]_0 = 1.74$ M. Figures 5.5 and 5.6 are similar, except that they correspond to experiments with higher inimer concentrations that lead to higher levels of branching. The predicted values of $\bar{M}_w$ were generated using the parameter estimates from the current article in our traditional MC model,[14] starting from 20000 initial IM units and the corresponding number of IB units in the system. The MC results (not shown) agree with the other results shown in Figures 5.4 to 5.6. From Figures 5.4 to 5.6, it is apparent that the new estimated parameter values tend to produce better predictions of the experimental data than the old parameter values produced, particularly for [IB] and $\bar{M}_n$. In Figures 5.4d, 5.5d and 5.6d, the calculated B_{kin} data (shown as Δ), using experimental values of [IB] and $\bar{M}_n$, and simulated values of [IM], are better predicted by the model than the calculated B_{kin} data from Dos Santos that assumed complete

consumption of IM.[3] Predictions for $\bar{M}_w$ are also quite good using the new parameter values, but are not as good as the predictions for $\bar{M}_n$ because the $\bar{M}_w$ data were not used for parameter estimation (see equation 5.15).

As shown in Figure 5.7, the predicted MWDs of the internal segments and dangling segments (from simulation 2) match those obtained from the advanced MC model.[15] To obtain relatively smooth MWD curves, 10^5 polymer chains were constructed using the MC calculations. The results in Figure 5.7a from PREDICI and the MC simulation agree very well with each other. However, in Figure 5.7b, results for the dangling segments agree less well because of the limited by the number of dangling segments in the MC simulation. In the 1×10^5 polymer chains that were constructed, there are 244368 internal segments and only 9664 dangling segments. Less jagged MC results could be obtained using a larger number of molecules. Note that it took the advanced MC model about 22 mins to produce the 10^5 polymer chains and generate the MWDs in Figure 5.7, however, it took the proposed PREDICI model only 8.7 seconds to obtain the MWDs for the internal and dangling segments. Figure 5.7 shows that the internal segments and dangling segments tend to have similar chain lengths because most of the IB was consumed during the first 1800 s (see Figure 5.6a) to produce the linear segments, which could then be joined together via branching reactions later in the batch.

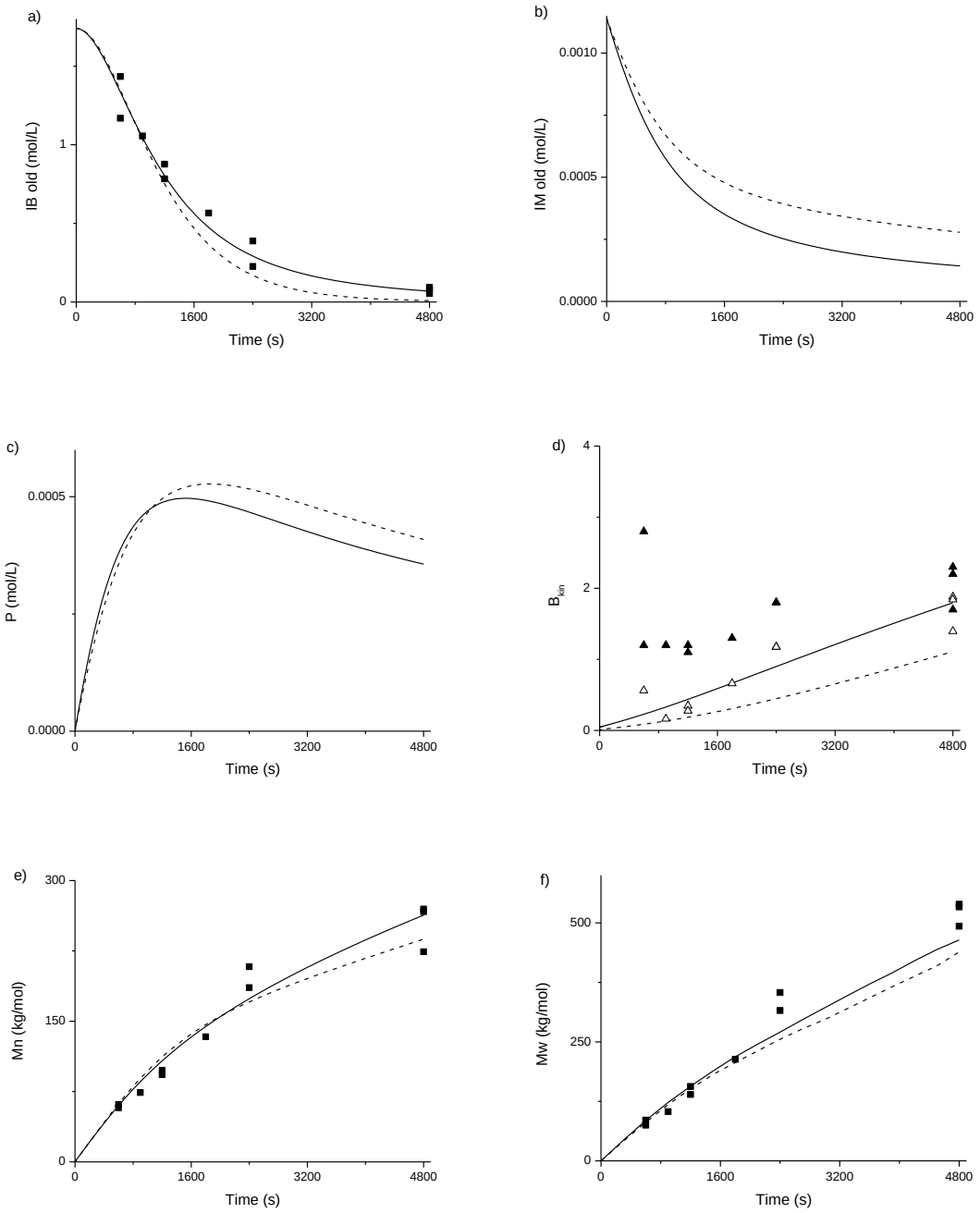

Figure 5.4 Comparison among experimental results and simulation results using old parameter values in Table 5.2 and new estimates in Table 5.7 for a batch reactor run with $[IM]_0$ = 0.00114 M and $[IB]_0$ = 1.74 M . ── simulation with newly estimated parameters; - - - simulation with old parameters; ■ experimental values; ▲ B_{kin} calculated from data with assumption [IM]=0; Δ B_{kin} calculated from data using simulated [IM]; a) [IB], b) [IM], c) polymer concentration, d) B_{kin}, e) M_n f) M_w.

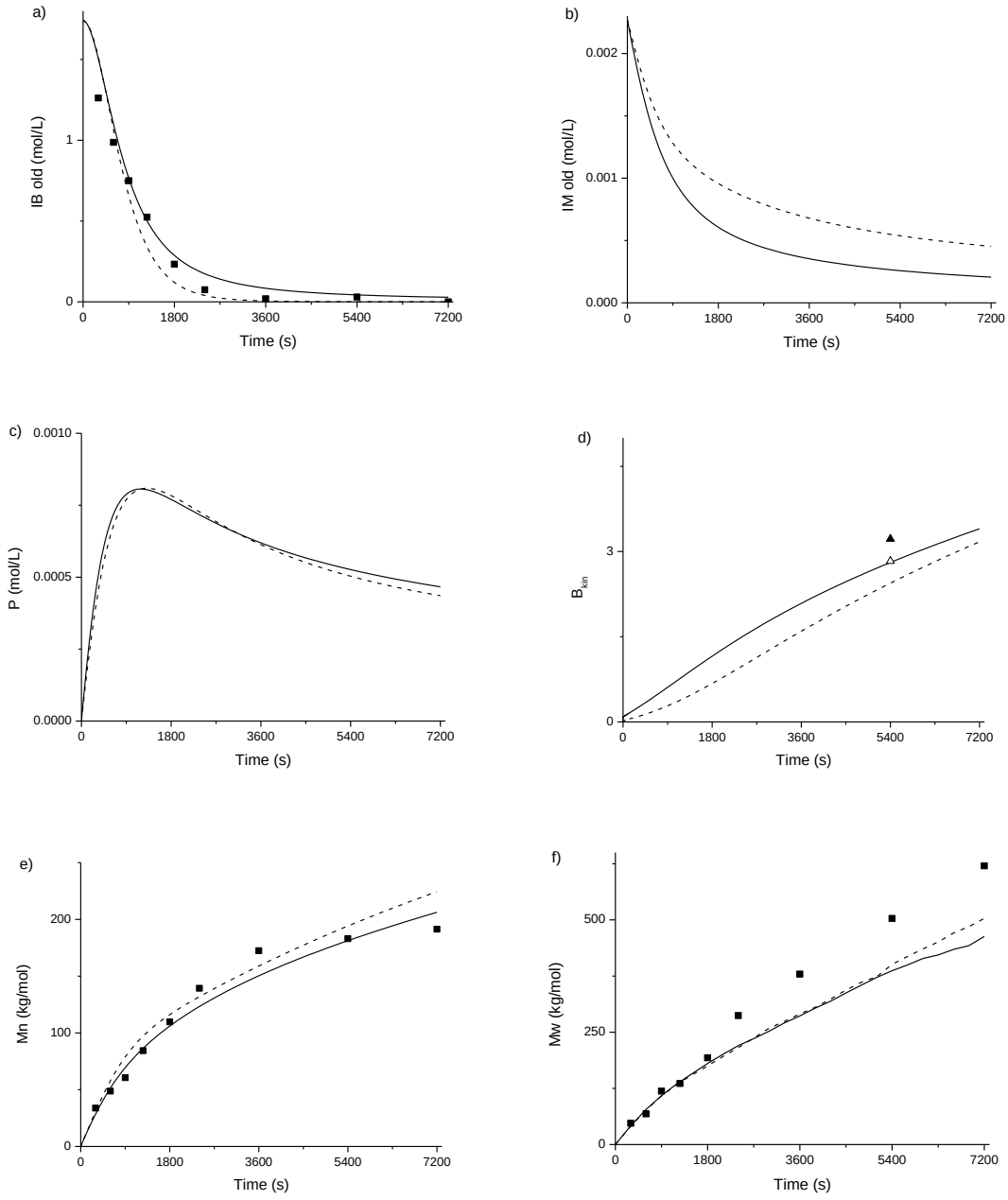

Figure 5.5 Comparison among experimental results and simulation results using old parameter values in Table 5.2 and new estimates in Table 5.7 for a batch reactor run with $[IM]_0$ = 0.00227 M and $[IB]_0$ = 1.74 M . ── simulation with newly estimated parameters; - - - simulation with old parameters; ■ experimental values; ▲ B_{kin} calculated from data with assumption [IM]=0; Δ B_{kin} calculated from data using simulated [IM]; a) [IB], b) [IM], c) polymer concentration, d) B_{kin}, e) M_n f) M_w.

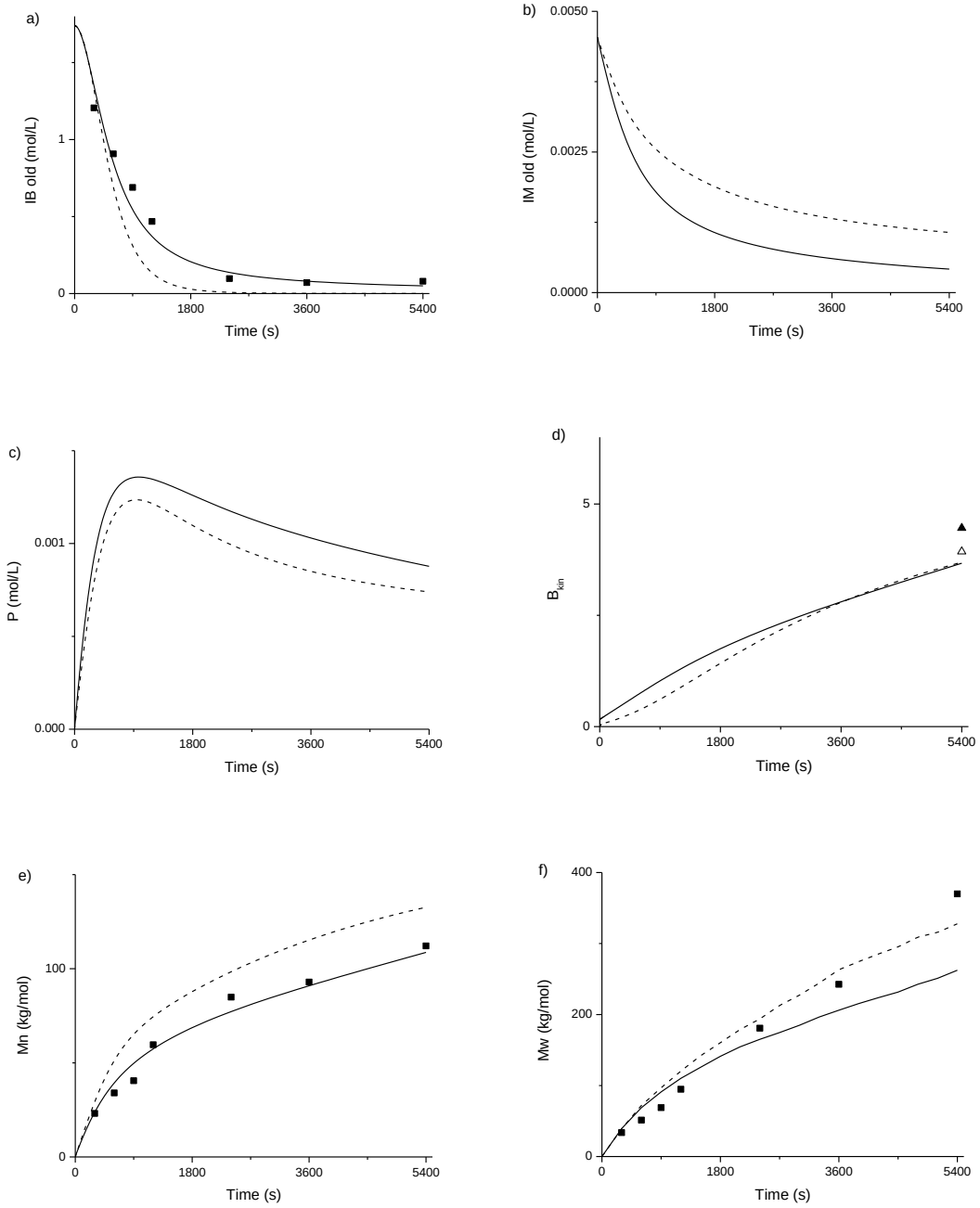

Figure 5.6 Comparison among experimental results and simulation results using old parameter values in Table 5.2 and new estimates in Table 5.7 for a batch reactor run with$[IM]_0$ = 0.00454 M and $[IB]_0$ = 1.74 M . ── simulation with newly estimated parameters; - - - simulation with old parameters; ■ experimental values; ▲ B_{kin} calculated from data with assumption [IM]=0; Δ B_{kin} calculated from data using simulated [IM]; a) [IB], b) [IM], c) polymer concentration, d) B_{kin}, e) M_n f) M_w.

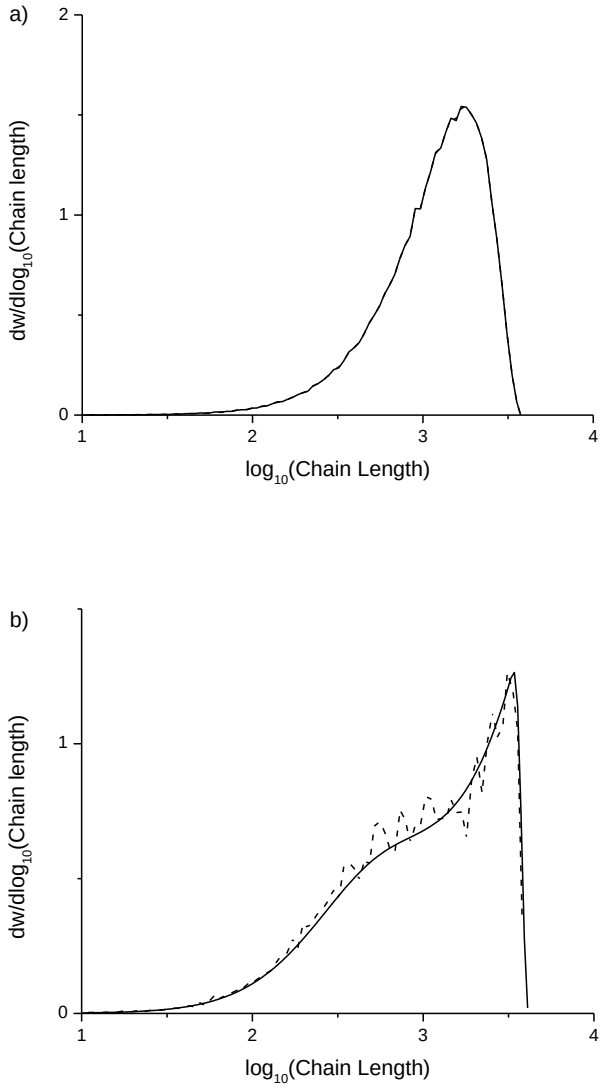

Figure 5.7 Predicted MWDs for a) internal segments and b) dangling segments at t = 5400 s from experiment with $[IM]_0$ = 0.00454 M and $[IB]_0$ = 1.74 M and parameter values from Table 5.7; ─ PREDICI, -- Advanced Monte Carlo. Note that the two curves in a) overlap.

5.5 Conclusions

A novel model consisting of parallel simulations was developed to predict key concentrations and polymer properties in the copolymerization of isobutylene and inimer via carbocationic polymerization. The proposed dynamic model predicts changing concentrations of isobutylene, inimer and polymer molecules, the MWDs of internal and dangling segments, and the branching level and $\bar{M}_n$ of the polymer molecules. Unlike our previous PREDICI model,[13] no restrictions on permissible branching levels needed to be introduced and all possible concentration ranges for inimer and isobutylene can be simulated. This model requires much less computational effort than our previous Monte Carlo models for the same copolymerization system,[14,15] which makes it suitable for parameter estimation. Twenty attempts at parameter estimation were performed, starting from different initial parameter values, because some attempts converged to local minima. In each attempt, the six apparent rate constants that appear in the model were ranked from most estimable to least estimable[49,52] and the number of estimable parameters was determined using a mean-squared-error-based criterion.[55] From 8 parameter estimation attempts, it was determined that all six parameters could be estimated, for the first time, using the data of Dos Santos.[3] Nevertheless, the relatively low inimer concentration and lack of [IM] monitoring in the available data set made it difficult to obtain precise estimates of three of the six model parameters (*i.e.*, k_{pIIapp}, k_{pSIapp} and k_{pSMapp}). The newly estimated parameters result in a better fit to the data for [IB] and $\bar{M}_n$ than parameter estimates from our previous model.[13] MWD predictions for internal and dangling segments agree well with those obtained using our advanced MC model, but require significantly less computational time to determine. In the future, there is opportunity to obtain improved parameter estimates using a larger data set that incorporates different concentrations of the Lewis acid and experiments involving inimer homopolymerization.[2,43]

5.6 References

1 Fréchet JMJ, Henmi M, Gitsov I, Aoshima S, Leduc MR, Grubbs RB. Self-condensing vinyl polymerization: An approach to dendritic materials. *Science.* 1995; 269: 1080-1083.

2 Paulo C, Puskas JE. Synthesis of hyperbranched polyisobutylenes by inimer-type living polymerization. 1. Investigation of the effect of reaction conditions. *Macromolecules*. 2001; 34: 734-739.

3 Dos Santos LM. *Synthesis of arborescent model polymer structures by living carbocationic polymerization for structure-property studies* [dissertation]. Akron, OH: University of Akron; 2009.

4 Puskas JE, Grasmüller M. Star-branched and hyperbranched polyisobutylenes. *Macromol. Symp.* 1998; 132: 117-126.

5 Puskas JE, Kwon Y. Biomacromolecular engineering: design, synthesis and characterization. One-pot synthesis of block copolymers of arborescent polyisobutylene and polystyrene. *Polym. Adv. Technol*. 2006; 17: 615-620.

6 Puskas JE, Kwon Y, Antony P, Bhowmick AK. Synthesis and characterization of novel dendritic (arborescent, hyperbranched) polyisobutylene-polystyrene block copolymers. *J. Polym. Sci., Part A: Polym. Chem.* 2005; 43: 1811-1826.

7 Hong CY, Pan CY. Preparation and characterization of hyperbranched polyacrylate copolymers by self-condensing vinyl copolymerization (SCVCP). *Polym. Int.* 2002; 51: 785-791.

8 He X, Yan D. Branched azobenzene side-chain liquid-crystalline copolymers obtained by self-condensing ATR copolymerization. *Macromol. Rapid Commun.* 2004; 25: 949-953.

9 Liu Q, Xiong M, Cao M, Chen Y. Preparation of branched polyacrylonitrile through self-condensing vinyl copolymerization. *J. Appl. Polym. Sci.* 2008; 110: 494-500.

10 Puskas JE, Dos Santos LM, Kaszas G, Kulbaba K. Novel thermoplastic elastomers based on

arborescent (dendritic) polyisobutylene with short copolymer end sequences. *J. Polym. Sci., Part A: Polym. Chem.* 2009; 47: 1148-1158.

11 Foreman EA, Puskas JE, Kaszas G. Synthesis and characterization of arborescent (hyper-branched) polyisobutylenes from the 4-(1,2-oxirane-isopropyl)styrene inimer. *J. Polym. Sci., Part A: Polym. Chem.* 2007; 45: 5847-5856.

12 Heidenreich AJ, Puskas JE. Synthesis of arborescent (dendritic)polystyrenes via controlled inimer-type reversible addition-fragmentation chain transfer polymerization. *J. Polym. Sci., Part A: Polym. Chem.* 2008; 46: 7621-7627.

13 Zhao YR, McAuley KB, Puskas JE, Dos Santos LM, Alvarez A. Mathematical modeling of arborescent polyisobutylene production in batch reactors. *Macromol. Theory Simul.* 2013; 22: 155-173.

14 Zhao YR, McAuley KB, Puskas JE. Monte Carlo model for arborescent polyisobutylene production in the batch reactor. *Macromol. Theory Simul.* 2013; 22: 365-376.

15 Zhao YR, McAuley KB, Iedema PD, Puskas JE. Advanced Monte Carlo model for arbores-cent polyisobutylene production in batch reactor. *Macromol. Theory Simul.* 2014; 23: 383-400.

16 Zargar A, Chang K, Taite LJ, Schork FJ. Mathematical modeling of hyperbranched water-soluble polymers with application in drug delivery. *Macromol. React. Eng*. 2011; 5: 373-384.

17 He X, Liang H, Pan C. Self-condensing vinyl polymerization in the presence of multifunc-tional initiator with unequal rate constants: Monte Carlo simulation. *Polymer.* 2003; 44: 6697-6706.

18 He X, Tang J. Kinetics of self-condensing vinyl hyperbranched polymerization in three-dimensional space. *J. Polym. Sci. Part A: Polym. Chem*. 2008; 46: 4486-4494.

19 He X, Liang H, Pan C. Monte Carlo simulation of hyperbranched copolymerizations in the presence of a multifunctional initiator. *Macromol. Theory Simul*. 2001; 10: 196-203.

20 Cheng KC, Chuang TH, Chang JS, Guo W, Su WF. Effect of feed rate on structure of hyperbranched polymers formed by self-condensing vinyl polymerization in semibatch reactor. *Macromolecules.* 2005; 38: 8252-8257.

21 Cheng KC, Su YY, Chuang TH, Guo W, Su WF. Kinetic model of hyperbranched polymers formed by self-condensing vinyl or self-condensing ring-opening polymerization of AB monomers activated by stimuli with different reactivities. *Macromolecules.* 2010; 43: 8965-8970.

22 Müller AHE, Yan D, Wulkow M. Molecular parameters of hyperbranched polymers made by self-condensing vinyl polymerization. 1. Molecular weight distribution. *Macromolecules.* 1997; 30: 7015-7023.

23 Yan D, Müller AHE, Matyjaszewski K. Molecular parameters of hyperbranched polymers made by self-condensing vinyl polymerization. 2. Degree of branching. *Macromolecules.* 1997; 30: 7024-7033.

24 Litvinenko GI, Simon PFW, Müller AHE. Molecular parameters of hyperbranched copolymers obtained by self-condensing vinyl copolymerization. 1. Equal rate constants. *Macromolecules.* 1999; 32: 2410-2419.

25 Litvinenko GI, Simon PFW, Müller AHE. Molecular parameters of hyperbranched copolymers obtained by self-condensing vinyl copolymerization, 2. Non-equal rate constants. *Macromolecules.* 2001; 34: 2418-2426.

26 Litvinenko GI, Müller AHE. Molecular weight averages and degree of branching in self-condensing vinyl copolymerization in the presence of multifunctional initiators. *Macromolecules.* 2002; 35: 4577-4583.

27 Lim GT, Puskas JE, Reneker DH, Jakli A, Horton Jr.WE. Highly hydrophobic electrospun fiber mats from polyisobutylene-based thermoplastic elastomers. *Biomacromolecules.* 2011; 12: 1795-1799.

28 Lim GT, Valente SA, Hart-Spicer CR, et al. New biomaterial as a promising alternative to silicone breast implants. *Journal of the mechanical behavior of biomedical materials*. 2013; 21: 47-56.

29 Puskas JE, Foreman-Orlowski EA, Lim GT, et al. A nanostructured carbon-reinforced poly-isobutylene-based thermoplastic elastomer. *Biomaterials*. 2010; 31: 2477-2488.

30 Kaszas G, Puskas JE. Kinetics of the carbocationic homopolymerization of isobutylene with reversible chain termination. *Polym. React. Eng.* 1994; 2: 251-273.

31 Puskas JE, Lanzendorfer MG. Investigation of the $TiCl_4$ reaction order in living isobutylene polymerization. *Macromolecules.* 1998; 31: 8684-8690.

32 Puskas JE, Peng H. Kinetic simulation of living carbocationic polymerizations I. Simulation of living isobutylene polymerization. *Polym. React. Eng*. 1999; 7: 553-576.

33 Puskas JE, Shaikh S, Yao KZ, McAuley KB, Kaszas G. Kinetic simulation of living carbo-cationic polymerizations. II. Simulation of living isobutylene polymerization using a mech-anistic model. *European Polymer Journal*. 2005; 41: 1-14.

34 Puskas JE, Dos Santos LM, Fischer F, et al. Fatigue testing of implantable specimens: effect of sample size and branching on the dynamic fatigue properties of polyisobutylene-based biomaterials. *Polymer*. 2009; 50: 591-597.

35 Puskas JE, Chain SWP, McAuley KB, Kaszas G, Shaikh S. Living carbocationic copoly-merization of isobutylene with styrene. *J. Polym. Sci. Part A: Polym. Chem.* 2007; 45: 1778-1787.

36 Schlaad H, Kwon Y, Sipos L, Faust R, Charleux B. Determination of propagation rate con-

stants in carbocationic polymerization of olefins. 1. Isobutylene. *Macromolecules.* 2000; 33: 8225-8232.

37 Gillespie DT. Exact stochastic simulation of coupled chemical reactions. *J. Phys. Chem.* 1977; 81(25): 2340-2361.

38 Sipos L, De P, Faust R. Effect of temperature, solvent polarity, and nature of Lewis acid on the rate constants in the carbocationic polymerization of isobutylene. *Macromolecules.* 2003; 36: 8282-8290.

39 De P, Faust R, Schimmel H, Ofial A, Mayr H. Determination of rate constants in the carbocationic polymerization of styrene: effect of temperature, solvent polarity, and Lewis acid. *Macromolecules.* 2004; 37: 4422-4433.

40 Roth M, Mayr H. A novel method for the determination of propagation rate constants: carbocationic oligomerization of isobutylene. *Macromolecules.* 1996; 29: 6104-6109.

41 De P, Faust R. Determination of the absolute rate constants of propagation for ion pairs and free ions in the living cationic polymerization of isobutylene. *Macromolecules.* 2005; 38: 9897-9900.

42 Puskas JE, Kaszas G, Kennedy JP, Kelen T, Tudos F. Quasiliving carbocationic polymerization. IX. Forced ideal copolymerization of styrene derivatives. *J. Polym. Sci. Part A: Polym. Chem.* 1982; 18:1315-1338.

43 Dos Santos LM, Puskas JE. Self-condesing vinyl polymerization of 4-(2-methoxy-isopropyl)styrene. *Polym. Prepr.* 2008; 49: 87-88.

44 Woloszyn JD, Hesse P, Hungenberg KD, McAuley KB. Parameter selection and estimation techniques ina styrene polymerization model. *Macromol. React. Eng.* 2013; 7: 293-310.

45 Woloszyn JD, McAuley KB. Application of parameter selection and estimation techniques in a thermal styrene polymerization model. *Macromol. React. Eng.* 2011; 5: 453-466.

46 Karimi H, Schaffer MA, McAuley KB. A kinetic model for non-oxidative thermal degradation of nylon 66. *Macromol. React. Eng.* 2012; 6: 93-109.

47 Cui WJ, McAuley KB, Whitney RA, Spence RE, Xie T. Mathematical model of palyether production from 1,3-propanediol. *Macromol. React. Eng.* 2013; 7: 237-253.

48 Cui WJ, McAuley KB, Spence RE, Xie T. Assesment of mass-transfer effects during polyether production from 1,3-propanediol. *Macromol. React. Eng.* 2014; 8: 476-492.

49 Thompson DE, McAuley KB, McLellan PJ. Parameter estimation in a simplified MWD model for HDPE produced by a Ziegler-Natta catalyst. *Macromol. React. Eng.* 2009; 3: 160-177.

50 Kou B, McAuley KB, Hsu CC, Bacon DW, Yao KZ. Mathematical model and parameter estimation for gas-phase ethylene homopolymerization with supported metallocene catalyst. *Ind. Eng. Chem. Res.* 2005; 44: 2428-2442.

51 Kou B, McAuley KB, Hsu JCC, Bacon DW. Mathematical model and parameter estimation for gas-phase ethylene/hexane copolymerization with metallocene catalyst. *Macromol. Mater. Eng.* 2005; 290: 537-557.

52 Yao ZK, Shaw BM, Kou B, McAuley KB, Bacon DW. Modeling ethylene/butane copolymerization with multi-site catalysts: parameter estimability and experimental design. *Polym. React. Eng.* 2003; 11: 563-588.

53 McLean KAP., Wu S, McAuley KB. Mean-squared-error methods for selecting optimal parameter subsets for estimation. *Ind. Eng. Chem. Res.* 2012; 51: 6105-6115.

54 McLean KAP, McAuley KB. Mathematical modeling of chemical processes-obtaining the best model predictions and parameter estimates using identifiability and estimability procedures. *Can. J. Chem. Eng.* 2012; 90: 351-366.

55 Wu S, McLean KAP, Harris TJ, McAuley KB. Selection of optimal parameter set using es-

timability analysis and MSE-based model-selection criterion. *Int. J. Adv. Mechatronic Syst.* 2011; 3: 188-197.

56 Wu S, K McAuley KB, Harris TJ. Selection of simplified models: I. Analysis of model-selection criteria using mean-squared error. *Can. J. Chem. Eng.* 2011; 1: 148-158.

57 Wu S, K McAuley KB, Harris TJ. Selection of simplified models: II. Development of a model selection criterion based on mean squared error. *Can. J. Chem. Eng.* 2011; 89: 325-336.

58 Polic AL, Lona LMF, Duever TA, Penlidis A. A protocol for the estimation of parameters in process models: Case studies with polymerization scenarios. *Macromol. Theory Simul.* 2004; 13: 115-132.

59 Zhao, YR. Mathematical modeling of arborescent polyisobutylene production in batch reactor using novel material balance and Monte Carlo methods [dissertation]. Kingston, Ontario, Canada: Queen's University; 2014.

Appendix 5.1 Additional Information about Parameter Estimation Attempts

Table 5.8 provides details about the 20 different initial values that were used for parameter estimation. It also gives the final values of *J* from each estimation. Table 5.9 is the final estimation results from all 20 estimations.

Table 5.8 Twenty different initial guesses used for parameter estimation. Note that the estimable parameters determined in each attempt are marked in **bold** and the best trial (Trial 19) is highlighted.

	k_{pIIapp}	k_{pIMapp}	k_{pMIapp}	k_{pMMapp}	k_{pSIapp}	k_{pSMapp}	J
1	7.500E-03	**1.580E-01**	**3.160E-02**	**1.580E-01**	1.000E-04	2.640E-01	6.807E+01
2	**7.500E-03**	**3.990E-04**	**1.950E-01**	2.126E+00	**1.000E-04**	**1.390E-02**	2.932E+01
3	7.740E-01	**3.200E-03**	**3.040E-01**	**5.560E-02**	5.700E-03	2.040E+00	1.256E+02
4	2.637E+00	1.389E+00	**2.376E-05**	**1.851E+00**	1.451E-01	**1.263E-04**	4.441E+02
5	7.348E+00	**1.100E-02**	**2.603E-01**	**1.500E-03**	1.280E-02	1.558E+00	1.455E+02
6	6.312E-01	**9.600E-03**	**5.294E-04**	**8.653E-01**	8.440E-02	**2.300E-02**	1.177E+02
7	**1.290E-02**	**7.649E-05**	**6.300E-03**	**5.377E-01**	**4.678E+00**	**1.834E-04**	8.455E+01
8	**2.250E-02**	**5.530E-01**	**7.000E-03**	**3.966E+00**	**2.460E-04**	**6.700E-03**	1.662E+02
9	**1.660E-01**	**3.450E-04**	**1.100E+00**	**3.410E+00**	**1.560E-02**	**1.480E-04**	3.741E+02
10	**4.800E-02**	**4.500E-03**	**1.520E-02**	**4.600E-03**	**1.030E-01**	**1.480E-01**	2.917E+01
11	**8.196E-03**	**3.640E-04**	**1.540E-01**	**2.110E+00**	**1.285E-03**	**1.652E-02**	2.892E+01
12	**1.351E-01**	**9.855E-05**	**1.131E-04**	**1.300E-03**	8.309E-04	**6.510E-04**	3.620E+01
13	**4.270E-02**	**4.300E-03**	**1.558E-05**	**1.400E-03**	5.132E+00	**2.480E+00**	2.055E+02
14	2.490E-01	**6.200E-03**	2.000E-03	**6.900E-03**	3.490E-02	1.470E-02	1.006E+02
15	**1.390E-02**	**8.438E-04**	**2.630E-01**	**5.379E-04**	4.408E+00	**1.843E-01**	2.205E+02
16	**1.055E-01**	**3.579E+00**	**6.923E-06**	**1.427E+00**	3.685E+00	**3.933E-01**	6.502E+02
17	**1.620E-02**	**7.630E-02**	**3.800E-03**	**5.371E-01**	**3.760E-01**	**1.357E+00**	2.916E+01
18	2.739E-01	**1.030E-02**	**1.102E-01**	**1.131E-01**	1.226E-01	8.148E-01	1.370E+02
19	**2.974E-02**	**8.000E-03**	**1.140E-04**	**1.467E+00**	**6.261E-01**	**2.075E-01**	2.886E+01
20	**5.560E-02**	**2.230E-02**	**2.850E-01**	**2.974E+00**	**6.139E-04**	**9.296E-01**	2.933E+01

Table 5.9 Estimation results from all 20 trials. Values shown as –- did not change from their initial values because the corresponding parameters were not selected for estimation.

	k_{pIIapp}	k_{pIMapp}	k_{pMIapp}	k_{pMMapp}	k_{pSIapp}	k_{pSMapp}
1	--	**2.665E-04**	**1.259E-01**	**2.131E+00**	--	--
	--	±5.748E-05	±3.005E-02	±2.670E-01	--	--
2	**1.345E-02**	**4.963E-04**	**5.429E-01**	**--**	**1.097E-02**	**4.110E-05**
	±9.061E-02	±1.158E-04	±1.765E-01	--	±5.737E-02	±3.315E-04
3	--	**3.157E-04**	**4.110E-06**	**7.764E-01**	--	--
	--	±1.199E-04	±1.698E-02	±1.287E-01	--	--
4	--	--	**1.034E-01**	**5.235E-01**	**--**	**4.110E+00**
	--	--	±3.269E-02	±1.692E-01	--	±1.502E+02
5	--	**2.241E-03**	**4.183E-03**	**4.758E-01**	--	--
	--	±7.933E-04	±2.002E-02	±8.479E-02	--	--
6	--	**2.941E-04**	**5.711E-06**	**9.708E-01**	--	**4.110E+00**
	--	±1.748E-04	±4.693E-02	±1.746E-01	--	±3.887E+02
7	**1.954E+00**	**1.878E-03**	**1.830E-01**	**1.134E+00**	**1.000E-04**	**4.110E-05**
	±5.675E+00	±3.882E-03	±2.287E-01	±8.823E-01	±4.579E-02	±6.304E-04
8	**5.541E+00**	**1.579E-02**	**2.989E-01**	**8.670E-01**	**1.000E-04**	**4.685E-05**
	±7.857E+01	±1.918E-01	±3.498E-01	±4.180E-01	±4.881E-02	±6.768E-04
9	**2.729E-01**	**3.913E-04**	**5.708E-01**	**2.956E+00**	**4.620E-03**	**4.110E-05**
	±7.574E-01	±5.374E-04	±6.589E-01	±2.586E+00	±6.623E-02	±7.264E-04
10	**3.682E-02**	**4.555E-04**	**5.390E-01**	**2.270E+00**	**5.182E-03**	**4.110E-05**
	±1.303E-01	±1.461E-04	±1.800E-01	±4.477E-01	±6.264E-02	±3.129E-04
11	**3.615E-02**	**4.508E-04**	**5.221E-01**	**2.265E+00**	**5.749E-03**	**4.110E-05**
	±1.469E-01	±1.453E-04	±1.751E-01	±4.724E-01	±6.425E-02	±3.124E-04
12	**1.050E-01**	**3.585E-04**	**4.612E-01**	**2.591E+00**	**--**	**4.110E-05**
	±1.268E-01	±1.190E-04	±1.648E-01	±7.819E-01	--	±3.285E-04
13	**7.500E-03**	**1.705E-04**	**2.811E-02**	**1.758E+00**	**--**	**4.110E+00**
	±2.301E-02	±8.067E-05	±1.653E-01	±5.180E-01	--	±4.859E+01
14	--	**1.351E-04**	--	**1.627E+00**	--	--
	--	±4.070E-05	--	±2.327E-01	--	--
15	**7.548E-03**	**1.401E-04**	**5.206E-02**	**1.811E+00**	**--**	**4.109E+00**
	±2.547E-02	±6.259E-05	±1.604E-01	±5.205E-01	--	±4.393E+01
16	**1.056E+00**	**1.298E-03**	**5.291E-02**	**5.139E-01**	**--**	**4.110E+00**
	±2.158E+01	±2.399E-01	±1.830E-01	±3.221E-01	--	±7.611E+01
17	**1.087E-02**	**4.561E-04**	**5.279E-01**	**2.217E+00**	**1.522E-02**	**4.110E-05**
	±1.066E-01	±1.433E-04	±1.805E-01	±4.237E-01	±5.610E-02	±3.383E-04
18	--	**1.056E-04**	**4.110E-06**	**1.127E+00**	--	--
	--	±5.817E-05	±1.622E-02	±1.931E-01	--	--
19	**3.323E-02**	**4.464E-04**	**5.188E-01**	**2.266E+00**	**6.447E-03**	**4.110E-05**
	±1.546E-01	±1.451E-04	±1.751E-01	±4.881E-01	±6.433E-02	±3.041E-04
20	**3.314E-02**	**4.580E-04**	**5.391E-01**	**2.267E+00**	**6.973E-03**	**4.110E-05**
	±1.252E-01	±1.465E-04	±1.809E-01	±4.404E-01	±6.277E-02	±3.225E-04

Chapter 6

Conclusions and Recommendations

6.1 Conclusions

In this thesis, four novel mathematical models are developed to describe the copolymerization of inimer and isobutylene to form arborescent polymer via living carbocationic polymerization. These four models have accomplished the goals mentioned in Chapter 1.

In Chapter 2, a lengthy PREDICI model has been developed. To my knowledge, this is the first model for a Self-Condensing Vinyl Copolymerization (SCVCP) system that does not apply equal-reactivity assumptions for different end groups and vinyl groups. Because of the simple approach used in this model (*i.e.*, to track separately the various polymer molecules with different numbers of end groups of different types), the model requires a large number of reaction steps and different species to describe the system accurately. Doing so would be impossible without making some simplifying assumptions. The assumption that were made (*e.g.*, only up to 15 inimer units per polymer molecule and two inimer molecules cannot react directly with each other) helped to reduce the number of reaction steps to 1430, the number of species to 122 and the number of different propagation rate constants from 6 to 4, making this model only applicable for low branching-level systems (*i.e.* average branches per polymer molecule < 5). This model can predict the concentration changes of inimer, isobutylene and different polymer species, the average branching level, M_n and M_w, the overall MWD and MWDs for polymers with different number of branches over time. Also for the first time, *arb*PIB experimental data are used for parameter estimation. It was shown that all four apparent propagation rate constants can be estimated by using the available literature data. The simulation results give a good fit to the experimental data. A secondary contribution of this modeling research is that it shows the ability of PREDICI to handle a surprisingly large number of species and reaction steps. Before doing this research, I

anticipated that PREDICI would stop working after implementing several hundred reaction steps, however, it works well even if there are more than a thousand steps. Perhaps even larger models for a variety of polymerization systems could be implemented in PREDICI in the future.

In Chapter 3, a traditional Monte Carlo model is developed, which is a great improvement over the RREDICI model in Chapter 2 because of the reduced number of simplifying assumptions. This MC model is the first model that can account for all six different types of apparent propagation rate constants in SCVCP systems without applying any equal reactivity assumptions for different end groups and vinyl groups. This model is also not limited by the number of branches (or inimer units) that polymer molecules can have, making it suitable for simulating the production of *arb*PIB or even inimer homopolymerization. A special matrix is used to track all the information about individual inimer and polymer molecules in a small reaction volume within the system, and to track reactions between different molecules. From this matrix, and the known initial concentrations in the batch reactor a variety of information can be determined over time (*i.e.* concentrations of isobutylene, inimer and polymer molecules, M_n and M_w, the overall MWD and MWDs for polymers with different number of branches). The main disadvantage of this MC model is that if we want reliable results for MWDs, a relatively large sample volume must be considered and an extremely large matrix is needed for tracking the results. The corresponding calculations for typical simulation can take several week on a typical laptop computer. This disadvantage could be addressed using advanced computing technology, including parallel computing, but even then, the proposed MC model would not be suitable for parameter estimation.

In Chapter 4, another MC model, which uses an advanced algorithm that I developed with assistance from Dr. Piet Iedema and Kim McAuley, is described. This advanced MC model uses a combination of dynamic material balances and stochastic calculations. It provides the same results as the MC model in Chapter 3, except that the MWD information is only generated for the polymer at the end of the batch (or at another user-specified time) where this information

is required. Also, the advanced MC model can easily provide information about dangling and internal segments that the traditional MC model does not provide. The advanced MC model has much shorter computational times (*e.g.*, by a factor of about 200 for the runs that were simulated). However, to achieve this remarkable performance, a much more complex algorithm is needed, which uses random number to make and track many more types of decisions than are made using the traditional MC approach.

In Chapter 5, a new type of model is developed in PREDICI, which contains three parallel simulation systems. The first simulation focuses on reactions between different types of end groups and vinyl groups. The second simulation provides information about dangling and internal segments. The third simulation provides information about the concentration of isobutylene, inimer and polymer molecules. Information from the first two simulations is required to compute the rate constants for the third simulation, accounting for the fact that polymer molecules of different sizes (with different numbers of end groups) tend to react at different rates. Based on the information provided from these three simulation systems, the value of average branching level and number average molecular weight can also be calculated. This new PREDICI model, which takes only several seconds to finish one simulation, is much faster and more efficient than the three models in Chapters 2 to 4. As a tradeoff, some information (*i.e.* weight average molecular weight and MWD) is not able to be obtained. Even if this PREDICI model did lose some information, it is still an excellent practical model for use in parameter estimation. This new model enabled parameter estimation for all six propagation rate constants in a SCVCP model, for the first time. The new parameter values provide a better fit to the experimental data than the previous values that I estimated using the model in Chapter 2. Also, the simulation results show that confidence intervals of parameters k_{pIIapp}, k_{pSIapp} and k_{pSMapp} include 0, which means they are not statistically significant at the 95% confidence level. The wide confidence regions seem to be caused by the low initial concentrations of IM in the experiments used to estimate the parameters

and the lack of information about concentration changes of IM over time. Additional experimental data could be used to obtain improved estimates of the model parameters.

Simulation results from the three models in Chapters 3-5 agree very well with each other and, for low branching-level systems, simulation results from the PREDICI model in Chapter 2 match the results from the three models in Chapters 3-5.

6.2 Recommendations for Future Work

Some recommendations arise from the research required to develop the four mathematical models in this thesis. These recommendations are listed below.

6.2.1 Modifications of Current Models

In the proposed models, there is a common assumption that all polymer chains are not allowed to react with themselves to form cyclic molecules. Also, steric hindrance effects are not considered for reactions between large highly-branched polymer molecules. These two assumptions may make reactions between large molecules occur faster in the simulations than in reality. It would be relatively easy to remove these assumptions in the traditional MC model by adding extra self-reaction steps into the model and some steric hindrance factors to the apparent kinetic rate constants for reactions involving large polymer molecules. However, it would be difficult to obtain the appropriate values for the cyclization rate constants and steric hindrance factors because literature values are not available and because the traditional MC model is too slow for parameter estimation.

Also, by using some of the ideas developed for the proposed *arb*PIB models, new models could be generated and applied to other branched polymerization systems (*e.g.*, involving controlled radical polymerization or condensation polymerization).

6.2.2 More Experimental Data for Parameter Estimation

The results in Chapter 5 shows that estimates for k_{pIIapp}, k_{pSIapp} and k_{pSMapp} may not be very accurate. These three parameters are related to the concentration changes involving IM and also end-groups that arise from the IM. Better estimation of these three parameters requires polymerization recipes that have high initial concentrations of IM and monitoring of the concentration of IM over time during the batch experiments. Also, it would help to have IM homopoly-

merization data with an initial $TiCl_4$ concentration that matches the concentration used in the SCVCP experiments used for parameter estimation in Chapters 2 and 5.

Moreover, the branching data available from Dos Santos were calculated from the concentration of IB and number average molecular weight, which does not provide any new information. Independent measurements of branching level (*e.g.*, by link destruction) would be helpful for parameter estimation. Note that the model developed in Chapter 5 will need to be revised to predict link-destruction measurements, because of the way that segments were defined. Link destruction destroys the benzene rings in the branched polymer chains and will result in longer "segments" than the types of segments that are predicted by the current models in Chapters 4 and 5.

In addition, only apparent rate constants were estimated in Chapters 2 and 5. If experiments are performed using a variety of initial $TiCl_4$ concentrations, then it should become possible to estimate a variety of true propagation rate constants and equilibrium constants. Note that the model developed in Chapter 5 could be used as an aid for selecting new experimental runs that will provide good information for parameter estimation and model validation. It will be important to use the models to predict data that are not used for parameter estimation, so that the predictive ability of the models can be assessed.